N O T I C E

THIS DOCUMENT HAS BEEN REPRODUCED FROM MICROFICHE. ALTHOUGH IT IS RECOGNIZED THAT CERTAIN PORTIONS ARE ILLEGIBLE, IT IS BEING RELEASED IN THE INTEREST OF MAKING AVAILABLE AS MUCH INFORMATION AS POSSIBLE

NAGW-1130

Workshop on Observations of Recent Comets (1990)

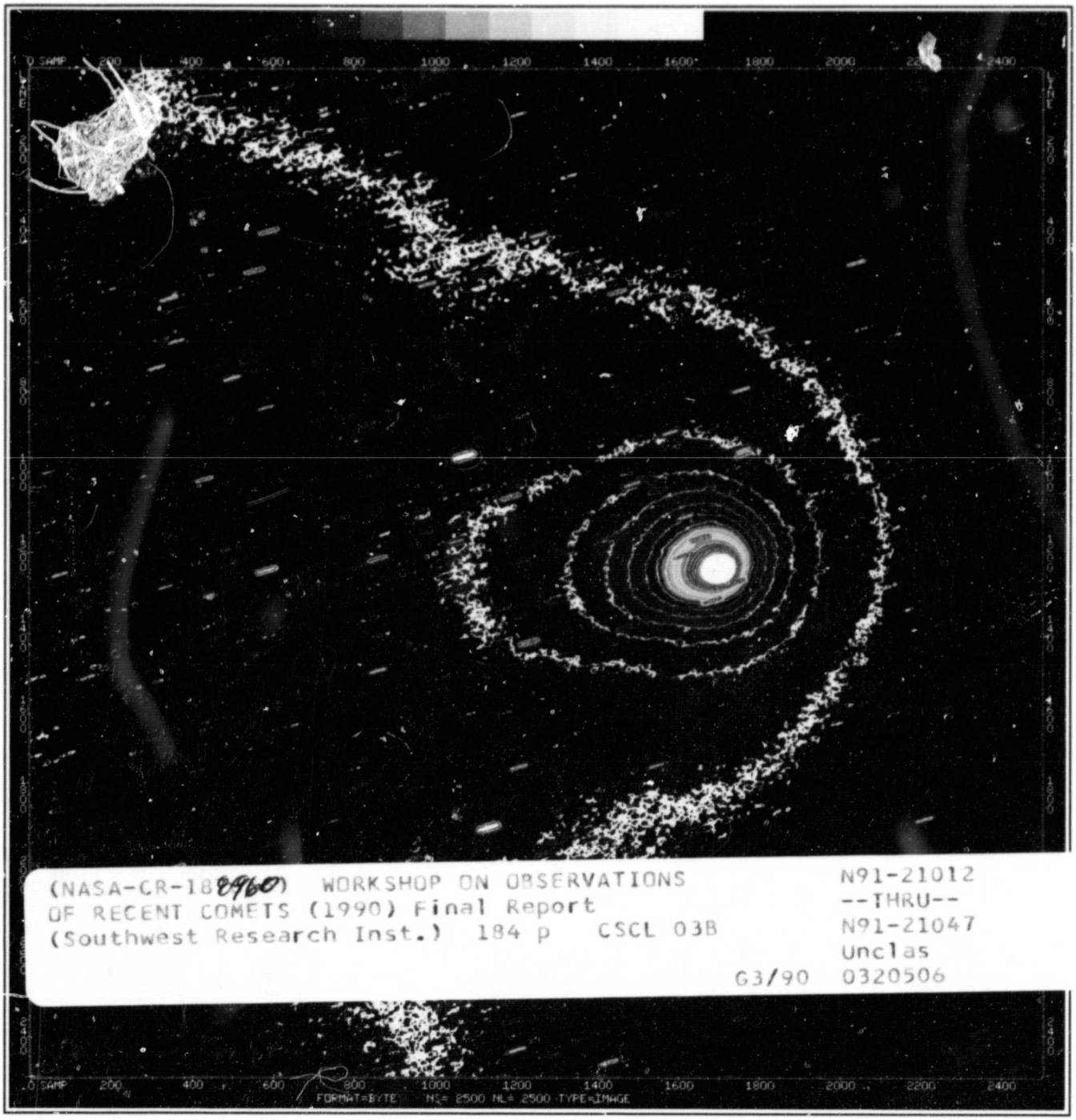

(NASA-CR-18[illegible]) WORKSHOP ON OBSERVATIONS OF RECENT COMETS (1990) Final Report (Southwest Research Inst.) 184 p CSCL 03B

N91-21012
--THRU--
N91-21047
Unclas
G3/90 0320506

Editors:
W. F. Huebner J. Rahe
P. A. Wehinger I. Konno

Albuquerque, New Mexico
June 15-16, 1990

Workshop on

Observations of Recent Comets (1990)

Proceedings of the

Albuquerque, NM Workshop, June 15-16, 1990

Editors:
W. F. Huebner
P. A. Wehinger
J. Rahe
I. Konno

Supported by

National Aeronautics and Space Administration
Planetary Astronomy Program

Published by

Southwest Research Institute
San Antonio, TX 78228-0510
1990

Foreword

This volume contains the proceedings of the Workshop on Observations of Recent Comets, 1990, held on June 15 and 16, at the Doubletree Hotel in Albuquerque, New Mexico, with the support of the Planetary Atmospheres Program of NASA. There were about 35 participants, including one from France. Two Japanese groups, who did not attend in person, submitted posters.

One-page abstracts were submitted in advance. These were made available to all participants at the time of the Workshop. All presentations were informal and about ten minutes in length, followed by about ten minutes of discussions. A written record of most, although not all, of the discussions was made. The presenters were encouraged to submit an expanded abstract of about five pages in length for inclusion in the Proceedings. The recorded discussions follow each of these presentations.

At the time of the Workshop about three years had passed since the highly successful and extensive spacecraft and Earth-based observing campaigns of Comet P/Halley. During this time, data have been reanalyzed and reinterpreted. In light of the new findings from the *in situ* measurements and coordinated Earth-based observations and the somewhat earlier *in situ* measurements from the P/Giacobini-Zinner flyby of the ICE spacecraft, the objective of the Workshop was to focus on potential interpretations of the observations of recent comets. Since much of the data on the recent comets Brorsen-Metcalf (1989o), Okazaki-Levy-Rudenko (1989r), Aarseth-Brewington (1989a1), and Austin (1989c1) was only partially reduced and not fully analyzed or interpreted, these extended abstracts have not been refereed. Consistent with this objective, it was felt that the Proceedings should get into the hands of the participants, as well as other colleagues who were unable to attend, without delay. This is another reason for not refereeing these extended abstracts. Thus the reader is warned of the preliminary nature of these Proceedings and is encouraged to contact the authors directly. We hope that such contacts will lead to profitable collaborations.

The editors wish to acknowledge the interest of the Planetary Atmospheres Program of NASA in sponsoring the Workshop and the publication of the Proceedings.

Walter F. Huebner
Peter Wehinger
Jurgen Rahe
Ichishiro Konno

TABLE OF CONTENTS

RESULTS FROM THE COMET GIACOBINI-ZINNER AND HALLEY CAMPAIGNS

W. F. Huebner
Southwest Research Institute
San Antonio, TX 78228-0510

N91-21013
51-90
P.7

The spacecraft flybys of Comets Giacobini-Zinner and Halley were highly successful. They confirmed many untested theories and provided additional clues to decide between competing models, but without leading to a clear preference. They also raised new questions. Based on the improved knowledge, research efforts will now be much better focused than was possible before the encounters. Moreover, we should be better equipped to interpret Earth-based (ground-based, air-borne, rocket-borne, and Earth satellite) observations.

The goals of the workshop are defined in terms of the results from spacecraft measurements and Earth-based observations of Comets Giacobini-Zinner and Halley. A summary is presented of the new knowledge about the nucleus, the coma gas and dust, and the plasma. We realize that we must be extremely cautious when generalizing results from the Comet Giacobini-Zinner and Halley investigations to comets universally. The many surprises of the successful missions, the dangers inherent in generalizations to other comets, and the many still open and new questions are the reasons for the need of further spacecraft investigations. However, an unquestionably successful start has been made in expanding our knowledge about the physics and chemistry of comets and all the related implications, and the question about the similarities of and differences between comets can now be explored further.

1. Summary of the P/Giacobini-Zinner and P/Halley Investigations

Starting with the P/Halley nucleus, we have learned that its size of approximately 500 km^3 is about three times larger in volume than estimates before the P/Halley missions had indicated (Keller et al., 1987). The larger size, combined with the same response to the nongravitational forces acting on it (therefore the same mass of about 1.5×10^{14} kg), leads to a much lower density of about 300 kg/m^3 (Rickman, 1989). With the uncertainties in the volume and mass, the density could be as low as 200 kg/m^3 and as high as 700 kg/m^3. The axial ratio of the nucleus is about 2 : 1 : 1 with the major axis of the ellipsoidal shape being about 16 km; this is much more aspherical than had been anticipated. The surface morphology suggests subunits of the nucleus that may have been as large as one to several kilometers in size. Consistent with the large surface area of about 400 km^2, the albedo is only about 4%. The abundance of CO and probably some of the other coma gases is much lower in the nucleus than earlier coma observations had suggested. The nucleus itself appears to be inhomogeneous, as indicated by the relatively small active areas that are responsible for the jet-like dust features and most, if not all, of the coma gas. The rotational motion of the nucleus has been controversial since the spacecraft flyby of P/Halley, but a possible solution may now be in sight.

More relevant to ground-based observations are the coma and the dust. We have learned that the frozen gases in the nucleus of P/Halley consist mainly of water. About 85% of the coma gas near the nucleus is water. Approximately half to two-thirds of the CO comes from distributed sources in the coma, probably indirectly through the dissociation of complex molecules that are released from the dust. Closely related to the decay of these complex

molecules may be the production of H_2CO, CH, and CH_2. Even other species, such as CN, NH, NH_2, C_2, and possibly C_3, may come, at least in part, from distributed sources, as the jet-like structures of these radicals in the coma suggest. The ratio of $^{12}C/^{13}C = 65 \pm 9$, as determined by Wyckoff et al. (1989). This ratio, obtained from CN observations, is much lower than the older values of 89 and higher, which were obtained from C_2 observations in comets (Vanýsek and Rahe, 1978). The value of 89 is the terrestrial value. The carbon isotope ratio obtained from the P/Halley dust analysis varies from very low to very high values (Šolc et al., 1987). It would be interesting to know whether the carbon isotope ratios from CN and C_2 are consistently different and if the ratios from gas-phase molecules are different from those of comet dust. The ratio of $0.6 \times 10^{-4} < D/H < 4.8 \times 10^{-4}$ obtained by Eberhardt et al. (1987) is very similar to that of ocean water and of Titan. Very heavy molecules with molecular weight up to about 120 amu were detected (Korth et al., 1987). It is likely that these molecules are associated with the organic dust known as CHON particles. Gas "jets" have been observed in CN, OH, NH, and other molecular emissions. These are most likely also related to CHON dust particles. The detection of para- and ortho-water in IR spectra (Mumma et al., 1987) assumes a special importance: It has the potential to open a new era of investigations about the formation temperature of comet nuclei.

The dust size distribution does not appear to have a lower limit; particles as small as 10^{-16} g (the lower limit of particle sizes measurable by the instruments) were detected in large numbers (McDonnell et al., 1987). Could this distribution of small particles continue downward to the size of molecular clusters? There is evidence that dust particles fragment in the coma. Large amounts of organic dust, rich on carbon, hydrogen, oxygen, and nitrogen, the so called CHON particles have been detected (Clark et al., 1987). They also contain small amounts of sulfur. The CHON particles and their disintegration products are also responsible for the IR emissions in the 3.3 μm range. CHON particles can be divided into six categories: Those consisting primarily of (1) H and C, (2) H, C, and O, (3) H, C, and N, (4) H, C, N, and O, (5) C and O, and (6) H and O. These divisions are probably not sharp, diffusing from one group to the next. Nitrogen is underabundant by a factor of 3 or perhaps somewhat more as determined from the combined analyses of gas and dust in P/Halley.

The relative abundances of the rock-forming elements in the dust are within a factor of two of the CI chondrites, while H, O, and especially C and N are highly enriched, i.e., less depleted in comet dust relative to CI chondrites. Thus the dust in P/Halley is more primitive than CI chondrites, which testifies to the nearly pristine nature of comet dust. The distribution of the Fe/(Fe + Mg) ratio in P/Halley silicate dust resembles the distribution found in anhydrous interplanetary dust particles (IDPs). Comparing the ternary Mg-Si-Fe system, P/Halley dust differs greatly from layer lattice silicate IDPs and matches better with anhydrous IDPs (Jessberger et al., 1988). But there is an important difference between comet dust and anhydrous IDPs: Anhydrous IDPs are practically devoid of samples richer in Mg then those lying on the olivine-iron line, while in comet dust many silicon-poor and magnesium-rich grains occur. This is what one would expect from primitive Solar System material, i.e., silicates that never had been exposed to high temperatures. The dust–to–gas mass ratio is about 1 : 1 with an uncertainty of a factor of about 2. If the dust size distribution is extrapolated and integrated to the largest particles that can be lifted through entrainment by coma gas against the gravitational attraction of the nucleus, then the dust–to–gas mass ratio is about 2 in P/Halley.

Of equal importance, but less accessible for Earth-based observations, are the plasma effects that have been determined by *in situ* spacecraft measurements. The cometopause,

which is defined by a particularly steep increase of mass loading of the solar wind, was discovered between the bow shock and the contact surface (Gringauz et al., 1986). It was found that the bow shock is not sharp and that there exists a turbulent transition zone. From the ICE passage through the onset of the ion tail region of Comet Giacobini-Zinner, it was found that: (1) The model for field-draping is basically confirmed, but a magnetosheath forms at the ion tail boundary. (2) A thin plasma sheet with a total thickness of about 2000 km and a width of about 1.6×10^4 km exists at the center of the ion tail. (3) The plasma flow velocity gradually decreases to zero at the center of the ion tail. (4) The degree of magnetic field turbulence and plasma wave activity was seen to correlate with the production of ions from cometary neutrals in the solar wind. The study of plasma instabilities, waves, pickup ions, ring and shell distributions in velocity space, energetic ions, and charge exchange processes with cometary neutrals is afforded by the natural plasma laboratory that a comet provides without the interfering wall effects that are always present in plasma chambers.

2. Relationship to Earth-based Observations

The above summary is obviously incomplete, but it provides a starting point for discussions in this workshop. Among the questions that we may want to address is: How well can we define and interpret Earth-based observations in terms of the above results? Some observations of P/Halley, such as the gas "jets" (A'Hearn et al., 1986), were ground-based and can obviously be tried again. It would be very important to know how common these jet-like gas features are in other comets. Other observations will be much more difficult to make by remote sensing from the Earth. Here we summarize some of the questions that might be answered through such observations.

Many attempts have been made to determine the spin period of comet nuclei, but how well can one determine the combination of spin and precession of the nucleus from ground-based observations? What fraction of a nucleus is active? How is this fraction related to the dynamical age of a comet? What causes the development of inactive (mantle) areas on the surface of a nucleus? What fraction of the coma gas comes directly from the nucleus (i.e., from the ice) and what fraction comes from the distributed (i.e., dust) sources? How does the relative abundance of gas to dust change and how does the relative abundance of frozen gases (e.g., CO : CO_2 : H_2O) change from comet to comet? Very important for the origin of comets is the question about the ratio of CH_4/CO and NH_3/N_2. What are the parent species of C_2, C_3, CN, CH, NH, and NH_2? Are gases trapped in the ice of the nucleus? If so, Ar should also be trapped (Bar-Nun et al., 1985). The relative abundance of Ar may become an important test case for the trapping theory. Do clathrates exist in comets? How wide does the S_2 abundance vary from comet to comet? Are other sulfur compounds, such as H_2S, SO, SO_2 present in comets? What is the $^{12}C/^{13}C$ ratio in the ice and in the dust? Can this isotope ratio, as obtained from CN and C_2, be used to determine the sources of CN and C_2? For example, does a narrow range in the isotope ratio indicate that the source is in the ice and a broad range indicate that dust is the source? What is the D/H ratio in other comets? What is the gas production of comets at large heliocentric distances (say, $r > 4$ AU) and which species can be detected?

What is the ratio of silicate to CHON particles in dusty vs. "dust-free" comets? Do the silicate and CHON particle size distributions differ with respect to each other and as a function of cometocentric distance? What are the compositions and structures of CHON and mixed silicate-and-CHON particles? If "dust-poor" comets are rich on very fine dust

(particle radius $a < 0.1\mu$m), then the production of some "mother molecules", such as CO, H_2CO, etc., may be detectable in distributed sources from the ground (see, e.g., Feldman et al., 1988). Are jet-like gas features frequent phenomena in comets? Do jet-like features in OH (Clairemidi and Moreels, 1989; Clairemidi et al., 1990) originate from H_2O trapped in dust particles? Can IR observations detect fragmentation of dust particles? For example, does the relative intensity profile at different IR wavelengths change with cometocentric distance? Can we improve detection of distributed sources from Earth-based observations? Can unidentified spectral features be related to heavy molecules with masses larger than about 40 amu? What is the relationship between amorphous and crystallized silicates and how do they relate to other features in comets (e.g., dust-poor or dust-rich comets, the 3.3 μm C–H stretch bonds of the organic grains, etc.)? What is the relationship between C_2, C_3, CN, CO (CO^+), dust, etc., in short-period vs. long-period comets?

With regard to plasmas, can we detect any evidence for an inner shock? How stable is the contact surface? How important is the Alfvén critical velocity effect (anomalous ionization)? Can one identify the cometopause from ground observations, and if so, how stable is it? What are the energetic ions inside of the contact surface and what is their source? What are the causes and dynamics of disconnection events (DEs) in plasma tails? We may need simultaneous observation of DEs and spectroscopy of tail ions.

Many other questions can undoubtedly be asked. Some new questions and perhaps even some answers may result from discussions in this workshop. But most important for this workshop is to outline some of the thoughts and provide the stimulus for development of further research and collaboration.

References

A'Hearn, M. F., Hoban, S., Birch, P. V., Bowers, C., Martin, R., Klinglesmith, D. A. III (1986): 'Cyanogen jets in comet Halley.' *Nature* **324**, 649–651.

Bar-Nun, A., Herman, G., Laufer, D., Rappaport, M. L. (1985): 'Trapping and release of gases by water ice and implications for icy bodies.' *Icarus* **63**, 317–332.

Clairemidi, J., Moreels, G. (1989): ' 'Hot' OH and CN – evidence for organic molecules close to the nucleus of Comet Halley?' In *Physics and Mechanics of Cometary Materials.* ESA **SP-302**, 177–184.

Clairemidi, J., Moreels, G., Krasnopolsky, V. A. (1990): 'Spectro-imagery of P/Halley's inner coma in the OH and NH ultraviolet bands.' *Astron. Astrophys.* **231**, 325-240.

Clark, B. C., Mason, L. W., Kissel, J. (1987): 'Systematics of the "CHON" and other light-element particle populations in Comet P/Halley.' *Astron. Astrophys.* **187**, 779–784.

Eberhardt, P., Dolder, U., Schulte, W., Krankowsky, D., Lämmerzahl, P., Hoffman, J. H., Hodges, R. R., Berthelier, J. J., Illiano, J. M. (1987): 'The D/H ratio in water from comet P/Halley.' *Astron. Astrophys.* **187**, 435–437.

Feldman, P. D., Dymond, K. F., Roettger, E. E., Weaver, H. A. (1988): 'The distribution of carbon monoxide in the coma of Comet P/Halley.' *BAAS* **20**, 827–828.

Gringauz, K. I., Gombosi, T. I., Tátrallyay, M. Verigin, M. I., Remizov, A. P., Richter, A. K., Apáthy, I., Szemerey, I., Dyachkov, A. V., Balakina, O. V., Nagy, A. F. (1986): 'Detection of a new "chemical" boundary at Comet Halley.' *Geophys. Res. Lett.* **13**, 613–616.

Jessberger, E. K., Christoforidis, A., Kissel, J. (1988): 'Aspects of the major element composition of Halley's dust.' *Nature* **332**, 691–695.

Keller, H. U., Delamere, W. A., Huebner, W. F., Reitsema, H. J., Schmidt, H. U., Whipple, F. L., Wilhelm, K., Curdt, W., Kramm, J., Rainer, T. N., Arpigny, C., Barbieri, C., Bonnet,

R. M., Cazes, S., Coradini, M., Cosmovici, C. B., Hughes, D. W., Jamar, C., Malaise, D., Schmidt, K., Schmidt, W. K. H., Seige, P. (1987): 'Comet P/Halley's nucleus and its activity.' *Astron. Astrophys.* **187**, 807–823.

Korth, A., Richter, A. K., Loidl, A., Anderson, K. A., Carlson, C. W., Curtis, D. W., Lin, R. P., Rème, H., Sauvaud, J. A., d'Uston, C., Cotin, F., Cros, A., Mendis, D. A. (1986): 'Mass spectra of heavy ions near Comet Halley.' *Nature* **321**, 335–336.

McDonnell, J. A. M., Alexander, W. M., Burton, W. M., Bussoletti, E., Evans, G. C., Evans, S. T., Firth, J. G., Grard, R. J. L., Green, S. F., Grün, E., Hanner, M. S., Hughes, D. W., Igenbergs, E., Kissel, J., Kuczera, H., Lindblad, B. A., Langevin, Y., Mandeville, J.-C., Nappo, S., Pankiewicz, G. S. A., Perry, C. H., Schwehm, G. H., Sekanina, Z., Stevenson, T. J., Turner, R. F., Weishaupt, U., Wallis, M. K., Zarnecki, J. C. (1987): 'The dust distribution within the inner coma of Comet P/Halley 1982i: Encounter by Giotto's impact detectors.' *Astron. Astrophys.* **187**, 719–741.

Mumma, M. J., Weaver, H. A., Larson, H. P. (1987): 'The ortho – para ratio of water vapor in Comet P/Halley.' *Astron. Astrophys.* **187**, 419–424.

Rickman, H. (1989): 'The nucleus of comet Halley: Surface structure, mean density, gas and dust production.' *Adv. Space Res.* **9**, 59–71.

Šolc, M., Vanýsek, V., Kissel, J. (1987): 'Carbon-isotope ratio in PUMA 1 spectra of P/Halley dust.' *Astron. Astrophys.* **187**, 385–387.

Vanýsek, V., Rahe, J. (1978): 'The $^{12}C/^{13}C$ isotope ratio in comets, stars and interstellar matter.' *Moon Planets* **18**, 441–447.

Wyckoff, S., Lindholm, E., Wehinger, P. A., Peterson, B. A., Zucconi, J.-M., Festou, M. C. (1989): 'The $^{12}C/^{13}C$ abundance ratio in Comet Halley.' *Astrophys. J.* **339**, 488–500.

Lewis Snyder
What is the present status of the formaldehyde polymer identification?

Walter Huebner
Laboratory experiments with H_2CO solutions in H_2O give a mass spectrum in the vapor phase that closely resembles the observed POM peaks. H_2CO in methanol solution produces the mass peaks in the vapor exactly and also shows some neighboring peaks to give a width to the spectral features, but the width does not fully account for the observed spectrum. Other species must be present.

Susan Wyckoff
Do the bulk properties of the Halley grains differ chemically from those analyzed by Anders and co-workers in primitive meteorites?

Walter Huebner
In layer lattice silicate interplanetary dust particles (IDPs) the ratio of Fe/(Fe + Mg) peaks sharply around 0.5 and is similar to a carbonaceous chondrite matrix. In anhydrous IDPs Fe/(Fe + Mg) peaks at low values and then is smeared out over the rest of the range. P/Halley silicate dust more closely resembles the latter. When comparing the ternary system Mg-Si-Fe, Halley silicate dust again is closer to the anhydrous IDPs, particularly in the pyroxene region. However, there is a clear difference between Halley silicates and IDPs: P/Halley silicates are relatively poor in Si and rich on Mg [there are no IDPs with Mg/(Mg + Si) > 2/3, i.e., richer in Mg than olivines].

Humberto Campins
Comment: The mass spectrometry of Halley's dust confirms the groundbased 10 μm spectrophotometry (Campins and Ryan, *Ap. J. 341*, 1059, 1989), which also shows that the silicates in Halley were anhydrous; more specifically crystalline olivine.

Walter Huebner
Yes, Halley silicate dust more closely resembles anhydrous interplanetary dust particles, particularly in the pyroxene region, but most Halley silicates are richer on Mg and poorer on Si. Does this mean that they have to be crystalline?

David Lynch
Are there models or observations of grain fragmentation which could guide those of us who do thermal IR spectroscopy as to the distance range on which fragmentation is expected to occur?

Walter Huebner
Observationally there are indications that the ratio of small particles relative to large particles increases with cometocentric distance, bursts of small particles have been measured indicat-

ing fragmentation at large cometocentric distances, and the images of "jets" near the nucleus show a behavior that is consistent with fragmentation at small cometocentric distances. Tomorrow you will hear about progress of modeling fragmentation, but particle lifetimes are only guesses at this time.

52-90
220608
8 5

N91-21014

PHOTOMETRIC NARROWBAND CCD IMAGING OF COMETS P/BRORSEN-METCALF AND AUSTIN (1989C1)

David G. Schleicher, David J. Osip, Robert L. Millis (Lowell Observatory), Andrea Thompson and Linda M. Sauter (Mass. Inst. Tech.)

Abstract

We have obtained simultaneous wide-field CCD images and conventional aperture photometry of Comets P/Brorsen-Metcalf (1989o) and Austin (1989c1). These data allow us to directly test our absolute calibration of the CCD images and our ability to generate full-coma, continuum-subtracted emission band images. Preliminary photometric calibration for a portion of the Brorsen-Metcalf observations yields reduced emission band and continuum fluxes which agree to within about 10% with those from the photoelectric observations. Conventional photometry of Comet Austin shows unusual variations among the production rates of the different species as a function of heliocentric distance.

Introduction

We have recently embarked on a program to obtain full-coma, narrow-band CCD images of comets. In addition to obtaining model-independent total abundances, a primary reason for imaging the whole coma is to obtain a complete spatial map of each species. These maps, in turn, can be used to improve model parameters such as lifetimes and scalelengths which are required to properly extrapolate to whole-coma values from small aperture measurements made with typical photometers and spectrophotometers.

Observations

In order to obtain digital images of the entire coma of a comet and to adequately sample the sky background, we have coupled a 200 mm Takahashi f/4 wide-angle telescope to our 800x800 TI CCD. This system gives a 50 arcmin field with 4 arcsec/pixel resolution. A set of image-quality IHW filters (2x2-inch to eliminate vignetting) isolate the CN, C_2, C_3, CO^+, and H_2O^+ bands, plus three continuum points. In the last year, a large number of photometrically calibrated narrowband images of Comets P/Brorsen-Metcalf and Austin were recorded with this equipment. A contour plot of a typical image is shown in Figure 1; note that the CN coma nearly fills even this large field.

By fitting model profiles to the actual radial profile extracted from the image, sets of viable parent and daughter scalelengths can be obtained. This family of solutions is considerably more restricted than would be the case if only the inner portion of the coma were measured. An example is given in Figure 2, where we show both the radial profile of CN (from Figure 1) and a contour plot showing χ^2 for each combination of parent and daughter Haser scalelengths. The two innermost contours are the domain of viable fits to the radial profile. The intersection of this domain with those found using images obtained at other heliocentric distances will progressively narrow the solution.

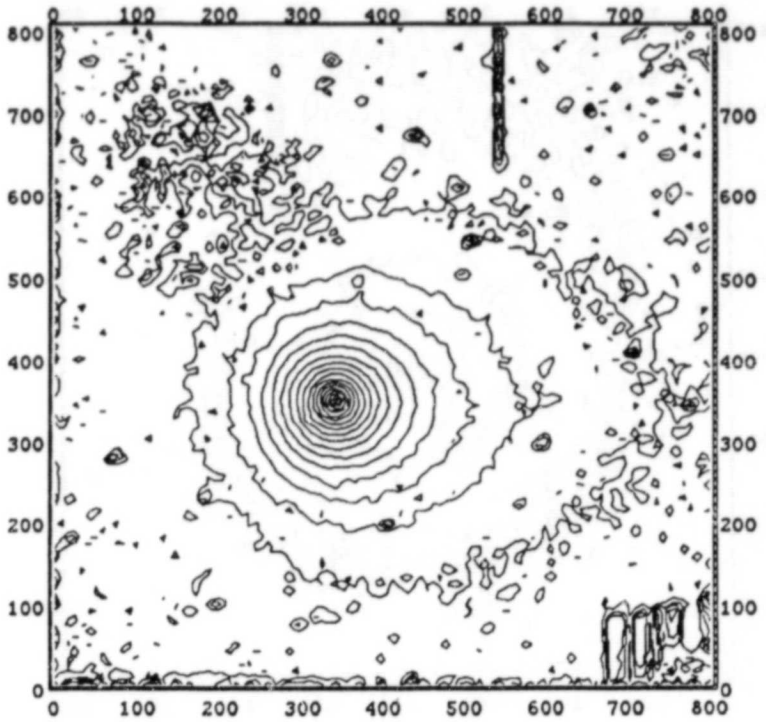

Figure 1. Contour plot of Comet P/Brorsen-Metcalf as observed in the CN molecular band (3870Å). The scale of the image is 50 arcminutes on a side.

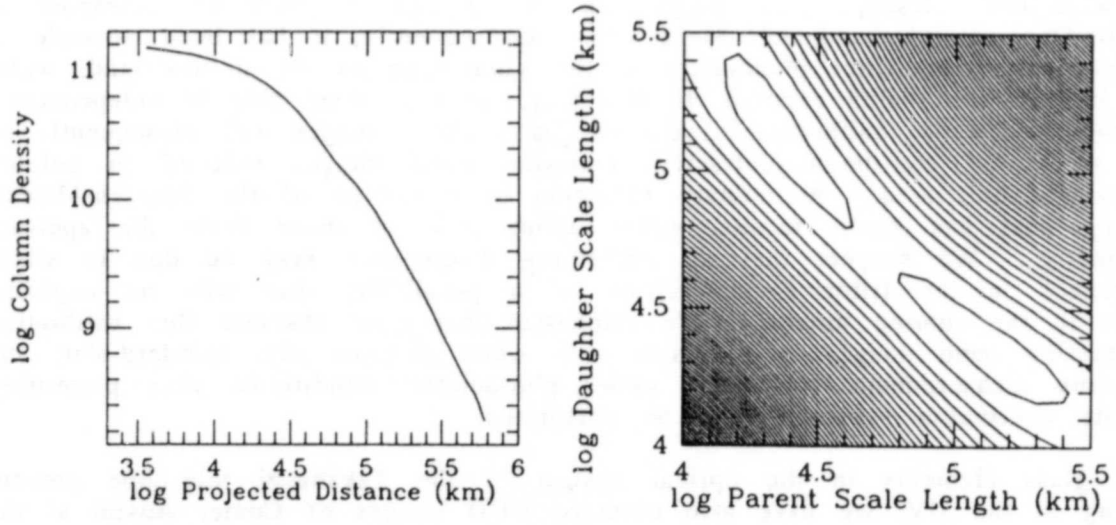

Figure 2. Radial profile of CN (left) extracted from the image shown in Figure 1 after continuum subtraction, and a contour plot of χ^2 for model fits to the radial profile as a function of assumed parent and daughter scalelengths (right). The two innermost contours are the domain of viable fits to the radial profile.

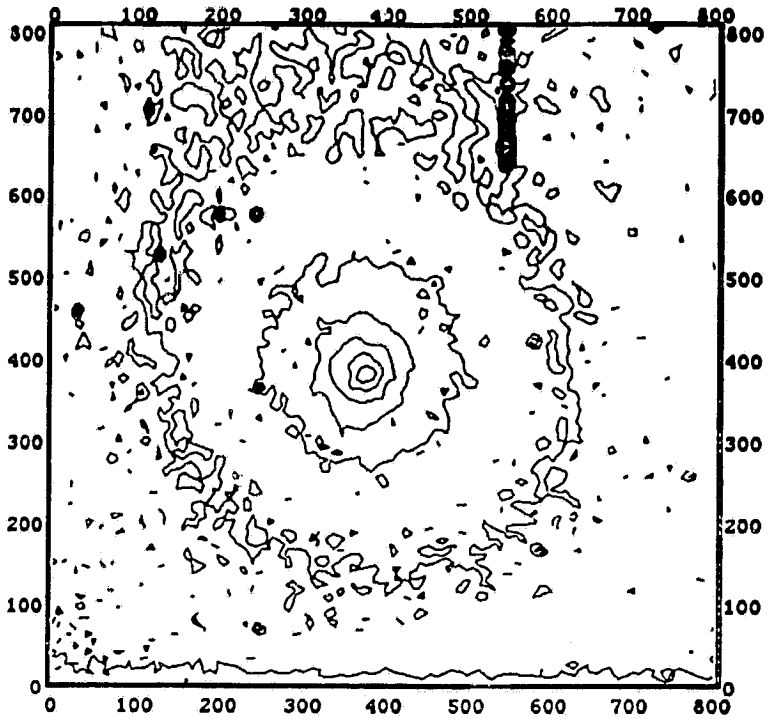

Figure 3. Contour plot of Comet Austin (1989c1) as observed in the OH molecular band (3080Å). Image scale is approximately 5 arcmin on a side.

The wide-field telescope rides piggy-back on the John S. Hall 42" telescope at Lowell Observatory's Anderson Mesa site. Consequently, it has been possible to obtain conventional filter photometry at the same time as the narrow-band, wide-field images were being exposed. In this way, we have been able to independently test the photometric calibration of the images. These images will subsequently be used to obtain continuum-subtracted, emission band images reduced to column density per unit area. Preliminary reduction of a portion of the Brorsen-Metcalf imaging data has given results within about 10% of those from the aperture photometry. We suspect that the remaining discrepancy may be due to slight differences in the filter characteristics — a possibility that will be explored further in the coming months. We emphasize that good absolute flux calibration of emission band images is attainable only when accurate sky, standard-star, and extinction measurements are made under photometric conditions, thus permitting accurate continuum subtraction to be performed.

Since glass elements in the optical system of the Takahashi telescope prevent working in the UV, we have also obtained CCD images of Comet Austin at the Cassegrain focus of the 42" telescope. These images give a measurement of the spatial distribution of the OH molecule (3080Å) in the inner coma. A sample is shown in Figure 3. These data will also be used to constrain OH model parameters.

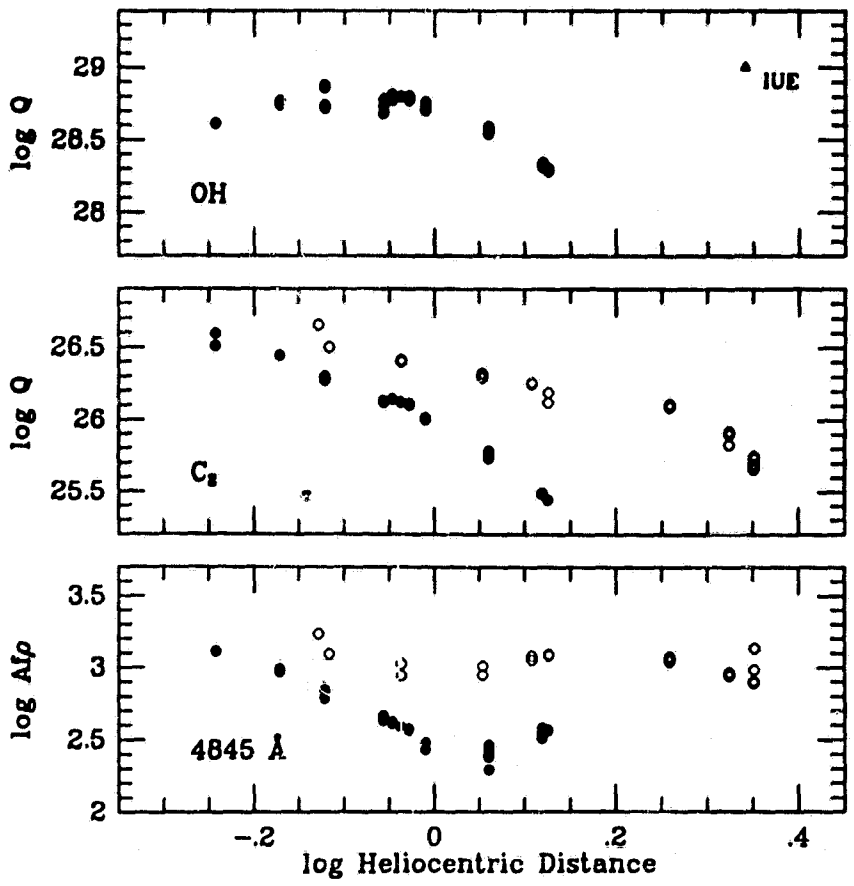

Figure 4. Production rates of Comet Austin as a function of heliocentric distance. Pre-perihelion points are shown as open circles, while post-perihelion points are shown as filled circles. Note the asymmetries about perihelion, as well as the differing behavior among the species.

The conventional aperture photometry obtained by ourselves and by Peter Birch at Perth Observatory give excellent heliocentric distance coverage of Comet Austin. These data clearly show that the initial rapid increase in brightness from December to January (which led to predictions of the "comet of the decade") slowed considerably during February and March (see Figure 4). While the production of dust by Comet Austin was essentially constant prior to perihelion (possibly tracking the OH production), our observations since late-April show the dust production dropping at a rate similar to those of all of the measured gas species except OH, which held constant for several weeks before it began to drop. The apparent minimum in the dust production near the end of the interval covered by our observations may be an aperture effect because minimum geocentric distance occurred at this time.

Comet Halley - 1910

In an unrelated development, we report the discovery by Schleicher and S. J. Bus of a 7.4 day periodicity in the brightness of Comet Halley during the comet's 1910 apparition. Although this period was previously identified in photometry obtained

during the 1986 apparition (Millis and Schleicher 1986), considerable debate has ensued as to whether this period directly reflects Halley's rotation period, or whether the nucleus is moving in a more complex manner. In fact, the initial evidence for a much shorter period of near 2.2 days emerged from the analysis of the morphology of dust jets recorded photographically during 1910 (Sekanina and Larson 1984; 1986). Reduction and analysis by Schleicher and Bus of brightness measurements of a homogeneous set of photographs taken on a nightly basis at the National Observatory of Argentina at Cordoba (Perrine *et al.* 1934) has yielded a period of approximately 7.4 days in each of the two monthly intervals covered by the 1910 data. Further, a simple phase shift of the 1910 phased lightcurve with respect to 1986 data yield a believable match in the shapes of the lightcurves. Although not conclusive due to the uncertainties in the 1910 data, this result strongly suggests that not only was a period of 7.4 days present in 1910, but that the same source regions were active. A paper discussing these results has been submitted to the Astronomical Journal.

References

Millis, R. L., and Schleicher, D. G. 1986, *Nature* **324**, 646.

Perrine, C. D., Winter, R., Symonds, F., and Glancy, A. E. 1934, ***Resultados del Observatorio Nacional Argentino. Vol. 25 -- Cometa Halley*** (Publicado per el Observatorio, Cordoba).

Sekanina, Z. and Larson, S. M. 1984, *A.J.* **89**, 1408.

Sekanina, Z. and Larson, S. M. 1986, *A.J.* **92**, 462.

OPTICAL AND NEAR-IR IMAGING OBSERVATIONS OF COMET AUSTIN 1989C1

N91-21015

J. Watanabe[1], N. Hiromoto[2], H. Takami[2], Te. Aoki[3], T. Nakamura[1], K. Takagishi[4], I. Hatsukade[4], B. Suzuki[5], H. Kurihara[6], S. Isobe[1], G. Sasaki[1], H. Agata[7], Y. Taniguchi[8], H. Sugai[3], S. Okamura[8], S. Ichikawa[1]

1:National Astronomical Observatory, Mitaka, Tokyo, 181, Japan
2:Communications Research Laboratory, Koganei, Tokyo, 184, Japan
3:Department of Astronomy, Faculty of Science, University of Tokyo, Bunkyo-ku, Tokyo, 113, Japan
4:Faculty of Engineering, Miyazaki University, Miyazaki-shi, Miyazaki, 889, Japan
5:Koshigaya High School, Koshigaya, Saitama, 343, Japan
6:Kanagawa kougyou High School, Yokohama, Kanagawa, 230, Japan
7:Sundai Gakuen High School, Ohji, Kita-ku, Tokyo, 114, Japan
8:Kiso Observatory, Institute of Astronomy, University of Tokyo, Mitake, Nagano, 397-01, Japan

ABSTRACT

Near-nucleus imaging observations of comet Austin 1989c1 were carried out by the Japanese CCD imaging team. Six telescopes were used to monitor the time variation of the near-nucleus images in C_2, CN, H_2O^+, Na, continuum in the optical region, and in J, H, K bands in the near-IR region. A featureless, round shape of the comet was revealed in all images. Although some of the jet features are recognized by using image enhancement technique, the azimuthal difference of the intensity distribution is about 10%. The images in the H_2O^+ band show complex ion structures near the nucleus.

1. INTRODUCTION

Comet Austin 1990c1 was one of the important object for cometary researches after the apparition of comet P/Halley, because of its brightness along with its good observational condition. In order to study the near-nucleus phenomena, we observed this comet with CCD imaging systems attached to six telescopes in Japan. This poster paper shows some of preliminary results in these observations.

2. OBSERVATIONS

The observations were carried out after the perihelion passage of the comet. Telescopes and CCD systems are listed in Table 1. Two observatories, C.R.L. and S.K.A.O., were engaged for imaging observations of this comet from April 20 through May 31! However, we could observe the comet only 6 nights in this period because of bad weather condition.

Near-nuceus images in the optical wavelength were taken from April 26 through May 26. We used the IHW standard filters of CN, C_2, H_2O^+ and correponding continuum bands. The R and I bands used at the K.O. and O.A.O. observatories are those in the Kron photometric system. The B and V at the K.O. are those in the Johnson system. The interference filters for Na D-lines used at the C.R.L. and T.O. are those of λ_c=589nm with $\Delta\lambda_{1/2}$ = 4nm. Near-nucleus images in the near-IR wavelength were obtained at the C.R.L. observatory on April 29, 30, May 9, 26, 27. The photometric bands are J, H, and K.

3. PRELIMINARY RESULTS

The reduction is proceeding with using an image processing software library SPIRAL(Ichikawa et al. 1987). Both the bias subtraction and the flat-field correction were applied with some relevant data, which were also taken during the observation.

Figure 1 shows a C_2 image on April 30 taken at the T.O. This image shows a featureless, round shape. However, a broad, northward jet-like structure is recognized in figure 2, which is the result of contrast enhanced image in figure 1, using the ring-masking method(Cosmovici et al. 1988). The azimuthal difference of the intensity distribution is about 10% at the distance of 2×10^4 km from the nucleus. On the next night, the position angle of this jet changed counterclockwise by 30°-40°. This gives information on the nucleus rotation(Sekanina et al. 1981). The images of CN are so poor that we can obtain the CN-jet structure(A'Hearn et al. 1986).

We are grateful to Dr. I. Konno for his arrangement of this paper presentation in the workshop.

REFERENCES

A'Hearn, M.F., Hoban, S., Birch, P.V., Bowers, C., Martin, R., and Klinlesmith III, D.A., 1986, Nature, 324, 649.

Cosmovici, C.B., Schwarz, G., Ip, W.I., and Mck, P., 1988, Nature, 332, 705.

Ichikawa, S., Okamura, S., Watanabe, M., Hamabe, M., Aoki, T., and Kodaira, K., 1987, Ann. Tokyo Astron. Obs., 2nd Ser., 21, 285.

Sekanina, Z., 1981, Ann. Rev. Earth Plant. Sci., 9, 113.

ORIGINAL PAGE IS
OF POOR QUALITY

Table I. Observing stations and instrumental data for optical wavelength

	(1) C.R.L.	(2) O.A.O.	(3) K.S.C.	(4) K.O.	(5) S.K.A.O.	(6) T.O.
Location						
Longitude	+139° 30'	+133° 36'	+131° 04'	+137° 38'	+138° 35'	+139° 53'
Latitude	+34° 42'	+34° 34'	+31° 13'	+35° 48'	+36° 27'	+34° 56'
Altitude	84 m	372 m	228 m	1130 m	1135 m	160 m
Telescope						
Aperture	150 cm	188 cm	60 cm	105 cm Schmidt	75 cm	60 cm
Focus	Nasmyth	Newtonian	Prime	Prime	Nasmyth	Newtonian
F number	18 reduced	4.9	4.5	3.0	12.0	4.7
CCD Detector	GEC P8603	RCA SID503EX	Sony ICX018CL	T: TC-215	Sony ICX018CL	Sony ICX018CL
Pix. number	576× 385	1024× 612	510× 492	1024× 1024	510× 492	510× 492
Pix. size(μm)	22× 22	15× 15	17× 13	12× 12	17× 13	17× 13
Imaging area	6'× 4'	5.8'× 3.6'	11.2'× 8.4'	12'.5× 12'.7	3.4'× 2.5'	10.7'× 8.0'
Imaging Bands	Na H_2O^+ Cont., IR	R	C_2 C_2 Cont.	B,V,R,I H_2O^+, H_2O^+ Cont.	C_2	H_2O^+, CN, Na C_2, C_2 Cont.

Names of Observing Stations
(1) Koganei Station, Communications Research Laboratory
(2) Okayama Astrophysical Observatory, National Astronomical Observatory
(3) Kagoshima Space Center, Institute of Space and Aeronautical Sciences
(4) Kiso Observatory, Institute of astronomy, University of Tokyo
(5) Sundai Gakuen Kitakaruizawa Observatory, Sundai Gakuen High School
(6) Tateyama Observatory

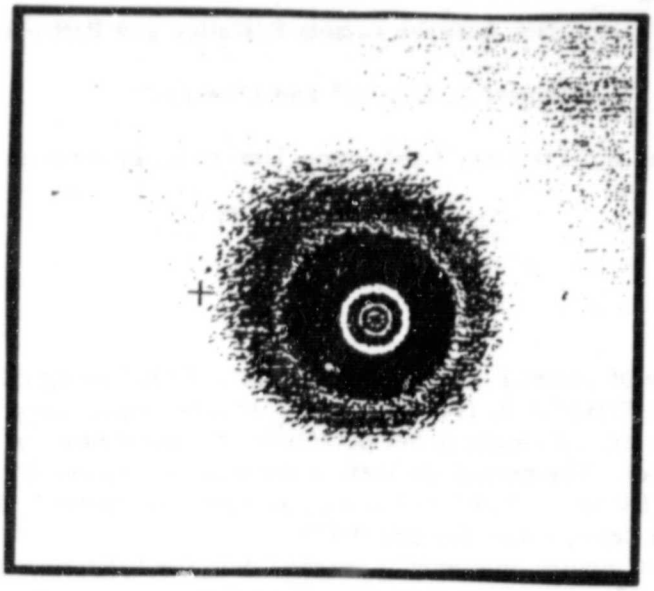

Figure 1
Comet Austin in C_2 band taken with the 60cm telescope at T.O. on April 30.77UT. North is left, and west is top. Field of view is 10.7'× 8.0'.

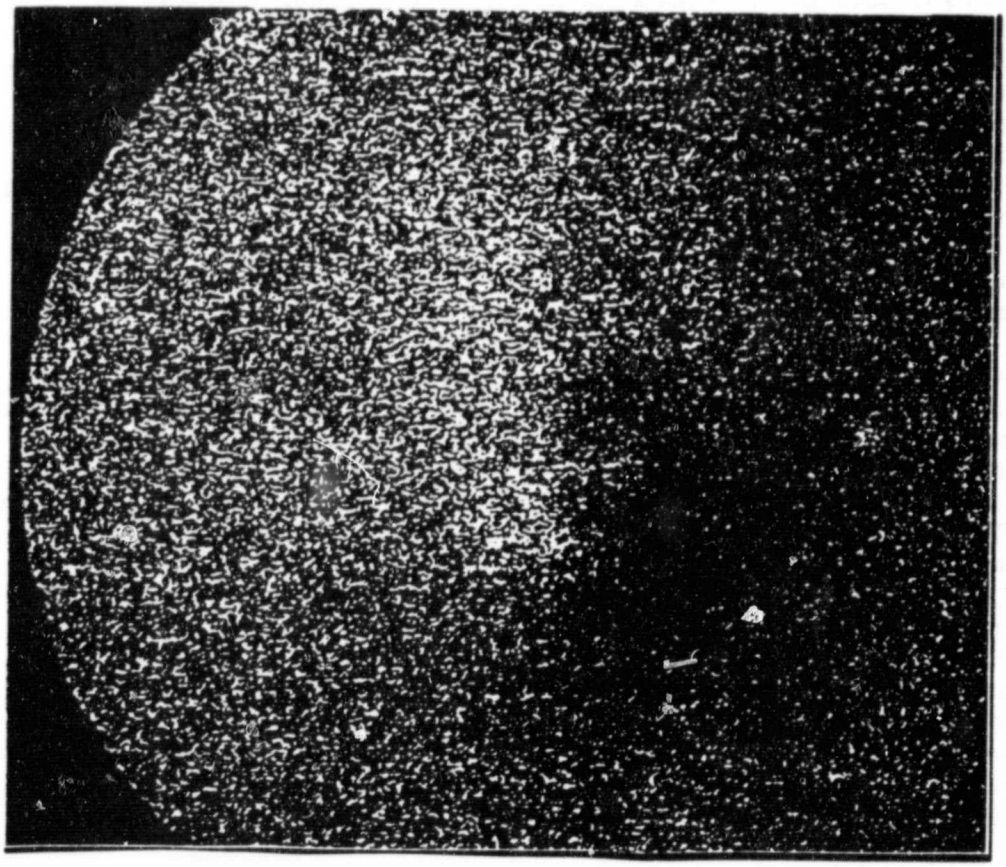

Figure 2
Processed image of figure 1. A broad, northward jet-like structure is shown.

ORIGINAL PAGE IS
OF POOR QUALITY

N91-21016
54-90
320510
P.4

A composition comparison between comets P/Halley and P/Brorsen-Metcalf

Michael A. DiSanti* and Uwe Fink

Lunar and Planetary Laboratory, University of Arizona

Tucson, Arizona 85721

The appearance of comet P/Brorsen-Metcalf in 1989 following only a few years on the heels of comet P/Halley in 1986 gave us an unusual opportunity to compare two comets of similar orbital elements but potentially different physical and chemical characteristics. The period, perihelion distance and eccentricity for comet P/Halley are 76.0 years, 0.587 AU and 0.967 while for comet P/Brorsen-Metcalf they are 70.6 years, 0.479 AU and 0.972.

We were able to acquire photometric spectral data for P/Brorsen-Metcalf on two dates: 1989 July 13 and 1989 August 02. The observations were carried out with the 154 cm Catalina Telescope of the University of Arizona Observatories. The instrumentation consisted of our wide field CCD camera with reducing optics and a fast spectrograph covering 5200 - 10400 Å, at a dispersion of 7.21 Å/pixel and a slit length of 200" at a spatial scale of 1.49"/pixel. Both the camera and spectrograph used an 800 x 800 Texas Instrument chip. Because of the reduced brightness of comet P/Brorsen-Metcalf we opened the slit to 5.0" compared to the 2.5" used throughout the comet P/Halley observations. This increased the acquired signal considerably while affecting the spectral resolution in only a minor way.

The spectrum for 1989 July 13 is compared to a P/Halley spectrum in Fig. 1. The general appearance of the spectra is very similar, both comets showing emissions due to C_2, NH_2, OI (^{1}D) and CN. Neither displays any emission features that are exclusive to only one of the two. The most notable difference between the two comets is the much lower continuum level of P/Brorsen-Metcalf as compared to P/Halley. Besides the differences in continuum, the spectra also show considerably weaker NH_2 emission for comet P/Brorsen-Metcalf as well as weaker CN emission and somewhat weaker C_2 emission when compared to the OI ^{1}D 6300 Å emission line.

Since water is now reasonably well established as the major driving force in the activity of a comet, we calculate the H_2O production rate for comet P/Brorsen-Metcalf in Table 1. We followed the same procedure recently applied to comet P/Halley (Fink and DiSanti 1990) and therefore do not repeat a discussion of our data reduction. The resulting water production rate for comet P/Brorsen-Metcalf is 16% of P/Halley at r=1.36 AU and 20% of P/Halley at r=1.01 AU (Table 1). Both measurements refer to pre-perihelion dates. The P/Halley water production rate in Table 2 is obtained from the relationship $Q(H_2O)=4.36 \times 10^{29} r^{-2.54}$ as derived in Fink and DiSanti (1990). For completeness we list the continuum flux, in Table 1, for the same aperture used for the water production rate. However, to effect a comparison in continuum fluxes, we turn to the values in Table 2 which used common apertures for both the P/Halley and P/Brorsen-Metcalf reductions. While for P/Halley the ratio of the continuum to OI flux is $-0.18 Å^{-1}$ for P/Brorsen-Metcalf it is $-0.0085 Å^{-1}$. Thus P/Brorsen-Metcalf exhibits only about 1/20 of the continuum of P/Halley when both are compared to their respective H_2O production rates.

We next present the relative ratios between the production rates of the various species which can be obtained from our data. The dilution factor correcting the measured intensity to the total flux emitted into 4 steradians is the same for all species of a given comet. Secondly for comets observed at the same heliocentric distance the scale lengths are identical and the correction factors from the finite observing apertures to an infinite observing radius are the same, provided the radii of the observing aperture (i.e. slit lengths for us) are chosen to be the same. To meet this criterion, we picked common apertures of 31 000 km for the observation pair P/Brorsen-Metcalf 1989 July 13 and P/Halley 1985 Dec. 08/09 and 43 000 km for the pair 1989 Aug. 02 and 1986 Jan. 10 (Table 2). For the first pair we were fortunate that both objects were at the same heliocentric distance r=1.36 AU. For the second P/Brorsen-Metcalf observation we interpolated our P/Halley data for 1985 Dec. 08/09 (r=1.36 AU) and 1986 Jan. 10 (r=0.87 AU) to the heliocentric distance of 1.01 AU.

Our results are summarized in Table 2. All species are compared to the H_2O production rate of the two comets. We set P/Halley = 100% for each flux ratio which we argued above is equal to their production rate ratios. The largest difference between the two comets occurs for their relative NH_2 production. For both observation dates P/Brorsen-Metcalf exhibits about one third the production rate ratio of comet P/Halley. The parent of NH_2 is thus definitely less abundant in P/Brorsen-Metcalf. While comet P/Brorsen-Metcalf is the first comet for which we have carried out such a comparison quantitatively, visual inspection of our other comet spectra (e.g. Johnson, Fink, and Larson 1984) shows similar variability for the NH_2 emissions. C_2 (at 80%) seems to be only slightly lower at r=1.36 AU but considerably lower at r=1.01 AU (40%). Cyanogen is down a factor of two but participates slightly in the above trend being 65% at r=1.36 AU and only 48% at r=1.01 AU.

The results presented in Table 2 give indications that C_2 originates from an extended source of dust particles or small polymers in addition to parent molecules. The lower production rates of C_2 and CN in P/Brorsen-Metcalf correlate well with both the lower dust production and their smaller increase as the comet approaches the sun. While the trend is there, we nevertheless note that the comparative dust production for P/Halley is down by a factor of twenty, but the production of C_2 and CN is only slightly off.

Even without a model, our spectroscopic observations of P/Brorsen-Metcalf allowed us to draw significant compositional conclusions. The NH_2 abundance is lower by about a factor of three which appears to be independent of heliocentric distance. Both C_2 and CN are less abundant in P/Brorsen-Metcalf than in P/Halley and do not seem to participate as much in the strong increase as the comet approaches the sun. The lower H_2O production rate implies that the active surface area of comet P/Brorsen-Metcalf is much smaller, or equivalently the comet as a whole is smaller. The substantially lower continuum level for P/Brorsen-Metcalf cannot readily be explained by smaller or larger active surface area, and must be intrinsic to the comet's embedded dust-to-ice ratio, or to an overall smaller-sized dust grain population in P/Brorsen-Metcalf.

References

Fink, U., and M.A. DiSanti 1990. *Astrophys. Journ.*, **364** (in press).

Johnson, J.R., U. Fink, and S.M. Larson 1984. *Icarus*, **60**, 351-372.

Table 1. H_2O production rate and continuum flux for P/Halley and P/Brorsen-Metcalf

	Halley	Brorsen-Metcalf	Halley	Brorsen-Metcalf
Date	85 Dec 08/09	89 Jul 13	85 Dec/86 Jan	89 Aug 02
Heliocentric distance (AU)	1.36	1.36	1.01	1.01
Aperture size (arc-sec)	151 x 2.5	151 x 5.0	151 x 2.5	151 x 5.0
(km)	77800 x 1300	97200 x 3200	140000 x 2400	71000 x 2400
6300 Å				
OI Flux (photons/s m^2)	1760 [1]	490	4000 [2]	2600
6250 Å				
Cont. Flux (photons/s m^2 Å)	270 [1]	6.4	820 [2]	32
Luminosity OI[3] (s^{-1})	12.5×10^{27}	2.0×10^{27}	26.6×10^{27}	5.4×10^{27}
H_2O Prod. Rate [3,4] (s^{-1})	20.0×10^{28}	3.17×10^{28}	42.5×10^{28}	8.60×10^{28}
$Q(H_2O)$ Halley=100%	100%	16%	100%	20%

Notes:
1. Average from Halley observations Dec 08 and 09 (Fink and DiSanti 1990).
2. Interpolated between our Halley 85 Dec 08/09 observations (r = 1.36) and our 86 Jan 10/11 observations (r = 0.86).
3. 6300 Å OI luminosity and H_2O production rate are independent of aperture used since they have been determined via a model.
4. For the production rate of Halley we used the relationship $Q(H_2O) = 4.36 \times 10^{29} r^{-2.54}$ (Fink and DiSanti 1990).

Table 2. Comparison of emission fluxes between P/Halley and P/Brorsen-Metcalf

		Halley [1]	Brorsen-Metcalf	Halley [2]	Brorsen-Metcalf
Date		85 Dec 08/09	89 Jul 13	85 Dec/86 Jan	89 Aug 02
Heliocentric distance (AU)		1.36	1.36	1.01	1.01
Aperture size (km)		31000 x 1300	31000 x 3200	43000 x 2400	43000 x 2400
6300 Å					
OI Flux (photons/s m^2)		1450	380	3800	2430
6250 Å					
Cont. Flux (photons/sm^2 Å)		230	3.2	770	20
F(continuum/OI) ($Å^{-1}$)		0.16	0.0085	0.20	0.0085
		100%	5.3%	100%	4.2%
$F(C_2/OI)$	v=-1	100%	80%	100%	42%
$F(NH_2/OI)$	0,10,0	100%	34%	100%	29%
	0,8,0	100%	32%	100%	32%
	0,6,0	100%	40%	100%	36%
	Avg.	100%	36%	100%	32%
F(CN/OI)	2-0	100%	55%	100%	47%
	1-0	100%	73%	100%	50%
	Avg.	100%	65%	100%	48%

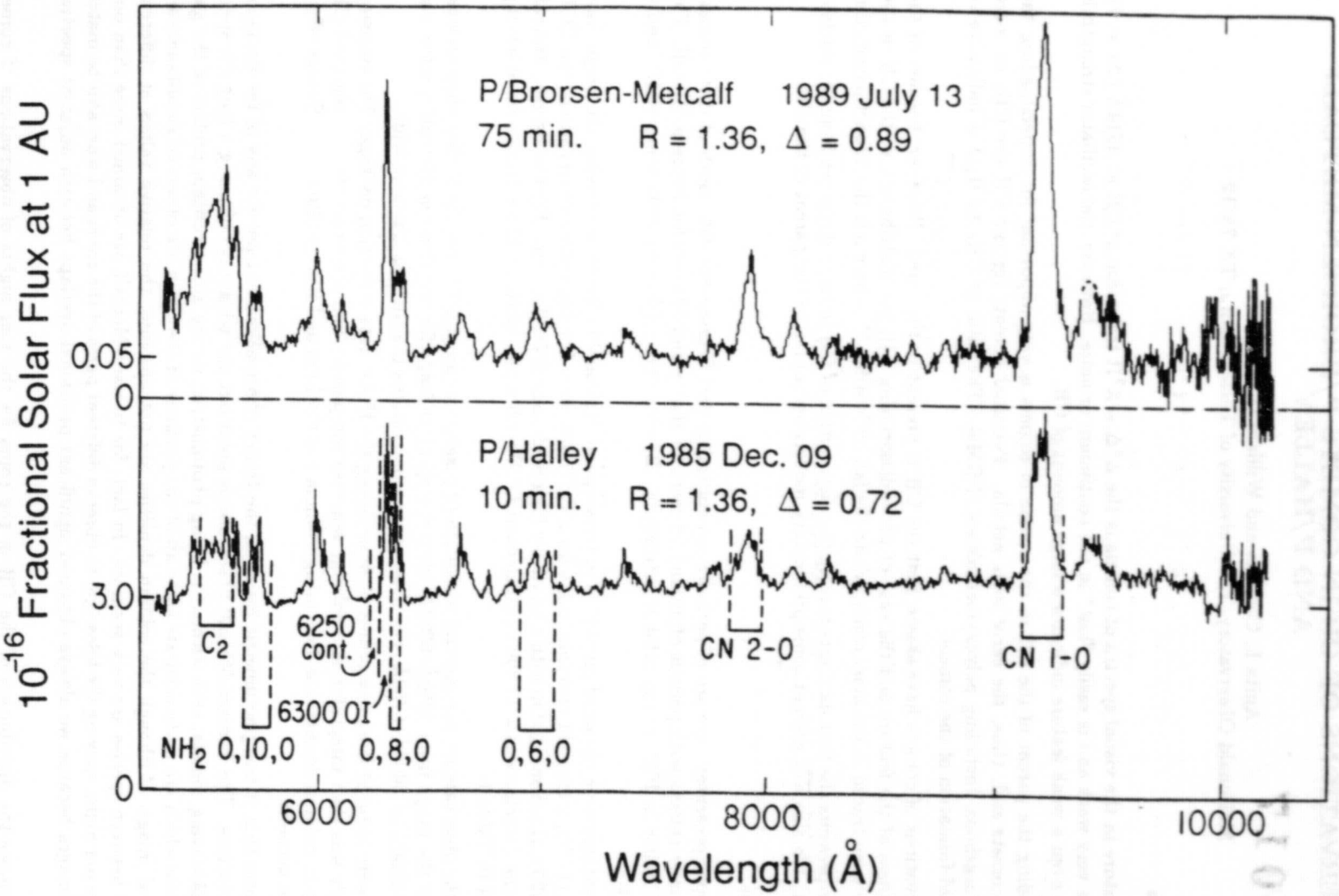

Fig. 1 Comparison between spectra of P/Brorsen-Metcalf observed in 1989 and those of P/Halley obtained during its 1985/86 apparition. Both spectra are divided by solar analogue stars and are integrated over a common 31000 km long window along the slit. Absolute flux levels are given at the side. The regions of spectral integration for the emission bands of C_2, OI, NH_2 and CN are marked.

55-90
32611
N91-21017

OBSERVATIONS OF CH IN COMETS P/BRORSEN-METCALF AND P/HALLEY

Anita L. Cochran and William D. Cochran
McDonald Observatory, The University of Texas, Austin, TX 78712

Introduction

A common feature in the visual spectra of comets is the $A^2\Delta - X^2\Pi$ transition of CH at 4314Å ($\Delta v = 0$). This feature is very weak and is easily "lost" in the continuum or noise. However, the oscillator strength is very small, so even a weak feature indicates a large amount of CH.

Understanding the parent of the CH in the comae of comets is very important for understanding the chemistry of comets and, thus, the early solar nebula. Potential parents for the CH are CH_4 or more complex hydrocarbons, including polyoxymethalenes (POMs). The ratio of CH_4 to H_2O is indicative of possible sites of formation of the comets.

Past observations of comets have shown that the CH is present in the coma. However, because of the intrinsic weakness of the feature and the ease of photodissociating CH, the distribution of the CH in the coma has only been traced in the inner coma, where the fall-off is still ρ^{-1}, where ρ is the impact parameter.

This paper presents the first data sets tracing the distribution of CH to large distances from the nucleus in two comets. We also will present some preliminary models pertaining to the parent of the CH.

Observations

The observations presented here are of periodic comets Halley and Brorsen-Metcalf. Both of these comets are Jupiter family comets with periods of around 76 years for Halley and 70 years for Brorsen-Metcalf. The inclination of Halley is 162° so the orbit is retrograde. Brorsen-Metcalf has an inclination of 19° and a prograde orbit.

The observations were obtained on the 2.7 m telescope at McDonald Observatory using the Large Cass Spectrograph (LCS), a long slit spectrograph with a CCD detector. For the Halley observations, the CCD was an RCA 320 × 512 element chip with a relatively high read-noise of 50 electrons. For the Brorsen-Metcalf observations, the detector was a TI 800 × 800 element CCD with a read-noise of 12 electrons. An observing log is included in Table 1.

For all of the observations, the spectral resolution (2 pixels) was around 7Å. For the Halley observations, the data cover the range from 3650Å–6800Å while the spectral range for the Brorsen-Metcalf spectra was either 3200Å–5950Å or 3000Å–5750Å. For most of the observations the slit was 2 arcsecs wide.

The data were reduced from raw counts to fluxes using the IRAF data reduction package. The emission from the bands was then integrated and column densities computed. The conversion from integrated CH band intensity to column density was done using formula 1 of Cochran and Barker (1985). No Swings effect was taken into account.

Table 1 notes that it was photometric for all of the Halley observations but not for any of the Brorsen-Metcalf observations. The Brorsen-Metcalf observations point out the advantage of using a long slit spectrograph for observing comets; even without it being photometric, we are able to obtain profiles of the gas within the coma which are quite accurate since all of the portions of the coma are observed simultaneously in one spectral image. Although the column densities are not absolute, the relative values at different positions and between species are very accurate. In fact, for Brorsen-Metcalf, we obtained more than one spectral image per night, moving the telescope to observe different parts of the coma and were able to match the spectral images because we always obtained significant positional overlaps between adjacent spectral images.

Figure 1 shows the distribution of the CH in the coma for the four nights of observations of comet Brorsen-Metcalf. The lack of scatter in the data gives a good indication that the errors are quite low. In most cases the CH information extends to 30,000 km. Figure 2 shows two representative nights of the Halley data (the data on the left hand and right hand panels is identical and the difference between the panels

Table 1: Observing Log

Comet	Date	R_h	Δ	Photometric?
Halley	9 Dec 85	1.36	0.72	y
	20 Mar 86	0.99	0.81	y
	21 Mar 86	1.01	0.79	y
	22 Mar 86	1.02	0.76	y
	23 Mar 86	1.04	0.74	y
	24 Mar 86	1.05	0.71	y
	10 Apr 86	1.32	0.42	y
	2 May 86	1.63	0.80	y
	9 May 86	1.75	1.05	y
	10 May 86	1.77	1.08	y
Brorsen-Metcalf	16 Jul 89	1.31	0.85	n
	1 Aug 89	1.04	0.65	n
	9 Aug 89	0.91	0.62	n
	11 Aug 89	0.87	0.63	n

will be explained in the next section). These two nights were chosen because they represent two extremes in heliocentric distance. The Halley data show much more scatter than the Brorsen-Metcalf data. There are two reasons for this: 1) Halley has a much higher dust/gas ratio than Brorsen-Metcalf so continuum subtraction introduces a much higher error; 2) The Brorsen-Metcalf data were obtained with the much lower noise TI chip.

Models

The lifetime of CH against photodissociation is very short, ~100 sec at 1 AU (Allen *et al*, 1989), because the threshold for photodissociation of CH is at 3500Å. Thus, wherever one observes the CH in the coma, the direct parent must be very near. We have assumed that the direct parent of CH must be CH_2. The photodissociative lifetime of CH_2 is 8.33×10^3 sec at 1 AU (Allen *et al*, 1989). If we further assume that CH_4 is the direct parent of CH_2 (the possibly logical daughter of CH_4, CH_3, is not seen in the lab), the photodissociative lifetime of CH_4 at 1 AU is 1.35×10^5 sec (Allen *et al*, 1987). We can derive scale lengths from these lifetimes if we assume some sort of velocity law. For this work we have assumed the velocity law of Delsemme (1982). Utilizing these derived scale lengths, we have fit Haser models to the data. These Haser models predict the distribution of the CH_2 but, as explained above, the CH_2 should be very near (~100 km) the CH, so the models also predict the distribution of the CH gas which we can then compare to the data.

Figure 1 shows the comparison of the models and the data. The fits are excellent. Note that the only assumptions we have made are a velocity law and the reaction pathway. The lifetimes are from straight physics. Thus, for Brorsen-Metcalf, the reaction pathway is plausible (but not necessarily unique). As has been often noted, the Haser model lacks for physical insight, but can empirically describe data well. This is certainly the case for CH. However, we also ran models of the physically more realistic Vectorial model (Festou, 1981). These models are almost indistinguishable from the Haser model. The only significant deviations between the models occur for data points where the optocenter is within the spatial bin, probably due to how the integration is handled by the two codes. This is a region which also suffers errors due to guiding and seeing effects.

We then tried to fit Haser models to all of the Halley data sets (not just the two shown) using the parameters discussed above. These fits were significantly and consistently worse than the Brorsen-Metcalf fits, with the greatest problem seen in the inner coma. In the left hand panels of figure 2, note that the models over-predict the CH in the inner coma. However, the Delsemme velocity law predicts that the outflow velocity should have been 0.61 km/sec at the time of the spacecraft encounter. The Giotto spacecraft measured a velocity of 0.9 km/sec (Krankowsky *et al*, 1986). If one assumes that the scaling of

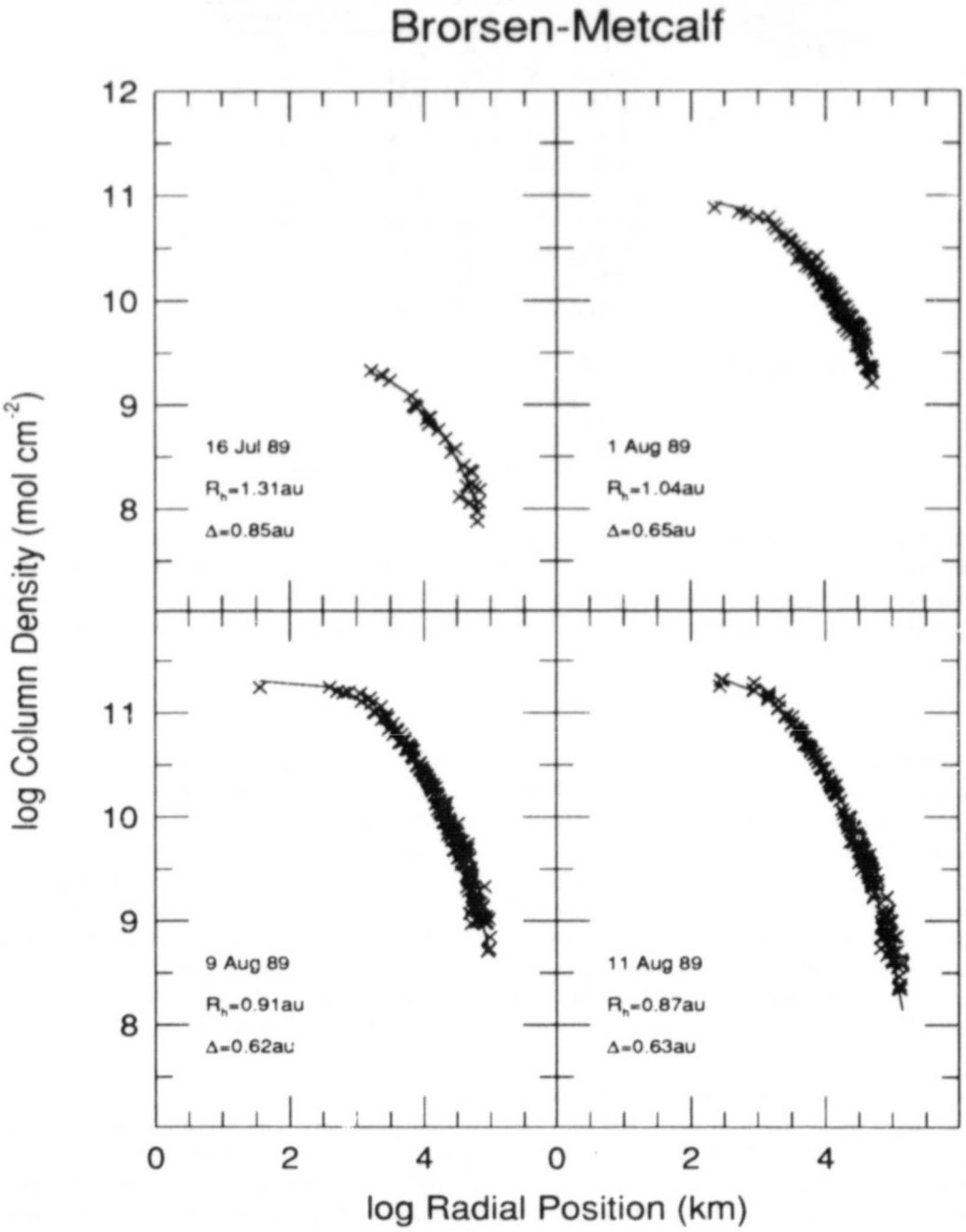

Figure 1: The distribution of CII gas for the 4 nights of observations of Brorsen-Metcalf. The Xs represent the data. The small scatter band indicates the high quality of the data. The line is the model described in the section on models.

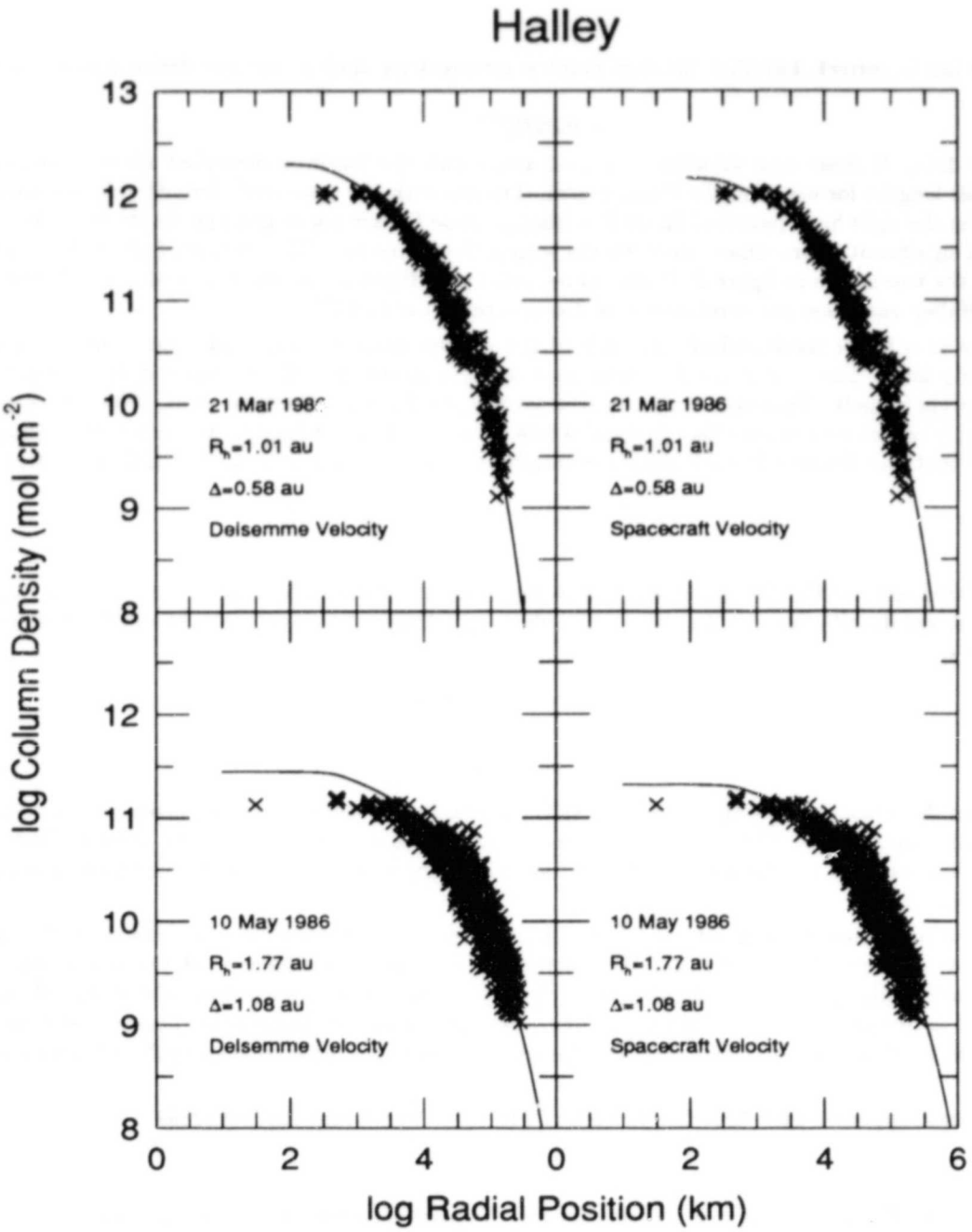

Figure 2: The distribution of the CH gas for 2 representative nights (smallest and largest heliocentric distance) of comet Halley. The Xs represent the data. The data in the left hand and right hand panels are identical. The line represents the models described in the text: The left hand panels utilizes the Delsemme velocity law while the right hand panels utilizes a law tied to the spacecraft velocity.

the Delsemme law is correct, but that the zero point is incorrect for Halley, one can derive a new scaling law of

$$v = 0.85 R_h^{-0.5}$$

for the Halley data. If these new velocities are used along with the lifetimes described above, when can derive new scale lengths for use with the Haser model. The fits with the spacecraft derived velocity scaling law are shown in the right hand panels of figure 2. Although these fits are not as good as the Brorsen-Metcalf fits, they are a significant improvement over the fits with a Delsemme law. This is true of all of the nights' data, not just the two shown in figure 2. It should be noted that there are actually several derived outflow velocities for Halley and these are summarized in Lammerzahl *et al* (1987).

Thus, there is a Haser model which fits each of the comets using the same lifetimes, but assuming different velocity laws. This is not the first time that we have noted that Halley has a different outflow velocity than other comets. This appears to be true for fits of NH_2 also (Cochran *et al*, 1989). However, Halley is the only comet we have studied in detail which does not fit the Delsemme velocity law. It should be noted here that the Brorsen-Metcalf data are totally incompatible with the higher Halley spacecraft velocities.

Conclusions

We have presented some of the first profiles of CH in the coma of a comet which are traced to large radial positions. These gas distribution profiles can be fit well using a Haser or Vectorial model and the following reaction pathway:

$$\begin{aligned} CH_4 + h\nu &\rightarrow CH_2 + H_2 \\ CH_2 + h\nu &\rightarrow CH + H \\ CH + h\nu &\rightarrow C + H \end{aligned}$$

The lifetimes for these reactions are the same for both comets and are given in the previous section. However, the velocities used to convert the lifetimes to scale lengths are different for the two comets: Brorsen-Metcalf velocities are derived from the Delsemme velocity law while Halley velocities are derived from a scaled spacecraft velocity.

Although the Haser model has no physical basis, it does a good job of describing the data with the scale lengths which we derived. This shows that the reaction pathway which we have employed is a plausible, but not necessarily unique, reaction pathway. We cannot rule out more complex hydrocarbons, although we do not need to invoke them either. More complex reaction pathways or parents are possible, as long as the scale lengths for these more complex reactions are comparable to the scale lengths for the CH_4 pathway given above.

This work was supported by NASA Grant NAGW 1477 and NSF Grant AST-8912869.

References

Allen, M., Bochner, B., van Dishoeck, E., Tegler, S., and Wyckoff, S., 1989, *Bull. AAS*, **21**, 934.

Allen, M., Delitsky, M., Huntress, W., Yung, Y., Ip, W., Schwenn, R., Rosenbauer, H., Shelley, E., Balsinger, H., and Geiss, J., 1987, *Astr. and Ap.*, **187**, 502.

Cochran, A. L. and Barker, E. S., 1985, *Icarus*, **62**, 72.

Cochran, A. L., Barker, E. S., and Cochran, W. D., 1989, *Bull. AAS*, **21**, 939.

Delsemme, A. H., 1982, in *Comets*, ed. L. L. Wilkening, p. 85, (Tucson, AZ: University of Arizona Press).

Festou, M. C., 1981, *Astr. and Ap.*, **95**, 69.

Krankowsky, D., Lammerzahl, P., Herrwerth, I., Woweries, J., Eberhardt, P., Dolder, U., Herrmann, U., Schulte, W., Berthelier, J. J., Illiano, J. M., Hodges, R. R., and Hoffman, J. H., 1986, *Nature*, **321**, 326.

Lammerzahl, P., Krankowsky, D., Hodges, R. R., Stubbemann, U., Woweries, J., Herrwerth, I., Berthelier, J. J., Illiano, J. M., Eberhardt, P., Dolder, U., Schulte, W., and Hoffman, J. H., 1987, *Astr. and Ap.*, **187**, 169.

Patrick Palmer
It was interesting that the Delsemme velocity law fits comet Brorsen-Metcalf, but the constant multiplier had to be changed by $\sim 50\%$ for Comet Halley to agree with spacecraft instruments and to make your data fit for P/Halley. Could you give an estimate for the error in mulitplier of this velocity law, as found by your measurements of Comet Brorsen-Metcalf?

Anita Cochran
In the past, we have found the Delsemme velocity law to hold for most comets and have found other species which point to the higher spacecraft velocity for Halley. The spacecraft velocities are 1.47 times higher than the Delsemme law. Our Brorsen-Metcalf data set is so clean one can easily rule out Halley-like velocities for Brorsen-Metcalf. I haven't tried putting a number to it, but I would imagine that one can say that Brorsen-Metcalf follows the Delsemme velocity law to about 10%. Of course, that assumes we have the lifetimes correct!

Susan Wyckoff
Ferro has also modeled the CH_4 photolysis. A comparison of a very preliminary version of his model with our observed P/Halley CH profile using van Dishoeck's photodissociation lifetimes does not indicate close agreement. Perhaps the difference in our results reflects the difference in the photodissociation lifetimes that we used in modeling the CH profiles.
This work is in progress.

Anita Cochran
We did a quick comparison of Ferro's model to our data during the coffee break and his model deviates from our data about the same way as it deviates from your data. An eyeball comparison of the data sets show them to compare favorably (except where yours turn back up - something which is non-physical). Clearly, we will have to check your scale lengths against our model more formally and you will have to check your model carefully.

Lewis Snyder
How do we reconcile the CO, H_2CO and CN extent of 1.5×10^4 km found for Comet Halley with the opacity radius on Comet Brorsen-Metcalf?

Anita Cochran
We do not see any conflict. First of all, Brorsen-Metcalf has an extremely high gas-to-dust ratio. Secondly, the spacecraft were able to image the nucleus of Comet Halley, even at 1300 km. The phenomena you talk about with molecules such as CO is not optical depth but is an extended source.

56-90
21014

AMMONIA AND NITROGEN ABUNDANCES IN COMETS

N91-21018

Susan Wyckoff
Department of Physics and Astronomy
Arizona State University

Introduction

Comets consist of pristine material preserved from an earlier galactic epoch. Determination of the molecular, elemental and isotopic abundances in the dust and volatile components of comet nuclei provide vital clues to the chemical evolution of both interstellar and solar nebula matter. Here the abundances of nitrogen-containing molecules in comets are considered. The molecular abundances of NH_3 in four comets are summarized (Tegler 1990, Wyckoff, Tegler and Engel 1990). From an inventory of nitrogen-containing compounds (Wyckoff, Engel and Tegler 1990, Wyckoff, Engel, Womack, Ferro, Tegler and Peterson 1990), an estimate of the elemental N abundance is also presented.

Ammonia Abundance

The hypothesis that NH_3 photolysis can account entirely for the NH_2 and NH observed in comets Halley and Thiele is tested by calculating the spatial distributions of NH and NH_2 assuming an NH_3 photolysis model,

$$NH_3 \rightarrow NH_2 \rightarrow NH \rightarrow N$$
$$\searrow \quad \nearrow$$
$$NH$$

In this photodissociation sequence, NH_3 is the only source of both NH and NH_2. The branching ratio into the NH_2 sequence is 97%, while direct photodissociation into NH occurs 3% of the time. A multi-generational Monte Carlo model (Ferro 1990) used to compute the NH distribution for comet Halley is compared with observations in Figure 1. In Figure 2 we present the NH_2 profile observed in comet Halley together with the profile computed using the vectorial model (Festou 1981). As input parameters to the models we have used photodissociation lifetimes calculated using the Solar Maximum Explorer satellite EUV flux for the dates of observation. In the vectorial model we have assumed an NH_3 outflow velocity of 0.8 km/s and that for NH_2 of 1.2 km/s. In the Monte Carlo model the velocities were calculated explicitly assuming conservation of momentum and energy. We assumed that 10% of the residual photon energy upon photodissociation of a molecule is transformed into internal energy, and 90% is converted into kinetic energy of the photodissociation products, following Tegler(1990). The fits of the models shown

in Figures 1 and 2 correspond to equal production rates of NH_3, namely $Q(NH_3)= 3.0 \times 10^{26}$ s^{-1}. We not only find that the *shapes* of the NH and NH_2 spatial profiles are well-predicted with the NH_3 photolysis model, but we also find that the *absolute scaling* of the column densities of both NH and NH_2 is consistent with a common source, namely, NH_3. Therefore the NH_3 photolysis model is self-consistent and provides strong evidence that both NH and NH_3 are the predominant photodissociation products of NH_3.

The agreement in the productions rates, $Q(NH_3) \sim Q(NH_2) \sim Q(NH)$ not only indicates that the NH_3 photolysis model adequately explains the NH and NH_2 observations of comet Halley, but also puts the ammonia abundances derived from the optical spectra on a very firm basis. The quality of the model fits to the data also indicates that no other species (*e. g.* hydrazine, N_2H_4) contribute significantly to the observed profiles, as Tegler (1990) has previously also demonstrated.

An analysis of four comets (Thiele, Halley, Hartley-Good and Borrelly) yields an average ammonia abundance, NH_3/H_2O =0.0013 (Wyckoff, Engel and Tegler 1990). In addition Tegler (1990) has found that the post-perihelion ammonia abundance agrees within a factor $\sim$2 with the pre-perihelion value. From this we conclude that the ammonia abundances in this small sample of dynamically heterogeneous comets is remarkably uniform, and that comet Halley is chemically homogeneous, at least on a scale of $\sim$6 meters which was the pre- to post- perihelion erosion depth (Keller *et al.* 1987, Tegler 1990).

Inventory of Elemental Nitrogen

An inventory of nitrogen-containing compounds in comet Halley has been compiled (Wyckoff, Tegler and Engel 1990). We find that NH_3 and CN are the predominant gas carriers of N, and that N_2 is a very minor source of the elemental nitrogen in the gas coma of this comet. Using the analysis of the comet Halley dust by Jessberger and Kissel (1990), we find that $\sim$95% of the nitrogen is partitioned into the dust grains in comet Halley and only $\sim$5% of the nitrogen is observed in the gas. Some nitrogen could be hidden from detection in large molecules such as cyanide polymers (Matthews and Ludicky 1986). In fact a weak feature detected in the spectrum of comet Halley at 4.45 μm has been attributed to a -C$\equiv$N stretch transition (Encrenaz and Knacke 1990). Estimates have been made that $\lesssim$10% of coma material is hidden in undetected grains or large molecules (*e. g.* Ip *et al.* 1990, Encrenaz and Knacke 1990). Thus even if all of the hidden(unobserved) material were in such nitrogen compounds, estimates of the amount of material unaccounted for in our inventory indicate that the large depletion of elemental nitrogen found for comet Halley would be virtually unchanged.

The elemental abundances in comet Halley, including the nitrogen abundance determined from our analysis (Wyckoff, Tegler and Engel 1990) are shown in Figure 3. As the figure indicates the nitrogen abundance in the gas component of the coma is $\sim$1/40 $N_\odot$,

and the elemental nitrogen abundance in the combined gas + dust components of the coma of comet Halley is depleted relative to the sun, N(gas + dust) $\sim$1/10 $N_\odot$. Here we have assumed a dust/gas mass ratio of two. The elemental abundances in the dust component were taken from Jessberger and Kissel (1990), and the abundances of light elements other than N were taken from Encrenaz and Knacke (1990) and Wegmann *et al.* (1987). The abundances in Figure 3 have error bars corresponding to factors of two. Analyses of the Giotto data have previously indicated deficiencies, although smaller, in the elemental nitrogen abundance in comet Halley (Geiss 1987, Encrenaz, d'Hendecourt and Puget 1988, Ip *et al.* 1990). These previous analyses adopted NH_3/H_2O $\sim$0.01-0.02, which is a factor $\sim$5-10 larger than used here, which accounts for the difference between this and previous N inventories in comet Halley. An estimate of the N_2 abundance in comet Halley confirms that it is a minor species with, $N_2 \sim 1/10$ NH_3 (Wyckoff, Tegler and Engel 1990).

A likely explanation for the nitrogen depletion in the comet is that a large amount of N_2 was excluded from the condensation process in the solar nebula. While N_2 can be incorporated into a clathrate hydrate, the process is very inefficient compared to enclathration of CO and CH_4. Thus N_2 would not have competed effectively with CO and CH_4 for the H_2O clathrate cage sites in the comet forming environment. Therefore unless temperatures in the comet-forming region were $\lesssim$20 K, N_2 is expected to have condensed into comet nuclei very inefficiently. In this scenario, an N_2-rich gaseous residue would have accumulated in the solar nebula as condensation and coagulation of cometesimals proceeded. Photodissociation, photoionization of the N_2 gas and subsequent expulsion from the solar system by radiation pressure, solar wind or other processes would have cleared the excess gas from the proto-solar accretion disk, leaving the comet nucleus depleted in elemental N. If on the other hand, the comet formed in temperatures $\lesssim$20 K where N_2 gas could have condensed as pure N_2 ice, then subsequent diffusion due to heating of the comet nucleus would have selectively depleted the highly volatile gas, N_2. In this case, the more thermally evolved a comet, the lower its N_2 abundance would be. Of course, some combination of condensation fractionation and thermal diffusion could explain the N deficiency. The fact that CO is less depleted than N_2 can be explained by the relative facility with which CO can bond with other compounds, especially to form organic molecules. In this regard we note that most($\sim$2/3) of the CO observed in comet Halley originated in a distributed source, and not the nucleus. Thus the abundance of CO would not be expected to correlate very tightly with that of N_2. The above scenario assumes that the comet ices condensed from the solar nebula, and that the bulk of the volatiles were not preserved as ice from their presolar environment.

Summary

We have demonstrated that the observations of NH and NH_2 in comets can be understood by assuming production of both species solely by NH_3 photolysis. The average ammonia abundance found for four comets was NH_3/H_2O ~0.0013 with an estimated uncertainty of a factor ~2. An inventory of the nitrogen compounds in comet Halley indicates that CN and NH_3 contain virtually all of the N in the gas coma, and that the dust coma contains ~95% of the total elemental nitrogen in the comet. We find that the elemental nitrogen is depleted by a factor ~40 in the gas coma, and a factor ~10 in the combined gas and dust coma. The depletion of elemental nitrogen in the comet may be the result of condensation fractionation of N_2 in the solar nebula or preferential diffusion of N_2 from the comet nucleus, or both. In a related program, we are surveying star-forming regions in the galaxy to determine the N_2 abundances in gas being assimilated into protoplanetary accretion disks (Womack 1990, Womack, Ziurys and Wyckoff 1990).

References

Encrenaz, T., d'Hendecourt, L. and Puget, J. 1988, *Astr. Ap*, **207**, 162.

Encrenaz, T. and Knacke, R. 1990, in *Comets in the Post-Halley Era*, eds. R. Newburn, M. Neugebauer and J. Rahe, in press.

Geiss, J. 1987, *Astr. Ap.*, **187**, 859.

Ferro, A. 1990, private communication.

Festou, M. 1981, *Astr. Ap.*, **95**, 69.

Jessberger, E. and Kissel, J. 1990, in *Comets in the Post-Halley Era*, eds. R. Newburn, M. Neugebauer and J. Rahe, in press.

Keller, U. *et al.* 1987, *Astr. Ap.*, **187**, 807.

Matthews, C. and Ludicky, R. 1986, in 20th ESLAB Symposium on the Exploration of Halley's Comet (ESA-SP-250), Vol II, eds B. Battrick, E. Rolfe, and R. Reinhard (Paris: ESA), p. 273.

Tegler, S. 1990, Ph. D. thesis, Arizona State University.

Wegmann, R., Schmidt, H.U., Huebner, W. F. and Boice, D. C. 1987, *Astr. Ap.*, **187**, 339.

Womack, M. 1990, this workshop.

Womack, M., Ziurys, L. and Wyckoff, S. 1990, *Ap. J (Letters)*, in press.

Wyckoff, S., Engel, L. and Tegler, S. 1990, *Ap. J.*, in press.

Wyckoff, S., Engel, L., Womack, M., Ferro, A., Tegler, S. and Peterson, B 1990, *Ap. J.*, in press.

Wyckoff, S., Tegler, S. and Engel, L. 1990, *Ap. J.*, in press.

Figure 1 – NH distribution in comet Halley.

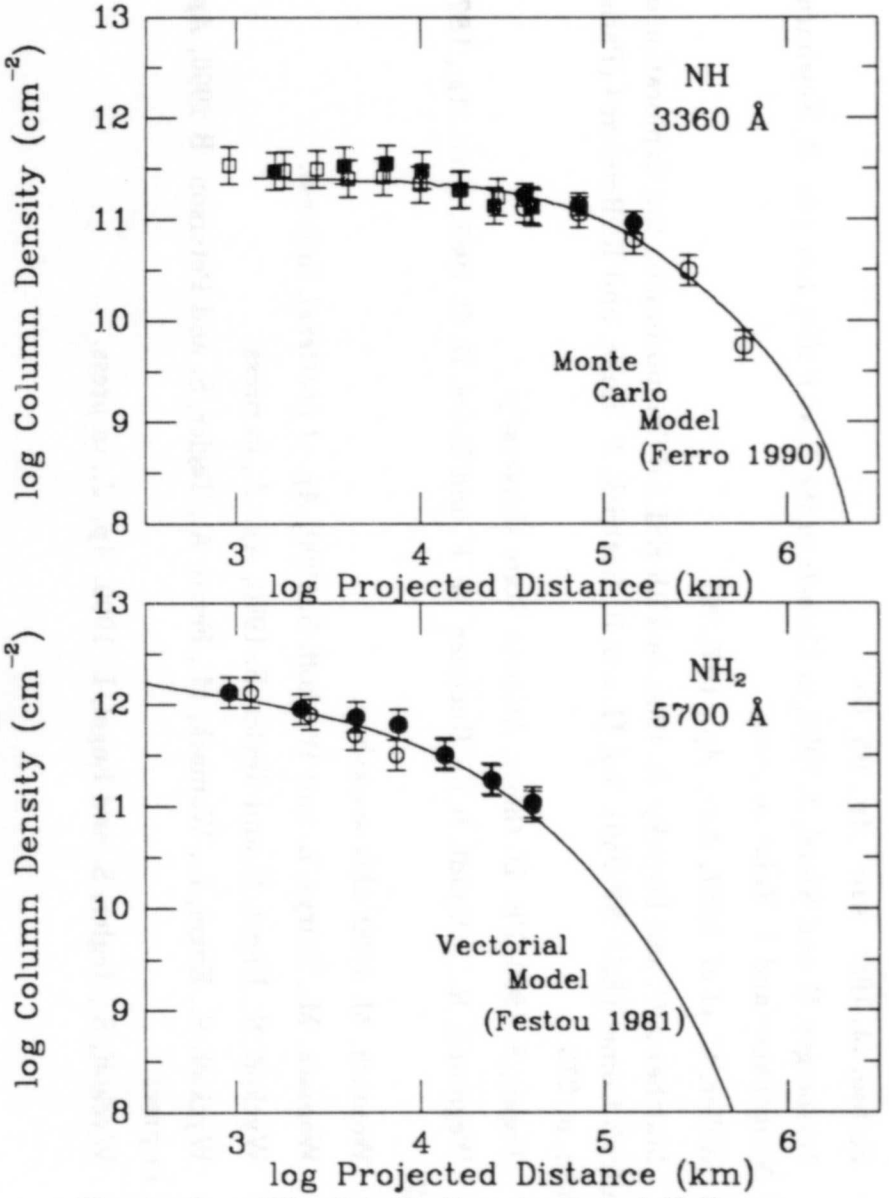

Figure 2 – NH_2 distribution in comet Halley.

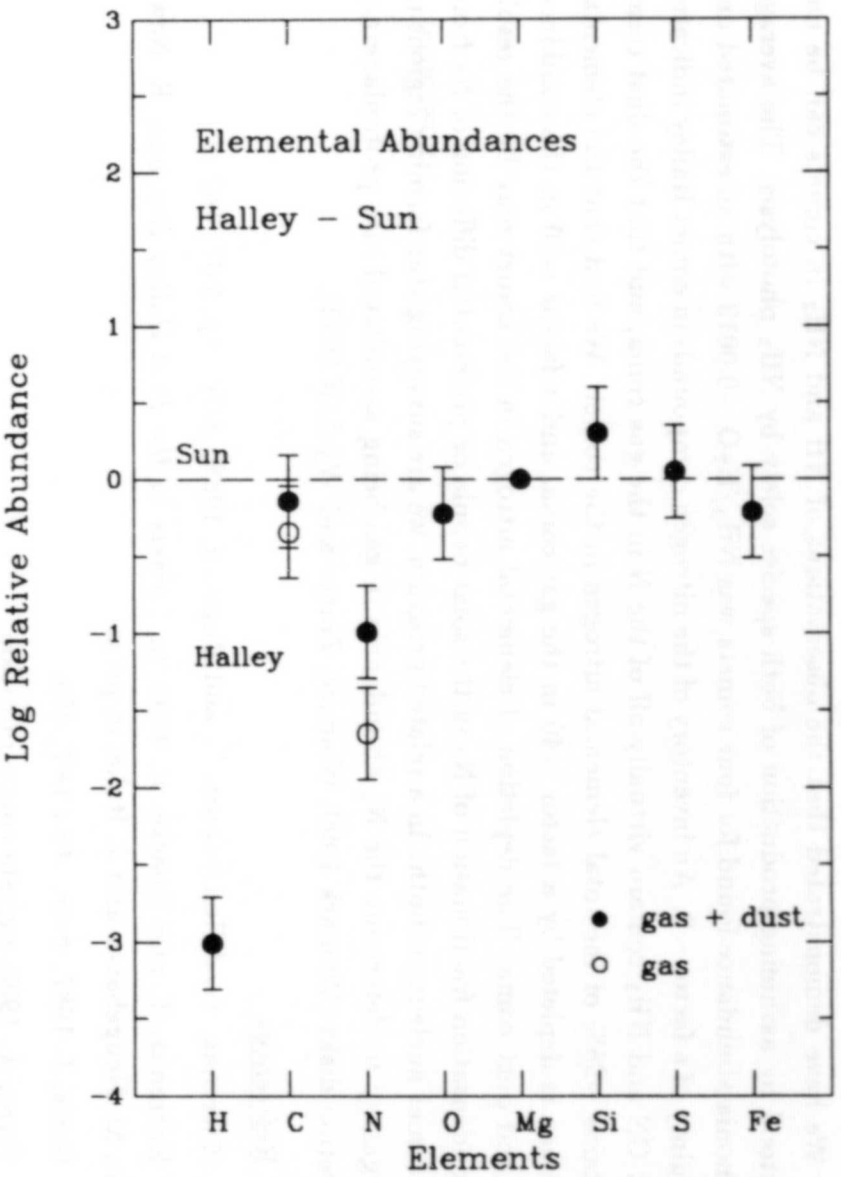

Figure 3 – Hydrogen and nitrogen depletions.

Walter Huebner
How did you determine the N_2 abundance?

Comment: Paul Feldman
In response to W. Huebner's question: on N_2: Loss of N_2 in Earth's atmosphere is principally through ionization (not dissociation). Rates for N_2 and CO are similar, so that to first order, $[N_2]/[CO]$ is probably not too different from $[N_2^+]/[CO^+]$ measured at a given point in the tail.

Susan Wyckoff
The estimate of the N_2/NH_3 we have given for Comet Halley (Wyckoff and Theobald 1989, Adv. Space Sci 9) was based on the above suggestion by Paul Feldman to measure the N_2^+/CO^+ ratio in our spectra. The ratio of the ion fluxes is relatively model independent, and with the ionization rates for N_2 and CO give an estimate of the N_2/CO ratio. We used $CO/H_2O \sim 0.1$ to convert to an abundance, $N_2/H_2O \sim 10^{-4}$. The result is acknowledged to be an estimate only with an accuracy of a factor of several. Even allowing for such a large error, the elemental nitrogen abundance would still be deficient by an order of magnitude in Comet Halley.

Paul Weissman
What is the condensation temperature for N_2 in the solar nebula?

Susan Wyckoff
The condensation temperature for pure N_2 ice is very low $\lesssim 20$ K. (See for example Prinn and Fegley, in "Origin and Evolution of Planetary and Satellite Atmospheres," U. Arizona press, p. 78, 1989).

N91-21019

UNIDENTIFIED IONS IN COMETS

Lisa Engel

Department of Physics and Astronomy

Arizona State University

Optical spectra were taken of comets Halley, West and Brorsen-Metcalf in the wavelength region 3200-6400 Å. These spectra were offset $\sim 10^{-5} - 10^{-6}$ km tailward from the nucleus so that the features detected were all ions with the exception of a very small residual C_2 emission at 5165 Å. The full labelled tail spectrum of comet Halley is shown in **Figure 1**. While most of the features detected are attributable to CO^+, H_2O^+, CO_2^+, CH^+ and OH^+, there are three moderately strong bands in the spectra of comets Halley and Brorsen-Metcalf which remain unidentified. These features were not detected in comet West. All three spectra in the 4800-5400 Å region are shown in Figure 2, in order of decreasing gas-to-dust ratio, Brorsen-Metcalf being the gassiest of the three. The central wavelengths of the unidentified features are 4930 Å, 5300 Å and 6000 Å. In an effort to identify the ions responsible for these features as well as to confirm previous identifications, laboratory spectra of ions were compared with the comet spectra.

H_2O^+ and CO^+ are known to have extensive emission in the 4800-6200 Å region. Therefore, the possibility that these unidentified features are due to H_2O^+ and CO^+ was investigated. A search for the following bands was conducted: H_2O^+ (11-0), H_2O^+ (12-0), H_2O^+ (13-1), CO^+ (1-1) and CO^+ (0-0). CO^+ (1-1) and CO^+ (0-0) have been previously identified and are present in all the spectra examined here. No positive identifications of the H_2O^+ (12-0) and (13-1) bands could be made. However, the H_2O^+ (11-0) band was identified. Comparison of the H_2O^+ (11-0) synthetic spectrum with comet Brorsen-Metcalf data is shown in Figure 3. The relative fluxes of the blended H_2O^+ lines in the synthetic spectrum match those of the cometary data. The central peak at 5198 Å may be due to residual night sky [NI] contamination in this region of the data.

After eliminating H_2O^+ and CO^+ as significant contributors to the stronger unidentified features, spectra of ions which have not yet been identified in the optical region of comets were compared to the data. These ions are NH^+, CS^+ and C_2^+ (Figures 4, 5, 6). None of these ions appears to be a significant contributor to the optical spectra of these three comets.

In conclusion, H_2O^+ (11-0) has been unambiguously identified in cometary optical spectra. However, no other molecular ions for which there are laboratory spectra can explain the unidentified features found in the ion tails of comets Halley and Brorsen-Metcalf.

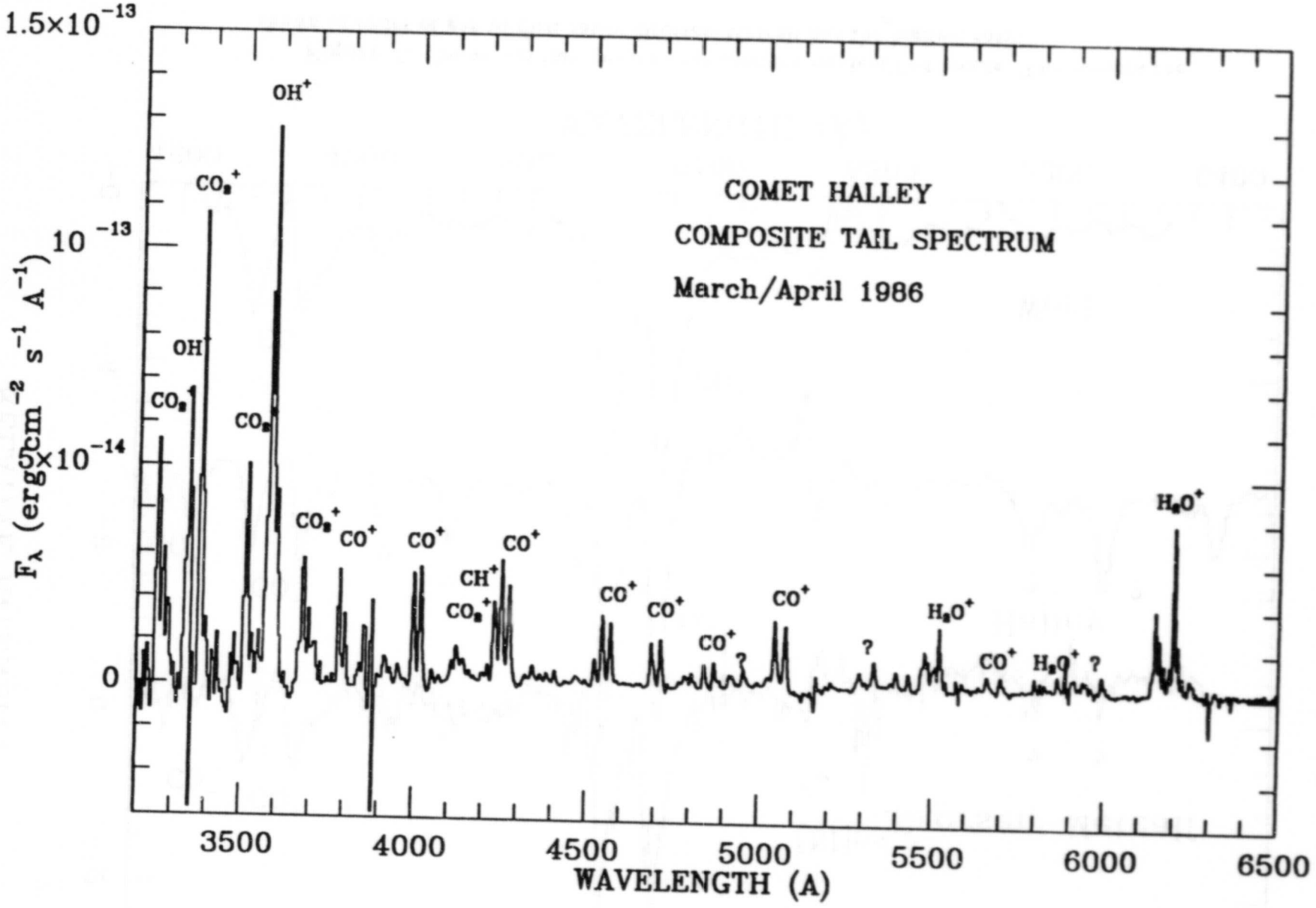

Figure 1. Comet Halley ion tail spectrum covering the optical wavelengths. Question marks denote unidentified bands.

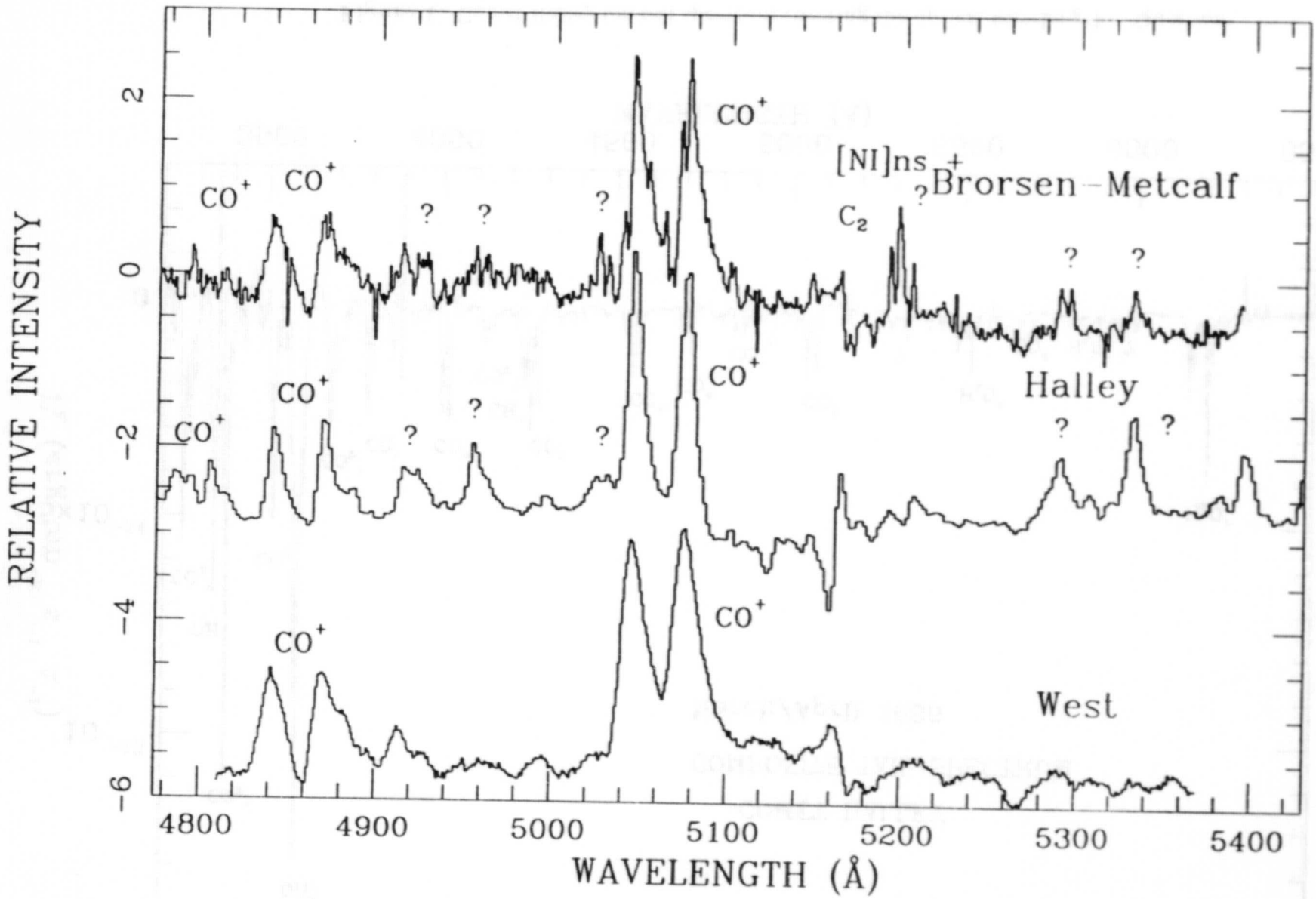

Figure 2. Comet ion tail spectra examined for unidentified bands. The spectra are shown in order of gas-to-dust ratio: Brorsen-Metcalf has the highest ratio.

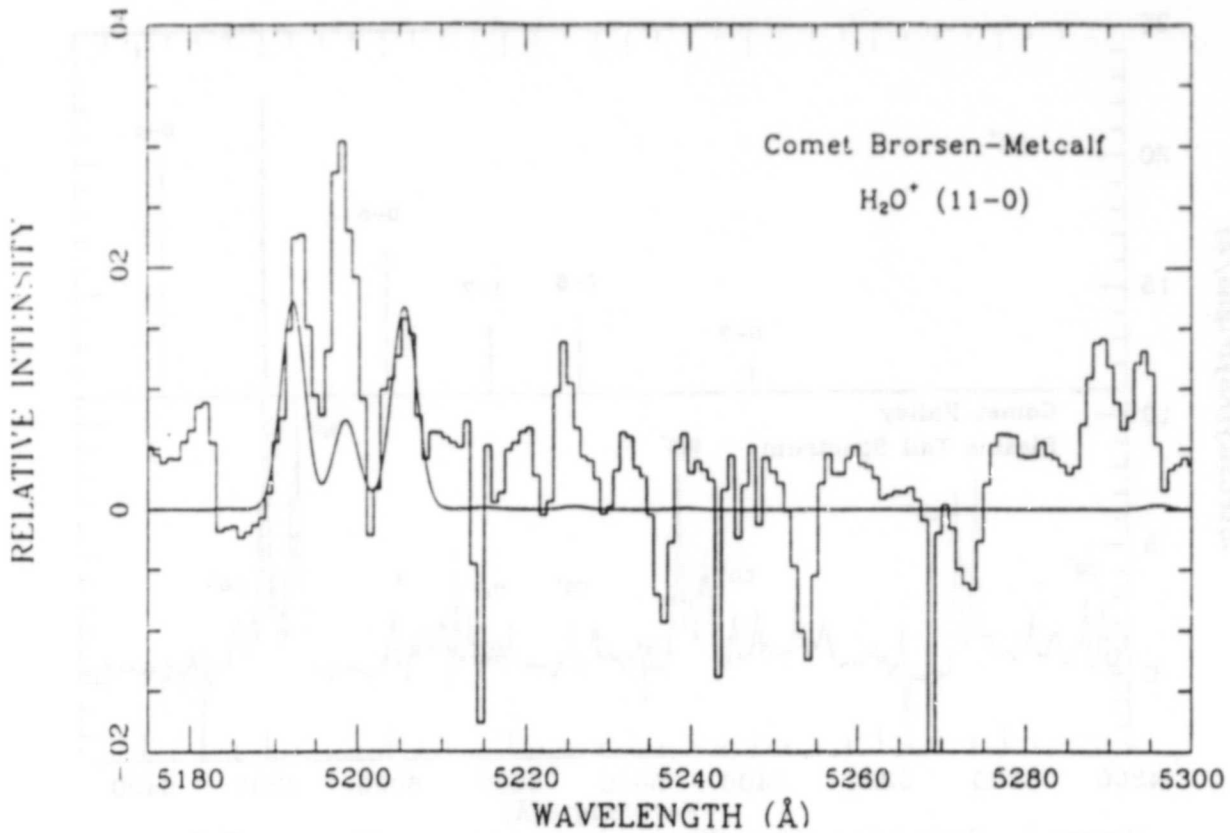

Figure 3. Comet Brorsen-Metcalf ion tail spectrum compared with the synthetic spectrum of the H_2O^+ (11-0) band.

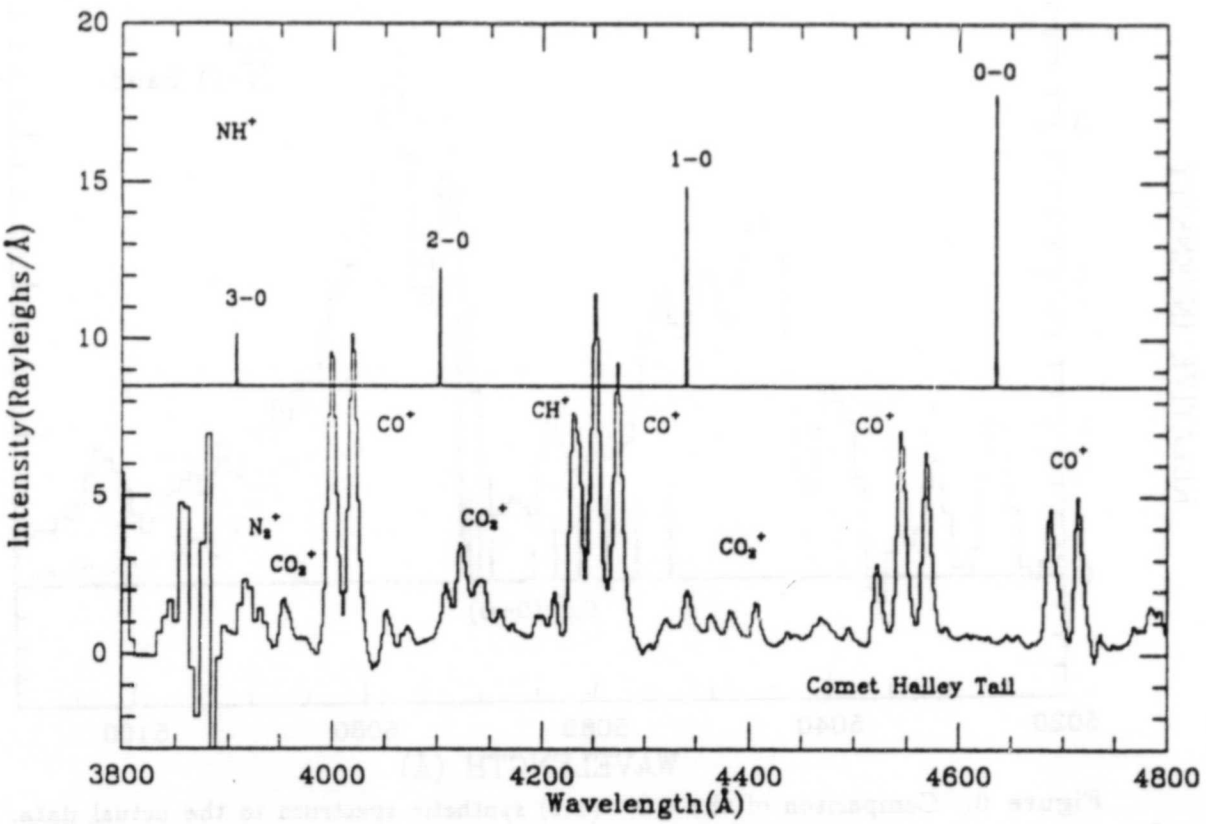

Figure 4. Comparison of NH^+ synthetic spectrum with comet Halley ion tail spectrum. Note the lack of wavelength coincidence between the NH^+ (0-0) feature and the actual data. The Swings effect has been taken into account.

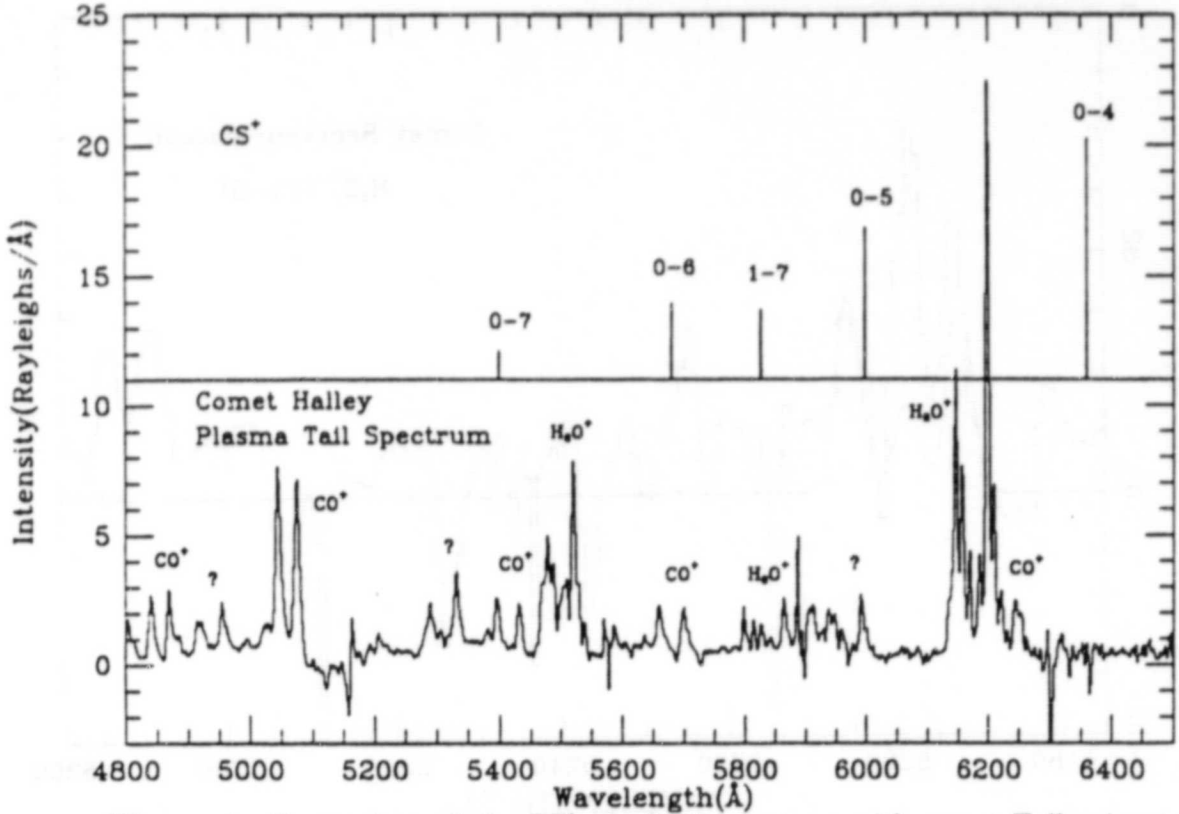

Figure 5. Comparison of the CS^+ synthetic spectrum with comet Halley ion tail spectrum. Note the lack of wavelength coincidence between the CS^+ (0-4) feature and the actual data. The Swings effect has been taken into account.

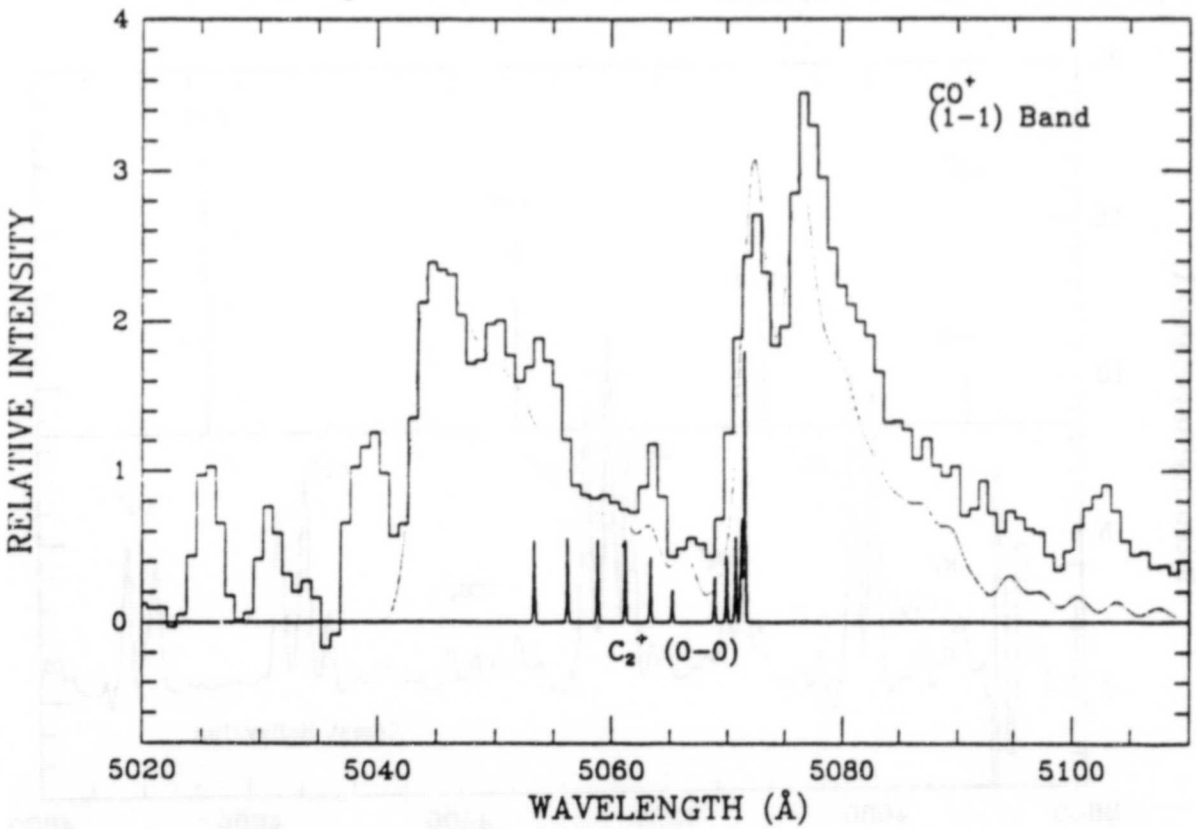

Figure 6. Comparison of the CO^+ (1-1) synthetic spectrum to the actual data. Rotational levels up to $J = 15$ have been considered. Further work will include rotational levels of $J > 15$. The C_2^+ (0-0) synthetic spectrum is shown at high resolution. It can be seen that the addition of this spectrum to that of CO^+ (1-1) will distort the synthetic spectrum beyond the peaks in the actual data.

Walter Huebner
Did you compare the unidentified lines with the very detailed spectrum of Greenstein and collaborator (1950's) which contained many unidentified lines?

Lisa Engel
That is the Comet Mrkos spectrum which covers a spectral region in the ultraviolet. We have concentrated here on the optical region.

William Cochran
You rejected several possible identifications of lines based on the presence of ions in the theoretical spectra that were absent in the data. However, the Swings effect can easily reduce the intensity of a single line by a large factor. Did your theoretical calculations include the Swings effect?

Lisa Engel
Yes, we did include the Swings effect. There are, however, problems with several coincidences.

Humberto Campins
Comment: There's a 1965 or 1966 spectrum by C. Slaughter of Comet Ikeya-Seki.

Lisa Engel
There are several unidentified features in this spectrum that are of interest to this work.

N91-21020

SIMULTANEOUS IMAGING OF OPTICAL *CN* LINES AND RADIO *HCN* LINES IN COMET AUSTIN

Patrick Palmer (U. of Chicago)
M. F. A'Hearn (U. of Maryland)
Imke de Pater (U. of California - Berkeley)
James J. Klavetter (U. of Maryland)
David Mehringer (U. of Chicago)
F. Peter Schloerb (U. of Massachusetts)
Lewis E. Snyder (U. of Illinois)
D. Wilner (U. of California - Berkeley)

Introduction

The parent molecule of cometary CN has been the subject of speculation for a long time. When HCN was detected at 3.4 - mm in Comet Kohoutek (Huebner *et al.* 1974), the problem seemed to be solved. But the much more detailed work on Comet Halley (Bockelée - Morvan *et al.* 1986; Schloerb *et al.* 1987) raised the quantitative question of whether HCN could be the only parent. Therefore comparative CN/HCN studies are vital for understanding the origin of cometary CN.

The striking observation of CN "jets" in Comet Halley (A'Hearn *et al.* 1986) raised another very interesting question about the origin of CN. Traditional theory permits only dust features to remain well defined far from the nucleus. Therefore the CN jets were interpreted as arising from submicron sized dust particles, perhaps $CHON$ particles. An estimated 10 - 50 % of the CN in the comet was in the jets in the Halley observations.

One can make several hypotheses: 1) some of the CN originates from the dust and has nothing to do with HCN; or, 2) at least some of the HCN is also produced from the dust in the coma rather than directly from the nucleus. (In the second hypothesis, whether HCN is or is not the parent of the CN associated with the dust would need to be established.) The extended scalelengths found for CO by Eberhardt *et al.* (1987) and for H_2CO by Snyder *et al.* (1989) also support ideas like hypothesis 2). A third hypothesis should be mentioned: contrary to the usual theory, the gas flow does not become isotropic (Combi 1987).

For all of the reasons mentioned above, it is essential to make a detailed comparison of the spatial distributions of CN and HCN. Furthermore, because of the variability of cometary emissions, it is necessary to make measurements simultaneously.

Instrumental Considerations

If one wishes to compare radio data with data like that of A'Hearn *et al.* , rather stringent conditions are placed on the instrumental parameters. The images shown by A'Hearn *et al.* are $\sim 5'$ $(= 10^5 km)$ square. To obtain even 100 radio pixels in this area would require better than 30 $''$ resolution. We also would like to have a resolution that corresponds to a fraction of the photodissociation scalelength of HCN (~ 40 $''$ in this case).

The radio project was designed to produce images with ~ 15 $''$ resolution over field 2'.3.

(During the period of observation this corresponded to $\sim$ 6500 km resolution over a field $\sim$ 60000 km in diameter.) In order to do this two instruments were used: the Five College Radio Observatory (FCRAO) 14 - m antenna and the Berkeley - Illinois - Maryland Array (BIMA) of three 6 - m antennas. The FCRAO antenna has 58 " resolution at this wavelength, the BIMA array has a 2'.3 field of view; its resolution depends on the locations of the antennas.

The instrumental limitation of the single dish antenna is that information is collected for only one beamwidth at a time. In order to map an area, the dish must be pointed at a sequence of different positions. In sum, one has only one resolution available at each frequency, and one must sacrifice signal - to - noise ratio in proportion to the size of area mapped.

Arrays have a different set of limitations. To understand the limitations, one must recall first that one measures the Fourier transform of what one wishes to know. The variable conjugate to the angular displacement in the sky is the projected baseline length. Therefore, because there is a maximum baseline, there is a minimum possible resolution. There is also a minimum projected baseline - the dish diameter - (otherwise one of the dishes shadows the other), so there is also a maximum size of feature to which an array is sensitive. Within these limitations, the array can make an image of a field of view as large as the primary beam of the individual antennas. Second, one does not measure the entire 2-dimensional Fourier transform of the sky brightness in any finite experiment, but only some of the Fourier components. The problem then is to reconstruct an estimate of the sky brightness from the finite set of data points. For an array like the VLA with 27 antennas, yielding 351 simultaneous independent measurements, in one day enough data is obtained to permit accurate reconstruction of the sky brightness over the range of sizes to which the array is sensitive. All existing mm - arrays have too few telescopes to permit this. With the BIMA array, one has 3 antennas, and therefore only 3 simultaneous independent measurements. The successful scientific programs carried out with mm - arrays so far typically use 5 configurations of antennas. The data acquisition is, then, spread out over a minimum of 5 days (for practical reasons, more typically a few months). For a comet, where we cannot trust that what we see will stay the same from day to day, one cannot use multiple configurations. Therefore, none of the existing mm- arrays obtain data fast enough to permit the construction of reliable images of comets.

The compromise approach that we chose was to use both a single dish and an array. This has several advantages. First, the single dish has no problem with sensitivity to large scale structures. Therefore, no part of the *HCN* distribution will fail to be observed because it is too smooth. Second, by judicious arrangement of the 3 antennas in the BIMA array, complementary data can be obtained which allow the resolution to be improved by a factor of 2 - 3 beyond that of the FCRAO antenna alone. Numerical simulations were carried out to verify the result of combining the single dish and the array data. (Unfortunately, the simulations were based on Comet Austin being at least as strong an *HCN* emitter as Comet Halley.)

Observations

The radio observations were scheduled at FCRAO and BIMA for 1990 April 24 through 1990 April 30. Because of bad weather in New England and other problems, valid

Table 1: Comet Austin Observations

Date	r	Δ	scale(20 ″)	λ_{HCN}	τ_s
Apr 27	.598 AU	.626 AU	9080 km	19000 km	0.13 day
Apr 28	.619	.606	8790	20400	0.13
Apr 29	.640	.587	8510	21800	0.12
Apr 30	.660	.568	8240	23200	0.12

data was obtained only April 27 through April 30. Some relevant parameters are summarized in Table 1. The first three columns are self - explanatory, the fourth is the linear size at the comet that corresponds to 20 ″, the fifth is the photodissociation scalelength of HCN, and the final column is the minimum time for HCN to move one resolution element. (An expansion velocity of 0.8 $\mathrm{km\,s^{-1}}$ was assumed in the last two columns.). The velocity resolution was 0.25 $\mathrm{km\,s^{-1}}$ at BIMA and 0.34 $\mathrm{km\,s^{-1}}$ at FCRAO. The total velocity range covered was $\pm$ 15 $\mathrm{km\,s^{-1}}$ at BIMA and $\pm$ 42 $\mathrm{km\,s^{-1}}$ at FCRAO. (Velocities are referred to the comet.)

Because Comet Austin was fainter than anticipated, it was decided not to attempt to map the entire field of view of the BIMA array with the FCRAO telescope. Therefore the chance of detecting the comet was improved, but the final field of view will be reduced to about 1 ′.

The optical observations were made at Lowell Observatory using the 42 inch J. S. Hall reflector equipped with the U. of Maryland CCD camera. CN images were obtained on April 20.5, 22.5, 23.5, 27.5 and May 9.5. Therefore, on only one night was data obtained simultaneously with both radio telescopes and the optical telescope.

Data reduction is still in progress. We have examined images made from each day's data at BIMA, and there are no miracles. Similarly, the raw spectra at FCRAO were examined; and, at best, there is a possible detection in this first pass through the data. Later this summer we expect to have the final calibrated and edited data from the two instruments so that we can combine them.

The Future

One may infer (correctly) that because of the faintness of Comet Austin, the most valuable feature of the current experiment may turn out to be that it provided a "dry run" for a future, better comet. It is also instructive to examine how the instrumental situation will improve for the radio part of the experiment.

First, the "speed" of the single dish observations will be improved enormously with the use of the very recently completed array feed at FCRAO. This feed provides 15 simultaneous independent beams for the 14 - m antenna. Therefore the entire field of view of the BIMA array can be imaged with only 5 pointings of the telescope (rather than 75 to do the same thing when we observed Comet Austin).

Second, more antennas are being added to the BIMA array. Mechanical assembly has just been completed for 4 new antennas. Therefore, we will have a 6 element array (usable to 1 - mm wavelength) within 2 years. (Three additional antennas are expected to be in operation shortly afterward.) With 6 antennas, one has 15 baselines, i.e. as many as are

obtained in many multi - configuration studies now. Therefore we will be at the stage of obtaining useful images in a single day from the array alone.

Third, the National Radio Astronomy Observatory has proposed building a mm - array of 40 8 - m antennas, to be operated in an innovative way so that the problem of a maximum size scale will be greatly relaxed. With 780 simultaneous baselines, one can obtain excellent images in a very short time. The total collecting area will be $\sim 2000\ m^2$, i.e. larger than that of any other mm - wavelength instrument in the world (and 12 times that of the 6 element BIMA array), so the resulting sensitivity will be correspondingly greater. Although many other astronomers might have something to say about the division of observing time, it is clear to me that this will be a wonderful comet telescope.

References

A'Hearn, M. F., Hoban, S., Birch, P. V., Bowers, C., Martin, R., and Klinglesmith, D. A. III 1986, *Nature*, **324**, 649.

Bockelée-Morvan, D., Crovisier, J., Depois, D., Forveille, T., Gérard, E., Schraml, J., and Thum, C. 1987, *Astr. Ap.*, **180**, 253.

Combi, M. R. 1987, *Icarus*, **71**, 178.

Eberhardt, P., Krankowsky, D., Schulte, W., Dolden, U., Lämmerzahl, P., Bertheiler, J. J., Woweries, J., Stubbemann, U., Hodges, R. R., Hoffman, J. H., and Illiano, J. M. 1987, *Astr. Ap.*, **187**, 481.

Huebner, W., Snyder, L. E., and Buhl, D. 1974, *Icarus*, **23**, 580.

Schloerb, F. P., Kinzel, W. M., Swade, D. A., Irvine, W. 1987, in *Cometary Radio Astronomy*, eds. W. M. Irvine, F. P. Schloerb, and L. Tacconi-Garman (Green Bank, WV: NRAO), p.65.

Snyder, L. E., Palmer, P., de Pater, I. 1989, *A.J.*, **97**, 246.

Anita Cochran
Your title talks of simultaneous optical images. What was Mike A'Hearn able to get from Lowell Observatory?

Patrick Palmer
Mike obtained CN images on April 20.5, 22.5, 23.5, 27.5, and May 9.5. Therefore one was simultaneous with the radio observations.

N91-21021

FABRY-PEROT OBSERVATIONS OF COMET AUSTIN

D. Schultz[1], F. Scherb[1], F.L. Roesler[1], G. Li[1], J. Harlander[1],
T.P.P. Roberts, D. Vanden Berk, S. Nossal, M. Coakley
Department of Physics
University of Wisconsin–Madison
Madison, WI 53706

and

R. Oliversen[1]
Laboratory for Astronomy and Solar Physics
Goddard Space Flight Center
Greenbelt, MD 20771

We present preliminary results of a program to observe Comet Austin (1990c1) from 16 April to 4 May and from 11 May to 27 May 1990 using the West Auxiliary of the McMath Solar Telescope on Kitt Peak, Arizona. The observations were made with a 15-cm dual-etalon Fabry-Perot scanning and imaging spectrometer with two modes of operation: a high resolution mode with a velocity resolution of 1.2 km/s and a medium resolution mode with a velocity resolution of 10 km/s. Scanning data was obtained with an RCA C31034A photomultiplier tube and imaging data was obtained with a Photometrics LN_2 cooled CCD camera with a 516 by 516 Ford chip. The results include: (1) information on the coma outflow velocity from high resolution spectral profiles of [O I]6300 and NH_2 emissions, (2) gaseous water production rates from medium resolution observations of [O I]6300, (3) spectra of H_2O^+ emissions in order to study the ionized component of the coma, (4) spatial distribution of H_2O^+ emission features from sequences of velocity resolved images (datacubes), and (5) spatial distribution of [O I]6300 and NH_2 emission from medium resolution images. The field of view on the sky was 10.5 arcminutes in diameter. In the imaging mode the CCD was binned 4 by 4 resulting in 7".6 per pixel and a subarray readout for a field of view of 10'.5.

High-resolution scans were obtained for heliocentric distances r_h of 0.46, 0.58, and 0.94 AU (see figure 1.) The [O I]6300 linewidth w (FWHM) as a function of heliocentric distance varied approximately as $r_h^{-1/2}$. Also, the [O I]6300 and NH_2

---

[1]Visiting Astronomer, National Solar Observatory, which is operated by the Association of Universities for Research in Astronomy, Inc., under contract with the National Science Foundation.

6298.6 linewidths were significantly less than those of Comet Halley's at comparable values of r_h.

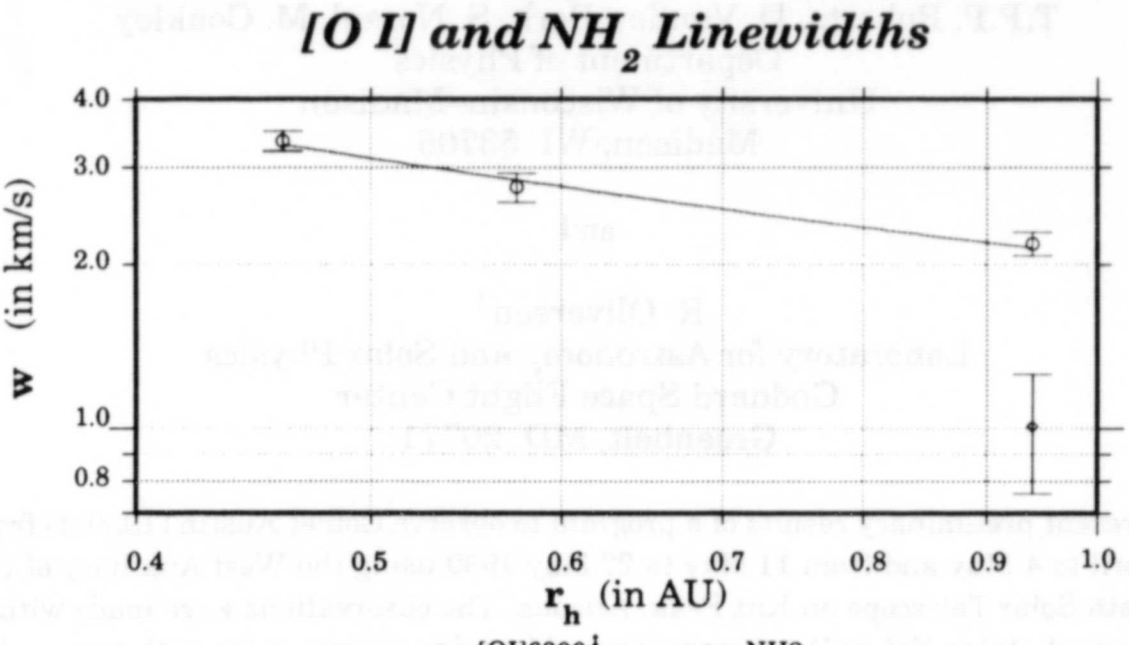

Figure 1: [O I]6300 and NH_2 6298.6 Linewidths

Post-perihelion water production rates were determined from medium-resolution [O I]6300 scans at heliocentric distances ranging from 0.44 to 1.11 AU (see figure 2.) The precision of these rates will be increased after careful study of [O I]6300 imaging data to determine reliable aperture corrections for the amount of emission outside our field of view. The [O I]6300 is cleanly resolved from any of the nearby NH_2 lines.

Medium-resolution scans of the H_2O^+ 6159 were obtained throughout the observational program. On four nights, both H_2O^+ 6159 and 6147 doublets were scanned. The intensity ratio of these two doublets (see table 1) can be used to test models of cometary ionospheres. In theory, our spectrometer could resolve the H_2O^+ 6147 doublet (6146.80Å and 6147.38Å), but the cometary H_2O^+ lines were broad enough to blend the two components.

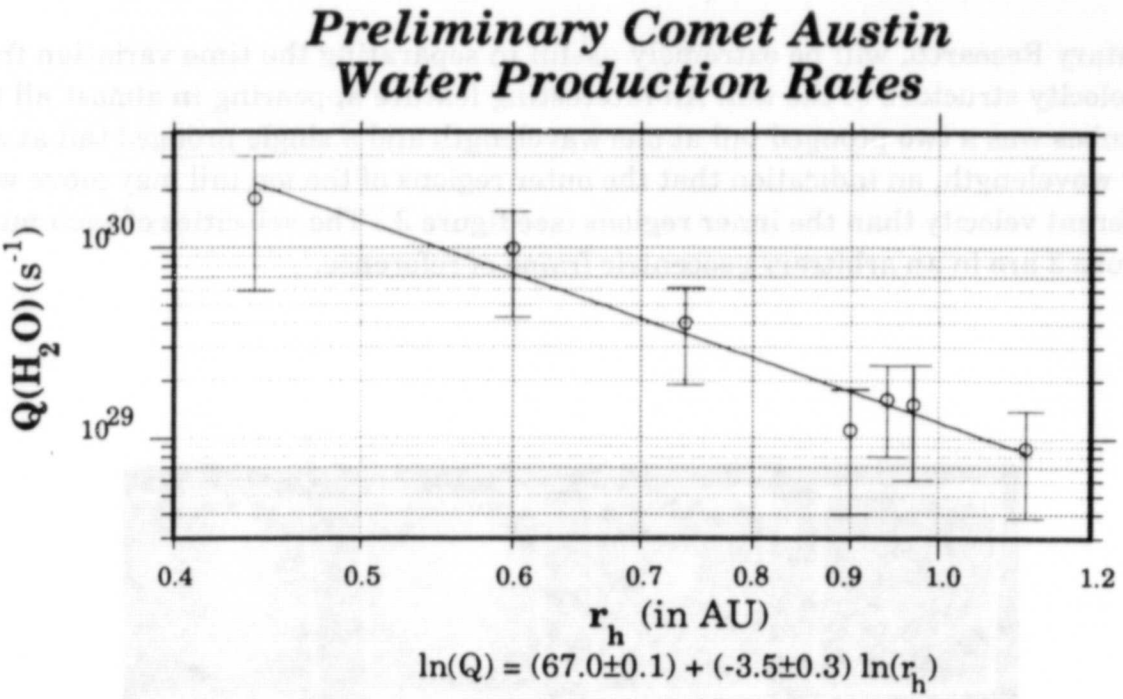

Figure 2: Preliminary H_2O Production Rates Based on [O I]6300 Intensity Measurements.

Table 1: H_2O^+ $\frac{\text{I(6147)}}{\text{I(6159)}}$

Date	I(6147) (arbitrary)	I(6159) (arbitrary)	$\frac{6147}{6159}$
21 May	191±14	170±20	1.1±0.2
23 May	97±13	104±16	0.9±0.3
25 May	96±12	60±30	1.5±1.0
26 May	115±14	73±18	1.6±0.5

A large amount of time in our program was used to obtain velocity-resolved images (datacubes) of cometary H_2O^+ emission in the medium resolution mode. The band-pass was 0.2Å and the images were taken 0.2Å apart. Datacubes of the 6159 doublet were obtained on 28 April and 3, 19, and 20 May. Datacubes of the 6147 doublet were obtained on 21, 23, 25, 26, and 27 May. Each image in a datacube was obtained in a five to fifteen minute exposure, with a complete sequence taking one to two hours to complete. A potential problem in analyzing these images will be the possible time variability of the comet ion tail. H_2O^+ images taken through narrow band interference filters, such as those obtained by the Joint Observatory for

Cometary Research, will be extremely useful in separating the time variation from the velocity structure of the tail. An interesting feature appearing in almost all the datacubes was a two pronged tail at one wavelength and a single pronged tail at another wavelength, an indication that the outer regions of the ion tail may move with a different velocity than the inner regions (see figure 3.) The velocities of each image in figure 3 are in an arbitrary geocentric frame of reference.

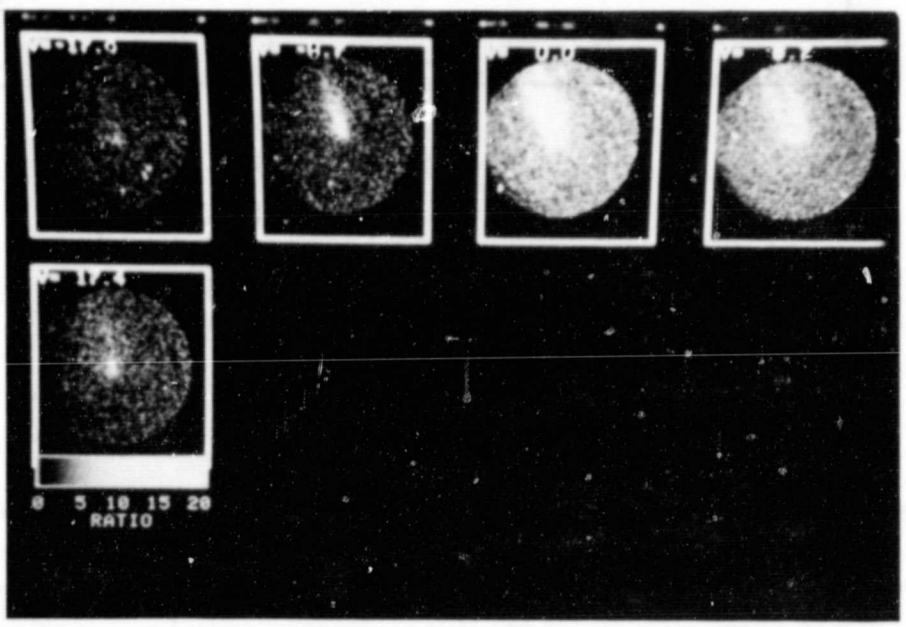

Figure 3: H_2O^+ 6147 Datacube.

ORIGINAL PAGE IS
OF POOR QUALITY

Anita Cochran
How long did it take to complete each data cube?

Daniel Schultz
Each image in a data cube took 5 to 15 minutes, with a whole sequence taking from one to two hours to complete.

Paul Feldman
Why are your values for $Q(H_2O)$ so high when Comet Austin was near the Sun?

Daniel Schultz
For these preliminary results, we estimated the aperture corrections. It is quite possible that our estimate was high for the first few points. We will analyze (OI) imaging data to obtain more accurate and precise aperture correction.

N91-21022

THE NEAR ULTRAVIOLET SPECTRA OF COMETS P/BRORSEN-METCALF AND AUSTIN

W. D. Cochran[1], R. O'Dell[2], C. O. Miller[2], A. L. Cochran[1], C. B. Opal[1], D. Valk[2], and E. S. Barker[1]

[1]McDonald Observatory, The University of Texas at Austin, Austin Texas USA 78712
[2]Department of Space Physics and Astronomy, Rice University, Houston Texas USA 77251

Abstract

We report results of spectrophotometric observations of comets P/Brorsen-Metcalf and Austin from 3000 to 3600Å at a spectral resolution of about 1.8Å. The strongest features are the OH (A-X) 0-0 and 1-1 bands, and the NH (A-X) 0-0 bands. We have clearly found, for the first time, the OH (A-X) 0-1 band. We verify the existence of, and quantitatively measure, the CN (B-X) 2-1 and 3-2 bands. We detect a feature at 3258Å that was first seen in uncalibrated spectra, and suggest identification as the NH singlet (c-a) 0-0 transition. We have also firmly identified the CO_2^+ features at 3378, 3504, and 3512Å. This ion was reported as being present in the tail of Comet Bester (1948 I) by Swings and Page (1950). We propose identification of a weak feature at 3547Å as the fundamental transition of H_2CO, which would make this the first optical cometary detection of this molecule which is very abundant in giant molecular clouds.

Introduction

The near ultraviolet (3000–3600Å) spectral region has not yet been fully exploited for the study of comets. Observations in this spectral region are difficult due to the high atmospheric extinction and the low throughput and sensitivity of spectrographs and detectors at these wavelengths. The first detailed study of the near-ultraviolet was by Swings, Elvey, and Babcock (1941), who first detected the strong OH (A-X) 0-0 band at 3090Å in Comet Cunningham (1941 I). One of the best ground-based ultraviolet spectra is that of Comet Kohoutek by Lane *et al.* (1975). The development of rocket and satellite observations has emphasized the importance of the OH bands, but with the exception of NH, the remainder of this spectral region remains largely unexplored. In this paper, we present spectra of comets P/Brorsen-Metcalf and Austin (1989c1) in the 3000–3600Å spectral region. Detailed results for P/Brorsen-Metcalf have been submitted for publication in The Astrophyscial Journal.

Observations

All observations were made using the Large Cassegrain Spectrograph mounted on the 2.7-m telescope at McDonald Observatory. The detector was a thinned, back-side illuminated TI 800×800 CCD. Prior to each of the observing runs, the CCD was soaked in dry NO gas at one atmosphere pressure and room temperature for about 15 minutes, in order to induce a negative charge layer on the back side of the chip. This process resulted in a 50-fold improvement in the response of the CCD at 3000Å. The spectrograph was used in long slit mode, with a scale at the detector of 1.28 arcsec per readout pixel, and a dispersion of 0.89Å per pixel. A log of the observations of both comets is given below.

Comet	Date	Exposure	R_h	Δ
P/Brorsen-Metcalf	30 July 1989	15 min	1.08 AU	0.66 AU
P/Brorsen-Metcalf	10 August 1989	15 min	0.89 AU	0.63 AU
P/Brorsen-Metcalf	10 August 1989	60 min	0.89 AU	0.63 AU
Austin (1989c1)	30 May 1990	109 min	1.24 AU	0.26 AU
Austin (1989c1)	2 June 1990	65 min	1.29 AU	0.28 AU

Separate exposures were made of spectrophotometric standard stars for absolute flux calibration. For cometary spectroscopy, proper subtraction of the sky spectrum is essential. In August 1989, a separate sky spectrum of 10 minutes was made after that of the comet. In July 1989 a set of planetary nebulae were observed before and after the comet. Since these objects did not fill the entrance slit length, the outer slit regions were used for determination of the sky spectrum. For the May 1990 observations, a separate sky exposure of 60 minutes was obtained. The average along the slit of the 10 August 1989 one hour spectrum of P/Brorsen-Metcalf is shown in Figure 1, and the central 15 pixels of the 30 May 1990 spectrum of Comet Austin in Figure 2. Note that the P/Brorsen-Metcalf spectrum has been calibrated to flux units, while the Austin spectrum is still in detector counts.

Identification of Spectral Features

OH. The well known OH (A-X) 0-0 and 1-1 bands, along with the NH (A-X) 0-0 band, are the strongest transitions in the spectra. Our spectra are at sufficiently high spectral resolution to resolve the rotational structure of these bands. The relative intensities of the lines within the 0-0 band should vary with heliocentric velocity due to the Swings effect. Our observed (0-0) line ratios are in good agreement with the theoretical values calculated by Schleicher (1983). The observed ratio of the integrated flux in the 1-1 to 0-0 OH bands is a good test of our understanding of the physics of cometary comae. Schleicher and A'Hearn's (1988) prediction of the OH 1-0 to 0-0 band ratio, together with their listed transition probabilities, leads us to expect a 1-1 to 0-0 band ratio of about 0.09. This value is only slightly outside the error bars of our measured value for P/Brorsen-Metcalf of 0.12±0.02. An independent measurement of this ratio in P/Brorsen-Metcalf obtained with the IUE at about the same time by P. Feldman (personal communication) gives a flux ratio of 0.082 ± 0.012. It is not yet obvious if there is any real discrepancy between theory and observations.

In the 3450–3485Å region we see an emission band which we identify as the first cometary detection of the $v' = 0$ to $v'' = 1$ band of the (A-X) transition of OH, based on the wavelength identification from Dieke and Crosswhite (1962). The relative intensities of the lines are the same as those in the 0-0 band, since they arise from the same upper level.

NH. The identification of the lines of the NH (A-X) 0-0 band at 3360Å are in good agreement with the results of Kim, A'Hearn, and Cochran (1989). We see no evidence, however, for the NH (A-X) 1-1 band, which should be shifted about 10.4Å longward of the 0-0 band.

We see a weak feature in the P/Brorsen-Metcalf spectrum at 3255Å, which was also see in Kohoutek by Lane *et al.* (1975). This feature is confirmed in our comet Austin spectrum, along with an additional feature at 3266Å. We reject an identification of these lines as the SH (A-X) electronic transition due to wavelength discrepancies with the observed feature. Instead, we propose the identification of the (c $^1\Pi$ - a $^1\Delta$) 0-0 band of NH. According to Pearse (1934), the strongest features of this band would be the Q branch at 3255Å and the P branch near 3267Å. This would be the first identification of the NH singlet transitions in a comet.

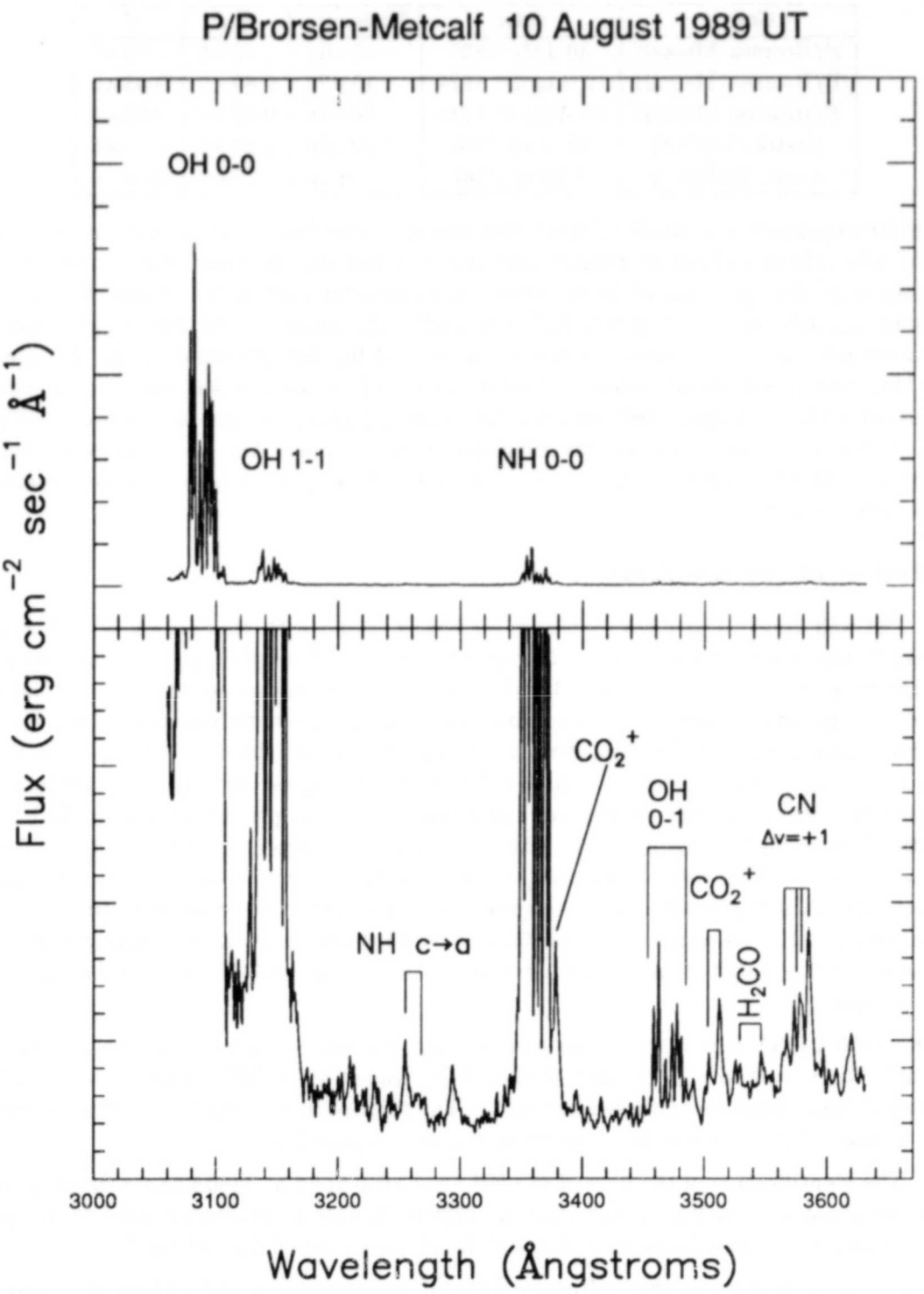

Figure 1: The spectrum of comet P/Brorsen-Metcalf on 10 August 1989. This 60-minute exposure has been calibrated to flux units. The upper panel is scaled so that the entire OH (0-0) band is visible, while the lower panel shows the weak features between the strong OH and NH bands.

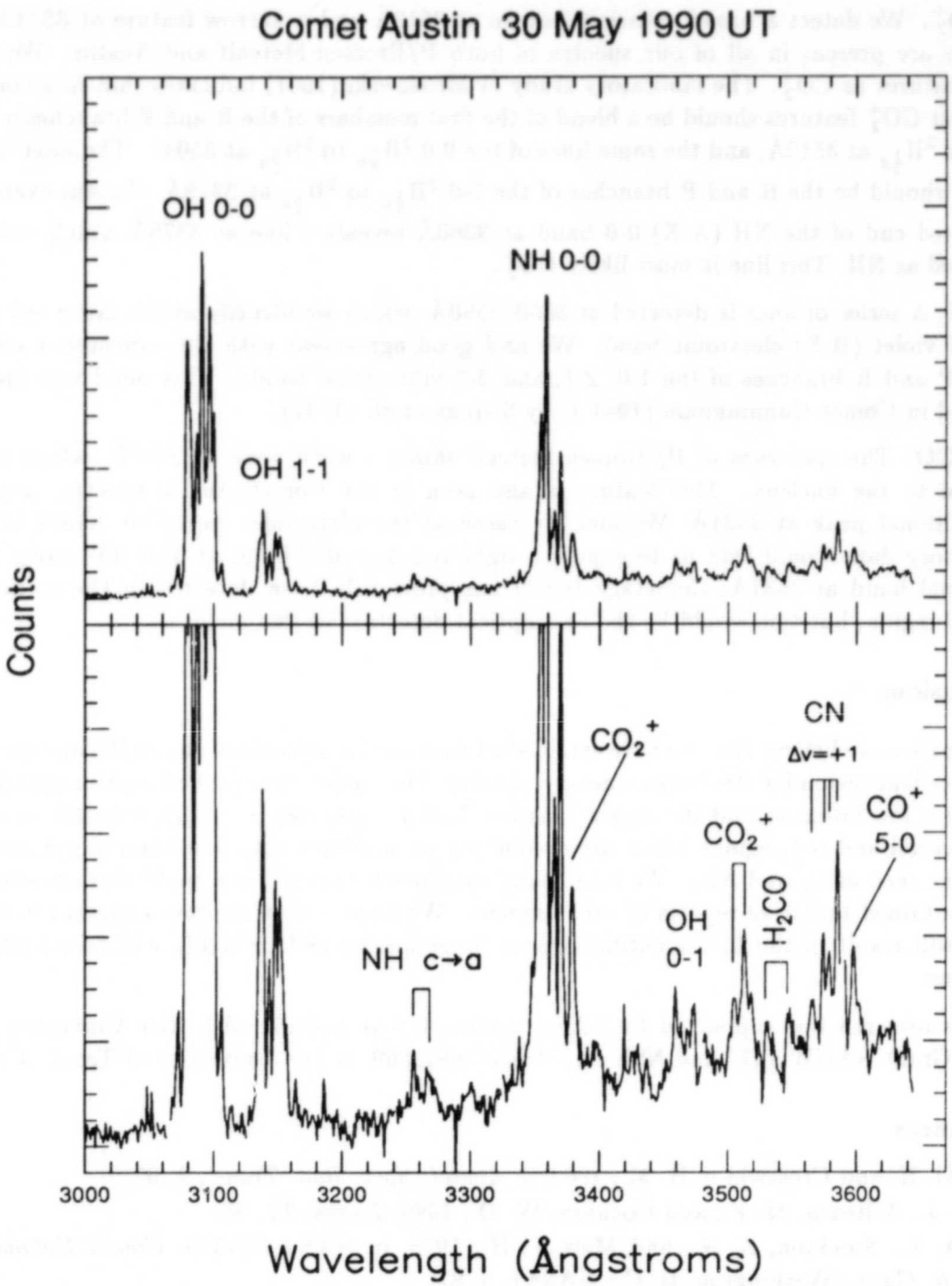

Figure 2: The spectrum of comet Austin on 30 May 1990. This 109-minute exposure has not yet been calibrated to flux, so the units are CCD counts. Thus, the decrease atmospheric transmission and CCD response near 3000Å serves to depress the strong OH (0-0) and (1-1) bands relative to the features at longer wavelength. The upper panel is scaled so that the entire spectrum is visible, while the lower panel shows the weak features between the strong OH and NH bands.

CO_2^+. We detect a broad emission feature at 3512Å and a narrow feature at 3504Å. These features are present in all of our spectra of both P/Brorsen-Metcalf and Austin. We identify these features as CO_2^+. The laboratory study of Mrozowski (1941) indicates that in a comet, the strongest CO_2^+ features should be a blend of the first members of the R and P branches of the 0-0 $^2\Pi_{\frac{1}{2}u}$ to $^2\Pi_{\frac{1}{2}g}$ at 3512Å, and the same lines of the 0-0 $^2\Pi_{\frac{3}{2}u}$ to $^2\Pi_{\frac{3}{2}g}$ at 3504Å. The next strongest feature should be the R and P branches of the 1-0 $^2\Pi_{\frac{1}{2}u}$ to $^2\Pi_{\frac{1}{2}g}$ at 3378Å. Careful examination of the red end of the NH (A-X) 0-0 band at 3360Å reveals a line at 3378Å which can not be identified as NH. This line is most likely CO_2^+.

CN. A series of lines is detected at 3560–3590Å, which we identify as the $\Delta_v = +1$ band of the CN violet (B-X) electronic band. We find good agreement with the expected wavelengths of the P and R branches of the 1-0, 2-1, and 3-2 vibrational bands. This band was previously reported in Comet Cunningham (1941 I) by Swings *et al.* (1941).

H_2CO. The spectrum of P/Brorsen-Metcalf shows a weak peak at 3547Å, which is highly confined to the nucleus. This feature is also seen in the Comet Austin spectra, along with an additional peak at 3531Å. We identify these as the ultraviolet electronic bands of H_2CO. Laboratory data would lead us to expect a tight red-degraded band at 3546.9Å, along with an additional band at 3531Å. Cometary H_2CO has previously been detected in the IR and radio spectral region, but this would be the first optical detection of this molecule.

Conclusions

In this paper, we believe that we have established that the far ultraviolet end of the optical window is an excellent region for studying cometary physics. The cometary scattered continuum light from the Sun is low intensity and the major emission lines are grouped into narrow bands, in contrast to the visual and red regions which are dominated by scattered solar continuum and spread-out emissions such as C_2 and NH_2. We have found evidence for several new molecular emissions, and have confirmed tentative reports of other species. We believe that improved spectra in the near future will result in the firm identification of these species and probably will reveal additional emissions.

This research was supported by NASA Contract NAG5-29451 with Rice University and by NASA Grant NAGW-1477 and NSF Grant AST-8912869 to The University of Texas at Austin.

References

Dieke, G. H. and Crosswhite, H. M., 1962, *J. Quant. Spec. Rad. Trans.*, **2**, 97.

Kim, S. J., A'Hearn, M. F., and Cochran, W. D., 1989, *Icarus*, **77**, 98.

Lane, A. L., Stockton, A. N., and Mies, F. H., 1975, in *NASA SP-355, Comet Kohoutek*, ed. G. A. Gary, (Washington, D. C.: NASA), p. 87.

Mrozowski, S., 1941, *Phys. Rev.*, **60**, 730.

Pearse, R. W. B., 1934, *Proc. Roy. Soc. London A*, **143**, 112.

Schleicher, D. G., 1983, PhD thesis, University of Maryland, College Park, Maryland.

Schleicher, D. G. and A'Hearn, M. F., 1988, *Ap. J.*, **331**, 1058.

Swings, P., Elvey, C. T., and Babcock, H. W., 1941, *Ap. J.*, **94**, 320.

Swings, P. and Page, T., 1950, *Ap. J.*, **111**, 530.

N91-21023 51-90

ROCKET OBSERVATIONS OF THE ULTRAVIOLET SPECTRUM OF COMET AUSTIN (1989c_1)

3-0517

D. J. Sahnow, P. D. Feldman, S. R. McCandliss and M. E. Martinez
Department of Physics and Astronomy
Johns Hopkins University
Baltimore, MD 21218

P4

Long slit ultraviolet spectra of Comet Austin (1989c_1) were obtained from a sounding rocket experiment launched from White Sands Missile Range, New Mexico, on 21 April 1990 at 1015 UT. The instrument, known as the Faint Object Telescope, consisted of an f/15.5 Dall-Kirkham telescope, a Rowland Circle spectrograph and a microchannel plate intensifier coupled to a Reticon diode array. An onboard television camera transmitted images to the ground during flight, which permitted real-time maneuvers in order to center the comet in the entrance slit. The comet was held near the center of the slit for approximately 270 seconds by sending six pointing corrections, all but one of which was less than 30 arcseconds. The comet's parameters at the time of observation, along with the characteristics of the instrument, are shown in Table I.

Table I Comet Austin parameters for NASA 36.073 UG

Heliocentric Distance	0.476 AU	
Heliocentric Velocity	31.44 km / sec	
Geocentric Distance	0.756 AU	
Geocentric Velocity	-37.63 km / sec	
Slit length at the comet	8.1 arcmin	(2.7 x 10^5 km)
Slit width at the comet	7.25 arcsec	(4.0 x 10^3 km)
Spectral Resolution	5.3 Å	
Wavelength Range	1150 - 1850 Å	
Time in slit	T+250 to T+520 sec	
Pitch/Yaw maneuvers	≤ 30"	

The data taken by the instrument consists of the (x,y) coordinates of the photons which fall on the Reticon diode array. Figure 1 shows a contour representation of the raw data (including detector dark counts) obtained during the time that the comet was in the slit. In this representation, wavelength runs along the horizontal axis, from approximately 1150 Å to 1850 Å over the 800 pixels, while the vertical axis is the spatial direction, with a span of approximately 3.7 x 10^5 km across the 544 pixels shown; the slit is 400 pixels long. The coordinates shown are actual photon positions on the face of the Reticon diode array after being corrected for a tilt of the entrance slit. Because of the centroiding algorithm used, the position could be determined to an eighth of a Reticon diode, although the instrument resolution is closer to ½ of a diode.

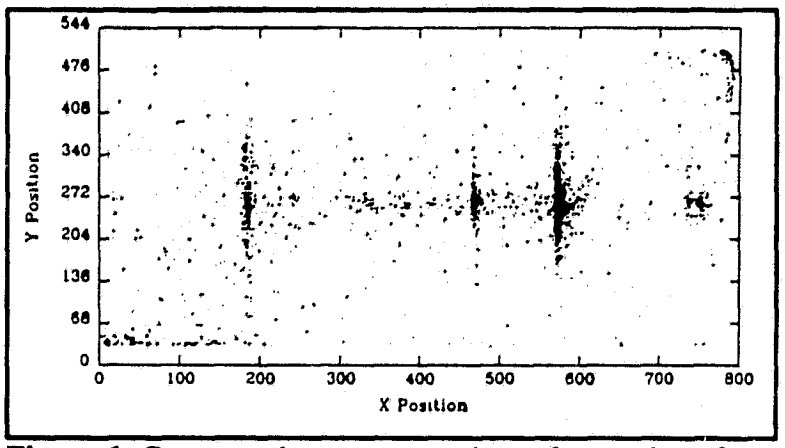

Figure 1 Contour plot representation of raw data from NASA 36.073 UG

The three brightest lines in the spectrum, O I (1304 Å) and C I (1561 Å and 1657 Å) are clearly visible in this picture, while others, including S I (1807, 1820 and 1826 Å) and the CO fourth positive bands (1380 - 1600 Å) can also seen in other graphical representations of the same data. A CaF_2 filter in front of the entrance slit attenuates all wavelengths below approximately 1240 Å by several orders of magnitude, which prevents H I (1216 Å) from being seen. The 15,808 counts in the spectrum shown include the detector dark count in addition to the photons from the comet.

Figure 2 shows a spectrum obtained from the above data by summing over 4 diodes in the spatial direction (40 arcseconds, or 21,500 km at the comet) around the center of brightness. Although the spatial resolution of the instrument is actually 10 arcseconds, because of pointing jitter and drift the spatial data is smeared out here over approximately 30 arcseconds. It will be possible to remove much of this degradation in resolution by taking into account the actual pointing at each instant in time during the flight, but this has not been done yet.

The data shown has been converted from raw counts to Rayleighs by folding in the instrument effective area at each wavelength. It has also been binned to ½ of a Reticon diode, had the detector dark counts subtracted, and then smoothed over 2 bins (7 Å). Only those wavelengths above 1250 Å have been included due to the effects of the CaF_2 filter mentioned above. The wavelength scale was determined by

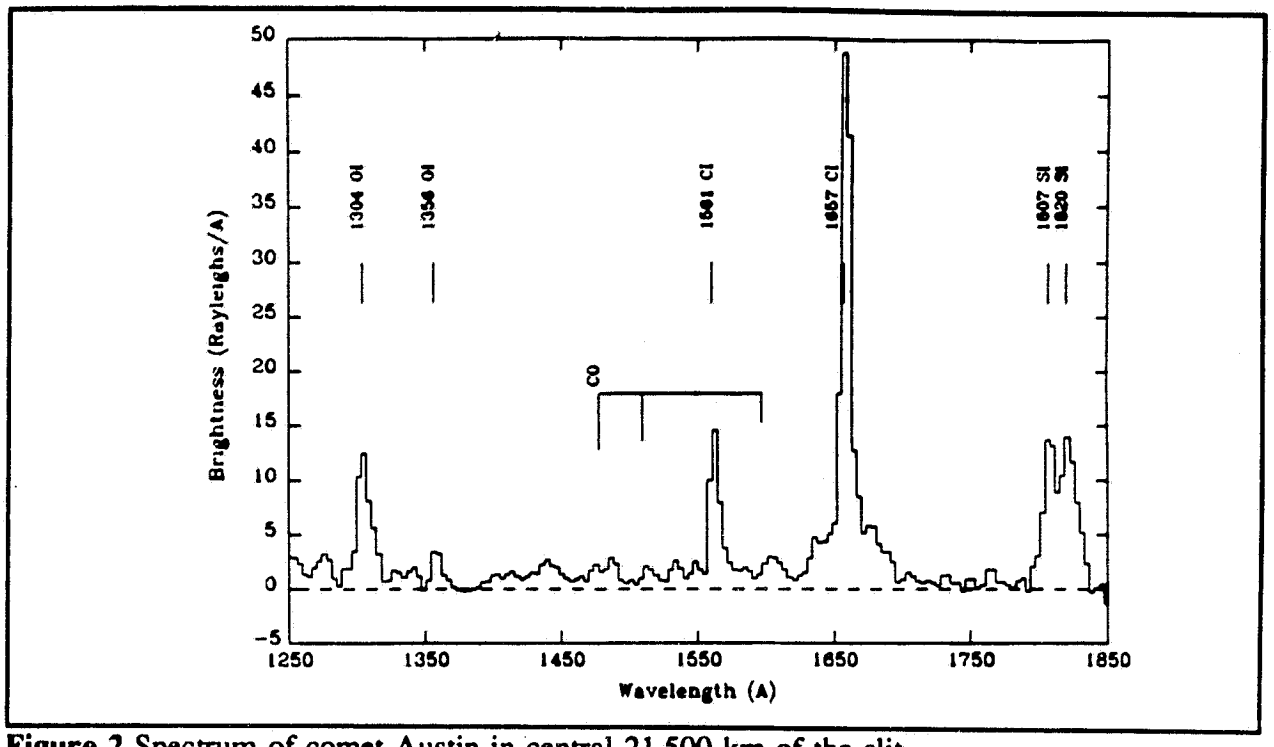

Figure 2 Spectrum of comet Austin in central 21,500 km of the slit.

measurement of the positions of the brightest lines seen. The slit is approximately 1.3 bins wide on the scale of this plot.

The brightest spectral features are labeled in the figure, and their preliminary brightnesses are tabulated for several projected areas on the comet in Table II. The errors associated with these values are mostly due to the 20% uncertainty in the absolute calibration of the instrument, although for the CO bands, the counting statistics become a significant source of error. This table also includes a comparison to the brightnesses measured in the central coma of Comet Halley (1986 III) with a similar rocket-borne instrument on 26 February and 13 March 1986 (Woods *et al.* 1986). The wavelength range did not extend above 1750 Å in the 1986 flights; thus the S I lines were not observed.

The O I (1304 Å) multiplet is much weaker relative to Halley due to the lower heliocentric velocity which shifts the absorption wavelength of the cometary oxygen atoms outside the solar line profile (Dymond *et al.* 1989) and results in excitation through Bowen fluorescence via H I Lyman-ß (Feldman 1982).

The measured CO brightnesses from the 40" column in Table II, when used in a simple radial outflow model, give a production rate of ~1.7 x 10^{27} s^{-1}, compared to 2.4 x 10^{29} s^{-1} for the first Halley flight, and 1 x 10^{29} s^{-1} for the second. Assuming a water production rate of ~1 x 10^{29} s^{-1}, based on ground-based optical and radio

Table II Brightnesses measured for Comet Austin compared with Comet Halley

	Comet Austin (1989c$_1$)			Comet Halley (1986 III)	
	21 April 1990			26 February 1986	13 March 1986
	0.48 AU			0.70 AU	0.90 AU
	7.25" x 20"	7.25" x 40"	7.25" x 80"	10" x 16"	
O I 1304 Å	80 ± 16 R	100 ± 20 R	105 ± 20 R	1460 ± 320 R	280 ± 65 R
O I 1356 Å	40 ± 8 R	25 ± 5 R	10 ± 2 R	60 R	< 10 R
CO 1478 Å	24 ± 12 R	21 ± 11 R	-	175 ± 50 R	65 ± 25 R
CO 1510 Å	24 ± 12 R	22 ± 11 R	-	140 ± 40 R	60 ± 25 R
C I 1561 Å	130 ± 25 R	100 ± 20 R	70 ± 15 R	480 ± 110 R	150 ± 35 R
CO 1597 Å	33 ± 17 R	15 ± 8 R	-	90 ± 25 R	30 ± 15 R
C I 1657 Å	400 ± 80 R	360 ± 70 R	300 ± 60 R	1600 ± 350 R	520 ± 115 R
S I 1807 Å	-	130 ± 25 R	75 ± 15 R	Not Observed	

observations made within a few days of the rocket flight and the relative constancy of the visual magnitude during this period, this value indicates an abundance of CO relative to water of approximately 2 percent.

This work was supported by NASA grant NAG 5-619.

References

Dymond, K. F., Feldman, P.D., and Woods, T.N. 1989, *Ap. J.*, **338**, 1115.

Feldman, P. D. 1982, in *Comets*, ed. L. L. Wilkening (Tucson: University of Arizona Press), pp. 461-479.

Woods, T. N., Feldman, P. D., Dymond, K. F., and Sahnow, D. J. 1986, *Nature*, **324**, 436.

N91-21024 S12-90
320-18
P5

IUE OBSERVATIONS OF COMETS P/BRORSEN-METCALF AND OKAZAKI-LEVY-RUDENKO

E. E. Roettger, P. D. Feldman, S. A. Budzien (Johns Hopkins University)
M. F. A'Hearn (University of Maryland)
and M. C. Festou (Observatoire de Besançon)

Comet P/Brorsen-Metcalf (1989o) was observed with the *International Ultraviolet Explorer* (*IUE*) on several dates from 27 July 1989 through 5 August 1989; comet Okazaki-Levy-Rudenko (1989r) was observed in low dispersion with *IUE* on 2 and 22 December 1989. The water production rates for P/Brorsen-Metcalf derived from OH measurements using the vectorial model of Festou (1981) were 4.2, 4.6, 5.3, 4.9, 6.2, and 6.7×10^{28} on 27.2 and 31.1 July, 1.8, 2.4, 3.9, and 5.2 August 1989, respectively. These are plotted in Fig. 1. For perspective, water production rates estimated from postperihelion visual magnitudes using the method of Newburn (1981; see also Roettger *et al.*, 1990) are also plotted. Fig. 2 shows the water production rates (squares) for comet Okazaki-Levy-Rudenko, which were 5.3 and 4.0×10^{28} on 21.9 and 22.2 December 1989. The 21 December measurement has a greater uncertainty, as it was derived from the OH (1,1) band, in a noisier region of the *IUE* camera. Results using a newer version code for the vectorial model are also plotted (diamonds); they are within a few percent of the previous results. The numbers listed are from the older code, to maintain consistency with published results for other comets. Also plotted in Fig. 2 are two estimates of the water production rate from the OI emission around 1304 Å (octagons). The higher point is from a Haser model, and should be an overestimation as oxygen is primarily a granddaughter product. The lower point was obtained by analogy with observations of comet Bradfield 1979X, a comet with similar *IUE* spectra and geometric parameters. These should be considered rough estimates only.

The ultraviolet continuum was not reliably measurable in comet P/Brorsen-Metcalf in most of the spectra, but we derive $Af\rho \sim 30$ cm for 2 August. For comet Okazaki-Levy-Rudenko, we derive $Af\rho = 50$ cm on 22 December. $Af\rho$ is the product of albedo, filling factor of grains in the aperture, and projected aperture radius (A'Hearn *et al.*, 1984); it is proportional to the dust production rate if the production is steady–state, and the grains move at constant velocity without fragmentation or albedo changes. Both comets had very little dust compared to other recently observed comets, as can be seen in Fig. 3.

The ratio of CS to water production rates are shown in Fig. 4. Relative to water, both comets had less CS than P/Halley in the same range of heliocentric distances. The CS production rates were obtained from a Haser model, assuming a short–lived parent (CS_2). For model-independent comparison, the column densities of observed species are listed in Table I. Because the dynamic range of the *IUE* spectrographs are limited, not all species can be measured in each spectrum. The P/Brorsen-Metcalf spectra from 31 July and 3 August were obtained from the NSSDC Archives. Due to the observing technique used for

these spectra, the exposure time and hence the brightnesses and derived quantities have a small uncertainty associated with them.

Mention was made previously (see O'Dell *et al.*, this volume) of a possible inconsistency of the OH g-factors from Schleicher and A'Hearn (1988) and the OH (1,1) to (0,0) band ratios. The (1,1) band is in a noisy region of the *IUE* camera, and so those measurements generally have a greater uncertainty than the OH (0,0) or (1,0) band measurements. Although individual band ratios vary from their theoretical values by typically 15%, the variation is in both directions and the average of the theoretical to measured ratios differ from the ideal value of 1.00 by only 2%. This is easily within the uncertainty of either the g-factors or the *IUE*. The nucleus and offset exposures were then averaged separately; the deviations from theory are higher but still within the expected uncertainties. These results and related calculations for the OH (1,0) band are presented in Table II.

Acknowledgements

This work was based on observations obtained at GSFC and Vilspa and supported by NASA under Grants NSG-5393 to the Johns Hopkins University and NAG 5-252 to the University of Maryland. Additional data courtesy of the *IUE* Science Working Group, National Space Science Distribution Center (NSSDC).

References

A'Hearn, M. F., D. G. Schleicher, P. D. Feldman, R. L. Millis, and D. T. Thompson 1984. *Astr. J.* **89**, 579.

Festou, M. C. 1981. *Astr. Ap.* **95**, 69.

Newburn, R. L. Jr. 1981. In *The Comet Halley Dust and Gas Environment Workshop* (ESA SP–174) (The Netherlands: ESA Publications Division), p. 3.

O'Dell, C. R., W. D. Cochran, C. O. Miller, A. L. Cochran, C. B. Opal, and E. S. Barker 1990. This volume.

Roettger, E. E., P. D. Feldman, M. F. A'Hearn, and M. C. Festou 1990. *Icarus*, in press.

Schleicher, D. G., and M. F. A'Hearn 1988. *Ap. J.* **331**, 1058.

Table I. Column densities (9"x15" aperture)

	P/Brorsen-Metcalf						O-L-R		
	27 Jul	31 Jul	1 Aug	2 Aug	3 Aug	5 Aug	2 Dec	21 Dec	22 Dec
r (AU)	1.12	1.06	1.03	1.02	0.99	0.97	0.78	1.04	1.04
Δ (AU)	0.69	0.65	0.64	0.64	0.63	0.63	0.52	0.81	0.81
$\dot{r}$ (km s^{-1})	-29.4	-29.6	-29.7	-29.7	-29.8	-29.8	+20.0	+25.5	+25.6
from	GSFC	NSSDCA	Vilspa	GSFC	NSSDCA	GSFC	GSFC	GSFC	GSFC
$B_{OH}(0,0)$ (kR)	11.2		20.0	19.3		31.8			32.5
$B_{OH}(1,0)$ (R)		740			1250				
$B_{OH}(1,1)$ (R)								1380	
N_{OH} (10^{13})	3.0	3.7	4.4	4.2	5.5	6.3		4.2	3.2
B_{CS} (R)	150	210	(240)	270	300	360	930	150	190
N_{CS} (10^{11})	2.8	3.4	3.6	4.0	4.2	4.9	8.1	2.3	2.9
N_{CS}/N_{OH} (10^{-3})	9.2	9.3	8.2	9.6	7.6	7.8		5.4	9.3
$B_{CO_2^+}$ (R)	50	110	(60)	70	100	120	280	100	120
$N_{CO_2^+}$ (10^{11})	2.9	4.7	2.9	3.5	4.8	5.4	2.2	4.9	6.2
$N_{CO_2^+}/N_{OH}$ (10^{-3})	9.6	13.	6.6	8.3	8.6	8.6		12	20
B_{OI} (R)	17		33				370		
N_O (10^{13})	1.7		2.9				2.7		
N_O/N_{OH}	0.58		0.65						
B_{CI} (R)	32		36				260		
N_C (10^{12})	3.9		3.7				4.3		
N_C/N_{OH}	0.13		0.084						
B_{SI} (R)	47	60	72				310		
N_S (10^{12})	1.4	1.6	1.8				5.0		
N_S/N_{OH} (10^{-2})	4.6	4.2	4.0						
B_{C_2} (R)							250		
N_{C_2} (10^{11})							4.2		

Table II. OH Ratios for Comet P/Brorsen-Metcalf 1989o

g_{11}/g_{00}	B_{11}/B_{00}	B/g^*	g_{11}/g_{10}	B_{11}/B_{10}	B/g^*	g_{00}/g_{10}	B_{00}/B_{10}	B/g^*
Avg0.0816	0.0803	0.980	1.75	1.84	1.05	21.33	21.29	0.998
dev 0.001	0.126	0.151	0.00	0.30	0.173	0.19	2.31	0.106
	off by	2.0%			5.4%			0.2%
				NUCLEUS exposures only				
Avg		1.028			1.12			0.997
dev		0.173			0.17			0.041
	off by	2.8%			12%			0.3%
				OFFSET exposures only				
Avg		0.923			0.966			0.999
dev		0.112			0.127			0.160
	off by	7.7%			4.4%			0.2%

* The ratios $(B_{11}/B_{00})/(g_{11}/g_{00})$, $(B_{11}/B_{10})/(g_{11}/g_{10})$, and $(B_{00}/B_{10})/(g_{00}/g_{10})$ were averaged after division.

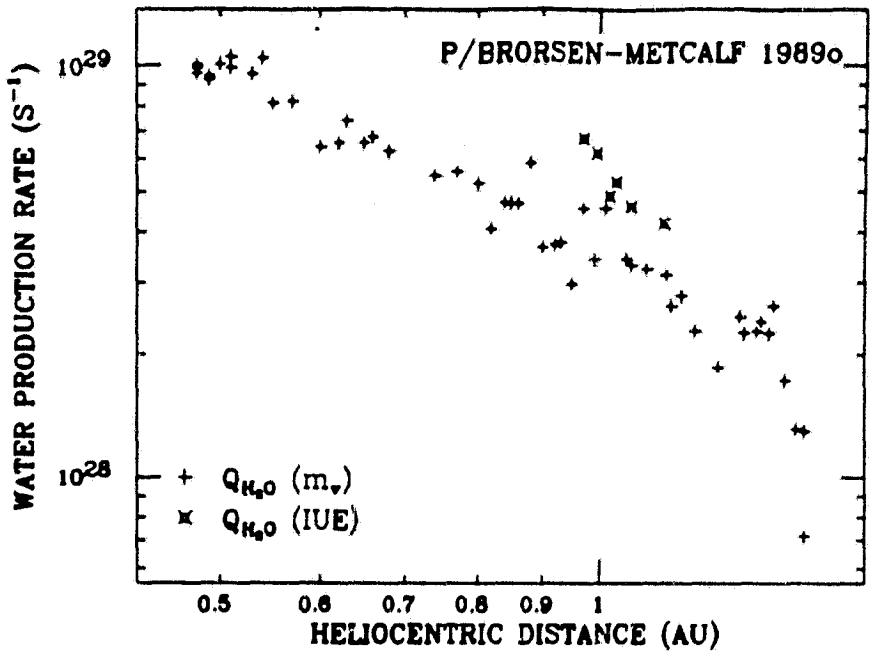

Figure 1. Preperihelion water production rates derived from OH emissions (pierced symbols) for comet P/Brorsen-Metcalf are plotted with production rates derived from visual magnitude estimates.

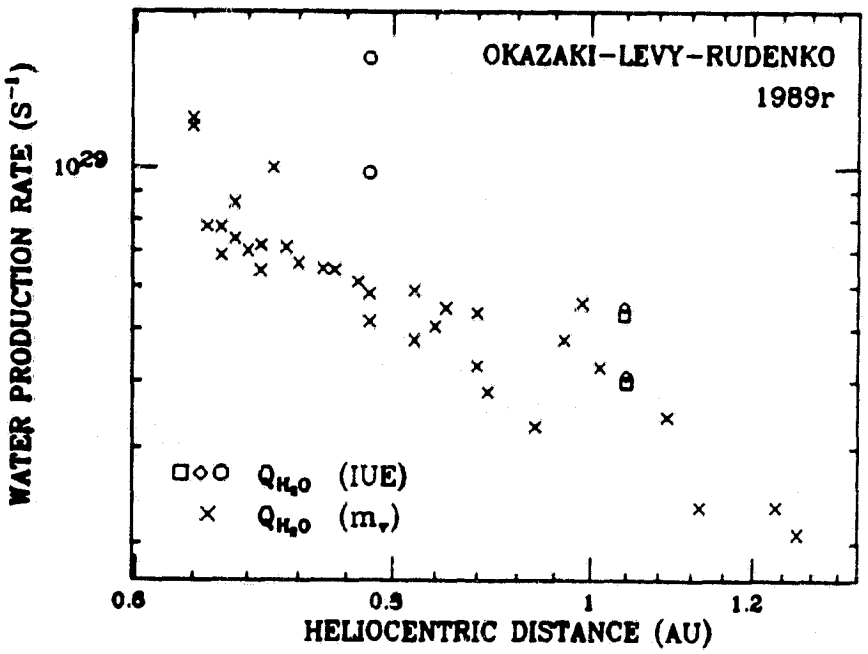

Figure 2. For comet O-L-R, postperihelion water production rates derived from OH emissions using older (squares) and newer (diamonds) vectorial codes are plotted with rates derived from visual magnitudes. Two estimates of the water production rate from the OI feature at 1304 Å are also plotted (hexagons); the upper is from a Haser model, the lower from comparison with comet Bradfield 1979X.

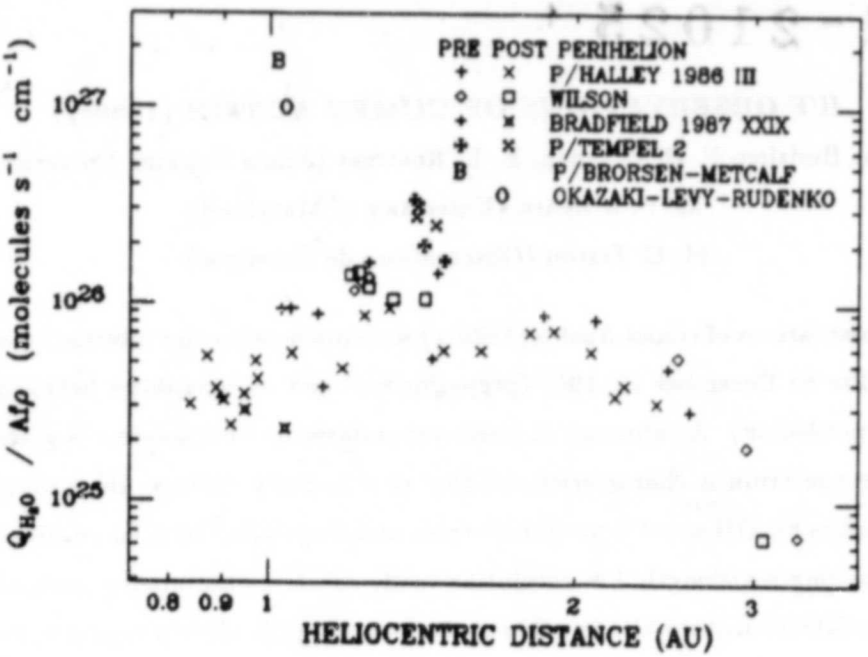

Figure 3. The gas-to-dust ratios of both comet P/Brorsen-Metcalf and comet Okazaki-Levy-Rudenko are much higher than those of other recent comets. $Af\rho$, a quantity approximately proportional to the dust production rate, is derived from reflected solar continuum measurements.

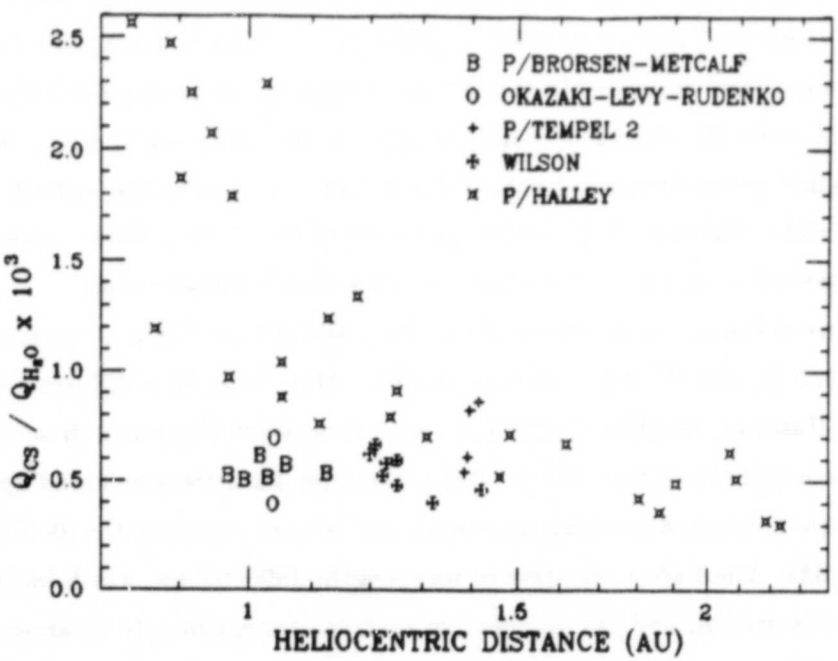

Figure 4. The relative CS production rate was derived from CS emissions around 2576 Å using a Haser model. Comets Brorsen-Metcalf and O-L-R both have lower Q_{CS}/Q_{H_2O} ratios than comet Halley at similar heliocentric distances.

513-90 N91-21025

p.5

IUE OBSERVATIONS OF COMET AUSTIN (1989c_1)

S. A. Budzien, P. D. Feldman, E. E. Roettger (Johns Hopkins University)
M. F. A'Hearn (University of Maryland)
M. C. Festou (Observatoire de Besançon)

Observations of comet Austin (1989c_1) were made using the *International Ultraviolet Explorer* satellite on December 22, 1989 (preperihelion) and on nine dates between May 7 and 24, 1990 (postperihelion). A summary of observation dates and parameters is given in Table I. The ultraviolet spectrum is characteristic of that of non-dusty comets. Here we present some preliminary results for OH and CS prodution rates and dust-reflected solar continuum emission based upon the long wavelength, low resolution mode spectra; photometry using the *IUE* Fine Error Sensor; a detection of the CO fourth positive system in the short wavlength, low dispersion spectra; and an upper limit on S_2.

Figure 1 depicts the H_2O production rates both pre- and postperihelion, based upon OH solar resonance fluorescence and a vectorial model (Festou, 1981) which was circulated by Festou in 1988. The preperihelion water production rate was 1.4×10^{29} s^{-1} at a heliocentric distance of 2.2 AU, and the postperihelion values are 1.0, 0.96, 0.85, 0.78, and 0.60×10^{29} for May 9.4, 13.7, 16.8, 19.7, and 24.3, 1990 at heliocentric distances from 0.80–1.13 AU. Since the longer exposures were saturated in the OH (0–0) band, for some dates the H_2O production rate was derived from the OH (1–0) band, scaling by the observed (0–0)/(1–0) band ratio. The post-perihelion production rate roughly follows an $r^{-1.6}$ power law during the period of observations. Production rates from visible photometry based on a Haser model (Schleicher, 1990) are also plotted, scaled by 1.7 to approximate vectorial model values.

Figure 2 shows the behavior of the H_2O and CS production rates, the $Af\rho$ dust parameter at 2950 Å, and the FES photometry from May 7–24. The CS prodution rate was derived using a Haser model (Haser, 1957), because the parent CS_2 has a dissociative lifetime ($\sim$ 500 s) short compared to CS ($\sim 10^5$ s). The CS column densities were based upon either the CS (0–0) or CS (0–1) band, depending upon exposure length, using the CS (0–0) g-factor from Jackson *et al.*, 1982. The FES is sensitive to wavelengths 380–650 nm, which include emissions of CN, C_2, and continuum, and has an effective aperture approximately 18 arcseconds square. The FES counts follow an $r^{-3.8}$ power law when normalized by heliocentric distance squared and geocentric distance to scale as a production rate. The $Af\rho$ parameter, which is the product of grain albedo, aperture filling factor, and projected aperture radius, assumes an r^{-2} dust density

distribution and is proportional to a dust grain production rate. The flattening of $Af\rho$ at larger heliocentric distances may be due to a combination of the decreasing geocentric distance and a dust distribution which falls off more sharply than r^{-2}. Using the $Q_{H_2O}/Af\rho$ as a measure of the gas-to-dust ratio, we find Austin at 1.0×10^{27} $s^{-1}cm^{-1}$ on May 16.8 is comparable to that of Okazaki-Levy-Rudenko and about 15 times higher than Halley at similar heliocentric distances (Roettger *et al.*, 1990).

Finally, we used multiple linear regression and the ratio-of-variances methods to fit synthetic spectra to observed spectra to determine CO and S_2 abundances. The CO fourth positive bands were observed in several short wavelength exposures with various signal-to-noise levels. From the May 9.4 exposure (Figure 3) we derive a CO production rate of $2.0 \pm 0.9 \times 10^{27}$ s^{-1}, or 2% the water production rate, based on a Haser model, and the solar maximum g-factors of Durrance (1981). From a 440 minute, long wavelength exposure on May 24.5, we obtained an S_2 production rate upper limit of upper limit of 2×10^{24} s^{-1}, or 3×10^{-5} that of water. For comparison, this abundance is an order of magnitude below the S_2 abundance of comet IRAS-Araki-Alcock (1983VII) when the species was discovered (A'Hearn *et al.*, 1983).

Acknowledgements

This work was supported by NASA grants NSG-5393 to the Johns Hopkins University and NAG 5-252 to the University of Maryland.

References

A'Hearn, M. F., Feldman, P.D., and Schleicher, D. G. 1983. *Ap. J.*, **274**, L99.

Durrance, S. T. 1981. *J. Geophys. Res.*, **86**, 9115.

Festou, M. C. 1981. *Astron. Astrophys.*, **95**, 69.

Haser, L. 1957. *Bull. Acad. Roy. Sci. Liége*, **43**, 740.

Jackson, W. M., Halpern, J. B., Feldman, P. D., and Rahe, J. 1982. *Astron. Astrophys.*, **107**, 385.

Roettger, E. E., Feldman, P. D., Budzien, S. A., A'Hearn, M. F., and Festou, M. C. 1990. Abstract submitted to *Workshop on Observations of Recent Comets.*

Schleicher, D. G. 1990, personal communication.

ORIGINAL PAGE IS
OF POOR QUALITY

TABLE I

SUMMARY OF *IUE* OBSERVATIONS OF COMET AUSTIN ($1989c_1$)

Year	1989	1990								
Month	Dec	May								
Day	22.31	7.45	9.37	11.46	13.68	13.75	16.84	19.69	19.75	24.33	24.49
r (AU)	2.209	0.795	0.839	0.879	0.924	0.925	0.987	1.042	1.044	1.132	1.135
Δ (AU)	2.248	0.445	0.410	0.377	0.343	0.342	0.299	0.267	0.266	0.238	0.238
$B_{OH(00)}$ (kR)	2.43		96.7		73.6			46.4		29.4	
$B_{OH(10)}$ (kR)						3.56	2.86		2.27		
N_{OH} (10^{13}cm^{-2})	2.95		13.6		11.4	10.4	9.4	8.2	8.3	5.7	
Q_{H_2O} (10^{29}s^{-1})	1.4		1.0		0.96	0.88	0.85	0.78	0.79	0.60	
$B_{CS(00)}$ (R))			1310		689	761	552	598	526	327	
$B_{CS(01)}$ (R)		189		175							41
N_{CS} (10^{12}cm^{-2})		1.20	1.31	1.35	0.84	0.93	0.77	0.93	0.82	0.60	0.53
Q_{CS} (10^{25}s^{-1})		6.2	6.3	6.1	3.5	3.9	3.0	3.4	3.0	2.1	1.9
$Af\rho$ (cm)		133		97			84		92		
N_{CO} (10^{14}cm^{-2})									0.5 ± 0.2		
Q_{CO} (10^{27}s^{-1})									2.0 ± 0.9		
N_{S_2} (10^{10}cm^{-2})											< 1.7
Q_{S_2} (10^{24} s^{-1})											< 2.2

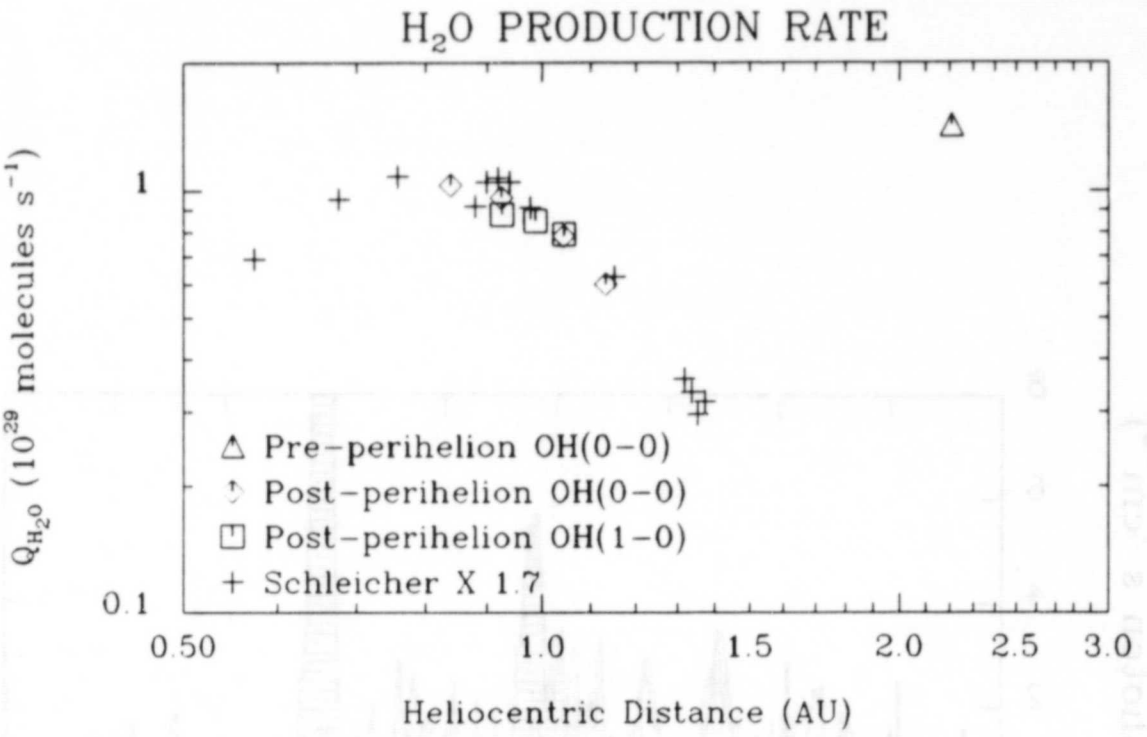

Figure 1: H_2O production rates vs. heliocentric distance.

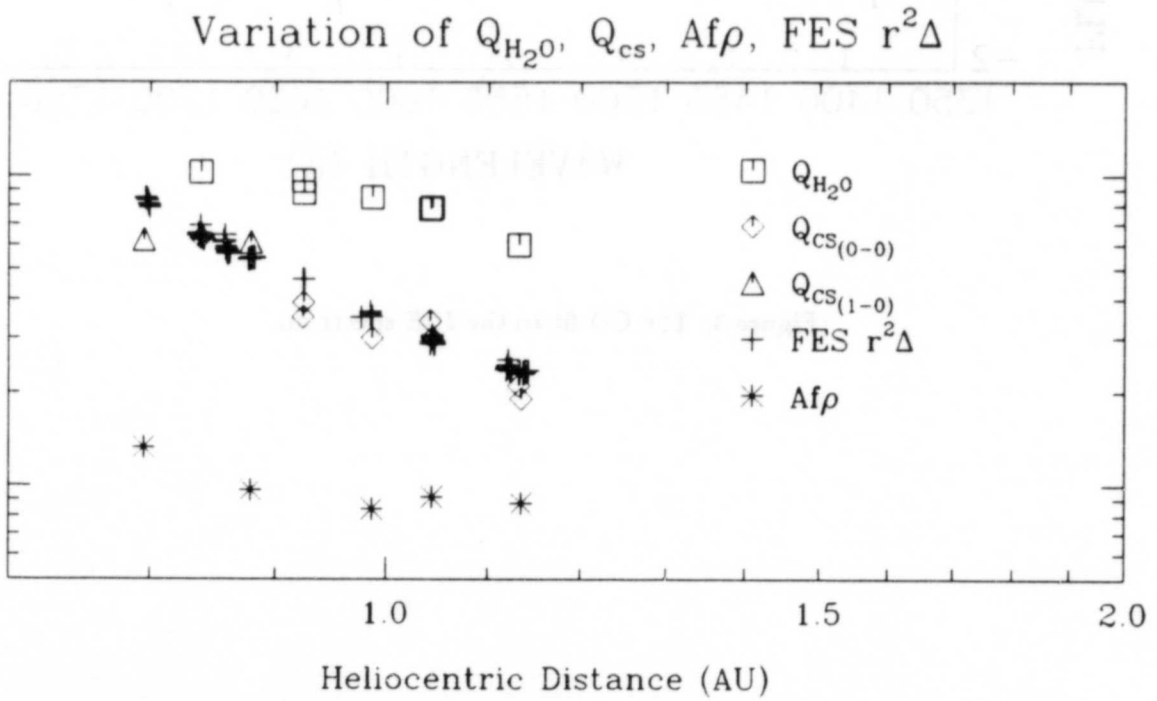

Figure 2: Postperihelion behavior of several species vs. heliocentric distance.

ORIGINAL PAGE IS
OF POOR QUALITY

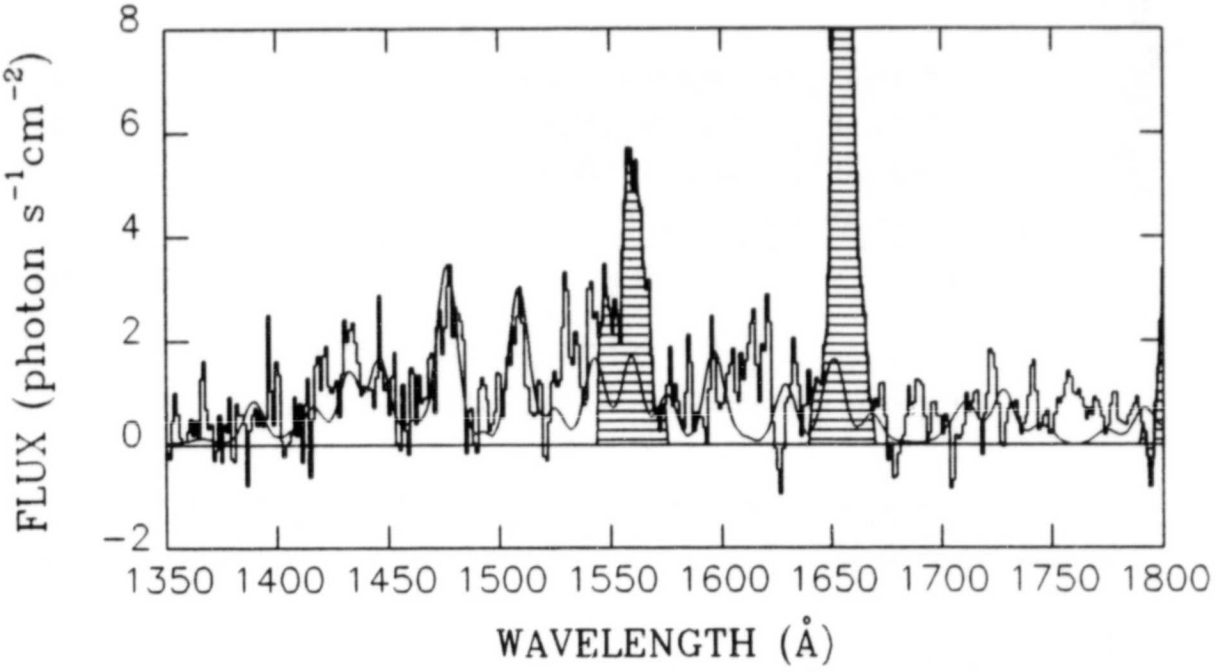

Figure 3: The CO fit to the *IUE* spectrum.

N91-21026

INFRARED SPECTROSCOPY OF COMETS

M. DiSanti, M. Mumma, S. Hoban, D. Reuter,
F. Espenak (NASA/GSFC), A. Storrs,
J. Lacy, R. Parmar (U. Texas) and R. Joyce (NOAO)

We have been engaged in an observational search for cometary parent molecules using infrared spectroscopy in the 1-5 μm region. The investigation involved two different observing programs, one at moderate spectral resolution and one at fairly high resolution.

The lower resolution program has been used to study cometary spectra in the vicinity of 3.5 μm at $\lambda/\Delta\lambda \approx 10^3$. Comets P/Brorsen-Metcalf (1989o), Okazaki-Levy-Rudenko (1989r) and Austin (1990c1) have been observed with the Cryogenic Spectrometer (CRSP) at Kitt Peak. The detector incorporated an InSb array with 58 spatial elements, each 2.7″ on the sky, and 62 spectral channels per spatial element.

An, as yet, unidentified feature has been detected at approximately 3.52 μm in Comet Austin (on 1990 May 4, 5 and 6). The feature is possibly present in P/Brorsen-Metcalf (observed on 1989 August 23 and 25), as well. Comet Okazaki-Levy-Rudenko exhibited continuum emission only in this spectral region at the time of our observations (1989 November 14 and 16). The data will be presented, and the relationship between the 3.52 μm feature and cometary activity (e.g. water production rate, visibility of the 3.4 μm emission feature) will be discussed.

The high-resolution ($\lambda/\Delta\lambda \approx 2\times10^4$) program probed comet Austin in the 4.8 μm region. These observations, conducted UT 1990 May 14-17 with the University of Texas Infrared Echelle Spectrometer (IRSHELL) on the IRTF atop Mauna Kea, were used to search for emission lines comprising the (1-0) vibration-rotation band of the ground electronic state of CO.

The instrument used a Si-As impurity band array detector with 10 spatial elements, each 1″ on the sky, and 64 spectral channels per spatial element. Two grating settings were employed. One was centered between the P2, P3 lines and the other between R2, R3. Retrieval of these lines allows a probe of the population distribution of levels $J'=1$ through 4 of the excited ($v'=1$) vibrational state within the ground electronic state of CO. Knowledge of this distribution can be used to constrain the rotational temperature. Preliminary analysis suggests the P3 line was present UT May 16 at roughly the 5σ level. Results concerning the existence of other lines, and physical conditions inferred therefrom will be discussed.

N91-21027

Comparison of p/Brorsen-Metcalf and p/Halley in the Thermal Infrared

5,5-90

David K. Lynch[a] and Ray W. Russell[a]
Space Sciences Laboratory
The Aerospace Corporation

Martha S. Hanner[a]
Jet Propulsion Laboratory

David J. Lien[a]
Steward Observatory
Bucknell University

[a] Visiting Astronomer, Infrared Telescope Facility, operated by the University of Hawaii under contract from the National Aeronautics and Space Administration

This work was supported by the Aerospace Sponsored Research Program in the Space Sciences Laboratory.

I. Introduction

Of the periodic comets, only comets Halley and Brorsen-Metcalf have periods of the order of 75 years and are bright enough to study spectroscopically in the infrared. In this paper we present thermal IR spectroscopy of comet p/Brorsen-Metcalf near perihelion and compare the results to comet p/Halley.

II. Observations

Spectra were obtained on comet p/Brorsen-Metcalf in the 8 to 13 μm region with a resolving power $\Re = \lambda/\Delta\lambda$ of about 50 using the 3.0 meter Infrared Telescope Facility on Mauna Kea with the liquid He-cooled facility circular variable filter (Tokunaga 1986) on August 28, 29, 30 and Sept. 4, 5, and 6, 1989 UT (14-6 days before perihelion). North-south chopper throws of 20 arc sec were used with a 7 arc sec aperture (5050 km at the comet) in August and 60 arc sec N-S chop with a 9.5 arc sec aperture in September (6860 km at the comet).

III. Results

In all, six 10 μm spectra of comet Brorsen-Metcalf were obtained. Within the 3-8% uncertainties, there was no variation in the shape of the spectra. Figure 1 shows one spectrum obtained on September 5, 1990 UT (R = 0.50, Δ = 1.00). The most obvious aspect of the spectra is their smoothness. Noticeably absent from the spectrum of Comet p/Brorsen-Metcalf in Figure 1 is any evidence for silicate emission. Indeed, no spectral feature was present at the 5% level. Also shown is a greybody fit to the data, which gives T = 399 K, consistent with the temperatures obtained by IR photometry (Lynch et al. 1990).

Figure 2 shows the spectrum of comet p/Halley obtained by Campins and Ryan (1989) taken with the facility CVF at the IRTF on Jan 16.08 UT (R = 0.79, Δ = 1.42) with an 8.2 arc sec aperture. Comet Halley displayed a strong, structured emission feature that Campins and Ryan identified with crystalline olivine.

IV. Discussion

In contrast to comet p/Halley which displayed significant photometric outbursts and brightness changes (Tokunaga et al. 1986; Lynch and Russell 1988), comet p/Brorsen-Metcalf showed little photometric variability. We note, however, that estimates of variability depend on the regularity and duration of observation. Halley was scrutinized closely for over a year whereas comet B-M was only observed episodically.

Like virtually all comets, both Halley and Brorsen-Metcalf showed IR color temperatures that exceeded the equilibrium by ~5% and ~20% respectively. The enhancement in temperature must occur via a small Q_{abs} in the IR and the usual assumption involves small grains. Grains small enough to show a significant temperature excess are, almost by definition, optically thin and will therefore show any band structure present in their emissivity curves (as opposed to optically thick particles which cannot show band structure in comets). If we adopt the small grain hypothesis as the origin of the temperature excess, then based on the featureless 8-13 μm spectrum and the detection of the 3.4-3.6 μm emission features by Tokunaga and Brooke (private communication) which are usually associated with carbon-rich species, then small carbon grains are the most likely candidates for the cometary dust population in Comet Brorsen-Metcalf. In contrast, the dust in comet p/Halley exhibited strong silicate emission, usually associated with oxygen-rich dust, as well as highly variable emission in the IR.

V. Summary and Conclusions

Except for their absolute brightness and similar orbits, comets p/Brorsen-Metcalf and p/Halley could hardly be more dissimilar. This is especially true of their IR spectra: Halley showed strong structured silicate emission, B-M showed no silicate emission. Halley was highly variable, B-M displayed no outburst activity or any variation which departed from a brightness variation that was monotonic with heliocentric distance. Indeed, if we were to ask what comets, periodic or otherwise, most resembled these two comets,

we would have to say that IRAS-Araki-Alcock (Hanner et al. 1985a; Feierberg et al. 1984), Grigg-Skjellerup (Hanner et al. 1984) and Churyumov-Gerasimenko (Hanner et al. 1985b) were comparable to B-M, while p/Bradfield 1987s (Lynch et al. 1989; Hanner et al. 1990; Russell et al. 1990) was most like p/Halley (Campins and Ryan 1989). The marked dissimilarities between the two comets suggests that the periodic comets do not comprise one class, but rather have very different histories.

VI. Acknowledgements

We are indebted to the IRTF staff for their support, particularly Ron Koehler, George Koenig, and Bill Golisch. M. Hanner's research was carried out at the Jet Propulsion Laboratory, California Institute of Technology, under contract with the National Aeronautics and Space Administration (Planetary Astronomy program). D. Lien acknowledges support as a JPL Summer Faculty Fellow. This work was supported by the Aerospace Sponsored Research Program in the Space Sciences Laboratory.

References

Campins, H. and Ryan, E. 1989 Ap.J., 341, 1059-1066.

Feierberg, M.A., Witteborn, F.C., Johnson, J.R. and Campins, H., 1984 Icarus, 60, 449-454

Hanner, M.S. Aitken, D.K., Knacke, R., McCorkle, S., Roche, P.F. and Tokunaga, A.T. 1985a Icarus, 62, 97-109.

Hanner, M.S., Aitken, D., Roche, P.F. and Whitmore, B. 1984 A.J. 89, 170.

Hanner, M.S., Newburn, R.L., Gehrz, R.D., Harrison, T., Ney, E.P., and Hayward, T.L. 1990 A.J., 348, 312-321.

Lynch, D. K. and R. W. Russell 1988, Proceedings of the NASA/Cornell Workshop on "Infrared Observations of Comets Halley and Wilson and Properties of the Grains," Aug. 10-12, 1987, p. 166, Cornell University, Ithaca, NY, NASA CP-3004.

Lynch, D.K., Russell, R.W. and Campins, H. 1989, "Contributed Papers", IAU Symposium #135 Interstellar Dust, Santa Clara, CA, July 26-30, 1988 A. Tielens and L. Allamandola, Ed. NASA CP-3036, 417-422.

Lynch, D.K., Russell, R.W., Hanner, H. and Lien, D. 1990 (comet Brorsen-Metcalf submitted).

Russell, R.W., Lynch, D.K. and Chatelain, M. 1990, Comet Bradfield 1987s (in preparation).

Tokunaga, A. 1986 "The Infrared Telescope Facility Photometry Manual," IRTF, Institute for Astronomy, Univ. Hawaii, Honolulu.

Tokunaga, A.T., Golisch, W.F., Griep, D.M., Kaminskim C.D. and Hanner, M.S. 1986 A.J., 92 (no.5), 1183-1190.

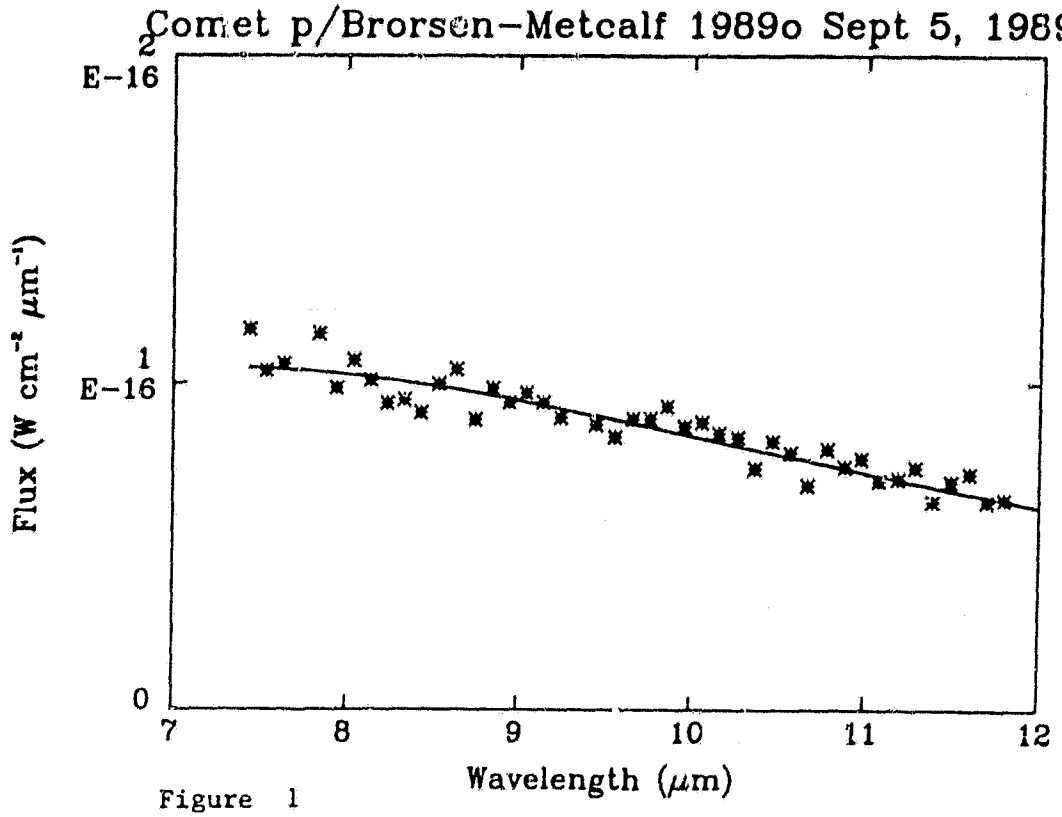

Figure 1

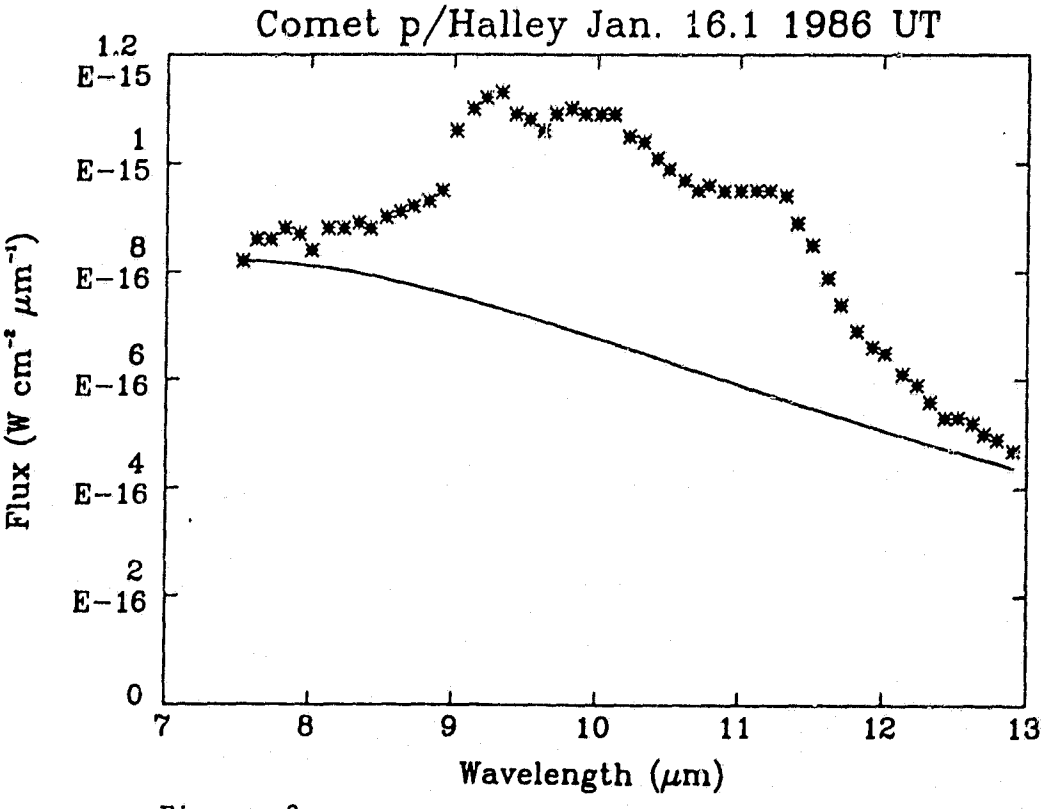

Figure 2

Walter Huebner
How well do the laboratory data of amorphous and crystalline olivine fit the Comet Bradfield observations? How does one produce crystalline olivine? Are there other materials, particularly non-silicates that could also explain the observed spectrum?

David Lynch
The laboratory data, combined with particle size distributions (which lead to temperature distribution) fit the observed data reasonably well. How does one produce crystalline olivine? There are lots of ways to do that. I think the real question is why should crystalline olivine dominate over amorphous olivine. A match in spectral shapes between laboratory and comet data does not nail down an identification; it only suggests one. Given the many processes that can alter the crystalline structure in comets (Cosmic rays, UV, chemistry, thermal cycling) I am amazed that the observers (including myself!) have been so eager to make mineralogical identification. There are many minerals that give plausible fits, mostly silicates. I would like to note that the best fit I could find for the 12.2 μm feature in Comet Wilson was a calcium tungstate!

Walter Huebner
How does an amorphous silicate become crystalline?

Comment by Ray Russell:
If grains of amorphous silicate are heated they can undergo a phase transformation to the crystalline form. Laboratory experiments with heating above 500 K, specifically to 700 K for hours, turns the amorphous material to crystalline form. There is a range of temperatures over different time periods that will accomplish this (i.e., 500 K for days would be expected to do a similar job as 700 K for hours). This has not been well documented, i.e., we have not made measurements of time required versus temperature.

David Lynch
We think this mechanism could happen for periodic comets whose volatiles would be cleaned from the surface, leaving a crust that can be heated repeatedly.

OH RADIO OBSERVATIONS OF COMETS P/BRORSEN-METCALF (1989o), OKAZAKI-LEVY-RUDENKO (1989r), AARSETH-BREWINGTON (1989a1) AND AUSTIN (1989c1) AT THE NANCAY RADIO TELESCOPE.

N91-21028

D. Bockelée-Morvan, J. Crovisier, E. Gérard, G. Bourgois

Observatoire de Paris, Section de Meudon, F-92195 Meudon, France

Abstract

The 1667 MHz and 1665 MHz transitions of the OH radical were recently monitored in several comets with the Nançay radio telescope: P/Brorsen-Metcalf (1989o) (August 4 to October 31, 1989), Okazaki-Levy-Rudenko (1989r) (October 3 to December 2, 1989), Aarseth-Brewington (1989a1) (December 8 to 30, 1989) and Austin (1989c1) (February 15 to June 14, 1990). We present gas expansion velocities measurements obtained from the analysis of the line shapes and discuss the long term variations of the water production rate, as measured from the OH radio lines. On October 13, 1989, we fortuitously observed the occultation of a background source by comet Okazaki-Levy-Rudenko (1989r). A preliminary report of this observation is given. Further analysis of the data is continuing.

Introduction

Thanks to their high spectral resolution, the observations of the OH 18-cm radio lines are a powerful tool to probe the neutral gas expansion velocity in the outer coma. This parameter is a requisite to the conversion of cometary molecular signals into production rates and is fundamental for the understanding of the thermodynamic of the coma. In order to separate the contribution of the OH ejection velocity v_d from that of the OH-parent velocity v_p in the OH radio profiles, Bockelée-Morvan et al. (1990) developed a deconvolution method, which consists in fitting trapezia to the observed spectra. The H_2O velocity is then derived from the half large base B_l of the best trapezium, which is assumed to be close to v_p+v_d.

Gas expansion velocities

The trapezoidal method was applied to several comets, including P/Halley, observed at Nançay over a variety of heliocentric distances and production rates. The inferred v_p were found to vary in the range 0.5 to 2 km s^{-1} and to depend, as expected from thermodynamical models, both on rh and on the gas production rate (Bockelée-Morvan et al., 1990).

As a complementary study, trapezoidal fitting has been performed to some selected integrated spectra of comets P/Brorsen-Metcalf (1989o), Okazaki-Levy-Rudenko (1989r), Aarseth-Brewington (1989a1) and Austin (1989c1). Fig. 1 shows the spectrum of comet Austin observed from May 21 to 25, 1990 with the fitted trapezium. The results of the fits, i.e. the half larger base B_l and the half smaller base B_s of the best trapezia with their 1-sigma formal errors, are given in Table 1, together with the observational parameters. Outflow velocities can be readily deduced by subtracting v_d = 0.9 km s^{-1} from B_l, according to our best observational estimate of the OH ejection velocity (one should note that the water photodissociation model of Crovisier (1989) predicts a somewhat larger value of 1.05 km s^{-1}).

The observations performed at small rh (< 1 AU) confirm the global increase of the outflow

velocity with decreasing heliocentric distances (Table 1). Outflow velocities as large as 1.6 km s^{-1} are found at 0.5 AU for production rates on the order of 10^{29} s^{-1}. On the other hand, when observed at large heliocentric distances, comets with similar production rates exhibit outflow velocity always below 1 km s^{-1}. The observations performed near rh = 1 AU are in agreement with the general trend of the outflow velocity with increasing production rate for constant rh found by Bockelée-Morvan et al. (1990) : at rh $\simeq$ 1 AU and below Q(OH) = 5 10^{28} s^{-1}, v_p is in the range of 0.7-0.8 km s^{-1}; a steep increase of the outflow velocity with increasing production rate then occurs at Q(OH) = 10^{29} s^{-1}, reaching values larger than 1 km s^{-1} and on the order of 1.8 km s^{-1} for Q(OH) = 6 10^{29} s^{-1}. For large rh (> 1 AU) and small Q(OH) (< 5 10^{28} s^{-1}), most inferred H_2O velocities are below 0.8 km s^{-1}.

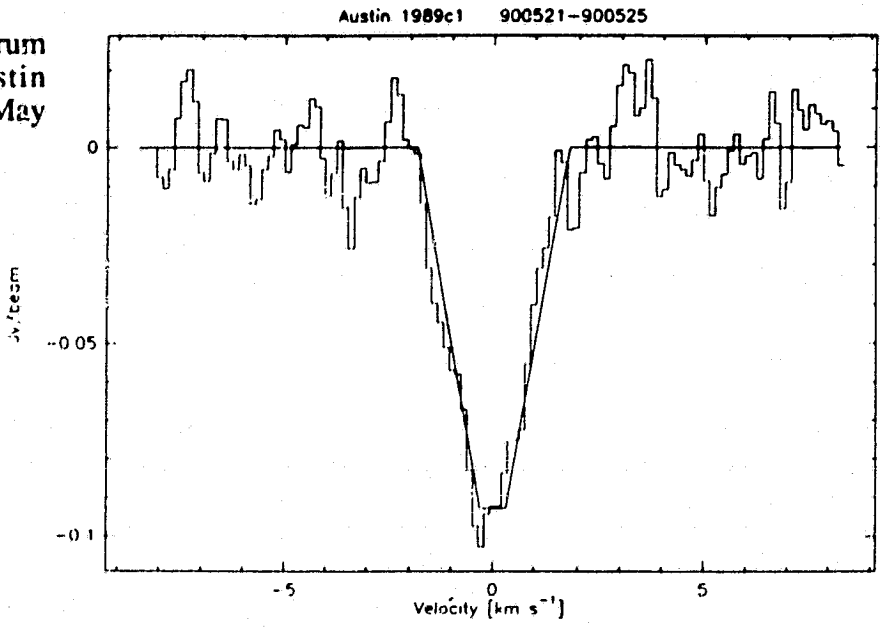

Figure 1: OH 18-cm spectrum observed in comet Austin (1989c1) from May 21 to May 25 and the fitted trapezium.

OH production rates

As detailed by Gérard (1990) and Crovisier and Schloerb (1990), the determination of the OH-parent production rate from the observed OH 18-cm flux density (Table 1) heavily relies on the density and excitation models assumed. We use here the model of Bockelée-Morvan et al. (1990), which brought radio OH production rates of comet Halley into reasonable agreement with UV-derived values. This model uses the Haser-equivalent formalism, in which the H_2O expansion velocities are those derived by trapezoidal fitting. In addition, the quenching of the OH maser lines by collisions is taken into account, using the quenching radius measured by Gérard (1990) in comet P/Halley and scaling the value for the production rate and heliocentric distance as discussed in Schloerb (1988). For comparison, OH production rates calculated with the set of Haser-equivalent parameters referred to as 1986a, assuming no quenching effect, are also given in Table 1. Both set of production rates are computed using the OH 18-cm maser inversion curve of Despois et al. (1981).

From the radio measurements, the OH production rate in P/Brorsen-Metcalf varied little through August 1989, from about 1 to 2 10^{29} s^{-1}. Roettger et al. (this workshop) report water production rates between 4.2 10^{28} and 6.7 10^{28} s^{-1} from July 27 to August 5, 1989, while DiSanti et al. (this workshop) measured about 9 10^{28} s^{-1} on August 8, from observations of the O_I ^1D line. For comet Okazaki-Levy-Rudenko, we infer production rates between about 2 and 7 10^{28} s^{-1} as the comet approaches the Sun from 1 to 0. 65 AU. For the pre-perihelion observations

ORIGINAL PAGE IS
OF POOR QUALITY

Table 1: Parameters of the OH spectra.

date	delta AU (1)	rh AU (2)	Vh km/s (3)	inv (4)	inv (5)	Tbg K (6)	S mJy.km/s (7)	Bl km/s (8)	Bs km/s (9)	Q[OH] E28s-1 (10)	Q[OH] E28s-1 (11)
P/Brorsen-Metcalf 1989o											
890804-890814	0.63	0.91	-29.7	-0.06	-0.11	3.0	-69 11	2.06 0.44	0.13 0.69	14.0 2.2	9.2 1.4
890826-890828	0.81	0.61	-24.3	0.38	0.35	3.0	154 11	2.21 0.17	0.17 0.52	9.2 0.9	7.2 0.7
890829-890831	0.87	0.57	-21.6	0.49	0.48	3.0	235 16	1.98 0.14	0.98 0.16	15.2 1.3	10.5 0.9
890901-890903	0.93	0.53	-17.8	0.42	0.43	3.0	194 14	2.12 0.16	1.13 0.15	19.5 1.6	12.5 1.0
Okazaki-Levy-Rudenko 1989r											
891003-891008	1.43	0.99	-25.1	0.33	0.28	3.0	27 8	1.39 0.42	1.05 0.35	1.8 0.6	2.0 0.6
891010-891015	1.35	0.89	-23.5	0.43	0.40	3.0	84 10	2.14 0.27	0.42 0.47	5.5 0.7	4.9 0.6
891017-891026	1.22	0.78	-19.9	0.50	0.51	3.0	117 4	1.83 0.07	0.47 0.12	6.7 0.4	6.0 0.4
891104-891108	0.91	0.65	-6.7	-0.30	-0.35	3.0	-82 11	2.29 0.33	1.24 0.41	6.5 0.9	5.5 0.7
891120-891123	0.59	0.68	11.6	-0.16	-0.23	3.0	-76 9	1.52 0.22	1.05 0.20	5.6 0.6	4.4 0.5
Aarseth-Brewington 1989a1											
891208-891217	1.08	0.52	-37.4	-0.24	-0.25	3.0	-99 7	2.89 0.21	1.72 0.22	22.4 1.8	15.4 1.3
Austin 1989c1											
900215-900315	1.64	1.02	-33.7	-0.16	-0.19	3.0	-51 5	2.19 0.26	0.51 0.36	11.5 1.2	9.6 1.0
900316-900325	1.39	0.64	-35.2	-0.19	-0.22	3.0	-68 6	2.63 0.27	0.79 0.34	20.6 2.9	15.1 2.1
900403-900405	1.15	0.38	-20.0	0.50	0.51	3.0	88 16	2.37 0.52	0.65 0.58	17.5 2.8	12.8 2.1
900421	0.75	0.48	31.5	-0.28	-0.24	3.0	-97 26	2.25 0.25	1.97 0.45	10.3 2.8	8.0 2.2
900516-900520	0.28	1.01	33.9	-0.18	-0.09	3.0	-102 10	1.70 0.16	1.07 0.20	2.0 0.3	2.1 0.3
900521-900525	0.25	1.11	33.1	-0.23	-0.15	3.0	-197 7	1.81 0.08	0.32 0.14	3.6 0.2	3.1 0.2
900526-900528	0.24	1.19	32.5	-0.26	-0.19	3.0	-186 11	1.44 0.08	1.04 0.09	1.9 0.1	2.7 0.2
900529-900530	0.26	1.23	32.1	-0.27	-0.22	3.0	-274 13	1.75 0.09	0.44 0.14	4.4 0.4	3.9 0.3
900531-900601	0.27	1.27	31.9	-0.28	-0.23		-437 17	1.62 0.07	0.13 0.17		
900603-900609	0.37	1.30	31.0	-0.28	-0.25	3.0	-117 9	1.60 0.14	0.24 0.22	1.9 0.2	2.3 0.2

(1) distance to the Earth.
(2) distance to the Sun.
(3) comet's heliocentric radial velocity.
(4) OH maser inversion from Despois et al (1981) which is used for computing Q[OH].
(5) OH maser inversion from Schleicher and A'Hearn (1988).
(6) assumed background temperature for the computation of Q[OH].
(7), (8), (9) parameters of the trapezoidal fit: area, larger half base, smaller half base.
(10) OH production rate computed according to Bockelee-Morvan et al. (1990) (see text).
(11) OH production rate computed using the OH density model 1986a, i.e. OH and OH-parent scalelengths of 1.E5 and 6.E4 km respectively, OH radial velocity of 1.4 km/s. Collisional quenching is not included.
Entries (7), (8), (9), (10) and (11) are given with their rms error.

ORIGINAL PAGE IS
OF POOR QUALITY

Figure 2: Geometry of the occultation. The origin of coordinates is the comet centre. The thick kine shows the relative position of the background source between the beginning (B) and end (E) of the observation.

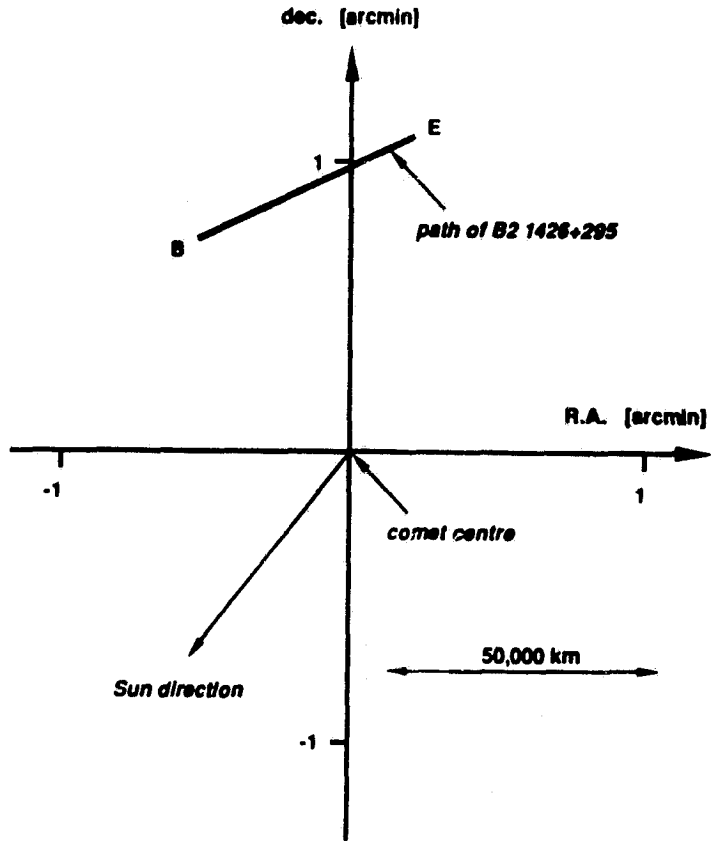

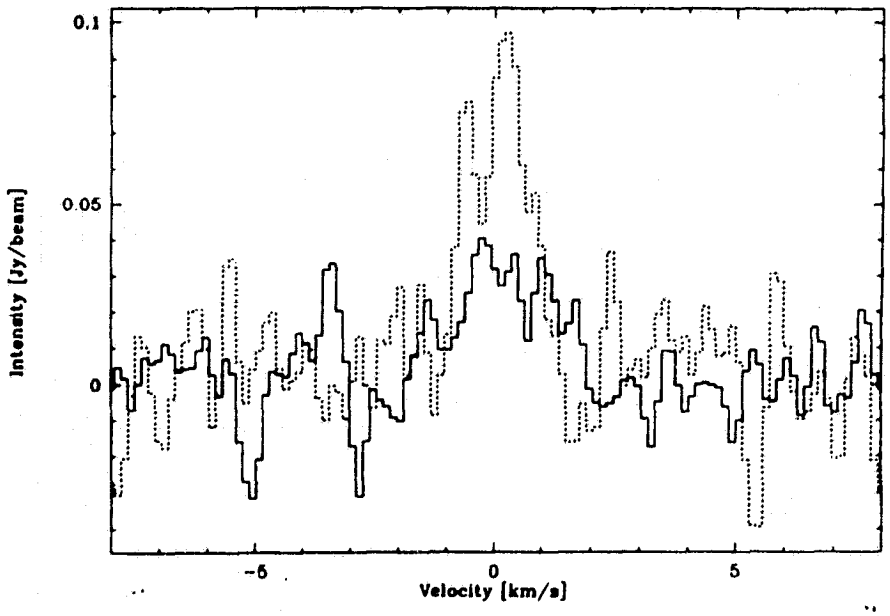

Figure 3: The OH spectrum observed on October 13.54 (dotted line) superimposed on the comparison spectrum averaged over the two preceding and two following days (full line).

of comet Aarseth-Brewington at rh $\simeq$ 0.5 AU, we derive an OH production rate of 2.2 10^{29} s^{-1}. From Table 1, it appears that the OH production rate in comet Austin was higher before perihelion than after, reaching 2 10^{29} s^{-1} at rh = 0.38 AU. A similar trend is present in the comet heliocentric magnitude. IUE OH observations lead to somewhat larger values than ours for the production rate of the end of May 1990 (6 10^{28} s^{-1} on May 24, Budzien et al., this workshop)

Comet Austin was hardly detected from April 6 to May 15 1990, mainly because the maser OH inversion rate was not favourable at that time. However, the observations performed during that period gave interesting results on the excitation mechanism of the cometary OH molecule: Schleicher and A'Hearn (1988) predict a change from absorption to emission at the heliocentric velocity of 35.1 km s^{-1}, while the model of Despois et al. (1981) predicts the turn-over at vh = 36.5 km s^{-1}. The observations from April 28 to May 9, which cover heliocentric velocities between 35.3 and 35.6 km s^{-1}, reveal a weak line in absorption and are in favour of Despois et al.'s model. On May 31 and June 1, comet Austin passed across the galactic plane, leading to an amplification by a factor of about 2 of its OH maser radio line. The exact amplification factor to be used for retrieving the OH production rate is still in study. Thus, in Table 1, we omit the production rate result.

Occultation

On October 13, 1989, we fortuitously observed the occultation of a background source by comet Okazaki-Levy-Rudenko (1989r) (Bockelée-Morvan et al. 1989). B2 1426+294, a point source of 0.4 Jy at 18 cm identified with a blue stellar object, passed at about 1' from the comet centre (corresponding to 60 000 km). The geometry of the event is shown in Fig. 2. The observed lines were enhanced by a factor of two with respect to the average of the spectra obtained before and after the occultation (Fig. 3). This is in agreement with the maser theory of the OH line excitation. There is a marginal evidence of a variation of the signal intensity during the occultation, while the line-of-sight to the source swept a path of about 50 000 km in the comet frame, which suggests that the OH distribution (or the excitation of the OH radicals) is not homogeneous within the coma (Crovisier et al., in preparation). The observation of such occultations is potentially very promising to investigate the coma structure, but such events are rare (only one is expected every several ten years at Nançay).

References

Bockelée-Morvan, D., Bourgois, G., Crovisier, J. and Gérard, E. 1989. IAU Circ. No 4882

Bockelée-Morvan, D., Crovisier, J. and Gérard, E., 1990. *Astr. Ap.* (in press)

Budzien, S.A., Feldman, P.D., Roettger, E.E., Festou, M.C. and A'Hearn, M.F., 1990. this workshop

Crovisier, J., 1989. *Astr. Ap.* **213**, 459

Crovisier, J. and Schloerb, F.P., 1990. in Comets in the Post-Halley Era, Edts R. Newburn and J. Rahe, Kluwer Academic Publishers, Dordrecht (in press)

Despois, D., Gérard, E., Crovisier, J. and Kazès, I., 1981. *Astr. Ap.* **99**, 320

DiSanti, M.A., Mumma, M.J., Hoban, S., Reuter, D.C. and Espenak, F., 1990. this workshop

Gérard, E., 1990. *Astr. Ap.* **230**, 489

Roettger, E.E., Feldman, P.D., Budzien, S.A., A'Hearn, M.F., and Festou, M.C., 1990. this workshop

Schleicher, D.G. and A'Hearn, M.F., 1988. *Ap. J.* **331**, 1058

Schloerb, F.P., 1988. *Ap. J.* **332**, 524

N91-21029

MILLIMETRE OBSERVATIONS OF COMETS P/BRORSEN-METCALF (1989o) AND AUSTIN (1989c1) WITH THE IRAM 30-m RADIO TELESCOPE.

P. Colom (1,2), D. Despois (3), D. Bockelée-Morvan (4), J. Crovisier (4) and G. Paubert (1)

(1) IRAM, Avenida Divina Pastora, 7, N.C., E-18012 Granada, Spain
(2) Centro Astronomico de Yebes, Apartado 148, E-19080 Guadalajara, Spain
(3) Observatoire de Bordeaux, BP 89, Avenue Pierre Sémirot, F-33270, Floirac, France
(4) Observatoire de Paris, Section de Meudon, F-92195 Meudon, France

Abstract

Millimetre observations with the IRAM 30-m telescope were conducted in comet P/Brorsen-Metcalf (1989o) on September 1989 and Austin (1989c1) on April and May 1990. The HCN J(1-0) and J(3-2) lines were detected in both comets. The HCN production rate relative to water in P/Brorsen-Metcalf is comparable to that previously measured in comet P/Halley, while that inferred in comet Austin might be smaller by a factor of two. The H_2CO 3_{12}-2_{11} transition, marginally observed in comet P/Brorsen-Metcalf, was firmly detected in May 1990 in comet Austin. Observations performed at offset positions suggest that the source of H_2CO might be distributed. The H_2CO abundance is on the order of 0.5% that of water for both comets, assuming a scalelength of 10^4 km at 1 AU from the Sun for the distributed source. During the May observing period of comet Austin, two new species were detected for the first time in a comet: hydrogen sulfide H_2S through its 1_{10}-1_{01} ortho line at 169 GHz, and methanol CH_3OH through J(3-2) $\Delta K = 0$ transitions at 145 GHz. Preliminary estimates of their abundances are 1.5 10^{-3} for H_2S and 8 10^{-3} for CH_3OH.

Observations

The observations were performed with the IRAM 30-m millimetre telescope on Pico Veleta in Spain. Comet P/Brorsen-Metcalf (1989o) was observed on September 2-7 1989 at rh = 0.51 AU from the Sun and Δ = 1 AU from the Earth. Comet Austin (1989c1) was first observed on April 2 1990 (close to its perihelion) at rh = 0.41 AU and Δ = 1.19 AU, and secondly in the May 21-25, 1990 period (around its perigee) at rh = 1.1 AU and Δ = 0.24 AU. We used four receivers in the double side band: 1. a 83-115 GHz SIS mixer receiver; 2. a 130-170 GHz SIS mixer receiver; 3. a 209-270 GHz SIS mixer receiver; 4. a 330-345 GHz cooled Schottky receiver. It was possible to use simultaneously 3 receivers, which allowed us to search for different lines at the same time. The backends consisted in two banks of 128x100 kHz channels (corresponding to a velocity resolution of 0.34 km s^{-1} and 0.11 km s^{-1} for the HCN lines at 89 GHz and 266 GHz respectively), and two banks of 512x1 MHz channels. In order to study the extension of the coma, observations at 6 arcsec and 12 arcsec North, East, South and West from the nucleus were performed in comet Austin during the May observing period. The observed integrated line areas or 3-sigma upper limits are shown in Table 1.

Hydrogen cyanide

The HCN J(1-0) (89 GHz) and J(3-2) (266 GHz) transitions were marginally detected in comet P/Brorsen-Metcalf. The HCN J(1-0) transition was only detected previously in comet Kohoutek 1973 XII and P/Halley despite many searches in other comets (Crovisier and Schloerb, 1990). Comet P/Brorsen-Metcalf is the first comet in which the HCN J(3-2) transition has been detected.

On April 2, the HCN J(1-0) line was not detected in comet Austin. However, during the May

Figure 1: The HCN J(1-0) spectrum of comet Austin observed on May 21 to 23, 1990 (centre and offset positions). Velocity scale is with respect to the comet rest velocity, for the F 2-1 main hyperfine component.

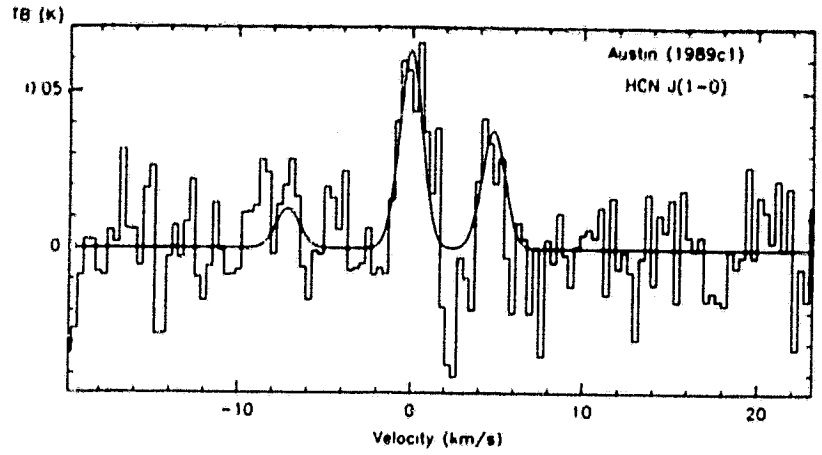

Figure 2: The HCN J(3-2) spectrum of comet Austin observed on May 23-24, 1990 (centre and offset positions).

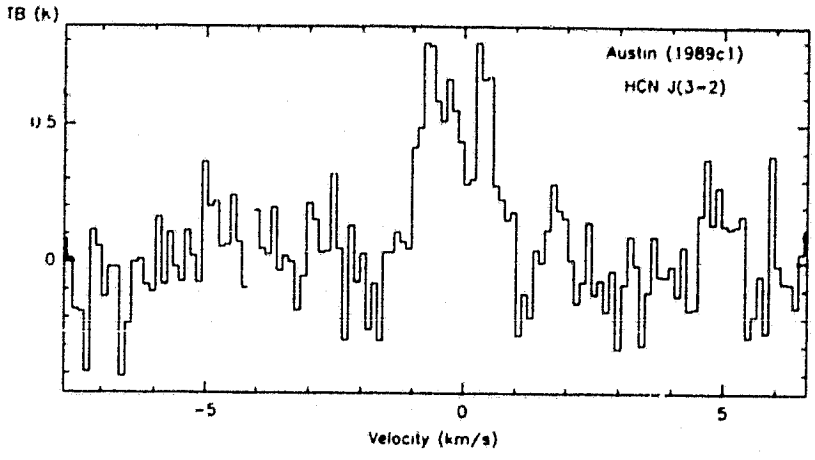

Figure 3: H_2CO 3_{12}-2_{11} spectrum of comet Austin observed on May 21, 22, 25 1990 (centre and offset positions).

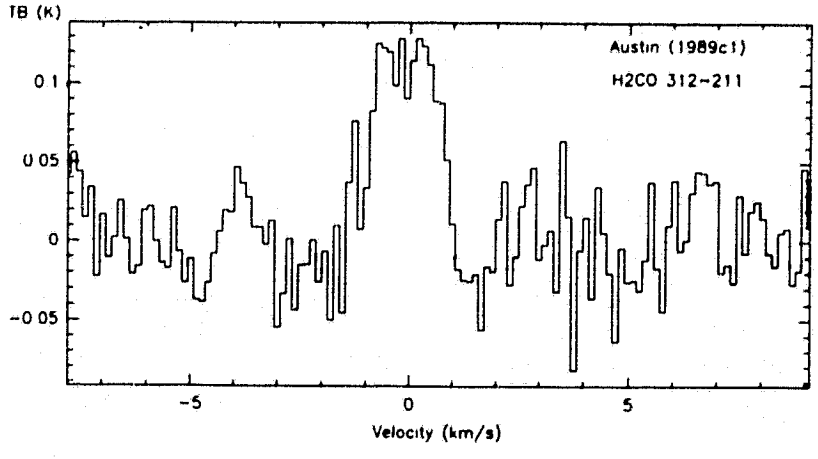

ORIGINAL PAGE IS
OF POOR QUALITY

observing session, both HCN J (1-0) and J(3-2) transitions were firmly observed in the comet (Bockelée-Morvan et al., 1990b; Crovisier et al., 1990a): some selected integrated spectra are shown in Figs 1 and 2.

In order to interpret the present observations in terms of HCN production rates, we used the observed J(1-0) intensities and the model of Crovisier (1987). The HCN abundance relative to water in P/Brorsen-Metcalf is in agreement with that of $\sim 10^{-3}$ measured in P/Halley (Table 1), but the HCN abundance in comet Austin is smaller by about a factor of 2. A similar deficiency was found in comet Wilson (1987 VII) (Crovisier et al., 1990b), suggesting a chemical difference in periodic and new comets.

Formaldehyde

The observations of the H_2CO 3_{12}-2_{11} transition at 226 GHz in comet P/Brorsen-Metcalf lead only to a marginal detection, with a signal-to-noise ratio of 4. However, it gave the first conclusive evidence for the possibility of observing cometary formaldehyde at millimetre wavelengths. Formadehyde was not detected in comet Austin in April. It was easily detected at 226 GHz in May (Bockelée-Morvan et al., 1990b), with a S/N ratio larger than 10 for the average spectrum obtained for May 21, 22, 25 shown in Fig. 3.

It has been suggested that formaldehyde gas originates from a distributed source in the coma (Snyder et al. 1989) which could be polyoxymethylene (POM) associated with the dust (Boice et al., 1990). Our observations of the 226 GHz H_2CO line performed at offset positions also suggest a distributed source for H_2CO. Indeed, formaldehyde is a short-lived molecule, with a photodissociation rate of $2.8\ 10^{-4}\ s^{-1}$ at 1 AU from the Sun, according to Huebner and Carpenter (1979). The line intensities expected for the 226 GHz transition at half-beam and one beam off the nucleus (6 arcsec and 12 arcsec corresponding to about 1100 km and 2200 km) are about 0.7 and 0.3 the intensity observed at the centre position, if one assumes that H_2CO comes directly from the nucleus, whereas the observed ratios are 0.8 ± 0.2 and 0.64 ± 0.14.

The density distribution of H_2CO in the coma being ill-known, it is difficult to give accurate estimates of its abundance. We tentatively compute production rates assuming a daugther Haser density distribution, with a parent scalelength of 10^4 km at 0.9 AU from the Sun and scaled proportionally to rh^2. We use a model where both collisional excitation and radiative excitation by the Sun are taken into account, and assume a kinetic temperature of 50 K in the coma. The derived production rates are given in Table 1: the H_2CO abundances relative to water are on the order of 0.5 % for both comets, i. e. much smaller than the 4.5 % found in comet P/Halley from the analysis of the 3.6 μm feature in the IKS-Vega spectrum attributed to H_2CO (Combes et al., 1988). For comparison, production rates computed using a parent distribution for H_2CO are also given in Table 1: as expected, much smaller abundances are derived for the May observing period of comet Austin.

Hydrogen sulfide

Hydrogen sulfide H_2S was unambiguously detected in comet Austin on May 23, 24 and 25 1990, through its 1_{10}-1_{01} transition at 169 GHz (Crovisier et al., 1990a), with a S/N ratio of 7 for the average spectrum shown in Fig.4. This is the first time that H_2S is observed in a comet, although it was highly suspected by the presence of H_3S^+ in the coma of P/Halley (Marconi et al., 1990).

A preliminary estimation of the H_2S production rate is given in Table 1. We assumed rotational LTE at 50 K and took a parent molecule density distribution. From the UV absorption spectrum of Lee et al. (1987) and the reference solar spectrum of Huebner and Carpenter (1979), we estimate the H_2S lifetime to be about 4000 s at 1 AU. H_2S is apparently a minor component of cometary atmospheres, with an abundance relative to water of $1.5\ 10^{-3}$.

Table 1: Line intensities and production rates

Molecule	Date	$\int T_B dv$[a] [K km s^{-1}]	Q [s^{-1}]	Q[H_2O] [s^{-1}]	Q/Q[H_2O]
P/Brorsen-Metcalf (1989o)					
HCN J(1-0)	89/09/04-07	0.18±0.03	3.0E26	2.5E29[b]	1.2E-3
HCN J(3-2)	89/09/02-03	0.96±0.21			
H_2CO 3_{12}-2_{11}	89/09/04-07	0.16±0.04	1.0E27[c]	2.5E29[b]	4.0E-3[c]
			6.8E26[d]	2.5E29[b]	2.7E-3[d]
Austin (1989c1)					
HCN J(1-0)	90/04/02	< 0.10	< 1.6E26	2.0E29[b]	< 8.0E-4
HCN J(1-0)	90/05/23	0.20±0.07	2.4E25	6.0E28[e]	3.9E-4
HCN J(3-2)	90/05/23	1.27±0.18			
H_2CO 3_{12}-2_{11}	90/04/02	< 0.07	< 9.1E26[c]	2.0E29[b]	< 4.6E-3[c]
			< 6.7E26[d]	2.0E29[b]	< 3.3E-3[d]
H_2CO 3_{12}-2_{11}	90/05/21-25	0.25±0.03	3.6E26[c]	6.0E28[e]	6.0E-3[c]
			3.3E25[d]	6.0E28[e]	5.5E-4[d]
H_2S 1_{10}-1_{01}	90/05/24	0.20±0.07	9.0E25	6.0E28[e]	1.5E-3
CH_3OH (3,0)-(2,0)A	90/05/25	0.25±0.05	4.9E26	6.0E28[e]	8.2E-3

a. Observations aimed at the nucleus.
b. From OH 18 cm observations (Bockelée-Morvan et al., 1990a).
c. Assuming a daugther density distribution with a parent scalelength of 10^4 km at 0.9 AU from the Sun and scaled as rh^2.
d. Assuming a parent distribution.
e. From OH IUE observations (Budzien et al., 1990).

Methanol

Methanol was observed in comet Austin on May 25 1990 through its J(2-1) $\Delta K = 0$ transitions at 96 GHz, and its J(3-2) $\Delta K = 0$ transitions at 145 GHz, using 512x1 MHz filter banks (corresponding to a velocity resolution of 2 km s^{-1} at 145 GHz). Two J(2-1) transitions are marginally present in the 96 GHz spectrum while four J(3-2) lines are detected with signal to noise ratios between 2 and 5 in the 145 GHz spectrum (Fig. 5), insuring an unambiguous detection of methanol in comet Austin and giving the first evidence of the presence of this molecule in comets (Despois et al., 1990).

Observing simultaneously several rotational lines of CH_3OH is fascinating since it provides clues on its excitation conditions. As a preliminary study we assumed a unique temperature Trot for describing the population distribution among the rotational states. From the reference solar

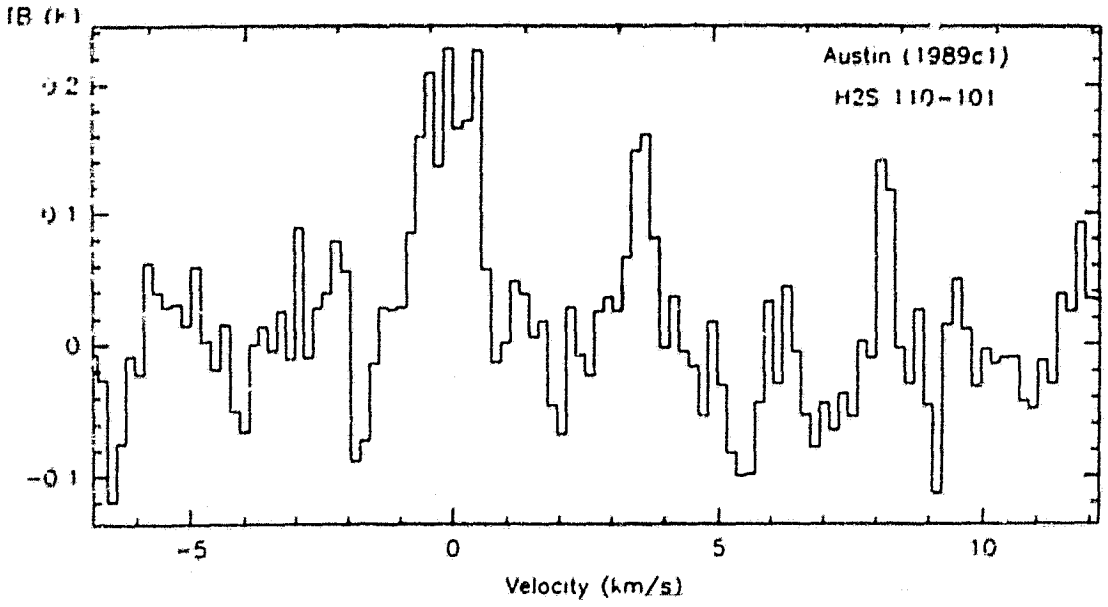

Figure 4 : The H_2S 1_{10}-1_{01} spectrum of comet Austin observed on May 24-25 1990 (centre and offset positions).

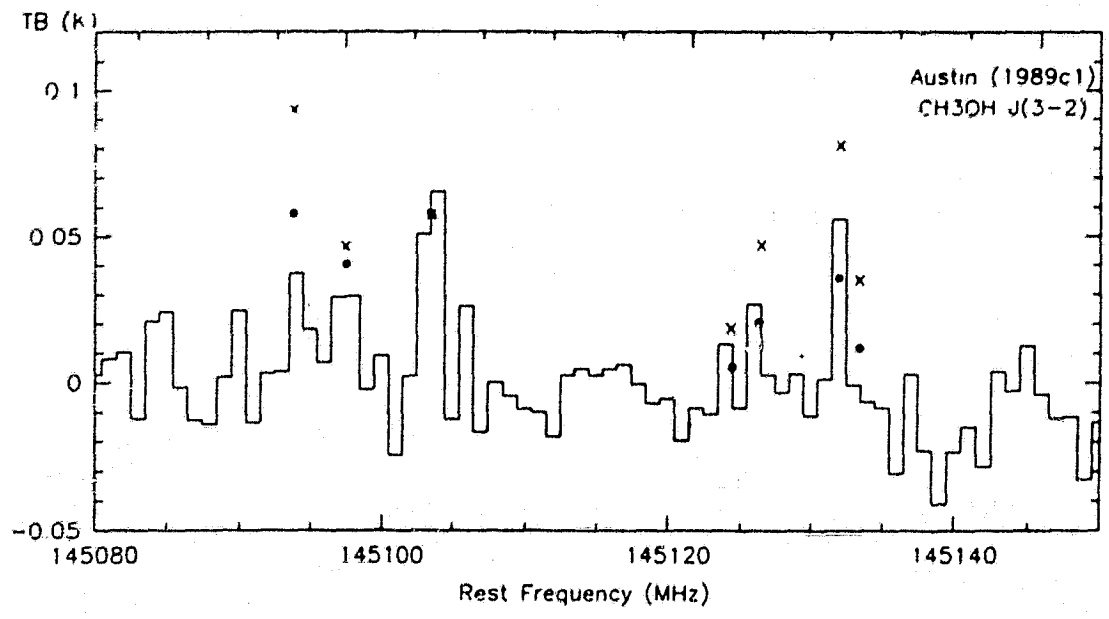

Figure 5 : J(3-2) $\Delta K = 0$ transitions of CH_3OH around 145 GHz observed towards comet Austin on May 25, 1990. Full circles and crosses indicate the line positions and the relative intensities expected for rotational LTE at Trot = 20 K and Trot =70 K, respectively.

ORIGINAL PAGE IS
OF POOR QUALITY

spectrum of Huebner and Carpenter (1979) and the UV absorption spectrum of Nee et al. (1985), we estimate a CH_3OH photodissociation rate of 1.3 10^{-5} s^{-1} at 1 AU. The line intensities computed with Trot = 70 K and Trot = 20 K are superimposed on the observed spectrum (Fig. 5). The observed transitions are much more easily explained by a rotational temperature of 20 K. Assuming this value and using the observed intensity of the (3,0)-(2,0) A line at 145.103 GHz (Table 1), we derive a methanol production rate of 5 10^{26} s^{-1}, corresponding to an abundance of 8 10^{-3} with respect to water.

Conclusion

These new detections confirm that microwave spectroscopy is an efficient tool to study cometary parent molecules. The presence of H_2S, H_2CO and CH_3OH, which are well-known constituents of the interstellar molecular clouds, supports the hypothesis that comets have retained, at least partly, some of the primitive matter of the Solar Nebula without alteration.

Detailed studies of observations made at offset positions, of the excitation of the new molecular species, and of the coma kinematics from the observed line shapes, are in preparation.

References

Bockelée-Morvan, D., Crovisier, J., Gérard, E. and Bourgois, G., 1990a, this workshop

Bockelée-Morvan, D., Despois, D., Paubert, G., Colom, P. and Crovisier, J., 1990b, IAU *Circ.* No 5020

Boice, D.C., Huebner, W.F., Sablik, M.J. and Konno, I., 1990, to be submitted to *Geophys. Res. Letts*

Budzien, S.A., Feldman, P.D., Roettger, E.E., Festou, M.C. and A'Hearn, M.F., 1990, this workshop

Colom, P., Despois, D., Paubert, G., Bockelée-Morvan, D., Crovisier, J. and Gérard, E. 1989, IAU *Circ.* No 4851

Combes et al., 1988, *Icarus* **76**, 404

Crovisier, J., 1987, *Astr. Ap. Suppl. Ser.* **68**, 223

Crovisier, J., Despois, D., Bockelée-Morvan, D., Paubert, G. and Colom, P., 1990a, IAU *Circ.* No 5022

Crovisier, J., Despois, D., Bockelée-Morvan, D., Gérard, E., Paubert, G., Johansson, L.E.B., Ekelund, L., Winnberg, A., Ge, W., Irvine, W.M., Kinzel, W.M. and Schloerb, F.P., 1990b, *Astr. Ap.* (in press)

Crovisier, J. and Schloerb, F.P., 1990, in Comets in the Post-Halley Era, Edts R. Newburn and J. Rahe, Kluwer Academic Publishers, Dordrecht (in press)

Despois, D., Bockelée-Morvan, D., Paubert, G., Colom, P. and Crovisier, J., 1990, IAU *Circ.* No 5027

Huebner, W.F. and Carpenter, C.W., 1979, *Los Alamos Informal Report* LA-8085-MS

Lee, L.C., Wang, X. and Suto, M., 1987, *J. Chem. Phys* **86**, 4353

Marconi, M.L., Mendis, D.A., Korth, A., Pin, R.P., Mitchell, D.L., and Reme, H., 1990, *Ap. J.* **352**, L17

Nee, J.B., Suto, M. and Lee, L.C., 1985, *Chem. Phys* **98**, 147

Snyder, L.E., Palmer, P. and de Pater, I., 1989, *Ap. J.* **97**, 246

5/8-90
3205
8.6

N91-21030

VLA SEARCHES FOR FORMALDEHYDE AND CYANOACETYLENE EMISSION FROM COMET P/BRORSEN-METCALF (1989o)

Lewis E. Snyder
Astronomy Dept., University of Illinois

Patrick Palmer
Dept. of Astronomy and Astrophysics, University of Chicago

Imke de Pater
Astronomy Dept., University of California

ABSTRACT

In 1989 September we conducted VLA searches for both formaldehyde (H_2CO) and cyanoacetylene (HC_3N) emission from Comet P/Brorsen-Metcalf (1989o). In early July, this comet was outgassing strongly at a brighter than average preperihelion rate, and our hope was that it would continue to do so through perihelion (1989 Sept. 11.9394). By observing the $1_{11} - 1_{10}$ transition of formaldehyde (H_2CO) at 4,829.659 MHz (6 cm. λ) during the phase of maximum outgassing, we expected to collect spectra with a high signal-to-noise ratio which would show the temporal behavior of formaldehyde relative to other molecules. During this same observing period, we also searched for the J=1-0, F=2-1 rotational transition of cyanoacetylene at 9098.3321 MHz (3.3 cm. λ).

I. INTRODUCTION

In order to investigate the composition and outgassing behavior of comets, one should observe as many comets as possible in order to get a statistically representative sample. We started radio interferometric studies of comets several years ago, and after several discouraging attempts, we finally succeeded to image OH in Comet Halley in 1985, and in Comet Wilson (1986l) in 1987 (de Pater, Palmer, and Snyder 1986; Palmer, de Pater, and Snyder 1989). We used the same techniques to detect H_2CO in comets Halley in 1985 and Machholz (1988j) in 1988 (Snyder, Palmer, and de Pater, 1989; 1990). We have other data on comets Liller (1988a), Machholz (1988j), and Okazaki-Levy-Rudenko (1989r) which are not yet fully reduced.

In 1989 July we proposed observing Comet Brorsen-Metcalf with the VLA because at the time it was outgassing at a brighter than average preperihelion rate. It was our hope that it would continue to do so through perihelion on 1989 Sept. 11.9, producing cometary H_2CO strong enough to image, rather than to simply detect. By observing H_2CO during the phase of maximum outgassing, we hoped to collect spectra with a high signal-to-noise ratio which would show the temporal variation of H_2CO relative to other molecules. The VLA referees' reports were generally favorable, except possibly for one comment: "H_2CO is a "known" comet parent molecule in the sense that it has been detected by a number of groups including this one. I think all of these detections are somewhat controversial, though, and it is important to verify them." Despite this, we were given time to search for the $1_{11} - 1_{10}$ transition of formaldehyde (H_2CO) at 4,829.659 MHz and

for the J=1-0, F=2-1 rotational transition of cyanoacetylene at 9098.3321 MHz (3.3 cm λ).

II. OBSERVATIONS

We used the VLA to search Comet Brørsen-Metcalf for the 1_{11} - 1_{10} transition of H_2CO on 1989 September 2, 3, and 7, and for the 1-0 of HC_3N on 1989 September 10 and 11. The initial data reduction for formaldehyde is farther along than for cyanoacetylene, so we will present our progress on the H_2CO observations in order to learn how they may correspond with other observations of P/Brorsen-Metcalf. The VLA was used with all 27 antennas in the D (the most compact) configuration and our observational parameters were set up just as they had been for our earlier H_2CO observations of comets Halley and Machholz (Snyder *et al.* 1989; 1990). As usual, D. Yeomans' cometary orbital elements were used in C. M. Wade's ephemeris program. Two identical spectrometers were used with a total bandwidth of 1.56 MHz each. Thirty one (Hanning smoothed) channels were recorded from each spectrometer; each channel had a width of 12.208 kHz (0.756 km s^{-1}). During the observations, the expected frequency of the cometary H_2CO line was positioned two channels above the center of the band in one spectrometer and two channels below the center in the other. This effectively served as a shift in the local-oscillator frequency when the 27 overlapping channels from the two data sets were combined to form the spectra discussed here. The H_2CO absorption against NGC 2024 was observed at the beginning of the comet observing session to monitor the overall performance of the system. The untapered beam was 20" x 20", and the tapered beam was 40" x 40". A cometocentric velocity system is used in which v = 0 is the predicted velocity of the nucleus.

III. DISCUSSION

In our reduction procedure used for Halley and Machholz (Figure 1),

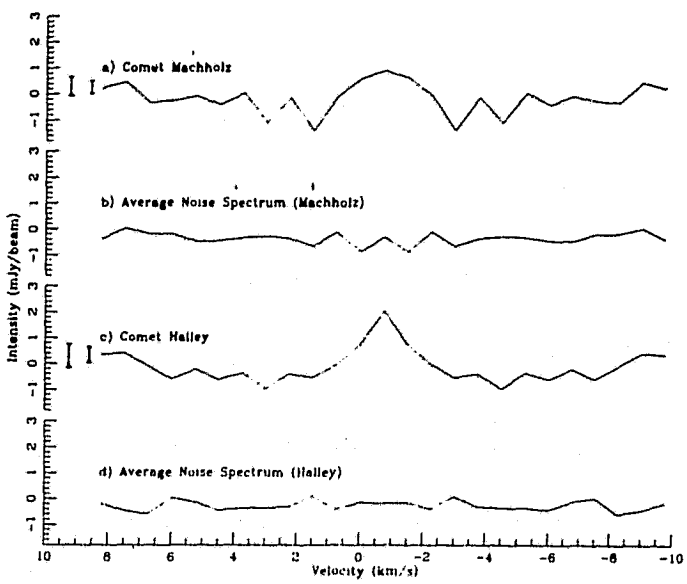

Figure 1. a) The 1_{11} - 1_{10} transition of H_2CO (folded about v = -0.76 km s^{-1}) observed in Machholz. b) The averaged, folded, background spectrum made as in 1a, but at 2 random points away from the nucleus. c) The 1_{11} - 1_{10} transition of H_2CO (folded about v = -0.76 km s^{-1}) observed in Halley. d) The averaged, folded background spectrum of 5 random points away from the nucleus. Ordinates: intensity in units of 10^{-3} Jy (mJy); abscissae: predicted radial velocity wrt the rest frame of the nucleus (from Snyder *et al.*1990).

ORIGINAL PAGE IS
OF POOR QUALITY

spectra were formed from the data cube - the set of the images of the comet for each velocity channel. By making a cut through the data cube at fixed position with respect to the cometary nucleus, a plot of intensity versus velocity for that position is obtained. Five spectra, taken in the direction of the cometary nucleus and at offsets 10" (≈ the half-power beamwidth) north, south, east, and west, were obtained and then averaged into one spectrum. Next, a version of Gérard's (1987) SYMCOMET routine was applied to the data. In this routine, a search for a symmetrical spectral line is conducted by folding the spectrum about an axis which is sequentially stepped through the velocity channels. The noise in the folded channels is reduced by $\sqrt{2}$ from its original value; and when the axis passes through the center channel of the line, the standard deviation computed for all channels (excluding the center channel) will reach a minimum. Finally, the same averaging procedure was repeated with 5 spectra around each of several randomly selected points away from the position of the comet. Figure 1a shows the H_2CO emission spectrum and 1b shows the average of all of the off-comet comparison spectra for Comet Machholz. The value of σ for all channels except the center channel of the line is the smaller of the two error bars located on the left-hand side. The larger error bar on the left-hand side represents $\sqrt{2}\sigma$, the correct estimate of standard deviation for the unfolded data at $v = -0.76$ km s^{-1}, the center channel and peak of the H_2CO emission line. Figures 1c and 1d show similar data for Comet Halley. Both comets had a line of H_2CO centered at the blueshift $v = -0.76$ km s^{-1}. For both Machholz and Halley, the VLA was generally facing the sunlight hemisphere of the nucleus, and this small blueshift is consistent with anisotropic outgassing of the nucleus in the solar direction. This is illustrated in Figure 2. Also, in the case of

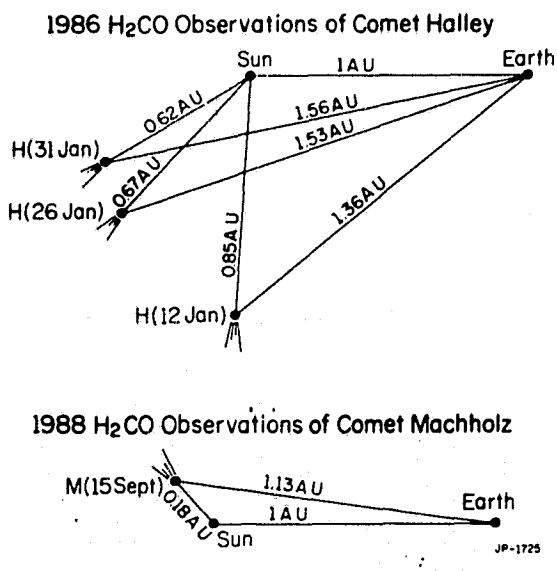

Figure 2. The geometry of comets Halley and Machholz at the time of the observations in the sun-earth coordinate system. (from Snyder *et al.*1990).

Halley, a similar blueshift was found for other cometary species such as HCN and H_2O.

For Comet Brorsen-Metcalf, we used a new technique for reducing the data. Figure 3 shows a hypothetical representation of a data cube which is constructed from the interferometric observations of cometary H_2CO. A

pixel, represented by a shaded square, is 10"x10" in tapered data and 5"x5"

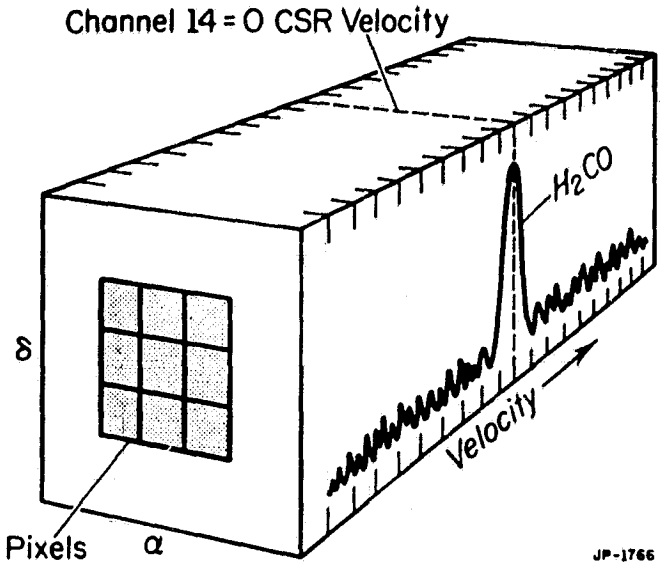

Figure 3. The data cube represents the set of images of the comet for each velocity channel as a function of α and δ. By making a cut along a pixel (which is at fixed position wrt the cometary nucleus) through the data cube, a spectrum of intensity versus velocity for that position is obtained. Averaging over the appropriate number of pixels simulates the synthesized interferometer beam. Here channel 14 is at 0 km s^{-1} cometocentric radial velocity.

in untapered data. For the data reductions, we used blocks which were either 3x3 pixels or 5x5 pixels. Note that 3x3 pixels untapered=15"x15", 5x5 pixels untapered= 25"x25", 3x3 pixels tapered=30"x30",and 5x5 pixels tapered=50"x50", so that the size of the untapered synthesized beam is bracketed by the untapered 3x3 and 5x5 pixels and the size of the tapered synthesized beam is bracketed by the tapered 3x3 and 5x5 pixels. This illustrates one of the strengths of using arrays for the radio observations of comets: within the field of view, different pixel clusters can be sampled to optimize the coupling of the synthesized beam to the gas distribution. This is particularly important in the case of comets, because small pointing errors caused by an inaccurate ephemeris can be corrected after the array observations have been made-a feat which is impossible with single dish radio observations. Figure 4 shows a composite spectrum displaying the spectra from the 5x5 tapered pixels (solid line), 5x5 untapered pixels (lightly dashed line), 3x3 tapered pixels (dotted line), and the 3x3 untapered pixels (heavily dashed line). There may be a weak H_2CO emission feature at channel 13; since channel 14 is 0 km s^{-1} in the cometocentric rest frame, this would correspond to a redshift of 0.756 km s^{-1}. However, we won't know the statistical significance (if any) of this feature until we finish the noise analysis of the data.

IV. CONCLUSIONS

We are finishing the noise analysis of our formaldehyde data in order to determine its statistical significance and later this year we hope to finish the cyanoacetylene data analysis. It will be important to compare our centimeter wavelength formaldehyde results with the millimeter wavelength formaldehyde results for Comet Brorsen-Metcalf presented by D. Bockelée-Morvan at this workshop (Colom *et al.* 1990). In order to compute the formaldehyde production rate, it will be necessary to model an extended

formaldehyde scalelength with a nuclear source and a coma source.

Both L. E. S. and P. P. wish to acknowledge NASA grant NAGW-1131 to the University of Illinois. I. dP. acknowledges support from NSF grant AST-8900156 to the University of California, Berkeley.

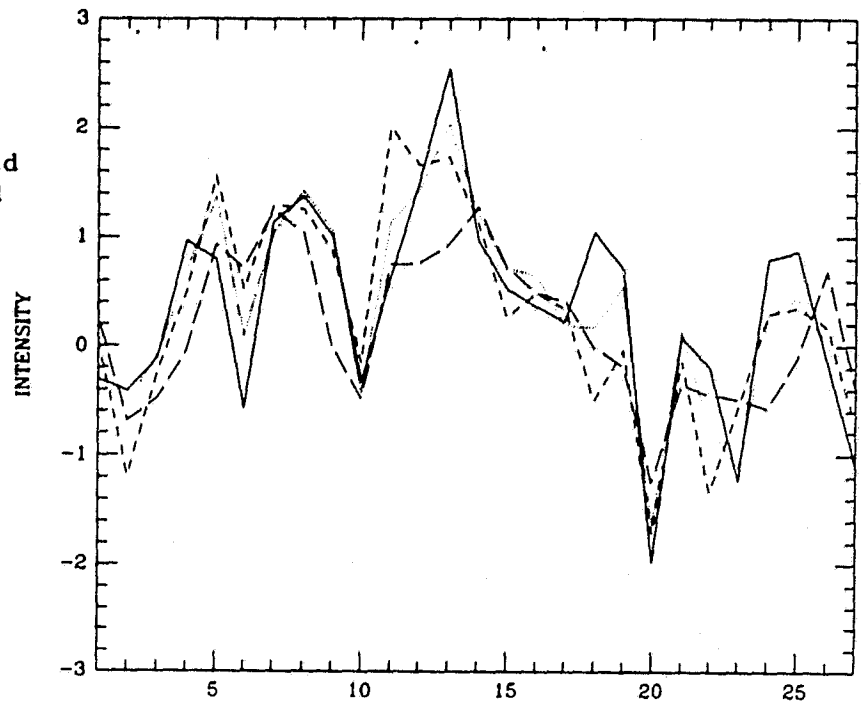

Figure 4: Spectra obtained by averaging over different pixel combinations or cuts through the data cube. Solid line: 5x5 tapered pixels. Lightly dashed line: 5x5 untapered pixels. Dotted line: 3x3 tapered pixels. Heavily dashed line: 3x3 untapered pixels. Ordinate: intensity in mJy; abscissae: channel number, which runs in the direction opposite to radial velocity wrt the rest frame of the nucleus. In this rest frame, channel 14 = 0 km s^{-1}.

REFERENCES

Colom, P., Despois, D., Bockelée-Morvan, D., Crovisier, J., Paubert, G., and Gérard, E. 1990, this workshop.

de Pater, I., Palmer, P., and Snyder, L. E. 1986, *Ap. J. (Letters)*, **304**, L33.

Gérard, E. 1987, In *Cometary Radio Astronomy*, NRAO Workshop No. 17 (W. M. Irvine, F. P. Schloerb, and L. Tacconi-Garman, Eds.), p. 91, NRAO, Green Bank, WV.

Palmer, P., de Pater, I., and Snyder, L. E. 1989, *Astron. J.*, **97**, 1791.

Snyder, L. E., Palmer, P., and de Pater, I. 1989, *Astron. J.*, **97**, 246.

Snyder, L. E., Palmer, P., and de Pater, I. 1990, *Icarus*, in press.

Dave Schleicher
Since the H_2CO is observed with the 5×5 grid, but not the 3×3 grid, can the 3×3 grid location be adjusted to search for the peak in the H_2CO distribution?

Lewis Snyder
Yes, we are working on this, but it will take some time to complete.

N91-21031

SILICATES AND VARIABILITY IN COMETS OKAZAKI-LEVY-RUDENKO (1989r) AND AUSTIN (1989c1)

Ray W. Russell and David K. Lynch
Space Sciences Laboratory, The Aerospace Corp.

Abstract

Comet Okazaki-Levy-Rudenko (1989r) was studied over a wide range of wavelengths from the UV to the submillimeter. Using visual magnitude estimates from the IAU Circulars and reported submillimeter fluxes in conjunction with our thermal IR spectroscopy and filter photometry, the nature of the grains and the behavior of the comet can be assessed and compared to other comets studied under this program. In addition, preliminary results from a collaborative IR study of Comet Austin are presented which address the nature of the dust in that comet. Progress on a model for cometary properties and brightness behavior is discussed.

Introduction

An extensive IR spectroscopic study of comets was begun with Comet G-Z, continued with Halley, and has been extended to include Wilson, Bradfield, Brorsen-Metcalf (BM), Okazaki-Levy-Rudenko (OLR), and Austin. Several others did not brighten up sufficiently or were unobservable due to weather. The goal of this on-going study is to develop a comprehensive cometary dust model that can account for the spectral signatures (or lack thereof) in the thermal IR, and predict, or at least explain in an objective fashion, the time variability (or lack thereof) in the cometary brightness curve. The current data base of spectroscopy in the IR is not large enough to fully accomplish this, but the situation is improving rapidly. This is indicated by the above list of comets, all of which have been studied in the last 6 years. This report represents the status of this work as applied to Comets OLR (1989r) and Austin (1989c1).

Observations

IR circular variable filter wheel (CVF) spectroscopy and filter photometry of Comet OLR were obtained during 5-8 Nov. 1989 UT using the NASA Infrared Telescope Facility (IRTF) circular variable filter wheel spectrometer (AT1) and the bolometer filter system (BOLO1) with about 9.5" apertures. Magnitudes on 8.8 Nov. 1989 UT were L=6.7, M=4.4 and [10.3]=0.6.

As part of a collaboration with M. Hanner and H. Campins, Comet Austin CVF and filter data were obtained at the 3 m IRTF on 6.8 May 1990 UT with the facility CVF spectrometer (AT1), with a resolving power of $\lambda/d\lambda \sim 50$. A 5 mm (9.3 arc sec) aperture and 45 arcsec N-S throw were used to allow for the extended nature of the comet at a distance from the earth of only .457 au. In addition to the usual 7-12.5 μm CVF wedge and moderate resolution filters used for the Halley watch observing program, two new filters were installed for this program and left in the AT1 CVF dewar. They are a 3.44 μm filter with a full width at half maximum transmission (FWHM) of 0.20 μm and an M filter which was measured cold in our lab to have a center wavelength of 4.73 μm and a FWHM of 0.61 μm. The filters were then tested cold in the AT1 dewar at the telescope with a monochromator and hot source to check for out-of-band spectral leaks. No leaks were found, lending credence to the technique of using data from these filters in conjunction with the longer wavelength data to derive color temperatures.

The addition of these filters to AT1 allows the characterization of the cometary dust continuum through the mid-IR without having to change instruments and calibrate two separate systems. In view of the difficulties inherent in trying to observe close to the sun in the daytime, this can be a significant advantage. The AT1 sensitivity at short wavelengths is reduced by the low quantum efficiency of the doped Si detector, but it was found to be adequate (about 10^{-12} W/root Hz at 3.44 μm) for the study of a comet bright enough to be studied spectroscopically at 10 μm. The 3.44 μm filter also permits a rough assessment of the strength of a possible "3.4 μm" emission feature above the nominal continuum.

Results and Discussion

The Comet OLR spectra reported by Lynch and Russell (B.A.A.S. 22, 834, 1990) and shown in Figure 1 show a strong, structureless 10 μm silicate emission feature extending about 20% above the continuum. It was present on all three days, but was about a factor of 1.5 brighter on 7 Nov. At the same time, the visual magnitude estimates shown in Figure 2 (IAUC 4892, 4904, and 4908) indicated a .5 -.8 magnitude brightening as well. This comet seems to be more variable than, for example, Comet Wilson (1986l), and of the order of or a little less variable than Comet p/Halley. The variability of OLR was reported to be about a factor of 3 during three days of observations in the submillimeter (IAUC 4914) in the 18-23 Nov. time frame.

The L-M-7.8 micron color temperature was 380 K, approximately 10% above the equilibrium temperature of 345 K. Figure 3 shows the spectroscopy data along with a normalized black body curve at the equilibrium and elevated temperatures for comparison. The grain temperature elevation compared to a black body at the same heliocentric distance indicates that the grains were inefficient radiators, and therefore small compared to the wavelength of the observation. This, in concert with the existence of silicate emission which is indicative of a wavelength dependent emissivity, suggests that the dust grains were optically thin at these wavelengths. We can compare the estimates of dust mass derived from the IR and submillimeter data, and find them to be discrepant by about three orders of magnitude. The source of the disagreement is being investigated. It may be model dependent or may simply reflect the variation in the dust production rate during this apparition of Comet OLR.

Several spectra of Comet Austin were obtained in different modes in an effort to defeat the effects of thermal changes in the optics due to differential heating by the sun shining on the telescope structure. The two best, complete spectra showed no 10 micron silicate emission exceeding 20% of the continuum and are consistent with the absence of silicate emission. However, to accurately determine the presence or absence of a silicate feature with low contrast, the level of the continuum must be precisely determined. We chose to use the measurements of the continuum at 3.44 and 4.73 microns (where blackbody flux distributions for typical cometary temperatures exhibit exponential dependence on temperature and thus even fairly large measurement errors translate into relatively small temperature uncertainties) and at the edges of the 8-13 micron window where the silicate has much lower emissivity than in the 9-11 micron region.

The IR magnitudes of Comet Austin obtained with the fixed filters were 3.44 microns, 6.4+/-0.35; M(4.73 microns), 4.7 +/-0.1; N(10.1 microns), 0.18 +/-0.05; 10.3 microns, 0.13+/-0.05. These data are consistent with a slightly elevated color temperature and the presence of a 3.4 μm emission feature (Mumma et al. IAUC 5012).

Fitting a 300 K greybody to the ten micron spectrum only results in a curve which misses the 3.44 and 4.73 micron values completely. Figure 4 shows a 335 K greybody normalized to the 4.73 micron point and just below the ends of the 10 μm spectrum, allowing for the fact that typical interstellar silicate emissivity curves are not zero at either 8 or 12.7 microns. The cometary spectral flux is normalized to the level of the 10.3 filter data, and is about 8 % lower than the other good quality, complete spectrum obtained the same day. If the comet spectrum in Figure 4 were raised to the level of the other narrowband spectroscopic data, the silicate feature would be correspondingly larger relative to the continuum. On the other hand, if one were to increase the comet flux at 4.73 microns by one sigma (10%) and then fit the 335 K greybody to that value, no silicate feature would be present.

We believe the intermediate normalization based on the 10.3 μm filter photometry shown here to be the most probable. Furthermore, considering the shape of the smoothest comet spectrum we obtained (Figure 4), the most likely choice is that there was a small silicate feature (about 10%) and that there may even be a break in the spectrum just past 11 microns which is seen in both complete spectra. This break was seen in Halley (Campins and Ryan 1989, Ap.J., 341, 1059) and Bradfield (Russell et al. 1990, in preparation) and identified by Campins and Ryan as due to a small admixture of crystalline olivine grains in the cometary dust.

It should be pointed out that a small silicate feature like that possibly present here would not

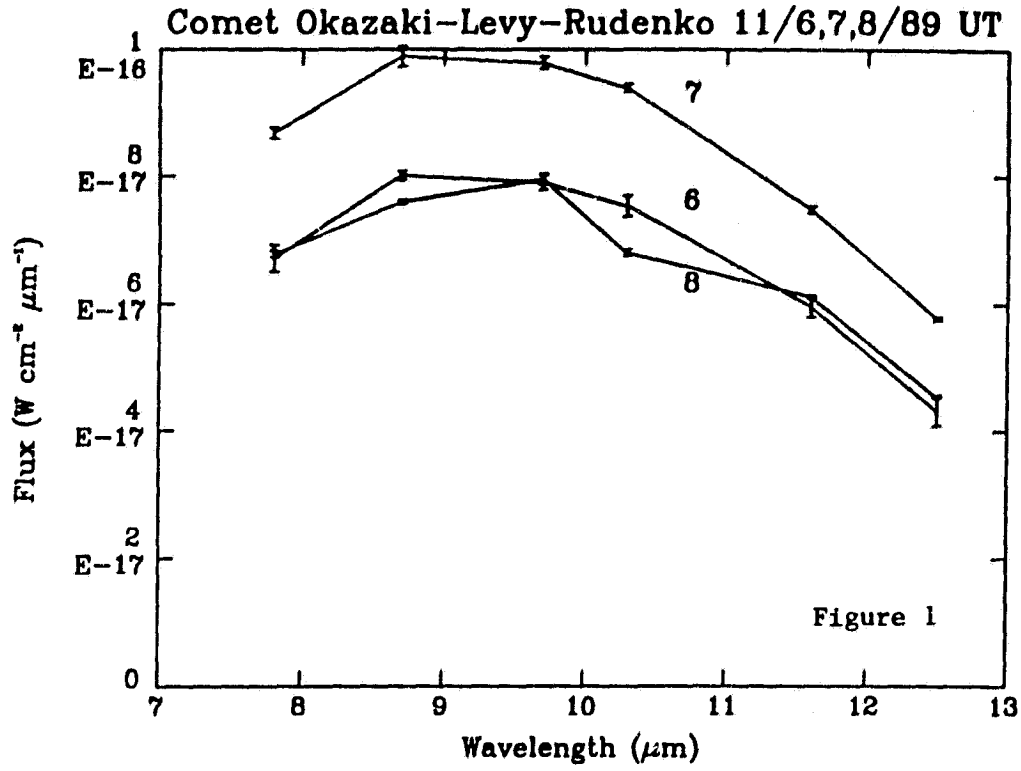

Figure 1

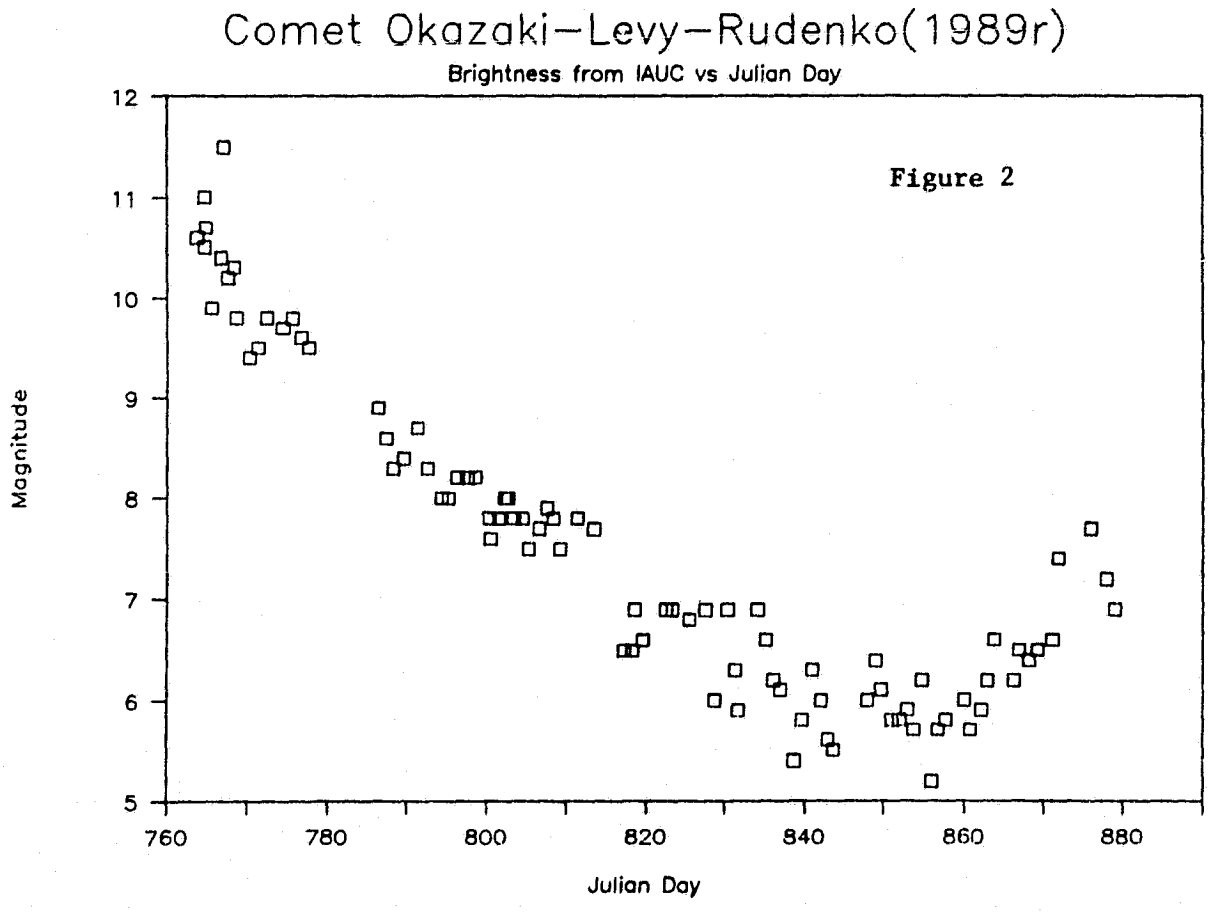

Figure 2

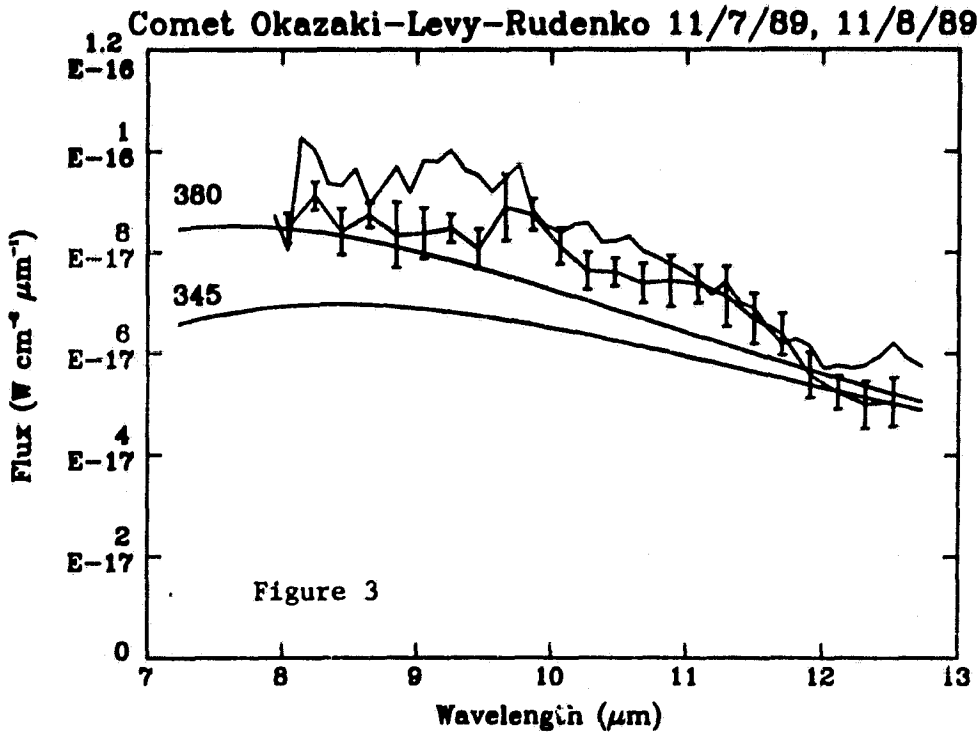

Figure 3

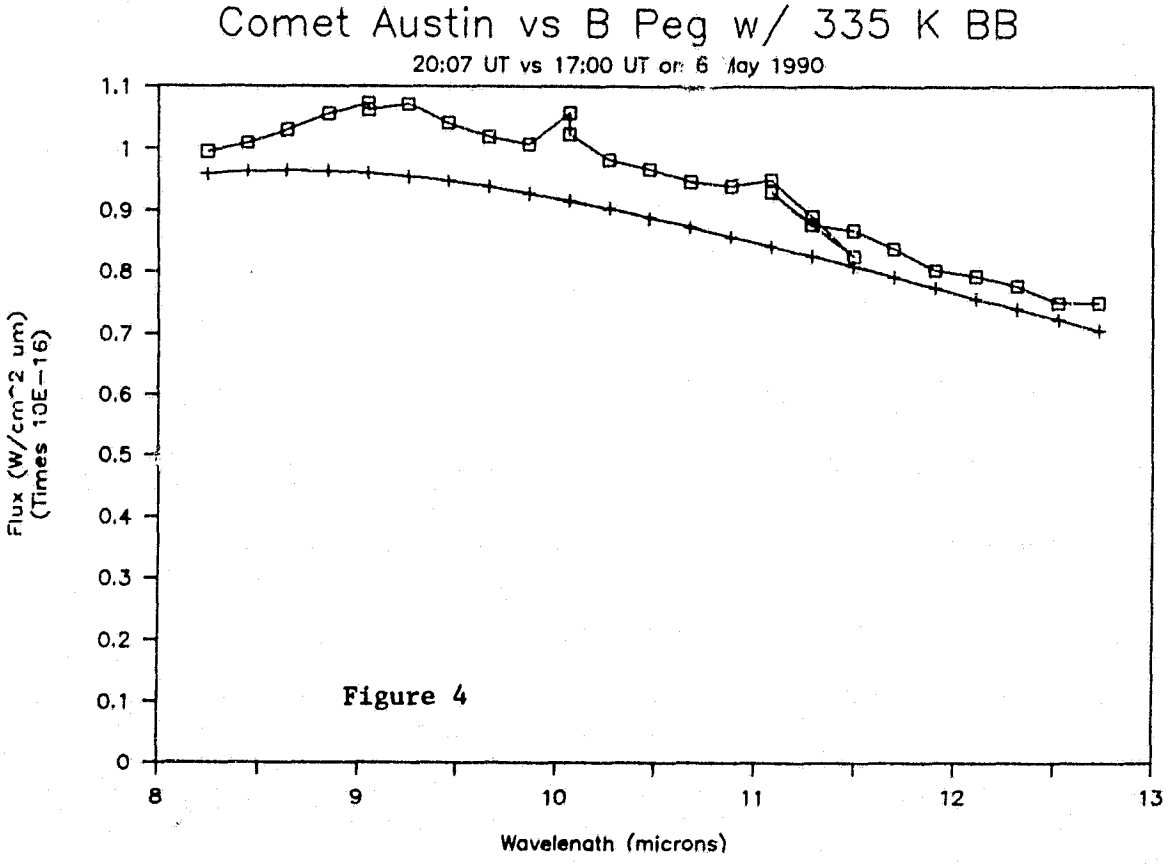

Figure 4

be detected at all by broadband filter photometry. This emphasizes the value of the two new filters in AT1 in conjunction with the CVF wedges for this type of program. The use of one dewar also means that all of the data can be taken through the same aperture with the same optics, thus removing another potential ambiguity from the data.

These comets fit well in a picture where the properties of the dust and the behavior of the brightness during the course of the apparition determine the type of comet under study. This approach to studying comets is in contrast to one in which models for different types of comets are based on their orbits (short or long period, or first time/one-visit comets). The comets which are not dusty seem (based on our observations of Brorsen-Metcalf, for example; Lynch et al., this volume), to have a carbon rich grain population which emits greybody spectra with little or no silicate feature in the 10 micron region. They seem to lack the dramatic variability seen in Comet O-L-R (1989r) or p/Halley, both of which had substantial silicate emission features. Austin may be an intermediate case between these two classes. The visual magnitude estimates from the IAU Circulars for Austin indicate, with the exception of one period of steady brightening, an essentially non-periodic variability of about a factor of 2 over the span of a few days.

In a comet with a lot of volatile material on the surface, a more or less steady outflow is expected. In contrast, a comet with a crusty surface could behave either in a minimalist fashion (i.e., very little sublimation at all, and thus fairly steady in brightness but at a low level) or in the very sporadic, outburst mode observed for p/Halley. This tough, crusty surface may well be mostly hydrocarbons which form a sticky layer, essentially black, which shields the inner parts of the cometary nucleus and emits the grey-body shape reported for B-M and closely approximated by the data shown here for Austin (silicate enhancement only about 10% above the greybody continuum).

Additional spectra of a statistically significant sample will be required to test this model and flesh out the classification characteristics. We have such an ongoing program using our new broadband array spectrograph to span the 3-13.5 μm region simultaneously, thus avoiding problems of tracking and spatial structure which have plagued our CVF measurements. The first of these runs is scheduled for the next quarter on the IRTF.

Summary

Thermal IR spectroscopy and mid-IR filter photometry of Comet OLR have been reported which show a strong silicate feature and significant temperature enhancement over a black body in equilibrium. Even though OLR was a "new" comet, it has many similarities in its spectral shape and temporal behavior to p/Halley. Similar observations of Comet Austin are suggestive of a small (about 10%) silicate feature superposed on a 335 K greybody continuum, and less temporal variation than Halley or OLR, but more than Wilson. The temperature derived for the dust in Austin is quite close to the blackbody equilibrium value of 314 K, and may be indicative of grains whose size is in the 1-10 micron range. The data are also consistent with a carbon-rich grain population which would be expected to emit essentially greybody emission. As noted above, the comet exhibited variability in the visual and IR which was intermediate in nature between that of Halley and Brorsen-Metcalf, silicate- and carbon-rich comets respectively.

This program clearly points out the need for IR spectrographic data on a statistical sample of comets to take our understanding of cometary dust grains and nuclear sublimation forward.

Acknowledgements

This work is supported in the Space Sciences Laboratory by the Aerospace Sponsored Research program. We gratefully acknowledge the responsiveness of the IRTF to the target of opportunity proposals through which many of the ten micron spectroscopy programs on comets have been conducted. IRTF personnel went out of their way to install and assist in the testing of the new filters for AT1, which made a significant improvement in our observing efficiency. M. S. Hanner and H. Campins are the collaborators on the Comet Austin part of this study.

N91-21032 520-90 220526 P5

DETECTION OF THE 3.4 MICRON EMISSION FEATURE IN COMETS P/BRORSEN-METCALF AND OKAZAKI-LEVY-RUDENKO (1989r) AND AN OBSERVATIONAL SUMMARY

T.Y. Brooke, A.T. Tokunaga
Institute for Astronomy, University of Hawaii
2680 Woodlawn Dr., Honolulu, HI 96822
and
R.F. Knacke
Space Sciences Lab ES-63
NASA Marshall Space Flight Center, Huntsville, AL 35812

We are continuing a survey of the 3 μm spectral region of comets, including the broad 3.4 μm emission feature due to C–H bonds in organic molecules. One goal is to determine how the strength of the emission band varies with heliocentric distance r in comets. This depends on both the production rate of the organic molecules and the emission mechanism, neither of which is well determined at present.

In 1989, the 3.4 μm feature was detected in two comets: the periodic comet P/Brorsen-Metcalf and new comet Okazaki-Levy-Rudenko (1989r), hereafter OLR. Spectra of the two comets obtained at the NASA Infrared Telescope Facility on Mauna Kea are shown in Fig. 1. The feature was clearly evident in P/Brorsen-Metcalf down to $r = 0.48$ AU, the smallest heliocentric distance at which these cometary organics have been detected.

The 3.4 μm features in P/Brorsen-Metcalf and OLR were spectrally similar to those observed in other comets. But the feature-to-continuum ratios in these two comets were higher than those expected from the trend seen in other comets to date. Fig. 2 shows the feature-to-continuum ratios at 3.36 μm as a function of heliocentric distance for all published 3 μm spectra of comets, including 3σ upper limits for spectra in which no feature was evident. Complete references for the data are given in Brooke, Tokunaga, and Knacke (1990).

The spectral contrast of the 3.4 μm feature in comet P/Halley was generally lower at smaller heliocentric distances for r in the range $1 - 2$ AU (Fig. 2). Comets Wilson (1987 VII) and Bradfield (1987 XXIX) appear to follow the Halley trend, though the data are limited. The feature-to-continuum ratios in P/Brorsen-Metcalf and OLR were higher than any reasonable extrapolation of this trend. This shows that the flux of the 3.4 μm emission is in general *not* coupled to the flux of the underlying continuum.

Separate comparisons of the dust continuum and 3.4 μm band fluxes of comets suggest a plausible explanation for the higher feature-to-continuum ratios in P/Brorsen-Metcalf and OLR. Fig. 3a shows the dust continuum flux at 3.36 μm ratioed to the water production rate at the time of the observation for each of the observations represented in Fig. 2. Water production rates are used as a means of normalizing fluxes of comets with widely different levels of activity. Measured continuum fluxes were reduced to a common viewing geometry assuming conservative radial outflow, i.e., flux proportional to the projected radius of the aperture. Details of the reduction and references for the water production rates are given in Brooke, Tokunaga, and Knacke (1990).

Fig. 3a clearly shows that comets P/Brorsen-Metcalf and OLR, along with P/Encke, had lower 3.36 μm continuum fluxes relative to their water production rates than the values that would be expected for Halley, Wilson, or Bradfield at comparable heliocentric distances.

Integrated 3.4 μm band fluxes were estimated by subtracting continuum fluxes from the spectra. Fig. 3b shows the band fluxes and upper limits ratioed to the water production rates for the same sample of comets shown in Fig. 3a. The same scaling to a common viewing geometry was used. In marked contrast to their continuua, the normalized 3.4 μm band fluxes of P/Brorsen-Metcalf and OLR are consistent with the values of other comets.

There is an approximate correlation between the 3.4 μm band flux and the water production rate at a given heliocentric distance for all of the comets in this sample (Fig. 3b). The high feature-to-continuum ratios in comets P/Brorsen-Metcalf and OLR are thus most likely due to their weaker 3 μm dust continuua relative to water. These two comets also had weak dust continuua in the visible (Schleicher *et al.* 1989) and ultraviolet (Roettger *et al.* 1990) compared to their gas production rates; in fact, the two are among the most "dust-poor" comets. The present results suggest that comets with low dust-to-gas ratios will exhibit higher feature-to-continuum ratios at 3.4 μm.

The heliocentric distance dependence of the normalized 3.4 μm band flux (Fig. 3b) can be used to constrain the emission mechanism if the production rate of organics relative to water is assumed to be the same in all comets. The present data are consistent with fluorescence by molecules excited by solar radiation, in which case the normalized band flux goes as r^{-2}. But simple models of thermal emission by a population of small, hot grains can also match the data (Brooke, Tokunaga, and Knacke 1990). Possibly both processes contribute. If the emission is from grains, it is interesting that the 3.4 μm flux from these grains is better coupled to the water production than the dust continuum, suggestive of two separate grain populations.

The observations to date are consistent with cometary organics being present in all comets at comparable abundances relative to water. Loss of contrast in the 3.4 μm feature as comets get closer to the sun is then easily explained by dilution by thermal emission from the continuum grains, whose flux rises more steeply with heliocentric distance than that of the organics. The lack of a definite 3.4 μm feature in some comet spectra for $r \lesssim 1$ AU could be due to insufficient signal-to-noise (Fig. 2). Upper limits to the band flux (Fig. 3b) suggest that 3.4 μm emission could have been present in these comets at levels consistent with those of other comets.

REFERENCES

Brooke, T.Y., Tokunaga, A.T., and Knacke, R.F. 1990, *A. J.*, submitted.

Roettger, E.E., Feldman, P.D., Budzien, S.A., A'Hearn, M.F., and Festou, M.C. 1990, these proceedings.

Schleicher, D.G., Millis, R.L., Oslip, D.J., A'Hearn, M.F., and Birch, P.V. 1989, *Bull. AAS*, **21**, 936.

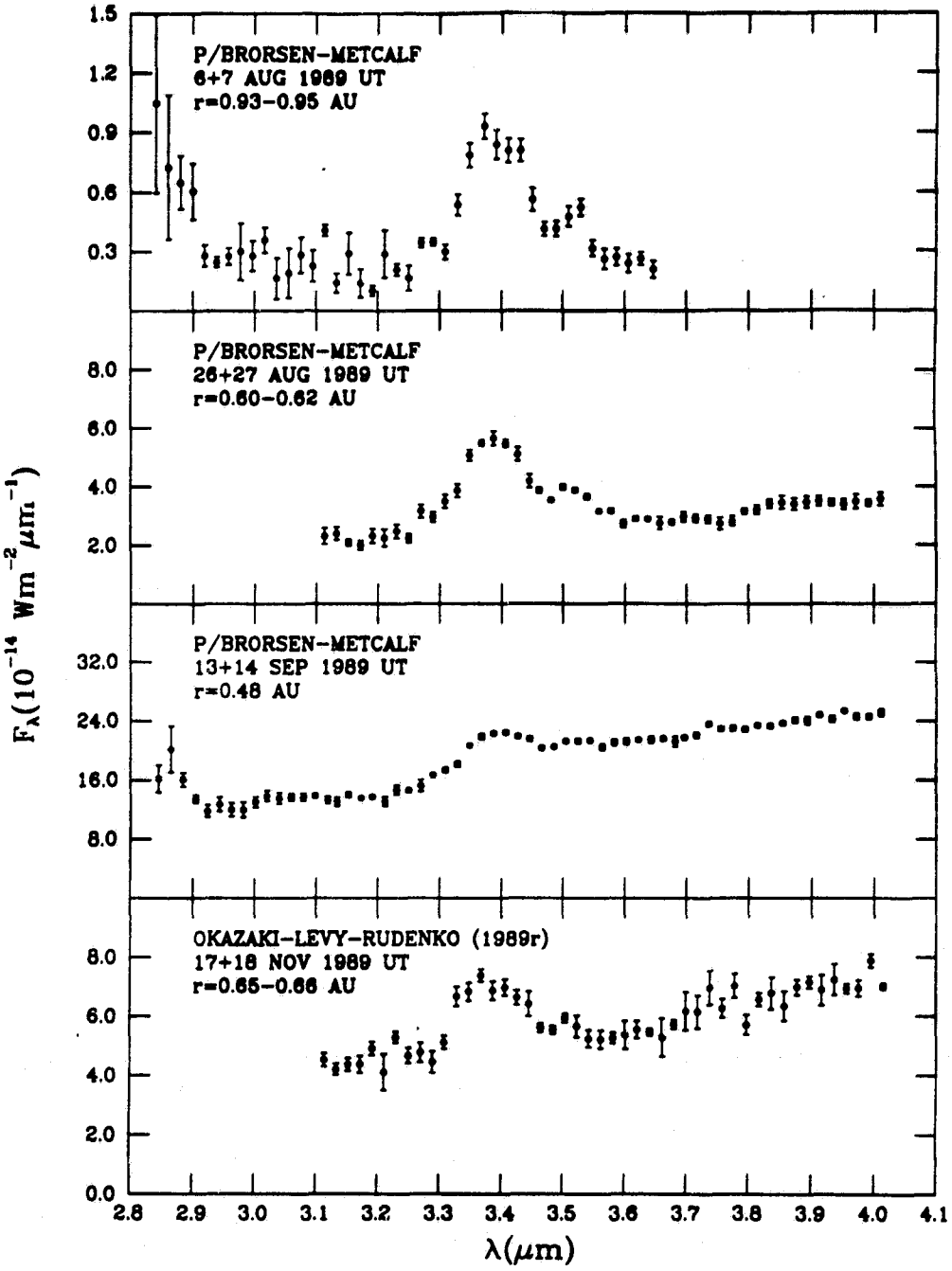

Fig. 1–Spectra of comets P/Brorsen-Metcalf and Okazaki-Levy-Rudenko taken with the Cooled Grating Array Spectrometer ($\lambda/\Delta\lambda = 150 - 200$) at the NASA Infrared Telescope Facility on Mauna Kea. The spectra are composites of data taken on successive days with different grating positions. All spectra were obtained with a 2.7 arcsec diameter aperture centered on the infrared peak. The uncertainty in the absolute flux calibration is approximately 30 %. From Brooke, Tokunaga, and Knacke (1990).

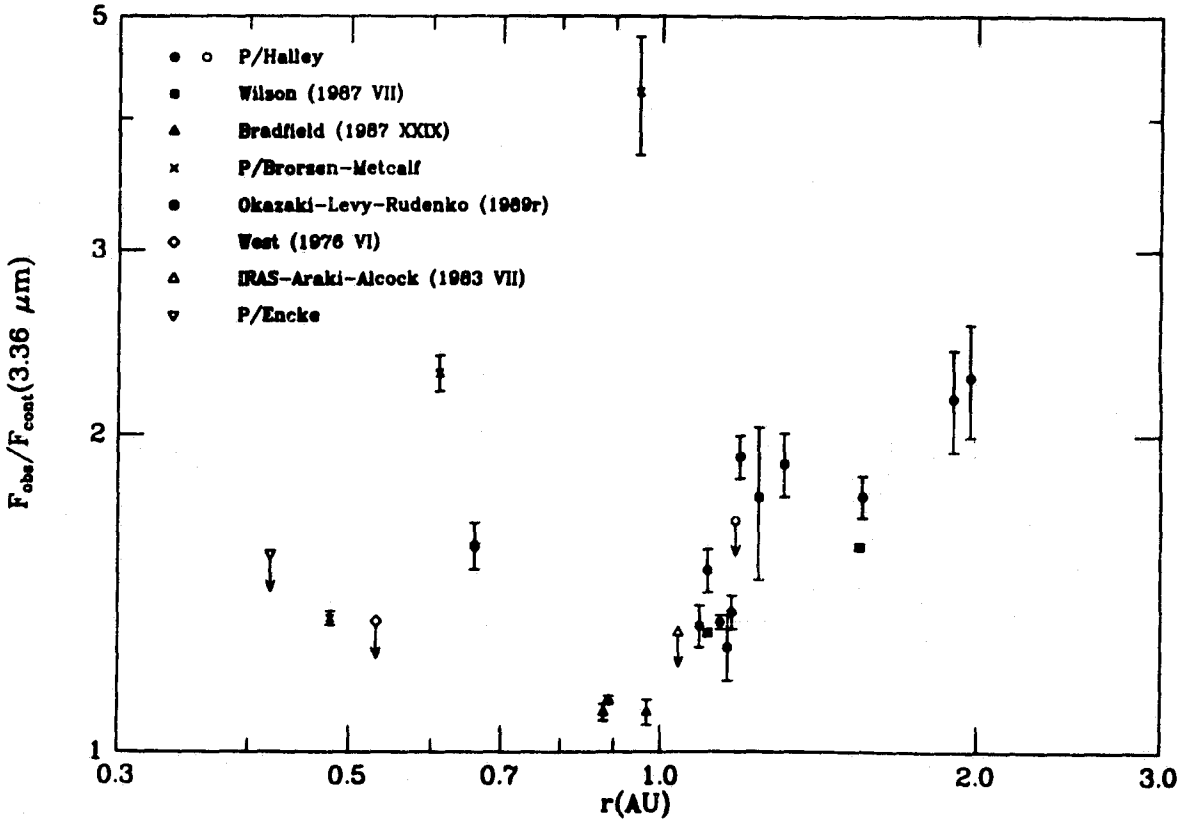

Fig. 2–Feature-to-continuum ratios as a function of heliocentric distance in comets. Downward arrows indicate 3σ upper limits.

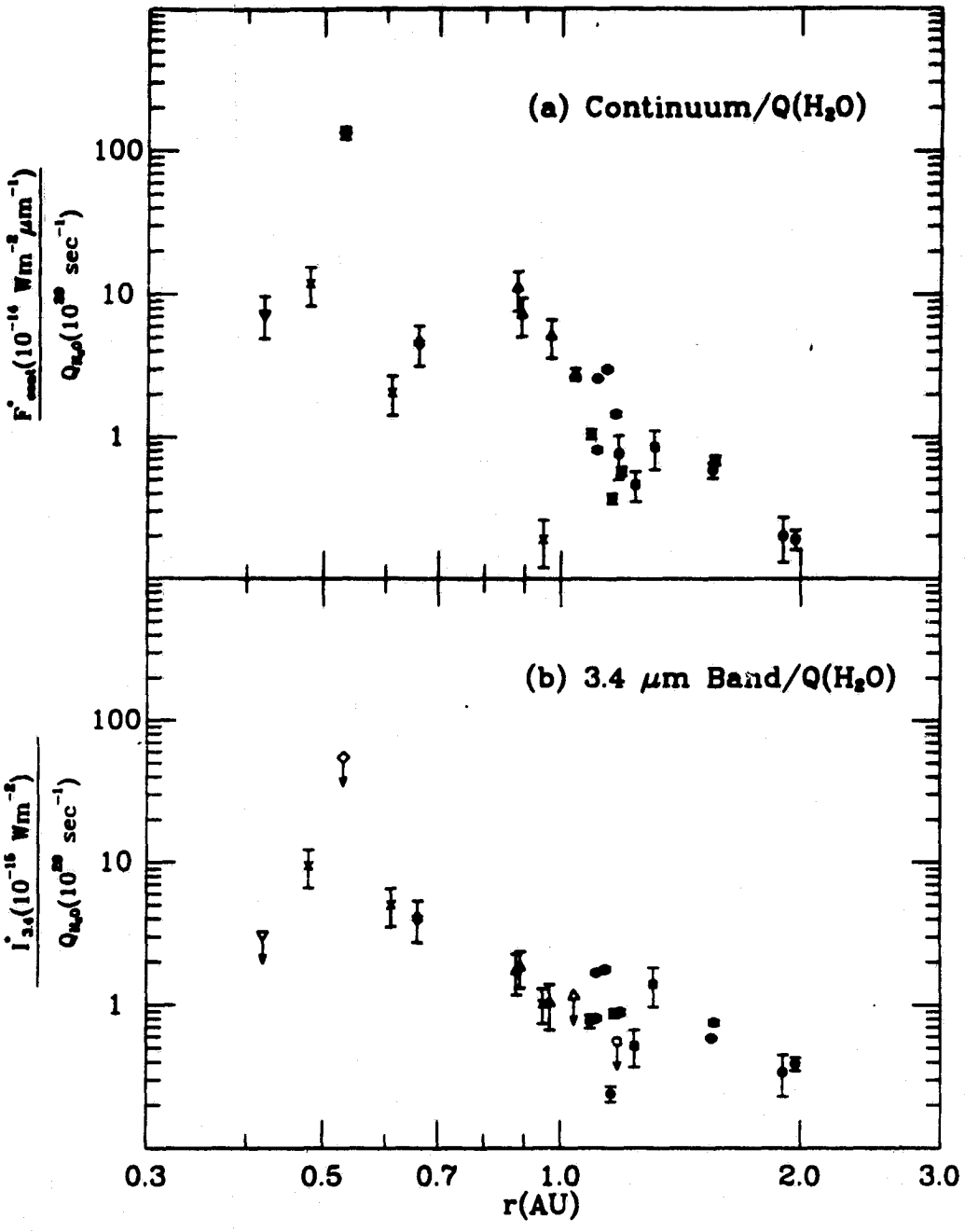

Fig. 3–(a) Dust continuum fluxes at 3.36 μm normalized by the water production rates. F^*_{cont} is the dust continuum flux reduced to a geocentric distance of 1 AU and a projected aperture radius of 980 km. (b) Integrated 3.4 μm band fluxes normalized by the water production rates. $I^*_{3.4}$ is the integrated band flux reduced to a geocentric distance of 1 AU and a projected aperture radius of 980 km. Symbols are the same as Fig. 2.

S21-90
ABS. ONLY
20527
p.1

N91-21033

COMET BRORSEN-METCALF IN THE 3.5 MICRON REGION

A. D. Storrs (U. Texas), M. J. Mumma, and S. M. Hoban (GSFC)

We observed comet Brorsen-Metcalf on UT August 21-24 1989, using the CRSP spectrometer and the 1.3m telescope at Kitt Peak National Observatory. The cometary continuum was detected on all nights. The data are very noisy, due to the short observation window and the untried nature of the instrument. Low resolution (0.0227 micron) spectra show the 3.4 micron C-H stretch feature having a contrast of at most a factor of two to the neighboring continuum. High resolution (0.00331 micron) spectra between 3.4 and 3.6 microns some 1 sigma features that might be attributed to the nu5 band of formaldehyde (H2CO). Similar spectra of the region between 3.2 and 3.4 microns show one 3-sigma line at 3.34 microns, which is as yet unidentified. Although the cometary spectra were more spatially extended than the spectra of standard stars, no extension of the line emission beyond the continuum was observed.

N91-21034

CARBON ISOTOPES IN COMETS

Peter A. Wehinger

Physics-Astronomy Department, Arizona State University

This paper is a progress report based on high resolution spectra of selected bright comets with the goal of determining the carbon isotope abundance ratio, $^{12}C/^{13}C$. The $^{12}C/^{13}C$ ratio has been determined for various Solar System objects (in the atmospheres of the giant planets, meteorites, the Earth, and the solar photosphere), where $^{12}C/^{13}C$ = 89/1. In the interstellar medium, optical and radio observations give a range of $^{12}C/^{13}C$ = 43-67/1 depending on the observing techniques used and the specific interstellar cloud observed. For comet P/Halley, Wyckoff *et al.* (1989 *Ap. J.*, **339**, 488) found $^{12}C/^{13}C$ = 65/1±8. Previous determinations of the $^{12}C/^{13}C$ ratio in comets by other investigators, involving lower resolution spectra, dealt with the C_2(0,1) Swan system with band heads at 4737 Å for $^{12}C_2$(0,1) and at 4745 Å for $^{13}C^{12}C$(0,1). However, there is an NH_2 feature with four lines which coincide with the $^{13}C^{12}C$ band head, thus making a determination of the $^{12}C/^{13}C$ ratio very uncertain based on the C_2(0,1) band structure.

Here we present echelle spectra of the CN(0,0) violet system in three additional comets: P/Brorsen-Metcalf (observed during August 1989), C/Okazaki-Levy-Rudenko (C/1989r) (December 1989), and C/Austin (C/1989c1) (May 1990). P/Brorsen-Metcalf has a period of 70 y (prograde) compared with P/Halley which is 76 y (retrograde). The similar periods made P/Brorsen-Metcalf of special interest for comparison with P/Halley. The other two comets were simply comets of opportunity. While not shown here, we have also acquired echelle spectra of C/Wilson. All four comets were observed when they were at or close to maximum brightness, ~5-6 mag for the integrated magnitude of the coma. Of the four comets discussed here, only P/Halley (~4.0 mag) has relatively high dust-to-gas production rates. Little or no scattered solar continuum was detectable in comets P/Brorsen-Metcalf, C/Okazaki-Levy-Rudenko, and C/Austin.

All of the spectra were acquired with the Mount Stromlo Observatory's 1.9-m reflector near Canberra, Australia, except for P/Brorsen-Metcalf which was observed with the Kitt Peak National Observatory 1-m coudé-feed telescope. Our observations consist of coudé-echelle spectrograms of the CN(0,0) $B^2\Sigma^+ - X^2\Sigma^+$ violet system. Our immediate objective is to search for $^{13}C^{14}N$(0,0) lines in the R-branch ($\Delta J=+1$) and to compare these spectra with those of P/Halley at approximately the same spectral resolution.

The instrumental details for the Mount Stromlo observations are: 1.9-m f/32 coudé focus, spectral range: $\lambda\lambda$ = 3862-3876 Å, spectral resolution: $\lambda/\Delta\lambda$ = 80-100,000, $\Delta\lambda$ = 40-50 mÅ(FWHM), typically ~2.5 pixels, with slit dimensions: 0.8 x 22 arc sec. The 600 line/mm echelle grating was used with a cross disperser and an 81.3-cm focal length Schmidt camera. The two-dimensional detector is a photon counting array (PCA) which employs two Litton micro-channel-plate intensifiers, an f/1 Nikon transfer lens, and a Fairchild 244 x 750 CCD. The PCA has inherently low noise characteristics and is read out continuously at tv-frame rates, thus making it an ideal system for detecting weak spectral lines at low contrast in extended objects such as comets.

The spectra of P/Brorsen-Metcalf were acquired with the 1-m f/30 coudé feed telescope at KPNO. The slit dimensions were: 1.5 x 134 arc sec, while the spectral range was the same as the Mount Stromlo spectra. The detector was a Texas Instruments 800 x 800 CCD with quantum efficiency of about 20% at 3870 Å. The No. 5 Schmidt camera was used with an echelle grating and an order-sorting filter centered on the 3860-3880 Å region, giving a spectral resolution of 100,000. The quality of the data was limited by the readout noise (12 e^- per pixel per read) which was comparable in intensity with the $^{13}C^{14}N$ lines. Integration times were limited to 15 min because of frequent and numerous cosmic ray hits.

In Figure 1 we present a moderate resolution spectrum of the CN(0,0) violet system in P/Halley showing both the P- and R-branches covering the spectral range 3850-3890 Å obtained with the Mount Stromlo 1.9-m reflector, 81.5-cm camera, and a plane grating, with a spectral line width of ~200 mÅ (FWHM). Figure 2 shows the CN(0,0) R-branch in P/Halley (1986 April 4). Figure 3 is a composite spectrum of the CN(0,0) R-branch in P/Brorsen-Metcalf coadded over five nights (1989 August 15-19). Figure 4 shows the CN(0,0) R-branch and part of the P-branch in C/Austin (1990 May 19 and 20). Detail of the weak $^{13}C^{14}N$ R4, R5, R6 lines are shown for P/Halley (Figure 5), P/Brorsen-Metcalf (Figure 6), C/Okazaki-Levy-Rudenko (Figure 7), and C/Austin (Figure 8).

In Figures 6, 7, and 8 possible detection of $^{13}C^{14}N$ lines is indicated by the vertical arrows. However, we must stress that the identification of these weak features, as well as any resulting $^{12}C/^{13}C$ abundance ratios, depend on comparisons with computed synthetic spectra, which simulate the Doppler-shifted solar flux for each integration over the course of two nights to two weeks. In a separate paper presented at this workshop, by Marvin Kleine (Arizona State University), full fluorescence calculations for the CN violet system are described. Comparison of our observations and Kleine's synthetic spectra are currently in progress.

These observations, their reduction, and analysis represent the collaborative effort of Bruce Peterson (Mount Stromlo Observatory), Susan Wyckoff, Marvin Kleine, Maria Womack (all at Arizona State University), and Eric Lindholm (Boston University). We are grateful to the Directors of Mount Stromlo Observatory (Alex Rodgers) and Kitt Peak National Observatory (Dave De Young) for telescope time. This program is supported, in part, by NASA Grant NAGW-547 and the NSF U.S.-Australian Cooperative Science Program. I am most grateful to Bruce and Vickie Peterson for their kind hospitality on numerous my visits to Canberra.

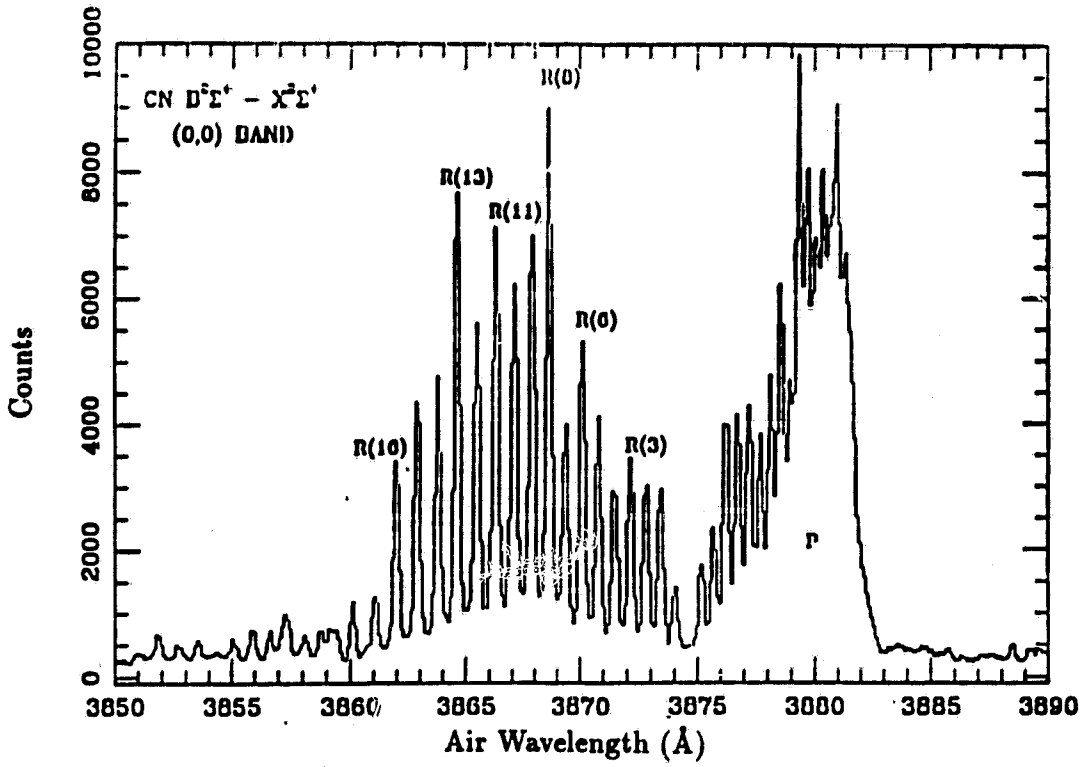

Figure 1. P/Halley CN(0,0) violet system P- and R-branch spectrum obtained with the 1.9-m Mount Stromlo reflector and a plane grating coudé where $\lambda/\Delta\lambda$ = 25,000 (1986 March 26).

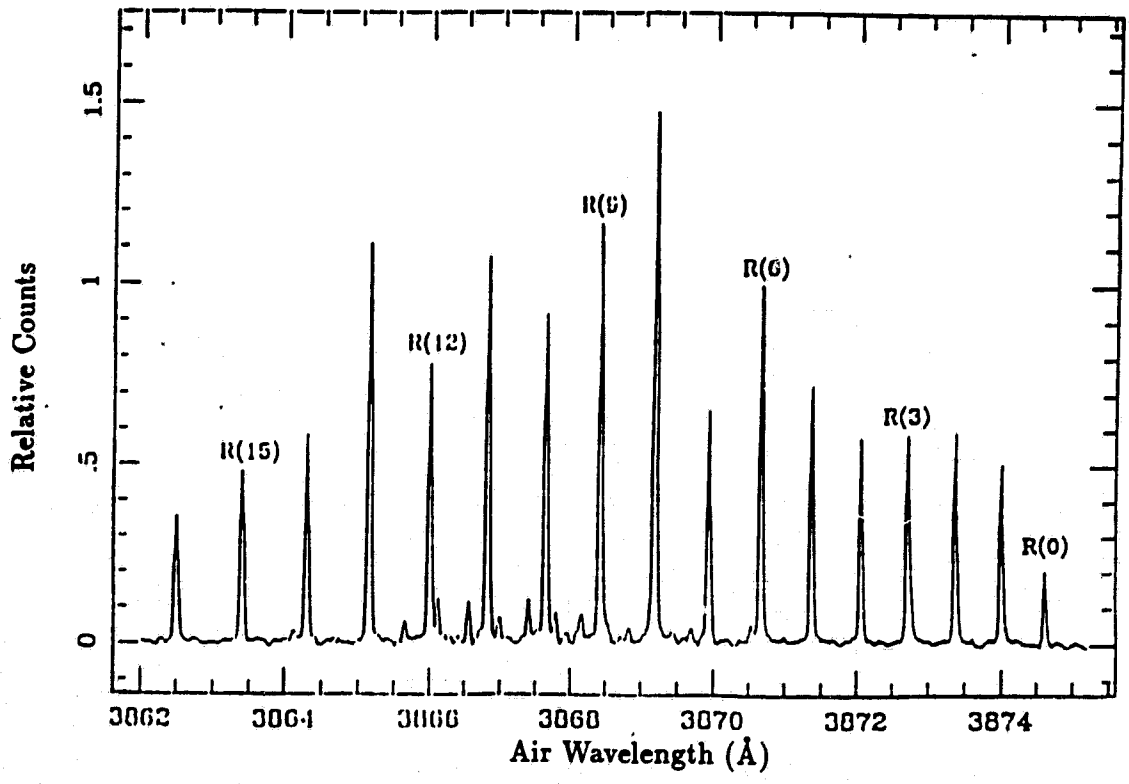

Figure 2. P/Halley CN(0,0) violet system R-branch spectrum obtained with the 1.9-m Mount Stromlo reflector and the coudé echelle spectrograph where $\lambda/\Delta\lambda$ = 100,000 (1986 April 4).

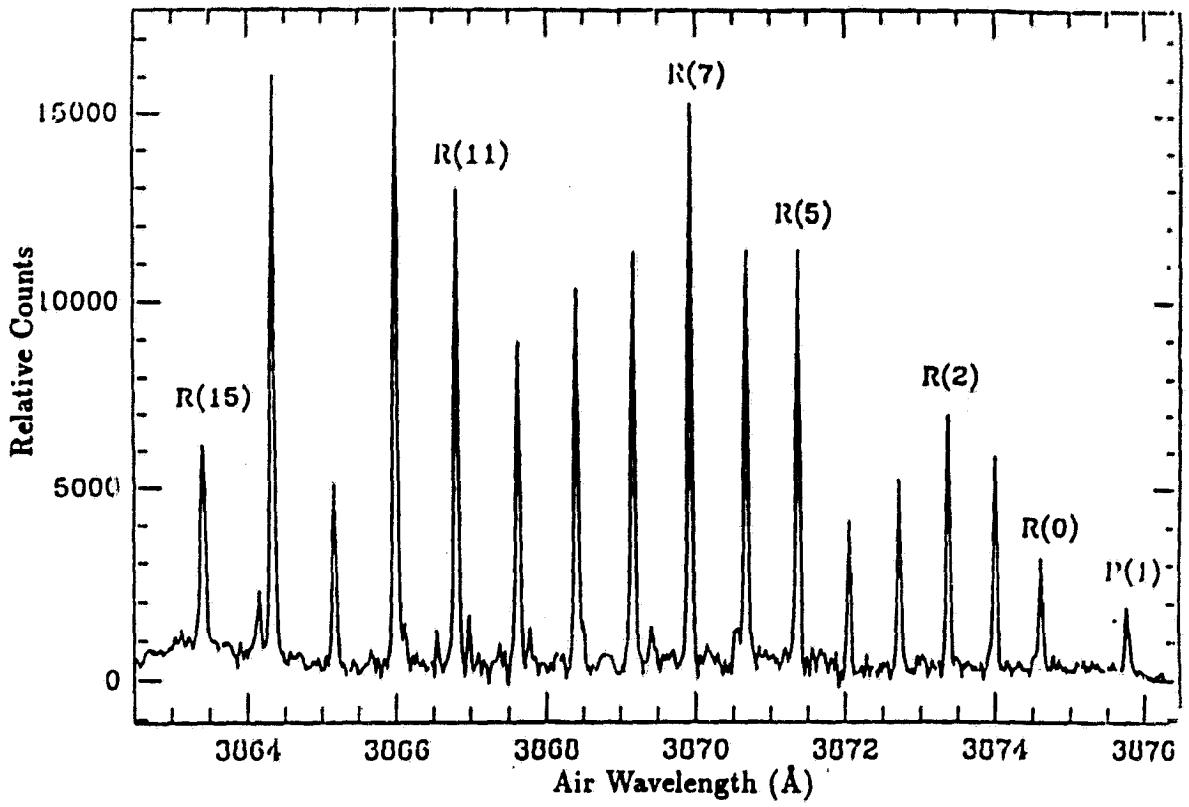

Figure 3. P/Brorsen-Metcalf CN(0,0) violet system R-branch spectrum obtained with the 1-m Coudé Feed telescope at Kitt Peak National Observatory where $\lambda/\Delta\lambda = 100{,}000$ (1989 Aug 15-19).

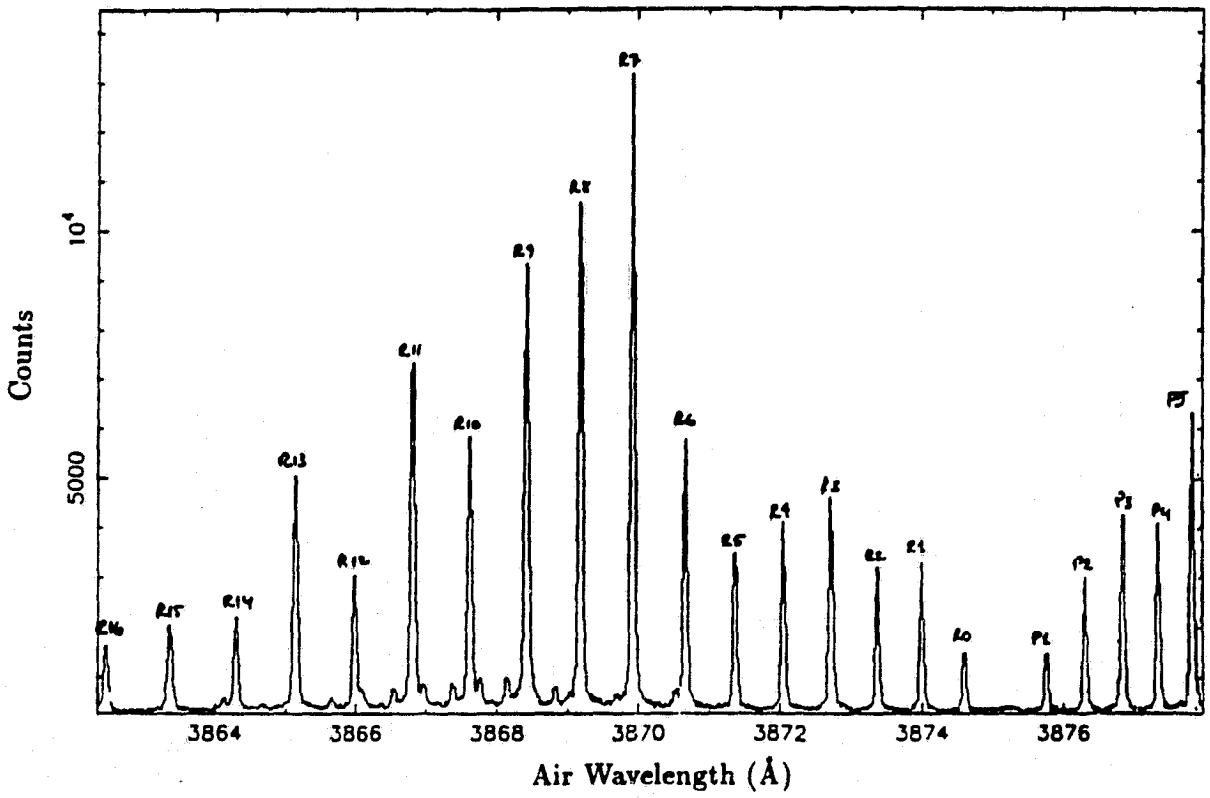

Figure 4. C/Austin CN(0,0) violet system R-branch spectrum obtained at Mount Stromlo (1990 May 19 and 20).

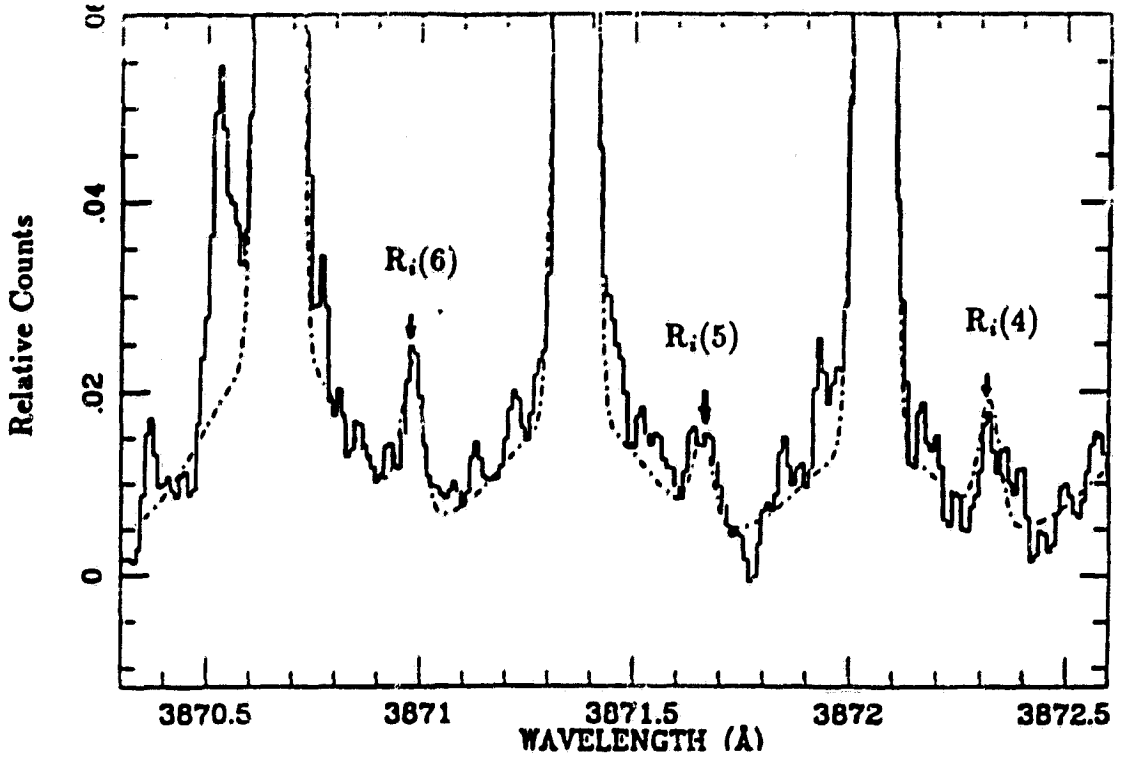

Figure 5. Detail of the $^{13}C^{14}N(0,0)$ rotational lines in P/Halley which are indicated by vertical arrows.

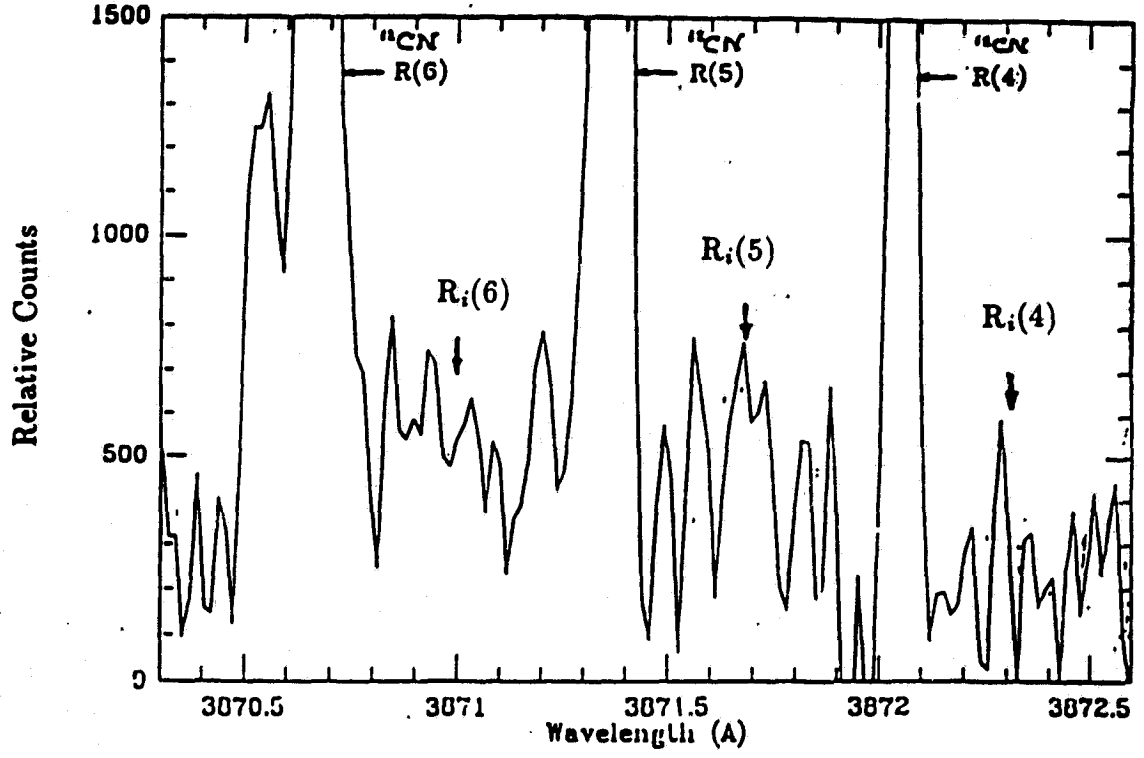

Figure 6. Detail of the $^{13}C^{14}N(0,0)$ rotational lines in P/Brorsen-Metcalf.

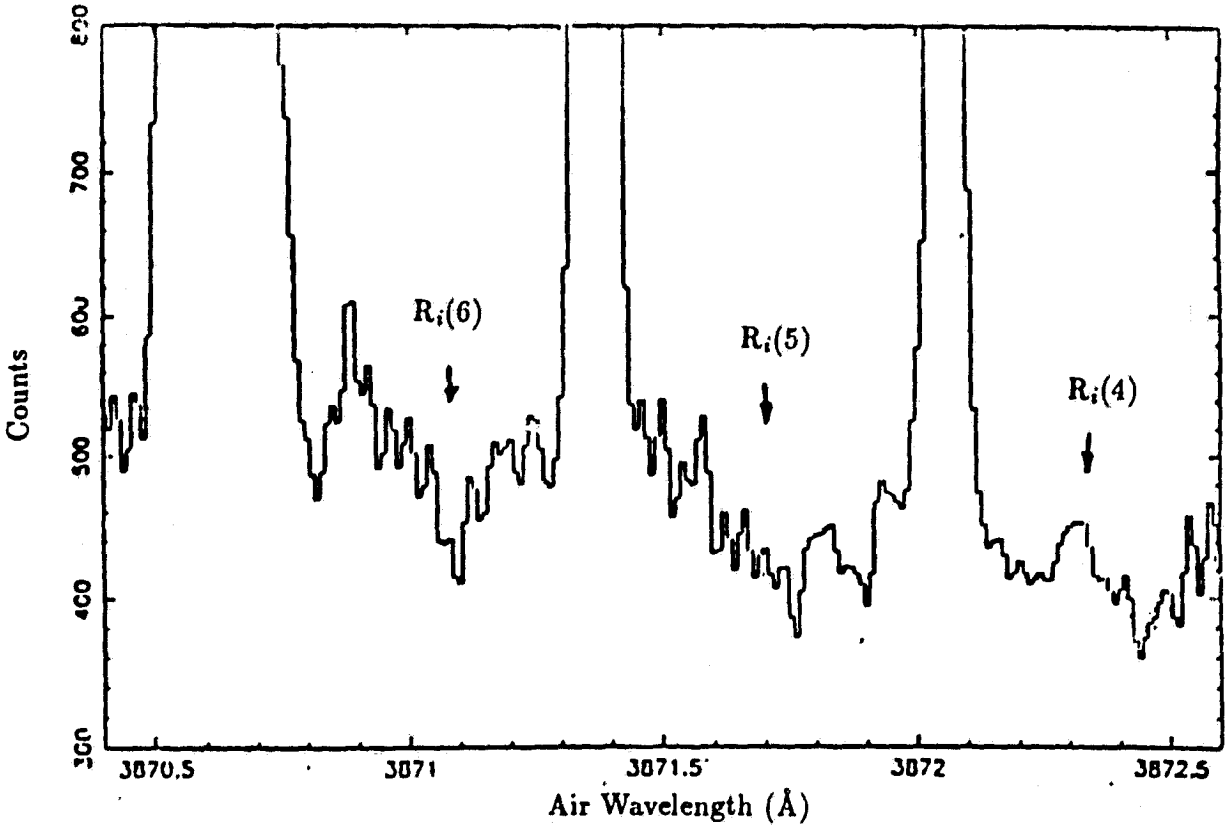

Figure 7. Detail of the $^{13}C^{14}N(0,0)$ rotational lines in C/Okazaki-Levy-Rudenko.

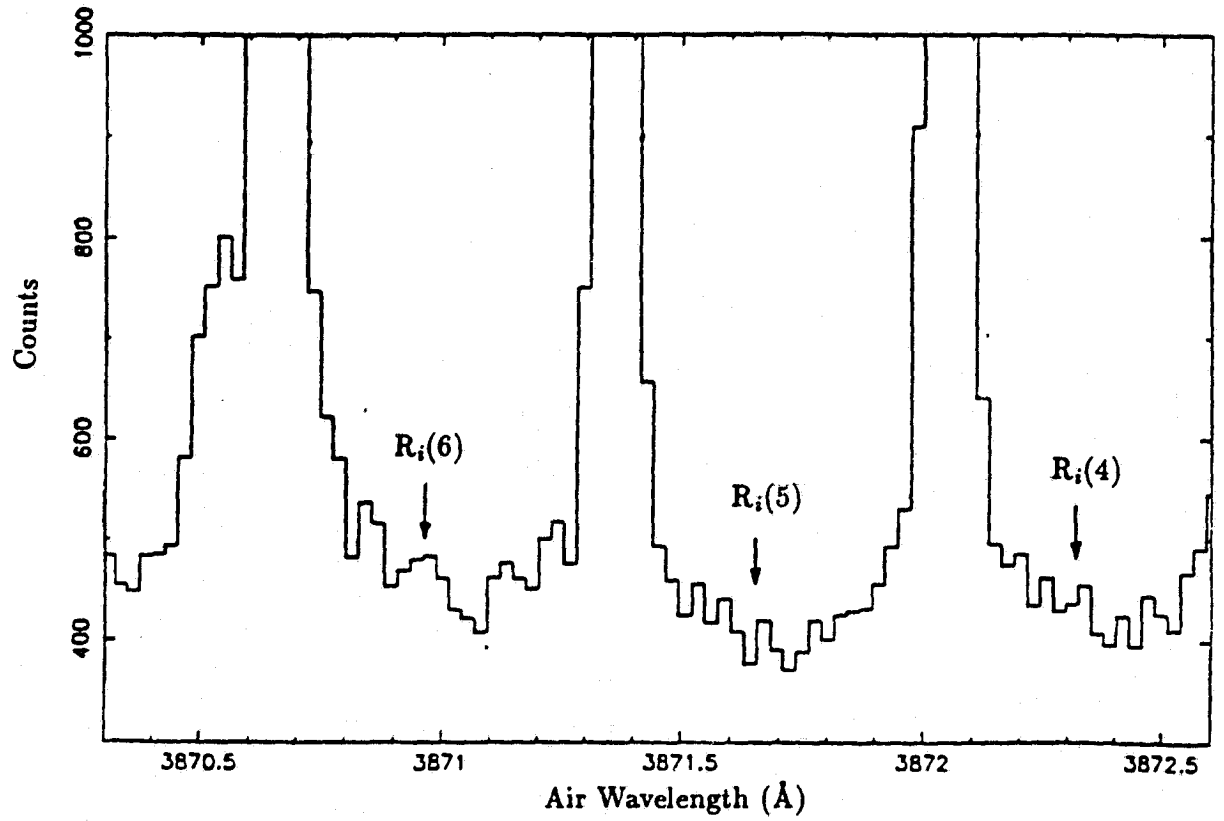

Figure 8. Detail of the $^{13}C^{14}N(0,0)$ rotational lines in C/Austin.

Dave Schleicher

1) What is the aperture size that was collapsed into the single spectrum?

2) Is the apparent continuum actually a continuum or just the wings of the strong CN lines due to the instrument profile?

Peter Wehinger

The typical slit dimensions were $\sim 20 \times 1$ arc sec.

In our spectra of comet Austin and Comet Okazaki-Levy-Rudenko scattered solar continuum has not yet been removed. However, with the low dust production in these comets, corrections for solar continuum is small, compared to Comet Halley.

N91-21035

N_2H^+ IN WARM AND COLD CLOUDS

Maria Womack

Department of Physics and Astronomy

Arizona State University

N_2/NH_3 Abundance Ratios in Star-Forming Regions

A topic of importance in both cometary and interstellar astronomy is the N_2/NH_3 abundance ratio in star-forming regions. A key test for solar system formation models is the N_2/NH_3 abundance ratio in comets, which are thought to be comprised of material from the protosolar nebula, and in molecular clouds, from which stars are thought to form. The N_2/NH_3 abundance ratio has been measured for comet Halley and found to be $\sim$ 0.1 (Wyckoff and Theobald 1989). The N_2/NH_3 abundance ratio has never been measured in the ISM, but is estimated from theoretical models (i.e. Herbst and Leung 1989) to be in the range of 100-200. If the theoretical models are truly representative of dense molecular clouds then the difference in the abundance ratios of N_2/NH_3 between comets and the ISM would imply that significant chemical processing must have occurred in the protosolar nebula that somehow altered the amount of N_2 relative to NH_3. We have undertaken a systematic survey of star forming regions to establish N_2 abundances and N_2/NH_3 ratios for comparison with cometary data.

Abundances of NH_3 in dense molecular clouds are well-established (e.g. Mauersberger *et al.* 1986). Molecular nitrogen, however, is not observable with radio techniques due to lack of a permanent dipole moment. Protonated N_2, (or N_2H^+), is observable and therefore N_2H^+ abundances can be measured and N_2 abundances deduced if we assume:

1) All of the N_2H^+ is produced from the reaction

$$N_2 + H_3^+ \rightarrow N_2H^+ + H_2$$

2) All of the destruction of N_2H^+ is due to electron recombination

$$N_2H^+ + e^- \rightarrow N_2 + H$$

3) Observed NH_3 and N_2H^+ line emission arise from the same volume.

4) $[N_2] \sim [N_2H^+](k_2/k_1)$ where k_1 = rate constant for electron destruction of N_2H^+ and k_2 = rate constant for formation of N_2H^+.

Observations of the N_2H^+ $J = 1 \rightarrow 0$ (93 GHz), $J = 3 \rightarrow 2$ (279 GHz) and $N^{15}NH^+$ $J = 1 \rightarrow 0$ (91 GHz) transitions were performed with the NRAO 12-m telescope on Kitt Peak. The N_2H^+ abundances were calculated using observed line temperatures of both the $J = 1 \rightarrow 0$ and $J = 3 \rightarrow 2$ transitions of the main isotope together with radiative transfer equations and a Large Velocity Gradient model. The spectra of the less abundant isotope transition were used to help constrain the optical depths of the clouds.

The dense ($n(H_2) \sim 10^4$ to 10^6 cm^{-3}) molecular clouds observed are listed in Table 1. Analysis of the observational data to determine the N_2/NH_3 abundance ratios in these sources is in progress.

TABLE 1

DENSE MOLECULAR CLOUDS WITH N_2H^+

Cold ($\lesssim$ 10K)	Warm ($\gtrsim$ 75K)
L134N	W3
TMC-1	NGC-7538
ORION-3N1E	W51
ρ Oph	W49
	IC443G
	DR21(OH)
	SGRB2
	ORION-S
	ORION-KL

Two Clouds At Orion-KL

A double velocity component was detected in N_2H^+ data obtained toward the Orion-KL (KL) region, which is located in the Orion Molecular Cloud, about 500 pc from the Sun. Orion-KL is considered to be a prototypical region of star formation, indeed it is the brightest infrared region of Orion (see Kleinmann and Low 1967).

Evidence for a shift in radial velocity ranging from +8 to +10 km/s across the KL region has been observed (Ho and Barrett 1978, Bastien *et al.* 1981 and Plambeck *et al.* 1985). Two possible explanations have been proposed:

1) The velocity shift is due to rotation about a central outflow source where the velocity differences are due to the redshift and blueshift of the rotating gas (Plambeck *et al.* 1985).

2) Two clouds with different radial velocities lie along the line of sight to Orion-KL. One to the north with $V_{LSR} \sim 9.8$ km/s and another to the south $V_{LSR} \sim 7.5$ km/s (Ho and Barrett 1978, Bastien *et al.* 1981).

Results

A spectrum of the N_2H^+ $J = 1 \rightarrow 0$ transition is presented in Figure 1. The hyperfine structure of the $\Delta F_1 = +1$ (93.173809 GHz), -1 (93.176310 GHz) and 0 (93.171947 GHz) (Sastry *et al.* 1981) transitions is seen. Two velocity components are apparent in the spectrum; one to the northeast (NE) of KL with an average velocity of 9.5±0.3 km/s and a weaker component to the southwest (SW) with an average velocity of 7.2±0.3 km/s.

In order to study the spatial extent of the clouds giving rise to the two velocity components, N_2H^+ was mapped around Orion-KL with a 70″ beam. A schematic diagram of the spectra obtained are presented in Figure 2. Measured velocities, V_{LSR}, from the individual spectra are plotted on a grid (α, δ) and two velocities are plotted for a given position if both velocity components were detected in a single spectrum. We have proposed boundaries of the two clouds with curved lines. Several compact infrared sources, including at least one protostar, have been found in the region and are plotted on top of our N_2H^+ data. The infrared sources lie at the projected overlap of the two clouds. Therefore we suggest that this may be evidence for a cloud-cloud collision triggering star formation.

Summary

A survey of N_2H^+ in 17 star-forming regions in the galaxy has been completed. N_2 abundances will be derived and N_2/NH_3 abundance ratios established in the molecular

clouds. The N_2/NH_3 abundance ratios will be compared with the same ratio in comets to assess the amount of chemical processing which may have occurred during the formation of the solar system.

As part of this survey, a double velocity structure was discovered toward Orion-KL, a region of substantial star formation. We propose a two cloud model for the Orion-KL nebula, where two velocity components are unambiguously detected - one to the NE of Orion-KL at $V_{LSR} \sim (9.5 \pm 0.3)$km/s and the other to the SW of Orion-KL at $V_{LSR} \sim (7.2 \pm 0.3)$km/s. Compact infrared sources (including at least one protostar) lie at the projected interface of the two clouds and suggest that a cloud-cloud collision may have triggered the observed star forming activities.

REFERENCES

Bastien, P., Bieging, J., Henkel, C., Martin, R.N., Pauls, T., Walmsley, C.M., Wilson, T.L. and Ziurys, L.M. 1981 *Astron. Ap. (Letters)*, **98**, L4.

Downes, D., Genzel, R., Becklin, E.E. and Wynn-Williams, C.G., 1981, *Ap. J.*, **244**, 869.

Herbst, E. and Leung, C.M. 1989, *Ap. J. Supp.*, **69**, 271.

Ho, P.T.P and Barrett, A.H. 1978, *Ap. J. Letters*, **224**, L23.

Kleinmann, D.E. and Low, F.J. 1968 *Ap. J. Letters*, **149**, L1.

Mauersberger, R., Henkel, C., Wilson, T.L. and Walmsley, C.M. 1986, *Astron. Ap.*, **162**, 199.

Plambeck, R.L., Vogel, S.N., Wright, M.C.H., Bieging, J.H. and Welch, W.J. 1985, *International Symposium on Millimeter and Submillimeter Wave Radio Astronomy*, 235.

Sastry, K.V.L.N., Helminger, P., Herbst, E. and De Lucia, F.C. 1981, *Chem. Phys. Letters*, **84**, 286.

Wyckoff, S. and Theobald, J. 1989, *Adv. Space Res. 9*, 157.

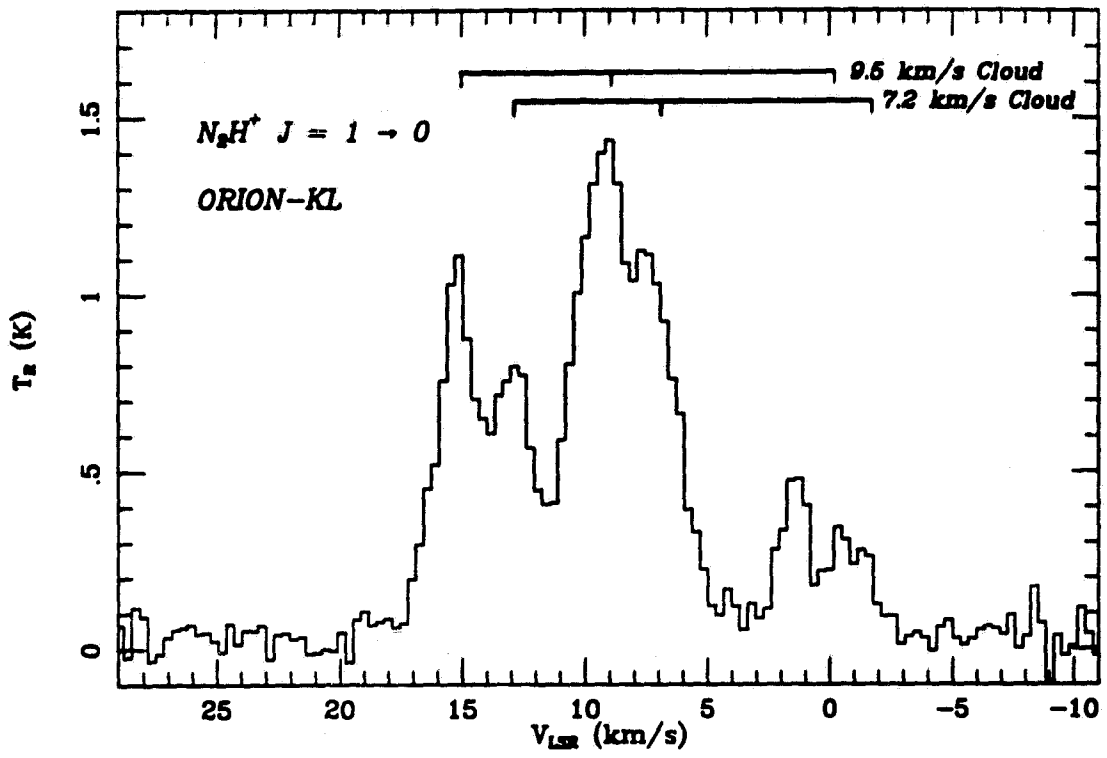

Figure 1. The N_2H^+ J = 1 → 0 emission toward Orion-KL. Two velocities are seen for each ΔF_1 hyperfine component of N_2H^+ and are separated by ~ 2.5 km/s.

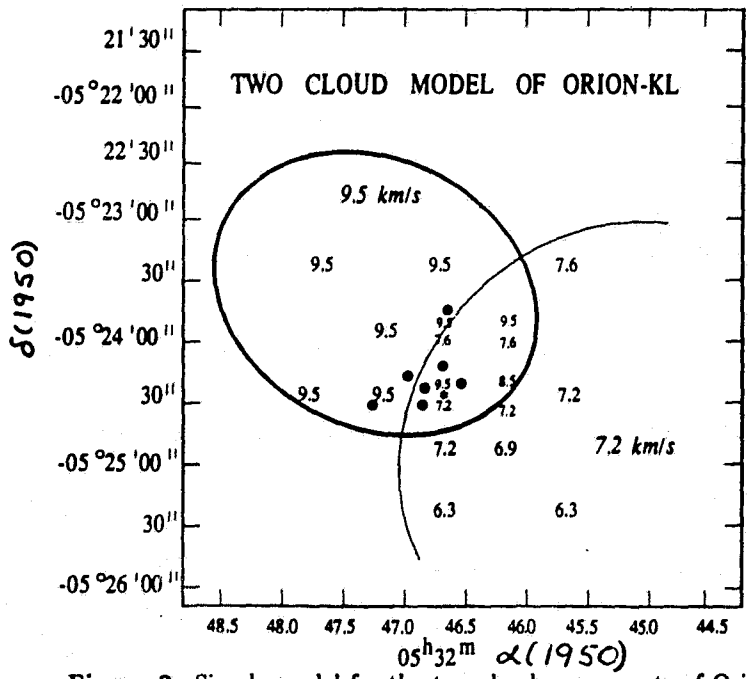

Figure 2. Simple model for the two cloud components of Orion-KL with the measured LSR radial velocities of two clouds as shown. Locations of compact IR sources (Downes *et al.* 1981) are plotted. The position of Orion-KL is noted with an *. Note that the IR sources are found within the projected overlap region of the two clouds, which we suggest is evidence for a cloud-cloud collision triggering star formation.

Ray Russell
Are there any other lines in this part of the spectrum that could act for the double set of lines?

Maria Womack
No. We were able to resolve the hyperfine lines of the N_2H^+ ($J = 1 \rightarrow 0$) transition in one of our sources, L134N. We used this spectrum to identify the $1 \rightarrow 0$ of N_2H^+ toward Orion - KL.

Walter Huebner
Since you base your N_2 abundance on N_2H^+, it is important to understand the production of N_2H^+. How does one produce an ion in the interior of a dense interstellar cloud? If this is not understood, then the N_2 abundance in the center of the cloud could be quite different since the observed N_2H^+ may be only on the surface of the cloud.

Maria Womack
N_2H^+ is thought to be produced by ion-molecule reactions, which typically proceed at low temperatures. The strength of both the $J = 1 \rightarrow 0$ and $J = 3 \rightarrow 2$ lines toward hot, dense regions was unexpected and we will work to identify the production mechanism of N_2H^+ in these hot, dense clouds. It has been suggested that grain chemistry may be important.

Timothy Brooke
Your technique will only give you N_2/NH_3 in the gas phase in molecular clouds. For comparison to comets, don't you also need a handle on the form nitrogen takes in grains?

Maria Womack
Yes, we will also consider the grains as a carrier of cometary nitrogen.

524-90
N91-21036

SPECTRAL SYNTHESIS OF CN IN COMETS

Marvin Kleine
Department of Physics and Astronomy
Arizona State University

Introduction

Measurement of the carbon isotope ratios in comets provides direct information about the chemical state of the interstellar medium (ISM) 4.5 billion years ago. All solar system objects (e.g. sun, planet atmospheres, meteorites and lunar rocks) for which the carbon isotope abundance ratio has been measured indicate $^{12}C/^{13}C = 89\pm2$. This value is different from the ratio measured in the present-day local interstellar medium (ISM) where the carbon isotope ratio has been measured to range from $^{12}C/^{13}C \sim 40$ to 70. Models for the chemical evolution of the ISM (e.g. Audouze 1985) attribute the difference between the solar system and ISM carbon isotope ratios as due to a gradual ^{13}C enrichment of the ISM largely from red giant stars and novae over the past 4.5 billion years. However, a measurement of the carbon isotope ratio in comet Halley (Wyckoff et. al. 1989) indicated a value significantly different from the solar system value, namely, $^{12}C/^{13}C = 65\pm 9$. If the comet formed coevally with the solar system, it is difficult to explain this abundance ratio.

Because of the importance of the carbon isotope ratio in understanding the formation of the solar system and the long-term chemical evolution of the ISM, we have initiated a program to observe the CN B-X (0-0) and C_2 Swan (0-0) bands in a sample of bright comets. An important factor in determining the carbon isotope ratio is the fluorescence model used in the analysis. Here we present high resolution CN spectra of several comets, and describe the model presently in the process of development which will be used to determine the carbon isotope abundance ratios from observations of the R-branch rotational lines of the CN B-X (0-0) band.

Swings (1941) was first to demonstrate that the CN band in comet spectra is excited by solar fluorescence. In fact he showed that the observed spectrum is extremely sensitive to the heliocentric velocity of the comet, because Doppler shifts of only a few km/s can cause large changes in the fluorescing solar flux due to the complex absorption line structure in the solar spectrum in the 3860 - 3880 Å region. In the model described here we assume fluorescence equilibrium (established on timescales of minutes in comet comae) and compute the relative populations of the rotational energy levels in the three electronic states: X, B and A. In exciting the upper electronic states we account for the relative Doppler shifts of the comet and the sun, the so-called Swings effect. The model includes 848 rotational levels of the molecule distributed between the three electronic states. The g-factors or fluorescence efficiencies are calculated from

$$g_{line} = x_i A_{ij}$$

for each observed line for each isotope, $^{12}C^{14}N$, $^{13}C^{14}N$, $^{12}C^{15}N$. The isotope abundance ratio is then computed from the observed line ratios, I/I_i, where I is the intensity of the normal isotope, and I_i is the line intensity of the less abundant isotope, from

$$N/N_i = (Ig_i)/(I_i g).$$

Fluorescence Calculations

The evaluation of the fluorescence efficiency for each transition, requires the solution of a set of linear equations. These linear equations describe the equilibrium occupancy of the molecular energy levels. The set of equations are

$$\frac{dx_j}{dt} = \sum_{i=j+1}^{N} (A_{ij}x_i - B_{ji}x_jU_\nu) - \sum_{i=1}^{i=j-1} (A_{ji}x_j - B_{ij}x_iU_\nu) = 0.0$$

and

$$\sum_{i=1}^{N} x_i = 1.0$$

where

N = number of energy levels,

A_{ij} = probability of spontaneous emission,

B_{ji} = probability of spontaneous absorption,

U_ν = energy density of fluorescing radiation,

x_i = fractional occupancy of the energy level,

x_j = fractional occupancy of energy level under consideration.

This results in a N x N matrix that must be inverted to deterime the x_i's. The g-factors or fluorescence efficiencies are calculated from

$$g_{line} = x_iA_{ij}$$

for each line.

To accurately model the Swings effect requires the use of a high resolution solar atlas. The atlas due to Kurucz et al. (1984) was utilized. The variability of the flux responsible for the pumping of the ground vibrational state of the electronic state B is shown in figure 1. The values for the molecular constants of CN are taken from Ito et al. (1988) and Koltar et al. (1980). The oscillator strengths were taken from the work of Knowles et al. (1988).

The input parameters to the CN spectral synthesis model are the heliocentric distance, heliocentric velocity, and parameters of the molecular isotope under evaluation.

Summary

The CN B-X (0-0) R branch fluorescence spectra for three comets (Austin, Bennett, Halley) were calculated and compared to the observe spectra (see figures 2,3,4). The synthesized spectrum in each case has been shifted to allow for the comparision of the individual line intensities. The Swings effect is clearly visible in each figure. In addition to the R(0-0) band in the CN spectrum, the P(1-1) band also contributes lines in the spectral

region of observation. This branch was calculated and compared to P/Halley (fig. 5). The overall agreement between observations and the CN spectral model is quite good. An exception to this statement would be the high J rotation lines intensities within the R(0-0) branch of P/Halley. Additional analysis is necessary to determine if this difference is due to mechanisms in addition to fluorescence (e.g. collisions).

Further sensitivity analysis of the model is planed to place the comparision with observations on a quantitative level. This model will be applied to cometary spectra (Wehinger, these proceedings) to calculate $^{12}C/^{13}C$ abundance ratios from the analysis of the B-X (0-0) band of the CN radical.

REFERENCES

Audouze, J. 1985, *Production and Distribution of C, N, O Elements*, ed. I.J.Danziger, F.Matteucci, and K.Kjar (ESO Conf. Proc. 21) (Garching:ESO) p.373.

Ito,H., et al.,J.Mol.Spectrosc,127,1988

Knowles,P., et al.,J.Chem.Phys.,89,1988

Koltar,A., et al.,J.Mol.Spectrosc,80,1980

Kurucz,R., et al.,1984,*National Solar Observatory Atlas No. 1*

Swings,P., 1941, Lick Obs.Bull.,19,No.408,131

Wyckoff,S., et al.,1989,Ap.J.,339,488

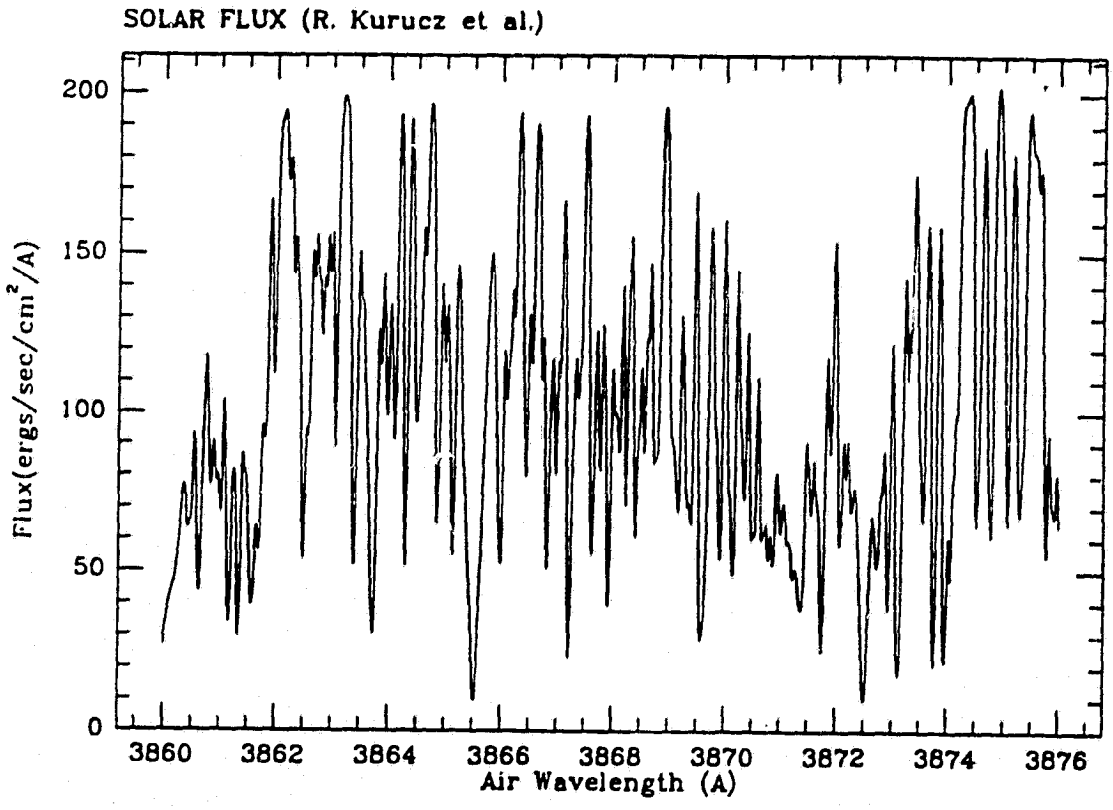

figure 1

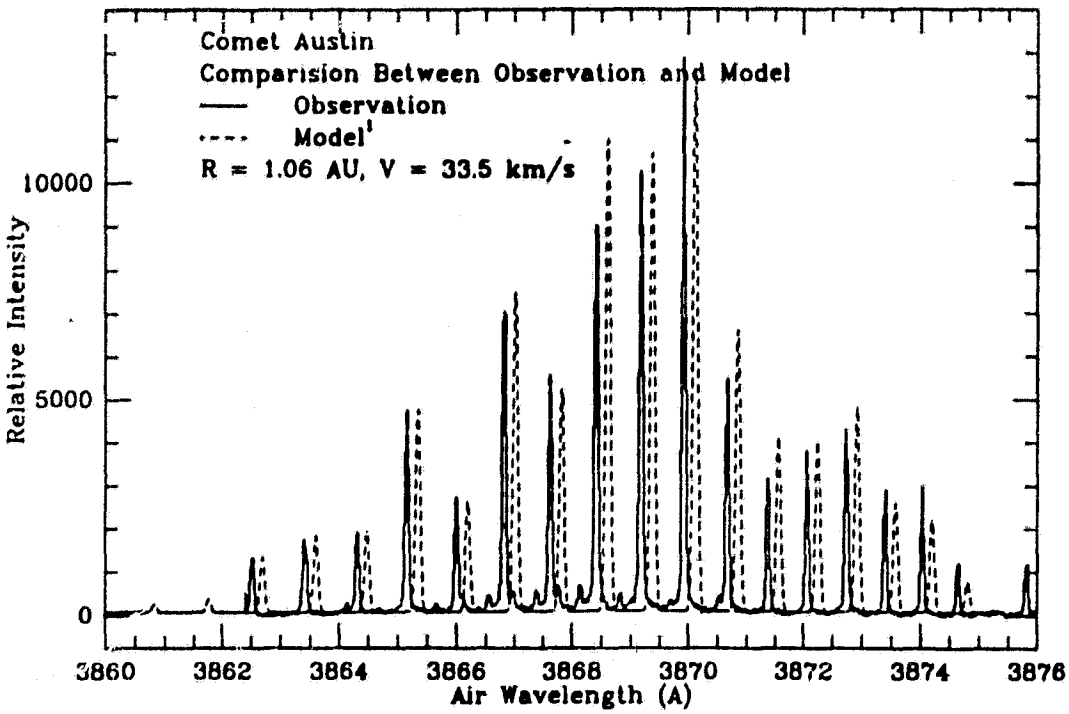

1 Spectrum shifted for comparision

figure 2

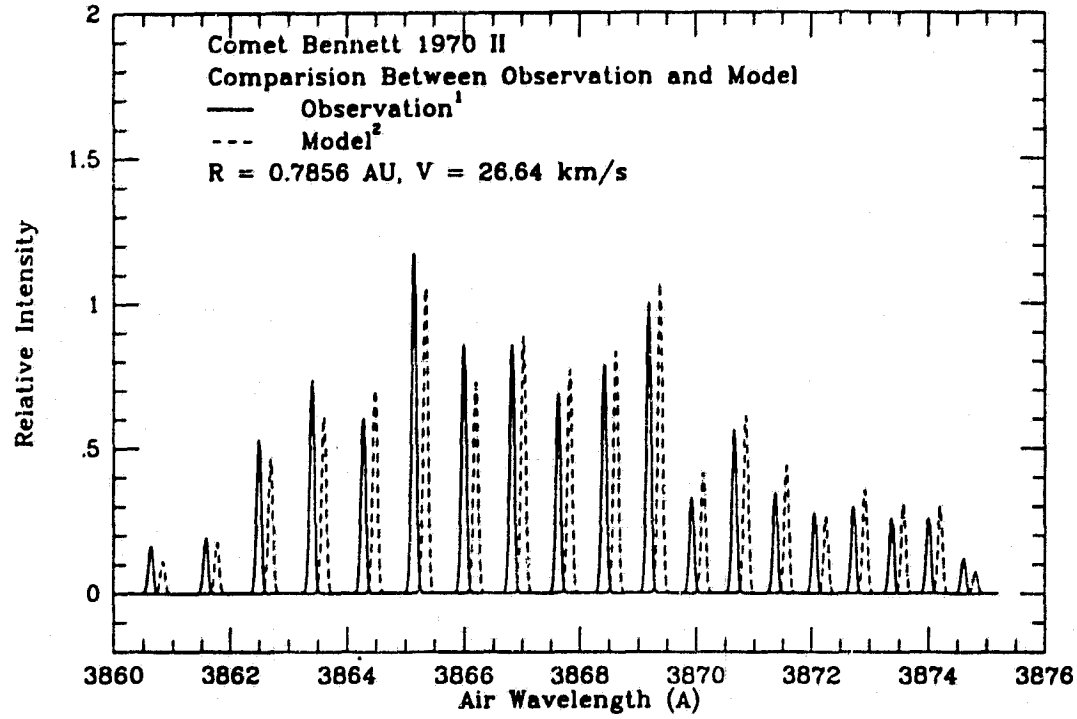

1 Aikman et al., Icarus 21, 1974, convolved with gaussian
2 Spectrum shifted for comparision

figure 3

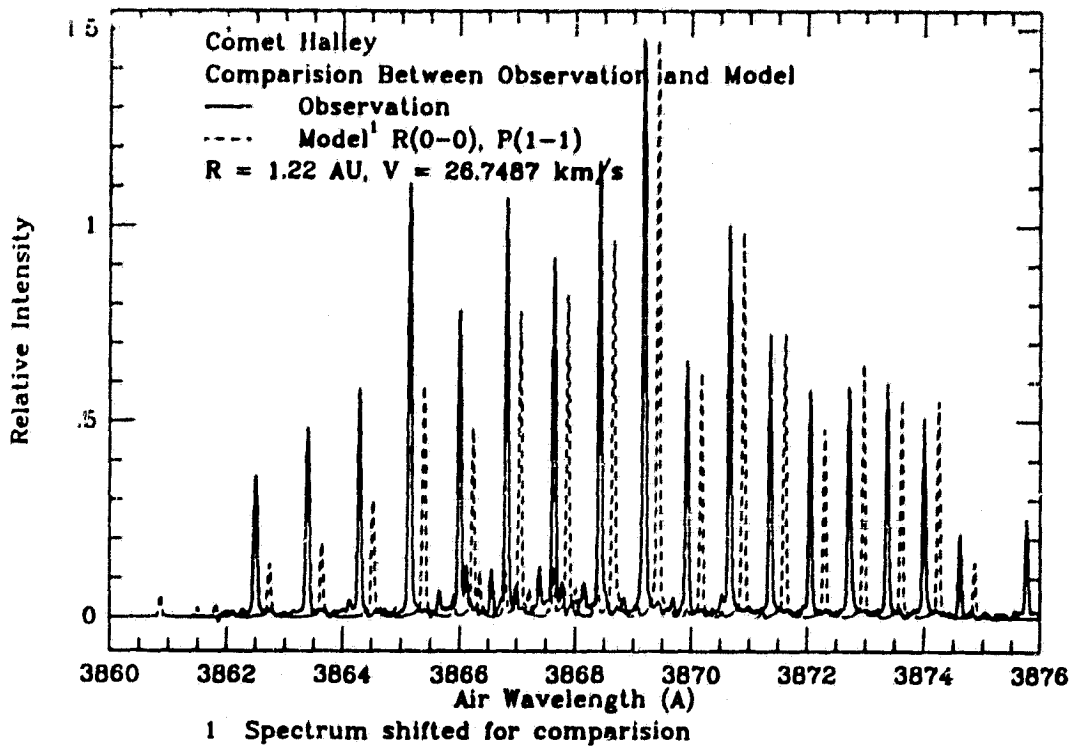

1 Spectrum shifted for comparision

figure 4

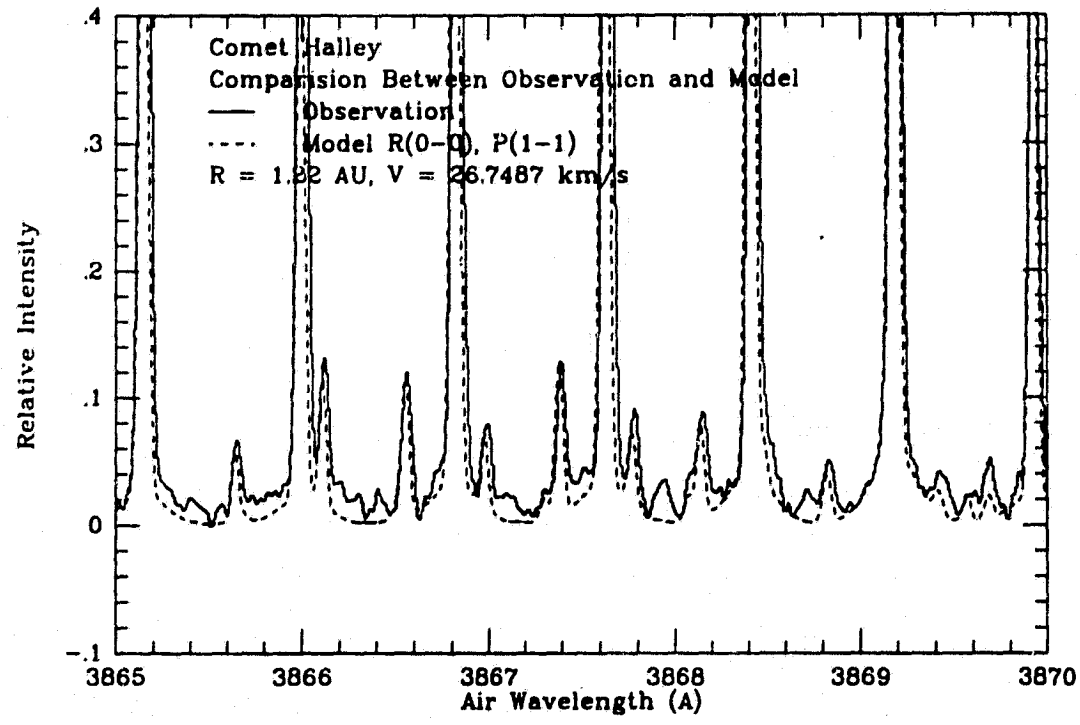

figure 5

N91-21037

NEAR-NUCLEUS H_2O^+ STRUCTURES IN COMETS BRORSEN-METCALF, OKAZAKI-LEVY-RUDENKO, AND AUSTIN

Stephen M Larson
Lunar and Planetary Laboratory
University of Arizona
Tucson, Arizona 85721

ABSTRACT

Comets P/Brorsen-Metcalf (1989o), Okazaki-Levy-Rudenko (1989r) and Austin (1989c1) were all observed to have well developed H_2O^+ structure close to the nucleus that showed changes on a time scale of only a few minutes. We present some preliminary data on the observed ion morphology and their evolution.

Introduction

Wide field groundbased imaging has provided a wealth of data on the spatial and temporal distribution of cometary ion tails resulting from the interaction of cometary and solar wind environments (e.g., Brandt, 1982; Ip and Axford, 1982). Although spacecraft experiments have measured the plasma distribution in Comets Giacobini-Zinner and Halley (e.g., Galeev, 1987; Brandt and Niedner, 1987), they refer only to the times of the encounters. On the other hand, groundbased time series imaging of cometary ion features may provide data on the large scale ion structure dynamics.

Comets P/Brorsen-Metcalf (1989o), Okazaki-Levy-Rudenko (1989r) and Austin (1989c1) were all dust-poor comets presenting an unusual opportunity to record ion structures in the coma relatively free of contamination by solar continuum. We took advantage of this fact to explore the temporal changes that occur at high groundbased resolution (~300 km per pixel) and time scales of a few minutes.

Observations

These CCD imaging observations were obtained with the 1.5 meter Catalina Observatory telescope using an RCA CCD at 0.7 arcsec/pixel and either a broad red-band (650-950nm) filter, or a narrow band filter transmitting the H_2O^+ (0,8,0) band.at 619nm. The field was slightly less than 4 by 6 arcmin. The length of the imaging

sequences were limited by the observing window and need for complimentary spectroscopic observations.

P/Brorsen-Metcalf (1989o) was observed on 1989 August 23 and 24 UT when r = 0.66 AU, D = 0.75 AU, and the phase angle was 91°. A continuous series of 5 minute exposures of over nearly 1.3 hours was obtained the first night, and less frequently over one hour on the second night. A one hour series of images of Comet Okazaki-Levy-Rudenko (1989r) was obtained on 1989 November 22 UT when r = 0.68 AU, D.= 0.58 AU, and the phase angle was 102°.Short sequences of Comet Austin (1989c1) were obtained over the nights of 1990 May 6-8 UT when r = 0.73 AU, D = 0.44 AU and the phase angle was 107°.

Image processing

The relative lack of dust in these comets improved the H_2O^+ visibility compared to most other comets. Large intensity gradients from the nucleus condensation to the outer tail, and some contamination by C_2 still caused some difficulty in seeing low contrast features We found that the best way to see changes of the rapidly moving ion features was to difference images in the sequence. This required careful registration by nulling the central condensation after shifting both images about the same amount to 0.01 pixel. The resulting derivative image shows changes in location of the features. Tracking errors sometimes show up as imperfect cancellation of the central condensation and causes a slight broadening of the feature edges, but do not significantly alter their location or shape.

Ion Feature Morphology

The August 23 sequence on P/Brorsen-Metcalf was the most extensive time series and will be discussed in detail; he sequences on the other comets showed a variety of H_2O^+ morphology consistent with that in P/Brorsen-Metcalf. The primary H_2O^+ features consisted of a central tail "core" flanked by "turning" rays which, in time, folded into the central tail. Virtually all features extend off the field edge 150,000 km from the nucleus. The apex of the main central tail edges was very close to the nucleus and merged into the seeing limited central condensation less than 600 km from the nucleus. The folding tail rays were fairly symmetric about the central tail axis in P/Brorsen-Metcalf, but significant deviations

were seen in the other comets. Modeling is underway to determine if the intensity profiles are consistent with either isolated rays, or conical sheets. If related, the viewing geometry of the projected neutral current sheet may complicate the appearance of the rays.

Evolution of the Ion Features

The figure shows an excerpt of the P/Brorsen-Metcalf sequence showing the formation of a set of folding rays. In this case, a "cloud" of ions accumulated in a uniform coma around the nucleus to a radius of at least 17,000 km before forming identifiable rays initially 65^{o} apart. At this scale, the rays then fold back and form the tail core in 40 minutes yielding an average folding rate of about 45^{o} per hour. The folding rate is slower as it approaches the tail core, and will yield a lower rate in wide angle images. The rays appear to be essentially parabolic forms with the central condensation at the focus. A second set of rays formed in the same way 40 minutes later.

The central tail core may appear to continue to stretch out behind the nucleus, and in some cases "detach" from the central condensation in a disconnection event. The first three frames in the figure shows a receding central tail segment that separated 15-20 minutes before the sequence started. The apparent velocity is about 60 km/sec.

Summary

CCD observations of rapidly changing H_2O^+ morphology in P/Brorsen-Metcalf with high spatial and temporal resolution show 40 minute production cycles of symmetric folding ray structure, extremely narrow central tail core extending to within 600 km of the nucleus, and a disconnected tail segment receding 60 km/sec from the nucleus. Comets Okazaki-Levy-Rudenko and Austin exhibited more complex asymmetric ray structure, but the motion of folding rays (observed over shorter time intervals) appeared consistent with those in P/Brorsen-Metcalf. More analysis will be required to see if these observations can provide constraints to models of ion tail formation and evolution, but qualitatively, it seems that the observed structure is consistent with models of draping solar wind magnetic field lines. The close proximity of H_2O^+ to the nucleus will certainly provide constraints on the ion transport mechanism.

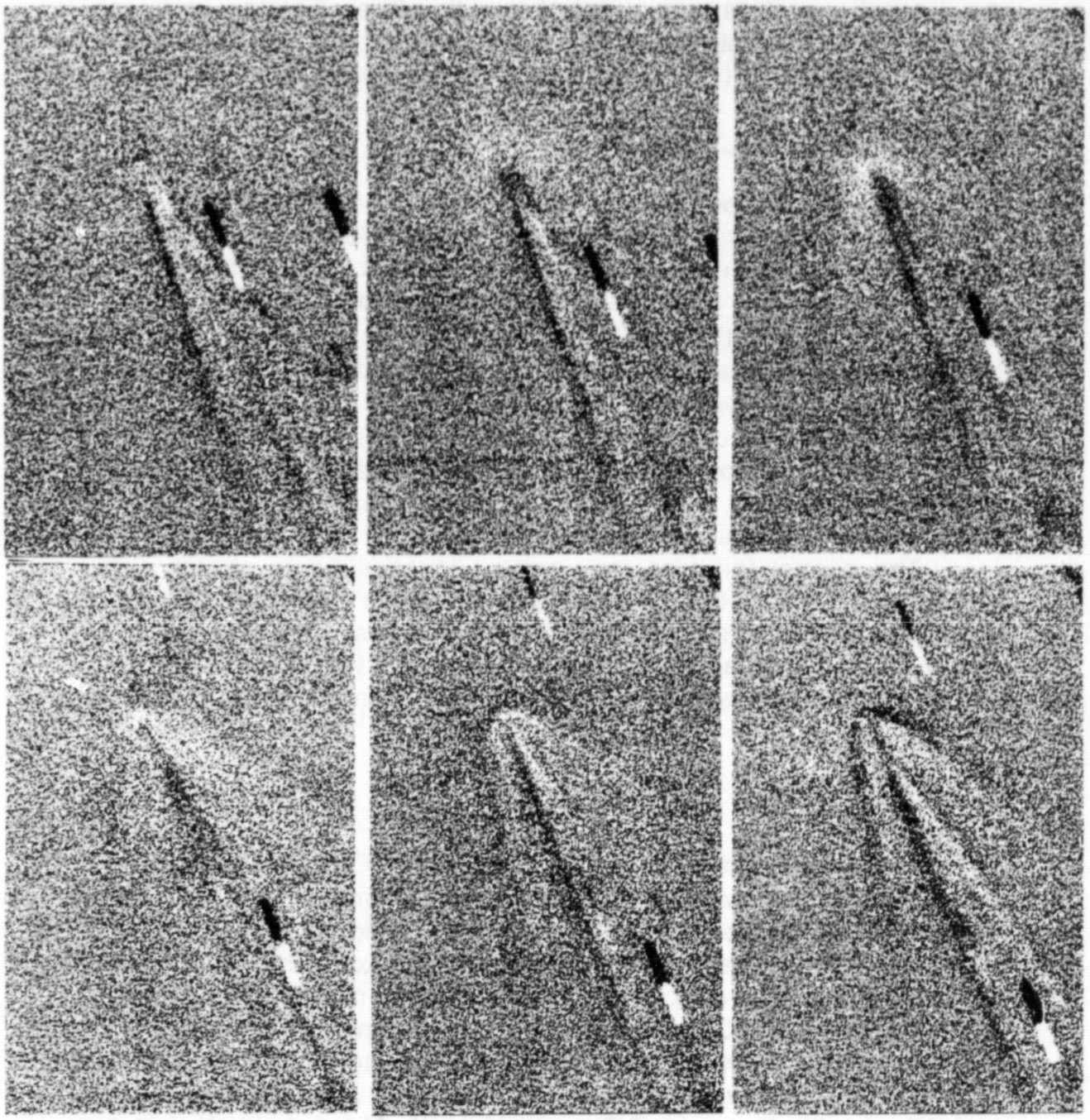

Sequence of 5-minute CCD difference images of P/Brorsen-Metcalf on 1989 August 23 UT. North is to the right, east is to the top, and the sun is to the upper left. The long edge of each frame is 195,000 km at the comet. The midtime of the light component of each difference image corresponds to 10:53, 10:59, 11:05, 11:11, 11:17 and 11:22 UT. Note the faint star trail near the central condensation in the first three frames.

ORIGINAL PAGE IS
OF POOR QUALITY

Acknowledgements

The author gratefully acknowledges the loan of the H_2O^+ filter from Uwe Fink. The Image Reduction and Analysis Facility software was written with NSF and NASA support by the National Optical Astronomical Observatory operated by the Association of Universities for Research in Astronomy. This work is supported by NASA grant NAGW 247.

References

Brandt, J.C., 1982. *Comets*, ed. L.L. Wilkening, 519.
Brandt, J.C. and Niedner, M.B., Jr., 1987. *Astr. Ap.* 1987, 281.
Galeev, A.A., 1987, *Astr. Ap.* **187.** 12.
Ip, W.-H. and Axford, W.I., 1982. *Comets*, ed. L.L. Wilkening, 588.

Walter Huebner
If the DE is caused by the passing of a sector boundary, should this not influence the tail rays also?

Stephen Larson
I would think so. It is not clear that I observed a "classical" DE, but I believe that I have seen published examples where the main tail broke off, but "new" rays were not affected.

Susan Wyckoff
What is the location of the tail ray vertex in your H_2O^+ images? Was it on the sunward or the tailward side of the center of the H_2O^+ brightness?

Stephen Larson
The tail rays appear to approximate parabolas of different sizes sharing the same focus at the central condensation.

Anita Cochran
You observed that the H_2O^+ seems to be starting very near the nucleus. In the past, observations of CO^+ have indicated this ion also started very near the nucleus. Do you have a feel for whether H_2O^+ and CO^+ start around the same distance and if not, which forms closer?

Stephen Larson
At the spatial resolutions that I normally work with, CO^+ and H_2O^+ are co-spatial.

Paul Feldman
Can you comment on the CO^+/H_2O^+ ratio in these comets and why you chose to image in H_2O^+ rather than CO^+?

Stephen Larson
The CO^+/H_2O^+ ratio was low in these comets. Images of Comet Austin in 1989o using the IHW (International Halley Watch) CO^+ filter were very weak.

William Jackson
Have you done any image processing? Do you expect to obtain more information with image processing?

Stephen Larson
Various image processing algorithms have been applied to improve visibility of features in individual images, but simple image differencing has been the most useful to show changes with time.

David Lynch
Your subtracted images are very nice and show lots of interesting structures. Can you tell us how you plan to analyze these and what you expect to learn from these images? Also, given the extreme sensitivity of the morphology in the image to minute registration shifts, how are you determining the best regestration?

Stephen Larson
The difference-images taken together will provide velocity, and perhaps acceleration maps. Registration on the central condensation is very important. I used the imcntr task in IRAF with a 15 pixel window to find the fractional pixel peak and shift the image the appropriate amount before differencing. Remaining asymmetries are due to imperfect telescope tracking over the 5 minute exposures. Registration was tested by shifting 0.1 pixel in each direction to establish the goodness of fit.

I. Konno
Comment: Takao Saito has found a case in which Comet Halley did not show a DE when it crossed the magnetic neutral plane. He also found DEs which are not related to sector boundaries. He proposed other models to explain DEs. DEs are not always necessarily related to the sector boundaries or the solar magnetic neutral plane.

Stephen Larson
I agree that the DE mechanism is not fully understood, but they seem to be triggered by some disturbance in the solar wind.

326-90
N91-21038

A TAIL-WAGGING EVENT IN COMET AUSTIN

Daniel A. Klinglesmith, Malcolm B. Niedner, Ronald J. Oliversen
Goddard Space Flight Center
Greenbelt, Maryland

David Westpfahl
New Mexico Institute of Mining and Technology
Socorro, New Mexico

ABSTRACT: On the morning of May 21, 1990 a sequence of images of Comet Austin was obtained in the light of H_2O^+. The filter was centered at 602.5 nm with FWHM of 5.0 nm. We were able to follow at least two waves out through the main ion tail structure. During the course of the observations, 2.5 hours, we saw two new tail rays form and undergo similar wave motion. Several condensations, possibly representing disconnected material, were seen to develop and move out along the tail ray with a velocity of about 60 km/sec.

INTRODUCTION

For the past 17 years the Joint Observatory for Cometary Research, JOCR, has been studying the large-scale interaction of bright comets with the solar wind and the interplanetary magetic field using photographic images of cometary ion tails obtained with a 14-inch Schmidt telescope and unfiltered IIa-0 plates. (See Brandt *et al.* 1975; Niedner, Rothe, and Brandt 1978; Niedner and Brandt 1978; Niedner and Schwingenschuh 1987). Recently we have installed a small, wide-field imaging system that uses a Tektronics CCD detector and narrow-band molecular emission filters. Comet Austin is the first bright comet available since the equipment has been installed. We were able to mount an extended observing campaign from the 16th of April through the end of June, during the time we were on the mountain we observed more than sixty percent of the nights when the comet was observable. We report in this paper the results from one night, May 21st, in which a series of ion tails formed and evolved. There are several other nights during which the ion tail was active, this paper is just the first in a series of studies of the variable structure within the ion, gas, and dust features.

INSTRUMENTATION AND OBSERVATIONS

Our optical system consists of the 300-mm f/2.8 Nikon lens originally used by Parker, Gull, and Kirschner (1979). A set of full-aperture molecular emission-line and continuum filters is available. The filters, their central wavelengths, and full-widths at half maximium are listed in Table 1. The detector is a cooled Tektronics

512 by 512 CCD camera system built by Princeton Scientific Instruments. As with the Parker, Gull, and Kirschner observations our system is mounted piggy-back on another telescope. The field of view of the CCD is 1.9 degrees square. Each pixel has a width of 13.6 arc seconds. On the morning of May 21 Comet Austin was at a distance from the Earth of 0.25 AU which translated into 2470 km per pixel as projected onto the plane of the sky or 2645 km projected onto the prolonged radius vector.

On the morning of May 21, 1990 a series of 13 images was taken through our H_2O^+ filter. All exposures were of 10 minutes duration. Table 2 below lists the frame number, image sequence number, and the UT at mid-exposure.

DATA REDUCTION

The basic data reduction was carried out at the NRAO-VLA Array Operations Center using IRAF running on a Convex C-1 and Sun workstations. The data reduction sequence consisted of 4 steps. The first was to subtract the average of the overscan columns (columns 1 and 2) to remove the bias level. This was supplemented by subtracting an average bias frame to remove any residual low-level fixed-pattern noise. The second was to divide by an average twilight sky flat field obtained through the H_2O^+ filter. Nineteen sky flats taken during a string of several clear nights were used to make the average flat. The third was to subtract the sky background level. A 5-by-5 pixel mode filter was applied to each frame. A two-dimensional surface was fitted to each smoothed image and subtracted from the initial image. The final images have a background level within 10 counts of zero. The final step was to correct for atmospheric extinction. The night's extinction was determined from aperture photometry of 32 stars which appear unblended in all frames and whose images had more than 5000 counts above the sky. Fitting a straight line to the magnitude as a function of airmass we obtained a slope of 0.058 ± 0.023. Using this slope we corrected all of the pixels within each frame to relative intensity per pixel outside of the earth's atmosphere. We have not yet transferred the data to an absolute system. The extinction correction ranged from 0.08 magnitudes when we first obsered the comet to 0.05 magnitudes at dawn.

DESCRIPTION OF THE INDIVIDUAL FRAMES

The 13 frames taken with the H_2O^+ filter have been made into a time-lapse movie showing the formation and evolution of the ion tail. Since, within the printed page, it is impossible to present a movie we provide a series of still photographs and a short description of the individual frames shown in Figures 1-1 through 1-13. The sequence number appears in the upper left corner of each frame. The images have been rotated so that the direction of the prolonged radius vector (PRV) is from left to right. The amount of rotation from a north up - east left orientation was 23.3 degrees counter clockwise. The width of each frame is about 860,000 km when projected onto the PRV. We have placed the brightest spot within the head at the same relative position in each frame. The displayed intensity is the logarithm of the number of counts, permitting display of details near the head of the comet as well

as in the tail. During the course of the observations three tails are seen, they will be referred to as T1 through T3. Some dust is being seen through the H_2O^+ filter. The dust cloud developing to the northwest of the comet head, above tail T1 is the beginning of the dust tail that will dominate Comet Austin by the end of May.

We will describe motions of the tails as if they are happening in the plane of the sky. It should be noted that we have limited knowledge of the true three-dimensional nature of the motions.

- Frame 1: In this frame T1 dominates and is already curved, concave up, near the head. T2 is very faint, below and well separated from T1. There is a hint of a condensation, C1, in T1 at a distance of 146,300 km from the head.
- Frame 2: T1 is bending down toward the position angle of the PRV. The condensation C1 has moved away from the head an additional 8000 km. T2 appears slightly longer and is moving up toward the PRV.
- Frame 3: T1 continues to bend down toward the PRV. It appears to have sharpened and split into two parallel tails at a distance of 186,200 km. We believe that this is the point of the condensation C1 seen in the previous two frames. T2 is lengthening and continues to move toward the PRV.
- Frame 4: T1 continues to bend down toward the PRV, parts of it are now parallel to the PRV near the head. It has a diffuse appearance with a very faint hint of the condensation C1 seen at 252,700 km from the head. Again the point C1 appears to be the beginning of two very narrow and separate rays. T2 is longer still and continues to move toward the PRV.
- Frame 5: This frame has some electronic noise but shows T1 bending down toward the PRV. T2 continues to lengthen and move toward the PRV while remaining straight. Due to the noise we are not certain of the location of C1.
- Frame 6: T1 is now parallel to the PRV for about one-third of its length, with the remaining length continuing to bend down. Another condensation, C2, in T1 has been identified 286,600 km from the head. The outer end of T1 is diffuse in this frame. T2 has begun to kink upwards above the PRV position angle near the head.
- Frame 7: T1 and T2 appear to merge near the head. One gets the impression that T1 is lying down on top of T2. No condensations are obvious in this frame.
- Frame 8: The declination tracking failed during this exposure but we can still see merging of T1 and T2. As a result of the tracking failure no condensations are visible.
- Frame 9: T1 and T2 are merged for most of their lengths. A condensation, C3, has appeared in T1 at 401,000 km from the head, just ahead of the two bright stars. The merged portion of T1 and T2 are close to the PRV.
- Frame 10: T1 and T2 continue to merge as T2 lengthens. The condensation C3 has moved down the tail with a velocity on the order of 60 km/sec and will continue to do so for the next 3 frames. Another tail, T3, has begun to form on top of T1.
- Frame 11: T1 is beginning to bend upwards toward T3 and away from the PRV near the head of the comet. T3 is lengthening. C3 continues to move out along T1. T2 has merged with T1.

• Frame 12: Dawn is beginning to affect our observations, but T1 and T3 are clearly bending up and away from the PRV. T3 is lengthing.

• Frame 13: The T1/T3 tail combination bends downward then upward near the head. It would appear that the process is about to begin all over again.

COMET HEAD PHOTOMETRY

We have measured the brightness, in instrumental magnitudes, of the comet head by doing aperture photometry on the individual frames. We present results at two extreme radii in Figure 2. The plus symbols show the brightness of the comet within a 54 arc second (4 pixel) diameter aperture as a function of time, the crosses show the brightness within a 272 arc second aperture. The magnitudes have been scaled to two different, arbitrary zero points. The changes with time are approximately the same. We wonder if the apparent fall in brightness is associated with the formation of tail T2 and if the later increase in brightness is associated with the formation of tail T3.

SPECULATION - TAIL WAGGING VERSUS DISCONNECTION?

While watching the movie of these frames one is reminded of a flag waving in a stiff breeze. A better analogy might be a flag which has been released from its flag pole but continues to wave as it is accelerated in the direction of the breeze. Like the flag, the tail of the comet continues to wave, raising the question of the cause of the waving. Magnetism almost certainly provides the restoring force, but what causes the displacement? Is it due to irregularities in the solar wind, and can those irregularities cause nearly periodic waving? Or is the tail waving because of eddy shedding, just like the flag?

High-resolution, large-scale displays of frames 9, 10, and 11 show discontinuities and condensations in the tail. Any of these frames viewed independently might be taken as evidence for a disconnection event. This leads us to speculate that the origin of tail wagging and disconnections could be the same. Could the trigger of tail wagging also trigger instabilites in the plasma tail, possibly associated with eddy shedding in the solar wind, waves in the plasma, or reconnection of the field? We hope that modeling of the tail motions in the movies of Comet Austin will allow some progress toward an answer.

ACKNOWLEDGEMENTS

We wish to thank the staff of the NRAO-VLA Array Operations Center for the opportunity to reduce the CCD frames, stack the frames into a movie, and record it on their video equipment. DW would like to thank the Kahlmeyer Foundation and acknowledge support under the NASA contract with New Mexico Tech for the operation of the Joint Observatory for Cometary Reserach. It should be noted that modernization of the JOCR facility was greatly helped by Steven N. Shore and Kevin Crain. We thank T. Calovini for help editing the manuscript.

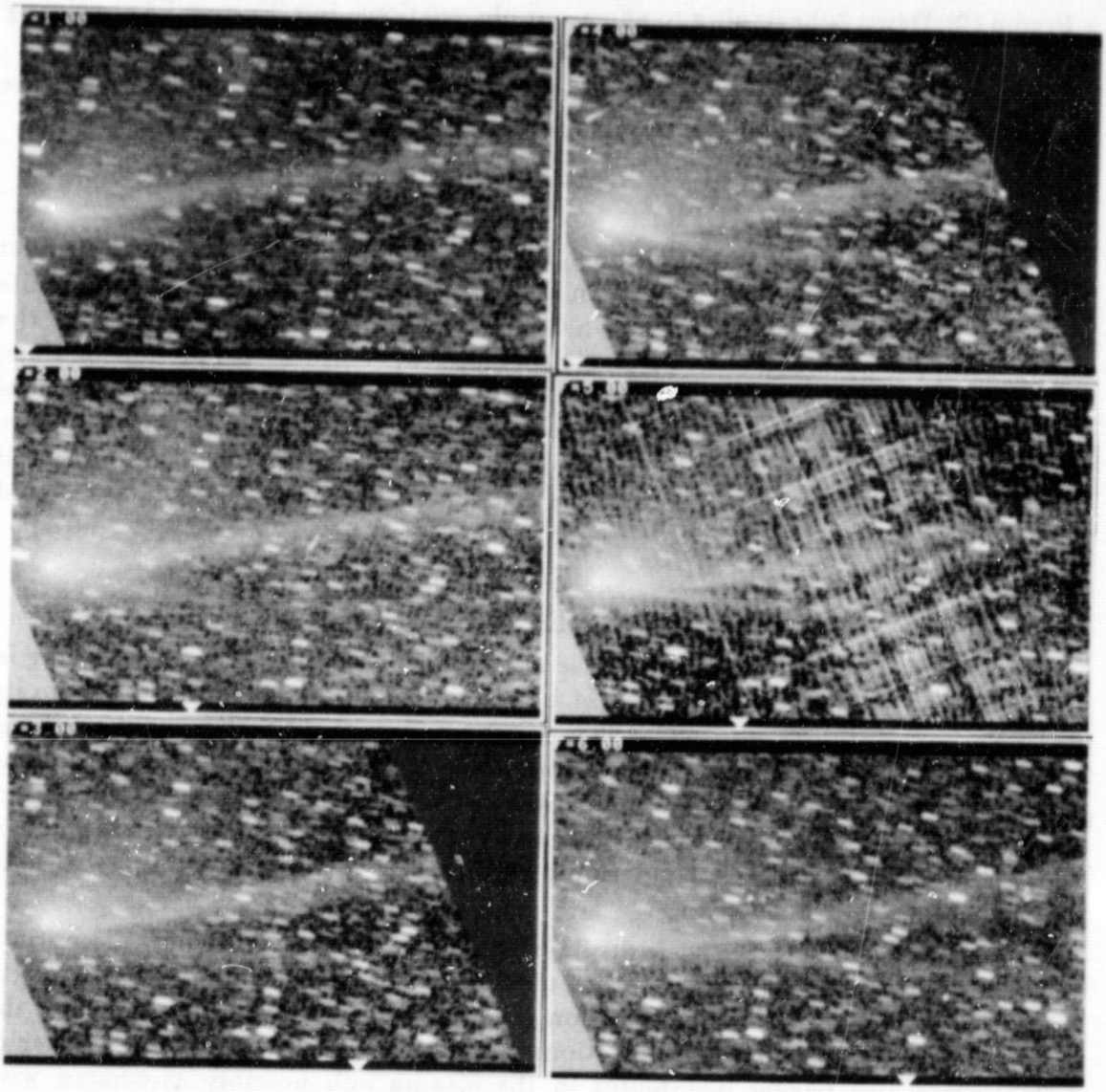

Figures 1-1 to 1-3 (left column) and 1-4 to 1-6 (right column) - H_2O^+ Images of Comet Austin. Each exposure is 10 minutes. Frames are described in the text. Frame 1-5 is dominated by noise.

ORIGINAL PAGE IS
OF POOR QUALITY

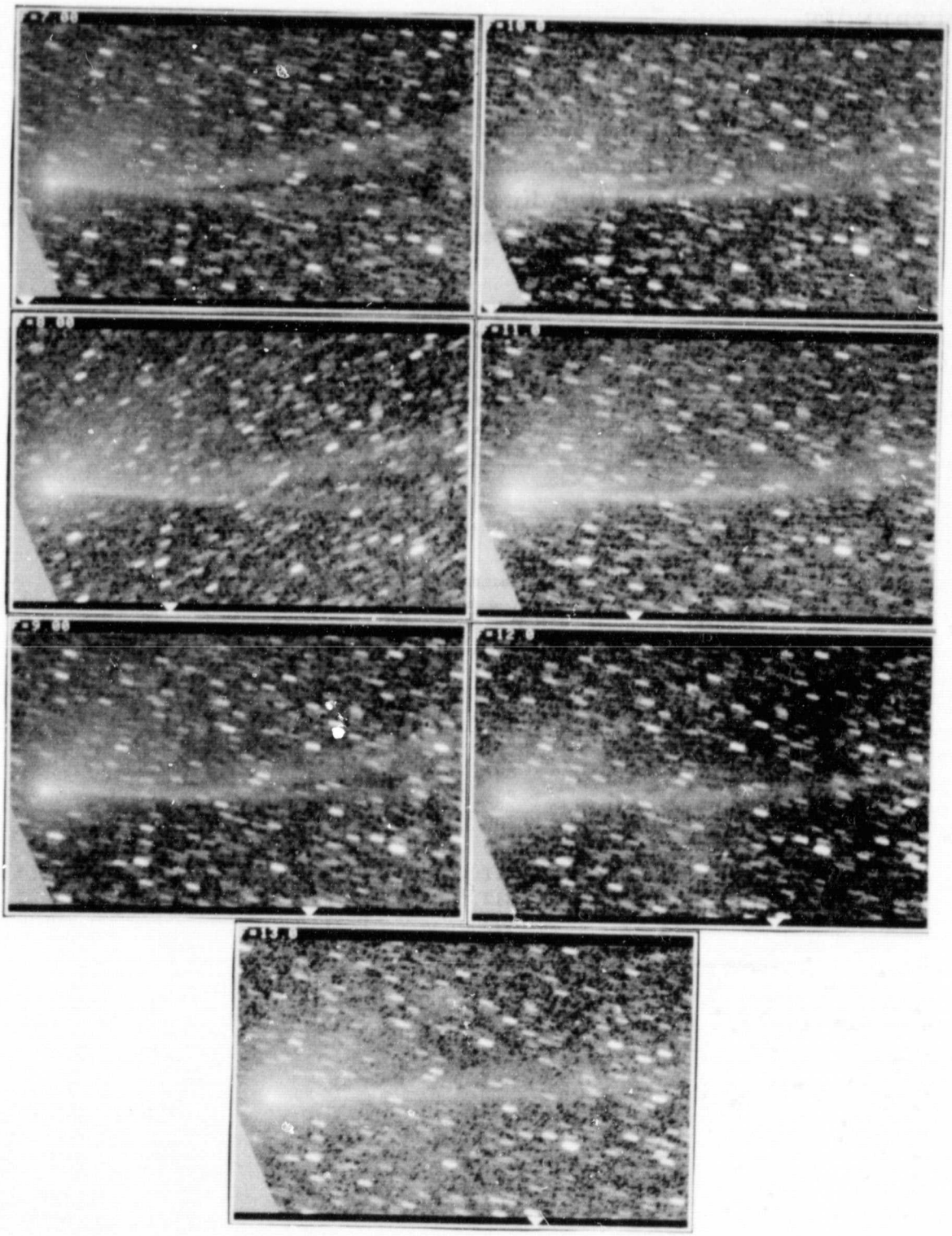

Figures 1-7 to 1-9 (left column), 1-10 to 1-12 (right column), and 1-13 (bottom) - H_2O^+ Images of Comet Austin.

ORIGINAL PAGE IS
OF POOR QUALITY

REFERENCES

J. C. Brandt *et al.* 1975, Mercury **4**, 12.

M. B. Niedner and J. C. Brandt 1978, Ap. J. **223**, 655.

M. B. Niedner, E. D. Rothe, and J. C. Brandt 1978, Ap. J. **221**, 1014.

M. B. Niedner and K. Schwingenschuh 1987, A&A **187**, 103.

R. Parker, T. R. Gull, and R. P. Kirschner 1979, NASA publication SP-434, *An Emission-Line Survey of the Milky Way.*

Table 1. Filters for Wide-Field Imaging

filter	central λ (nm)	FWHM (nm)
blue continuum	445.0	10
C_2	514.0	8
H_2O^+	620.5	5
red continuum	647.0	8

Table 2. H_2O^+ Frames from May 21

sequence number	JOCR archive	UT at mid-exp.
1	802	08:28.72
2	803	08:43.35
3	804	09:01.17
4	805	09:16.63
5	806	09:31.22
6	807	09:44.90
7	808	09:56.37
8	809	10:07.80
9	810	10:20.37
10	811	10:32.35
11	812	10:43.82
12	813	10:57.05
13	814	11:08.03

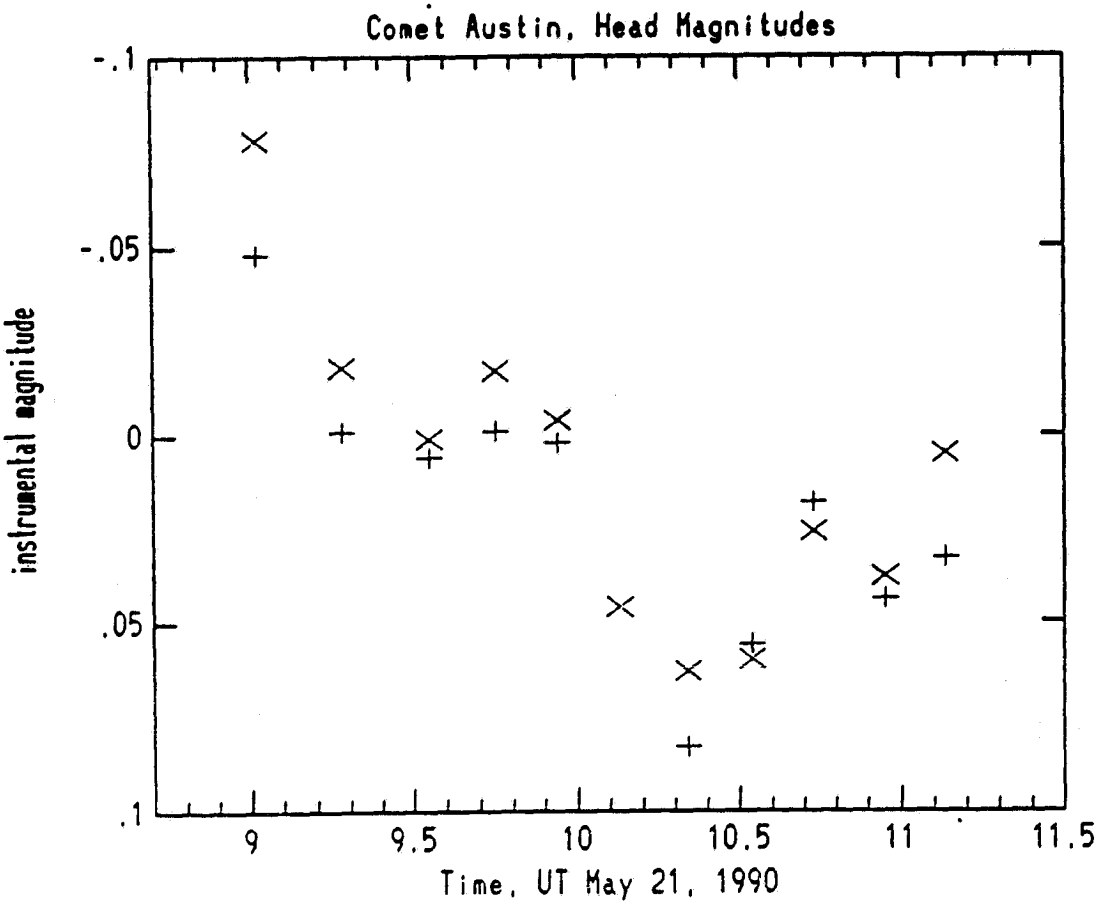

Figure 2 - Comet Head Photometry. The plus symbols show the magnitude of the comet head inside a 54 arcsecond aperture, the crosses show the magnitude within a 272 arcsecond aperture, both at arbitrary zero points.

Walter Huebner
Are there any data for coincidence of sector boundaries with the DEs? If sector boundaries cause DEs, why do they not disrupt the tail rays?

David Westpfahl
The data are being tabulated now.

Ray Russell
What happens to the center of the coma (< 5 arc minutes diameter) during a DE? Does it brighten or not? If so, before, during, or after the DE? This information would be most helpful in the interpretation of our spectroscopy in the thermal IR.

David Westpfahl
The CCD Frames have been calibrated but brightnesses have not yet been determined. We plan to do this in the next few months.

N91-21039

DISTURBANCES OF THREE COMETARY MAGNETOSPHERES AS EXPLAINED BY AN MHD SIMULATION

527-90
30033
P5

Y. Kozuka[1], T. Saito[1], I. Konno[2], and T. Oki[1]

1. Geophysical Institute, Tohoku University, Aramaki-Aza-Aoba, Sendai 980, Japan
2. Southwest Research Institute, 6220 Culebra Road, San Antonio, TX 78228-0510, USA

Summary

Outstanding disturbances of the plasma tails were observed in 1989 in three comets, Brorsen-Metcalf, Okazaki-Levy-Rudenko, and Aarseth-Brewington. Time variations of the tails were obtained from photographs provided by many astronomers. A two-dimensional MHD simulation was performed varying the speed and the direction of the solar wind flow. The simulation agreed quite well with the observations. Solar flares were identified as the sources of these disturbances. It was found that the sudden change in direction of the plasma tail axis occurs when the comet crosses a discontinuity surface of the solar wind structure accompanied by solar flares.

1. Introduction

A study of disturbances in plasma tails of comets is very useful in understanding the structure of the solar wind (Saito and Oki, 1987). We calculated how the plasma tail of a comet deforms with changes in the solar wind speed and direction, then we traced the time variation of the plasma tail disturbances using photographs sent to us from throughout Japan and compared them with the simulation.

2. Tail Bending Phenomena and the Variation of the Solar Wind Flow

During the last half of 1989 three active comets, Brorsen-Metcalf (B-M), Okazaki-Levy-Rudenko (O-L-R), and Aarseth-Brewington (A-B) appeared. Since the sun was very active during this time many disturbance phenomena of the plasma tails were observed.

In many observed disturbance phenomena there are cases for which the tail is bent or the axis of the tail changes greatly in a short time as seen in series of photographs. Such phenomena are thought to be caused by the change of the speed and direction of the solar wind flow crossing the comet (Brandt et al., 1980).

It is known that, in general, when there is discontinuity in the flow direction of the solar wind and the discontinuity surface is inclined relative to the flow, the flow direction is shifted as in Figure 1. The discontinuity surfaces inclined relative to the flow in the solar wind may be caused by a corotating stream or a solar flare. In the case of the corotating stream, the change of the flow appears as in Figure 2 (Dessler, 1987). A corotating stream and a solar flare are similar to each other in that their discontinuity surfaces are both inclined relative to the flow so that they may be thought to produce a similar change in the flow direction relative to the discontinuity surface.

3. Two Kinds of Plasma Flows

In the case of our earth's magnetosphere, the plasma flow is different on the inside and outside the magnetosphere. On the outside it is a solar wind flow which is nearly anti-sunward. On the inside it is plasma convection, which flows sunward, due to the $\vec{J_E} \times \vec{B_Z}$

force produced by the tail sheet current $\vec{J_E}$ and the tail field $\vec{B_Z}$.

In the case of a cometary magnetosphere, i.e., a cometary plasma tail, the outer flow is also the solar wind. The inner flow is the plasma convection due to the $\vec{J_C} \times \vec{B_C}$ force where $\vec{J_C}$ is the tail sheet current and $\vec{B_C}$ is the magnetic field component perpendicular to $\vec{J_C}$. However, if $\vec{B_Z}$ and $\vec{B_C}$ are in the same direction, then $\vec{J_E}$ and $\vec{J_C}$ are in opposite directions (See Fig. 3 of Saito et al., 1987). Therefore the inner flow of the cometary magnetosphere is in the anti-sunward direction. A cometary plasma is accelerated due to the inner flow from the speed of a few km/s near the nucleus, eventually reaching the solar wind velocity (Minami and White, 1986; Tomita et al., 1987). When the direction and the speed of the solar wind changes, the shape of the cometary or earth's magnetosphere will change and the deformation travels leeward nearly at the solar wind speed.

In this paper we solve the problem of deformation of a cometary magnetosphere, i.e., a plasma tail, and its transmission by the solar wind using simulation. Deformation of the magnetosphere is represented by deformation of the tail axis. Therefore, for the sake of computatinal convenience, we assume in this paper that the solar wind plasma "starts at the cometary nucleus" and flows with the given solar wind velocity.

4. Tail Bending Simulation

Pizzo (1989) has published a model of the variation of the solar wind parameters in the interaction region for a corotating stream (Figure 3) using a two-dimensional MHD simulation. We performed calculations to see how the plasma tail deforms, using the windsock theory, when a comet crosses the region where the solar wind has the speed and the direction as in Figure 3. In this model we assume that (1) a comet crosses a space with a structure in which the solar wind has the velocity as in Figure 3, and that (2) the plasma from the comet has the speed and direction of the solar wind at that moment, and that it flows away from the head keeping that velocity (Figure 4). We connect the the positions of the particles at a certain time that left the nucleus at a different time to determine the form of the plasma tail at that time. Then we trace how the plasma tail changes its form in time for a given velocity structure. In this way, we obtained the manner in which the deformation occurs for the cases with and without shocks (Brandt, 1970; Pizzo, 1989).

Figure 5 shows the simulation for the case when shocks formed. We see that the tail axis shifts greatly at the shock pair and at the discontinuity surface between them. Also even a slight change of the direction of a few degrees with the distance from the comet head causes a large structure with an acute angle. Similarly, Figure 6 shows the simulation for the case when no shocks formed. Although not as rapid of a change as in the case of a shock, it shows a fairly large deviation of the tail axis. We also see that a large structure with an acute angle appears similarly to the shock case.

5. Comparison with the Observational Results

We chose examples (Figure 7) from the three comets and compared them with the simulations. The first example is a phenomenon in Comet B-M on August 13, 1989, in which the direction of the tail axis changes suddenly from north to south (Figure 8A). There is a solar flare which is thought to correspond to the disturbance on the above date

DEVIATION OF THE FLOW DIRECTION
AN OBLIQUE CASE OF TANGENTIAL VELOCITY DISCONTINUITY
WITH RESPECT TO THE FLOW DIRECTION

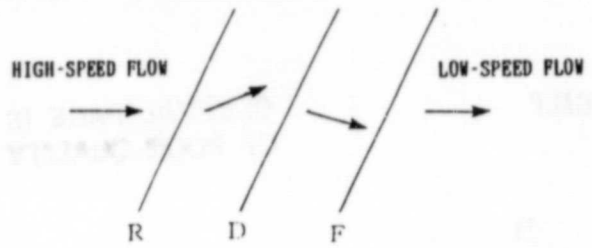

F : FORWARD SHOCK
D : TANGENTIAL VELOCITY DISCONTINUITY
R : REVERSE SHOCK

Fig.1

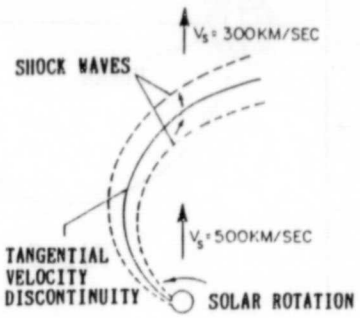

Fig.2

PIZZO (1989)

TWO-DIMENSIONAL MHD SIMULATION
SHOWING THE VARIATION OF THE SOLAR WIND PARAMETERS
BY A COROTATING STREAM INTERACTION

[CASE 1]:NO SHOCKS FORMED

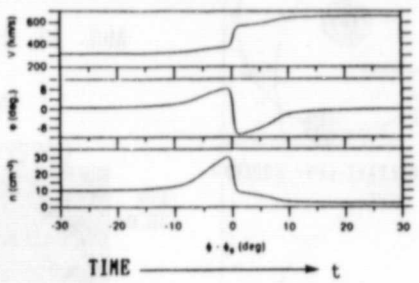

[CASE 2]:SHOCKS FORMED

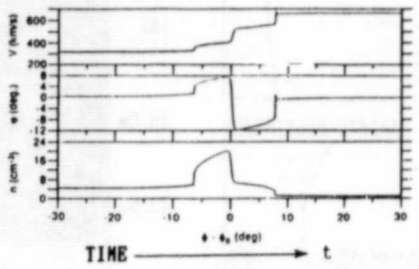

Fig.3

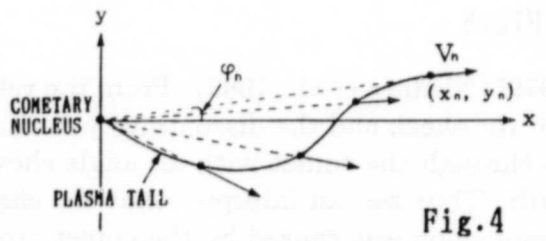

$$V = f(t)$$
$$\varphi = g(t)$$
$$\begin{cases} x_n = V_n \cos\varphi_n \cdot t_n \\ y_n = V_n \sin\varphi_n \cdot t_n \end{cases}$$

Fig.4

[CASE 2]:SHOCKS FORMED

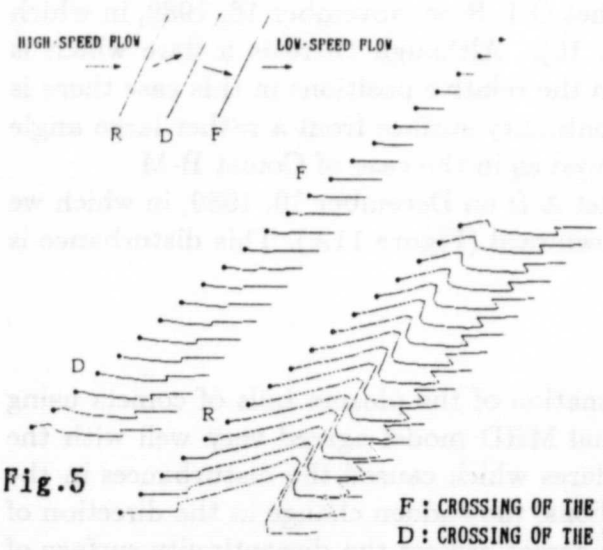

Fig.5

[CASE 1]:NO SHOCKS FORMED

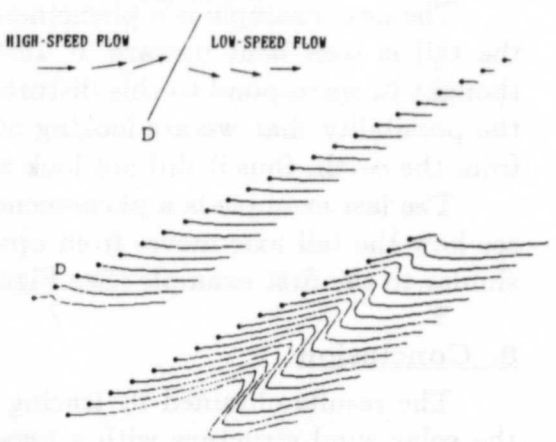

Fig.6

F : CROSSING OF THE FORWARD SHOCK
D : CROSSING OF THE TANGENTIAL VELOCITY DISCONTINUITY
R : CROSSING OF THE REVERSE SHOCK

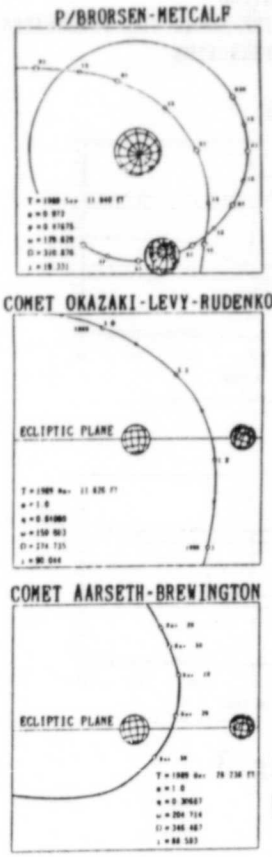

Fig.7

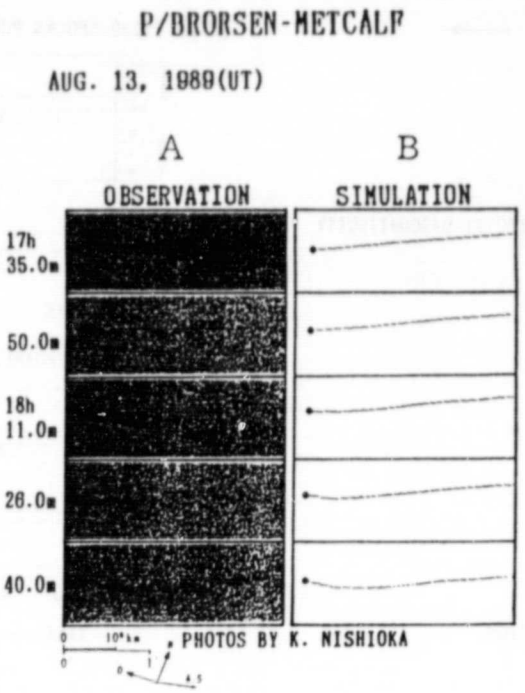

Fig.8

ORIGINAL PAGE IS
OF POOR QUALITY

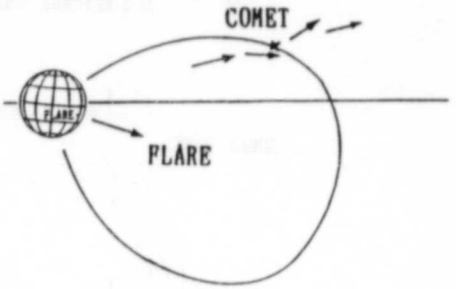

Fig.9

as in the case of Comet Bradfield, 1979l (Niedner et al., 1983). From the relative positions of the flare, the comet, and the earth, the shock and the discontinuity surface produced by the solar flare are expected to cross through the comet with an angle shown in Figure 9 when the comet is seen from the earth. Thus we can interpret that the change of the tail axis from north to south in this phenomenon was caused by the comet crossing the solar wind discontinuity surface produced by the flare. The way the tail deforms resembles very much the results at the time the tail crosses the discontinuity surface.

The next example is a phenomenon in Comet O-L-R on November 16, 1989, in which the tail is seen bent upward at 19:42 (Figure 10). Although there is a flare which is thought to correspond to this disturbance, from the relative positions in this case there is the possibility that we are looking at the discontinuity surface from a rather large angle from the earth, thus it did not look as pronounced as in the case of Comet B-M.

The last example is a phenomenon in Comet A-B on December 10, 1989, in which we see how the tail axis moves from upward to downward (Figure 11A). This disturbance is similar to the first example (See Figure 11B).

6. Conclusion

The results obtained by tracing the deformation of the plasma tails of comets using the solar wind structure with a two-dimensional MHD model agreed very well with the observed tail disturbances. There exist solar flares which caused the disturbances in the plasma tails of comets. From the relative positions, the sudden change in the direction of the tail axis is considered to happen when the comet crosses the discontinuity surface of the solar wind structure produced by the solar flare.

ORIGINAL PAGE IS
OF POOR QUALITY

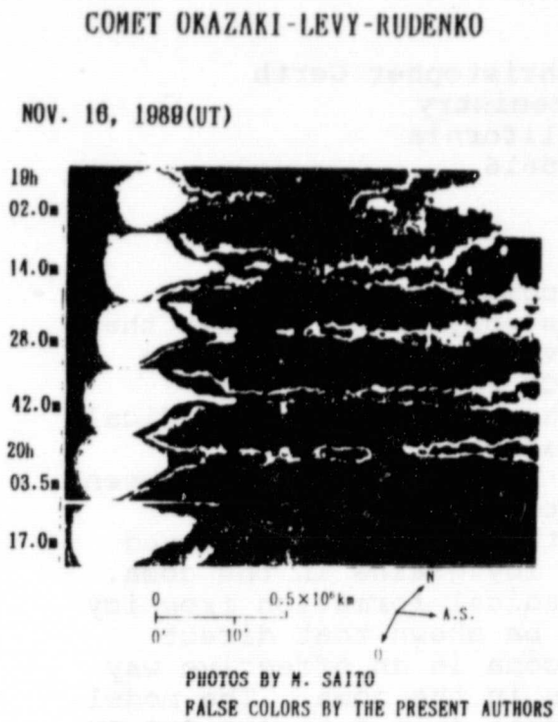

Fig.10

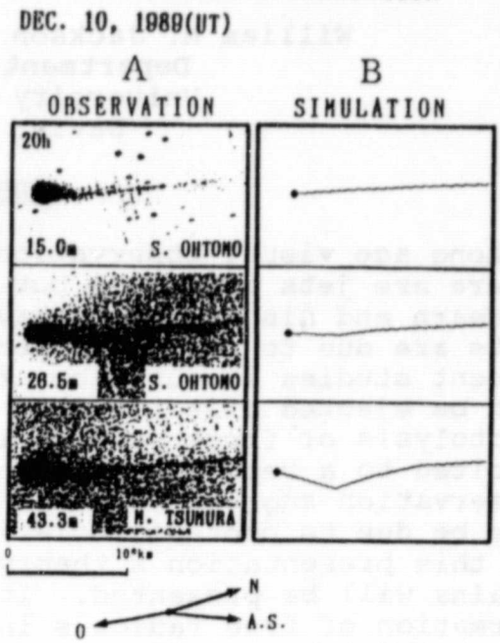

Fig.11

Acknowledgement

We are indebted to K. Nishioka, M. Saito, S. Ohtomo, M. Tsumura, and many others who kindly sent us photographs of comets used in this study.

References

Brandt, J.C., 1970, *Introduction to the Solar Wind*, W.H. Freeman and Company, San Francisco.

Brandt, J.C., Hawley, J.D., and Niedner, Jr., M.B., 1980, *Ap. J.*, **241**, L51.

Dessler, A.J., 1967, *Revs. Geophys.*, **5**, 1.

Minami, S. and White, R.S., 1986, *Geophys. Res. Lett.*, **13**, 849.

Niedner, Jr., M.B., Brandt, J.C., Zwickl, R.D., and Bame, S.J., 1983, in *Solar Wind V*, ed. M. Neugebauer (NASA SP-2280), p. 737.

Pizzo, V.J., 1989, *J. Geophys. Res.*, **94**, 8673.

Saito, T. and Oki, T., 1987, in *Laboratory and Space Plasmas*, ed. H. Kikuchi (Springer), p. 531.

Saito, T., Yumoto, K., Hirao, K., Minami, S., Saito, K., and Smith, E., 1987, *Astr. Ap.*, **187**, 209.

Tomita, K., Saito, T., and Minami, S., 1987, *Astr. Ap.*, **187**, 215.

N91-21040

RADICAL FORMATION IN THE COMA FROM PHOTODISSOCIATION OF ICE GRAINS

William M. Jackson and Christopher Gerth
Department of Chemistry
University of California
Davis, Ca. 95616

ABSTRACT

Long ago visual observations of comets suggested that there are jets in comets but it has only been recently that A'Hearn and his coworkers have proven that some of these jets are due to emission from the CN radical [1,2,3]. Recent studies in our laboratory have shown that CN radicals can be ejected directly into the gas phase from the photolysis of frozen vapors if the parent molecule has been excited to a repulsive excited state. This later observation suggest that the jets that have been observed may be due to photodissociation of icy grains in the coma. In this presentation a theory of radical formation from icy grains will be presented. It will be shown that direct formation of free radicals in the coma is an effective way to produce radicals from icy grains in the coma. The model predicts that icy grains could produce from 6 to 800,000 OH radicals/s per grain depending upon whether the radius of the grain is 0.3 to 100 μm.

Acknowledgements: The authors gratefully acknowledge the support of the NASA's planetary atmospheres program under grant number NAGW 1144.

1. Bobrovnikov, N. T. Astrophys. J. 66, 145-169(1927).
2. Bobrovnikov, N. T. Astrophys. J. 66, 439-464(1927).
3. A'Hearn, M. F. et al., Nature, 324, 649-651(1986).

omit

Lewis Snyder
What is the structure of NCCN?

William Jackson
It is linear.

Ray Russell
Would small silicate grains (strings of 100 - 200 $\AA$ spheres, stuck together in long twisted strings like IDP's) coated with organics provide a viable source for the radicals?

William Jackson
If we had 100 $\AA$ spheres each individual sphere would not give you enough of a yield to explain the jets. If thousands of these spheres are together then one might be able to obtain a high enough yield to explain the observations.

Carey Lisse
Were the production rates quoted in the final table for 1 grain or a jet of an estimated mass, made entirely of one given particle size? Also, what ambient grain temperature and pressure have been used for these calculations?

William Jackson
The production rates were total production rates for all grains of a given size. We used the flux measured in Halley for a given grain size. We used a grain composition of 2% HCN, 2% C_2N_2, and 90% H_2O.

No ambient grain temperature or pressure was needed for these calculations.

N91-21041

AN ALTERNATIVE TO THE DIRTY SNOWBALL MODEL OF COMETS

Tom Van Flandern
VF Associates / 6327 Western Ave, NW / Washington DC 20015

A. Comparison of Models

To be viable, a scientific theory or model must not be contradicted by observations or experiments. To be useful, a model must explain some phenomenon and aid our understanding of it. To be valuable, a model must make successful predictions.

By these criteria, the "Dirty Snowball" model for the nature of comets is now on shaky ground. By contrast, the "Satellite Model" easily passes all these measures of the worth of a theory. Although the Dirty Snowball model is familiar to all comet investigators, the newer Satellite Model may not be.

Briefly, in the Satellite Model,[1] comets consist of a cloud of asteroid-like debris of all sizes, which is gravitationally bound together. Typically, the comet's sphere of influence, within which it can keep material in stable satellite orbits against the attraction of the Sun, is dominated by a primary "nucleus", but also includes bodies of kilometer, meter, millimeter, and dust size, all of which contain volatiles. Comet tails are formed when solar radiation pressure drives gas and dust away. In the Dirty Snowball model, that material must be driven off the nucleus. In the Satellite Model, most of it is spread throughout the sphere of influence, and needs only to escape.

Let me briefly review each important physical characteristic of comets, and how it fits into each model. Surely a good model will automatically explain important physical properties. A failing model often needs to be patched up to accommodate new findings.

B. Albedos and Spectra

In the Dirty Snowball model, the chief ingredient of comets is water-ice. In the Satellite Model it is carbonaceous rock. In either model the surface is coated with an extremely black carbonaceous residue. The Dirty Snowball model does not expect this black coating; it merely accommodates it. The Satellite Model anticipates that the same carbonaceous material which coats asteroids and so many solar system moons also coats comets. Comets have a mean albedo of about 4%, primarily from this coating. Other solar system moons which are <u>icy</u> underneath their carbonaceous coatings have mean albedos of about 20%; whereas asteroids, which are rocky underneath, have mean albedos of about 4%, the same as comets.

The spectra of comets are very similar to those of asteroids. In the Dirty Snowball model that is coincidental, due to the

surface coating. In the Satellite Model, it is because comets and asteroids are made of the same basic materials throughout. The absence of ices in the reflection spectra of comets[2] is a noteworthy feature, arguing against the Dirty Snowball model. In Comet Halley, heavy molecules to 120 amu were detected[3]: fairly heavy stuff if comets are primitive objects, but quite expectable if they are like asteroids.

C. Densities and Strengths

We have no direct measurements of the densities or tensile strengths of comets. The Dirty Snowball model requires that both be low, partly to permit the solar non-gravitational forces to be as strong as is observed; and partly to account for the ease with which comets split, and the low accelerations and high surface brightnesses of the fragments. It is concluded that comets must be either flat and pancake-like (ruled out by spacecraft missions), or fluffy dustballs[4]. The Satellite Model expects asteroidal bodies with densities in the 2-3 g/cc range. In it, the high non-gravitational forces are brought about by the large surface area of the sphere of influence, typically 10,000 times greater than the area of the nucleus alone. All of the satellite bodies and dust within the sphere of influence (not just the nucleus) feel the push of solar radiation and affect the motion of the center of mass. Since a split event is just the gravitational escape of a satellite, and nothing actually breaks up, comet materials of normal strength are expected. The indirect observational evidence which is available tells us this: Micro-meteoroids collected in the upper atmosphere during meteor showers associated with comets are primarily of carbonaceous chondritic (normal density) material[5]. And fireballs associated with comets (because their orbits have aphelia far beyond Jupiter) survive to low altitudes in the Earth's atmosphere,[6] again suggesting they have the strength of rock, not fluffy dustballs.

D. Radar Reflectivity, Lightcurves, Comas

The radar reflectivity of comets is around 10%. This implies a non-porous surface, probably rocky,[7] as expected by the Satellite Model. The Dirty Snowball model specifically expects a porous surface.

Comet lightcurves are often complex. The well-observed lightcurve for Comet D'Arrest is of a distinctive triple-maximum, triple-minimum type associated with binary stars and asteroids.[8] In a few comets, multiple or "granulated" nuclei have been directly observed even in cases where no "split" event followed.

The Dirty Snowball expects the comas of comets to be formed as they approach the Sun, and grow in size as they get closer. The Satellite Model predicts that the comet's sphere of influence, and therefore the size of its ever-present coma, will generally shrink

as the comet approaches the Sun. Observations show that comet comas are already formed even when comets are first detected in excess of 10 au from the Sun, and generally diminish in linear size as they approach the Sun.

E. New versus Old Comets

Comets "new" in the Oort sense lose 2-3 magnitudes in absolute brightness on their first passage near the Sun. Old comets show no further absolute brightness losses, in a few cases even after dozens of revolutions. The Dirty Snowball model predicted that the brightness losses would continue, but at a reduced rate, due to the formation of a surface "frosting"; and that Comet Encke would be considerably diminished if not totally evaporated by this time. The Satellite Model predicts exactly the observed behavior: As comets approach the Sun for the first time, their spheres of influence shrink to a smaller diameter than ever before, causing the gravitational escape of much material which was previously gravitationally bound inside the coma. But on subsequent revolutions, as long as the comet's perihelion distance is not reduced further, a comet can lose only gas and small dust particles from solar radiation pressure. The millimeter and larger size bodies are virtually unaffected, insuring that the comet will maintain its general appearance at least until solar radiation pressure successfully removes all gas and dust from the coma.

Because there are numerous smaller spheres of influence within the primary one in the Satellite Model, this process of losing dust and gas can take many thousands of years. Moreover the volatiles are not lying in layers of ice near the surfaces of these satellite bodies. Instead, they are interstitial, just as is found in carbonaceous meteorites on Earth, which are about 15% interstitial water by volume. The Satellite Model obviously predicts that "new" and "old" comets will not differ in albedo. The Dirty Snowball model expects an albedo change when the surface "frosting" forms just after the first perihelion passage. Observations should soon tell us which prediction is correct.

F. Jets

In the Dirty Snowball model, volatiles must be ejected from the surface of the nucleus in high-speed jets to account for their abundances and relative independence of solar distance. Although the Satellite Model can accommodate jets, it does not predict them. Spacecraft encounters with Comet Halley photographed what appeared to be jets streaming sunward from the nucleus. However, unlike the expectations of the Dirty Snowball model, dust in the jets appears to be unaccelerated, and there is no evidence for pressure in cometary jets above the ambient pressure, and no supersonic flow in them. Moreover, bursts of dust particles were observed to come from sources in the coma other than the nucleus, as the Satellite Model would certainly predict.

Are the spacecraft-observed features really "jets"? The Satellite Model suggests another explanation of the pictures. The "jet" features eminate from surface spots of high albedo. One might have expected true jets to eminate from the hotter, darker regions, rather than the cooler, brighter ones. In the composite picture of Comet Halley, the "jets" look instead very much like sunlight back-scattered into the dust. But in the single frames, the "jets" seem concentrated in narrow, sunward beams. This seems likely to be the result of the well known "opposition effect" for asteroidal material, in which most of the reflected light is concentrated in a cone with a divergence of just plus or minus 3 degrees from the Sun direction. So the "jets" may be just dust backlit by sunlight over surface bright spots. A single "jet" not pointing exactly sunward, or not eminating from only the brightest surface spots, or visible in direct (not backlit) sunlight, would provide a counter-example to this proposal.

G. Split Comets

The Dirty Snowball model did not expect comets to split, but accommodates that by assuming low strength materials and explosive jets of volatiles. The Satellite Model expects major satellites to drift off on independent solar orbits if the comet's sphere of influence is reduced to smaller than the satellite's distance from the primary nucleus. These events would have the appearance of "splits", but could occur only on the inbound leg, or while the comet was close to perihelion. While the comet's distance from the Sun was increasing rapidly, its sphere of influence would also, preventing gravitational escapes or "splits". Observations show us that all 14 split events where the date of split is uniquely determinable occurred in the range from three years before perihelion to 10 days afterwards.[9] Of 18 other cases with too few observations to make a split date determination, 8 appear to have happened after perihelion. But considerable uncertainty exists in each of these cases; and it is impossible to distinguish a true split event from a chance alignment of well-separated comet components in the line of sight due to viewing geometry.

Perhaps the single strongest observation which distinguishes these two models is that of the relative fragment velocities resulting from split events. The square of relative fragment velocities must be proportional to the energy available to accomplish the split (from $2E = m\ v^2$). In the Dirty Snowball model, if the energy comes from solar forces which are inverse square (light, heat, gravity, radiation), then relative fragment velocities will be proportional to solar distance to the minus one power ($b = -1$). If the energy comes from entirely internal sources unaffected by solar energy, then relative fragment velocities will be independent of solar distance ($b = 0$). The Satellite Model makes a very specific prediction about relative fragment velocities, since they are gravitational escapes from the sphere of influence: relative velocity is proportional to solar distance to

the minus one-half power (b = -0.5). Observations (see the previous Sekanina reference) over two orders of magnitude in solar distance for comet splits show that b = -0.57 ± 0.10. Whereas this result is in precise agreement with the Satellite Model, it would seem to rule out the Dirty Snowball model with more than four standard deviations of statistical significance.

H. Conclusion

In conclusion, the Dirty Snowball may no longer be a viable model, even after its patches have been applied. Although it appeared for a while to aid understanding, its predictions have not been noted for their success; and it is now flatly contradicted by one line of evidence. The Satellite Model provides a whole new understanding of comets which happens to describe all of their physical properties rather well.

We cannot make progress in understanding comets until we get the model right. Research interpreted with the wrong model may be doomed to early obsolescence. So the question is one of importance. Let us therefore give the matter our most critical thinking, and our severest judgment. Can we move forward and gain understanding of comets without a change of models?

References

[1] Van Flandern, T.C. "Do Comets Have Satellites?". Icarus 47, 480-486; 1981.

[2] A'Hearn, M.F. and Dwek, E. "Where is the Ice in Comets?" (1981).

[3] Huebner, W.F. "Results from the Comets Giacobini-Zinner and Halley Campaigns." In Observations of Recent Comets, W.F. Huebner, ed. (1990).

[4] Donn, B. and Rahe, J. "Structure and Origin of Cometary Nuclei". In Comets, L.L. Wilkening, ed., 203-226 (1982).

[5] Millman, P.M. "The Chemical Composition of Cometary Meteoroids". In Comets, Asteroids, Meteoroids, A.H. Delsemme, ed., Univ. of Toledo, Toledo, OH, 127-132 (1977).

[6] Wetherill, G.W and ReVelle, D.O. "Relationships Between Comets, Large Meteors, and Meteorites". In Comets, L.L. Wilkening, ed., 297-319 (1982).

[7] Kamoun, P.G., Pettengill, G.H., and Shapiro, I.I. "Radar Detectability of Comets". In Comets, L.L. Wilkening, ed., 288-295 (1982).

[8] Tedesco, E., Drummond, F., Canoy, M., Birch, P., Nikoloff, I., and Zellner, B. "1580 Betulia: An Unusual Asteroid with an Extraordinary Lightcurve." Icarus 35, 344-359 (1978).

[9] Sekanina, Z. "The Problem of Split Comets in Review". In Comets, L.L. Wilkening, ed., 251-287 (1982).

William Jackson
How do you continue to have H, OH, CH, C_2, C_3, etc., in short period comets, e.g., Comet Encke?

Tom Van Flandern
The volatiles are not from surface ices, as determined by the reflection spectra. Since one must go below the surface to "boil off" volatiles, this is easily accomplished for rocky, chondritic material. Even carbonaceous chondrite meteorites still have about 15% interstitial water by volume.

Ray Russell
How does the satellite model explain the amount and size distribution of dust being released after so many apparitions as P/Halley and P/Encke have had? Wouldn't all the dust be swept out or wouldn't your model require such a high density for collisions to occur so that the whole gravitational sphere would be optically thick (in which case the pieces would be seen in mm radio and in radar observations) and they would grind themselves to dust very quickly?

Tom Van Flandern
The preservation of the dust is no more difficult than in the Dirty Snowball model, because one has thousands of source bodies gravitationally binding dust, not just the nucleus. Just as for zodiacal dust, the time scale to remove dust depends on how close the comet gets to the Sun, how long it stays there, and the size distribution and lifetimes for the dust particles. In the Satellite Model, a continuum of sizes of dust particles are present, including sizes large enough to be very little influenced by solar radiation pressure. Russell's question seems to suppose that the gravitational binding forces in comets are too small to hold the dust for long against radiation pressure. But some of these gravitational binding forces are strong enough to hold larger dust particles indefinitely. As for the grinding of the smaller dust, Russell's own paper noted that the dust is not in thermal equilibrium, and Konno and Huebner discussed evidence of dust fragmentation in the coma, such as an increase in the number of small grains away from the nucleus.

General Discussion:
Many participants objected to the Satellite Model that had just been presented. It was felt that this model was untenable for several reasons. Some of the objections to the model included: (1) The lack of evidence of satellites of Comet P/Halley in the images from the Halley Multicolour Camera or the Vega cameras, (2) the difficulties that the model has in explaining the observed gas and dust production as a function of heliocentric distance which are easily explained with Whipple's Icy Conglomerate Model, (3) the statistics used for comet splitting, (4) the inconsistency with the persistence of dust over many revolutions of the comet around the Sun, and (5) inconsistencies with Sun-grazing comets. Tom Van Flandern replied with qualitative counter arguments to these objections, but the real test has to be a quantitative model based on physics and chemistry and its comparison with observational comet data.

N91-21042

MODELING THE DUST SIZE DISTRIBUTION IN COMETS WITH DUST FRAGMENTATION

Ichishiro Konno and Walter F. Huebner

Southwest Research Institute, P.O. Drawer 28510, San Antonio, TX 78228-0510

Summary

We have developed a hydrodynamic model of a spherically symmetric dusty gas flow in a cometary atmosphere assuming a single-fluid, inviscid, perfect gas. The hydrodynamics for gas and dust, which involves the gas drag force (momentum transfer), heat exchange between gas and dust, photodissociation energy for H_2O gas, and radiative heating and cooling terms for dust particles, are solved using the Gear method for stiff, coupled differential equations. Calculations have been done with a dust size distribution for radii $a = 0.01\mu$m to 10 cm with densities variable with the size. A nucleus size of 4.0 km radius with a density of 0.5 g cm^{-3} and a total dust-to-gas mass ratio $\chi = 1$ were adopted.

There are indications from *in situ* observations that dust particles fragment into smaller ones. Fragmentation of dust partilcles has been incorporated into the model. This is done by adding source and sink terms in the continuity equations for the dust. Lifetimes for the decay of dust particles were assumed as a function of particle size. It is also assumed that dust particles always fragment only into the next smaller size.

1. Introduction

Recent observations of dust in comets suggest fragmentation of dust particles at some distances from the nucleus. Fragmentation of dust is implied mostly from the relative increase in the number of smaller grains or the decrease of the intensity of scattered light less rapid than $1/R$, which is expected for dust with constant speed and no fragmentation. From Giotto's PIA and DIDSY data, McDonnell et al. (1987) found some evidence for possible fragmentation or evaporation of grains. Vaisberg et al. (1987) obtained several pieces of evidence for an evolution of the mass spectrum and the supply of new particles in the low-mass range while dust propagates from the source. There are also some ground-based observations suggesting dust fragmentation. It is thought that fragmentation may arise from the sublimation of a gluing material such as POM (polyoxymethylene) in the grain agglomerates of the dust (Boehnhardt et al., 1990).

We study the radial distribution of dust by solving hydrodynamic equations. In order to model the dust fragmentation in a comet, we assume the dust size distribution at the source (surface of the nucleus) and the lifetime of grains which is a function of the particle size.

2. Modeling

We solve sets of hydrodynamic equations for a dusty gas flow in a comet coma which assumes single-fluid, inviscid, perfect gas with the Gear method, a stiff differential equation solver. The equations contain the gas drag force on dust, heat exchange between gas and dust, and photodissociation energy for H_2O gas.

Calculations have been done with dust particles of sizes from 0.01 μm to 10 cm in radius with a continuous distribution approximated by 22 discrete particles sizes seperated by a logarithmic scale so that a particle always fragments into ten particles of next smaller size. It is assumed that the smallest particles have infinite lifetime against fragmentation. The size distribution at the nucleus surface is given by

$$\rho_a = \rho_{max}(a/a_{max})^{\beta},$$

where ρ_a is the spatial mass density of the particles of radius a and ρ_{max} is the density of the particles of the maximum radius a_{max} that can be entrained by the gas. The bulk density of dust particles is a function of the dust size:

$$\rho_{bulk} = 2.2 - 1.4a/(a_0 + a) \ \text{g cm}^{-3},$$

where $a_0 = 10^{-4}$ cm (Lamy et al., 1987). We assumed for the nucleus of Comet Halley that the radius $R_n = 4.0$ km, the density $\rho_n = 0.5$ g cm^{-3}, and the dust-to-gas mass ratio $\chi = 1$.

3. Results and Discussion

Figures 1 to 3 are obtained from calculations with $\alpha = -2.0, \beta = 1.0$, and $\tau_{max} = 300$ s. The gravity between the nucleus and the dust has been taken into account but the results show that the gravity of a Halley-class nucleus has very little effect on particles smaller than about 1 cm.

Figure 1 shows the average velocity of dust particles of different sizes as a function of cometocentric distance. The farther out in the coma particles fragment, the less acceleration the fragmented particles experience. Therefore the mass-averaged velocity of the fragmented particles starts decreasing at the distance of the scale length of their parent particles.

Figure 2 shows the dust size distribution at various cometocentric distances. The number density is plotted as a funcion of dust particle radius. The relative density of larger particles decreases with the distance because of fragmentation. The number density of small particles could increase with the distance because of rapid fragmentation despite the R^{-2} dependence of the number density when there is no fragmentation.

In Figure 3, the cumulative number density of dust particles at the surface of the nucleus ($R = 4.0$ km), and at $R = 1{,}000$ km and $R = 3{,}000$ km is shown. The result (Lamy et al., 1987) from observations by the Vega 2 spacecraft is also shown. The spacecraft results are deduced from observations made at much farther distances over several thousand kilometers assuming an R^{-2} dependence of the density. Therefore the spacecraft data may not give a true distribution at $R = 1{,}000$ km if there is fragmentation within the these distances.

In case of dust fragmentation, the dust size distribution at the nucleus of a comet may not be uniquely determined without the knowledge of the lifetimes of all kinds of dust particles. Spatial profiles of narrow band continua should give information on the scale lengths of the parent particles. Lifetimes of dust particles may be obtained from the scale lengths.

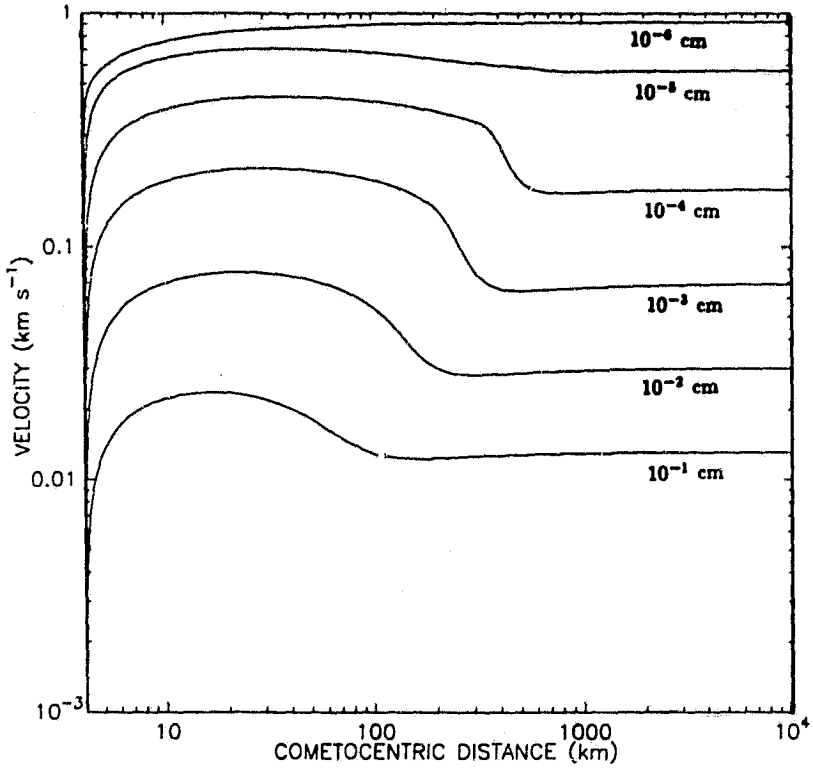

Fig. 1.– Mass-averaged dust velocity. Average velocity decreases because the particles fragmented at larger distances have lower velocities (typically that of their parents).

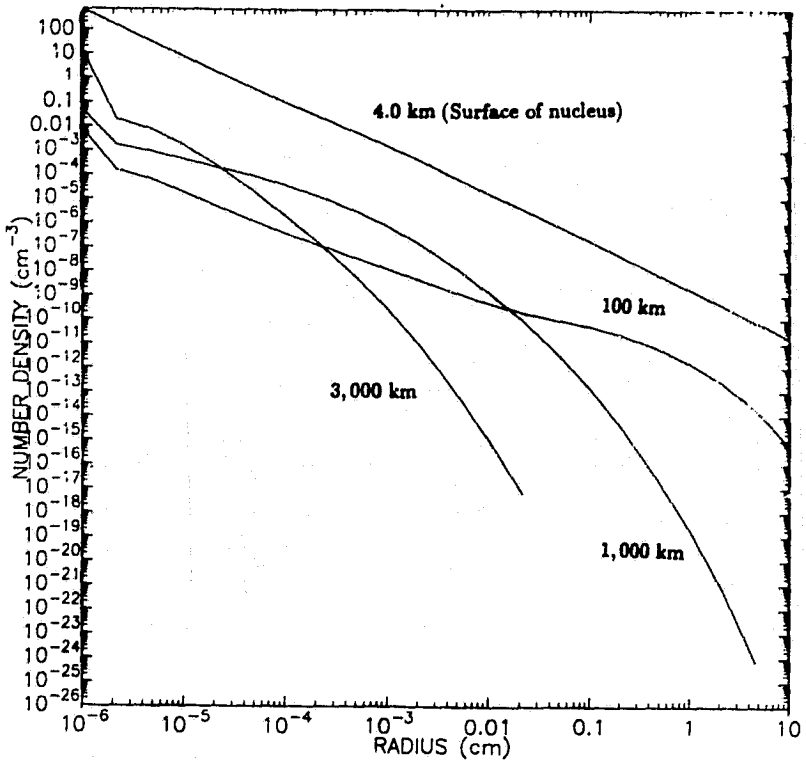

Fig. 2.– Dust number density at various cometocentric distances as a function of the particle size. Because of rapid fragmentation, the number density of small particles can increase at larger distances despite the R^{-2} dependence of the density in the case of no fragmentation.

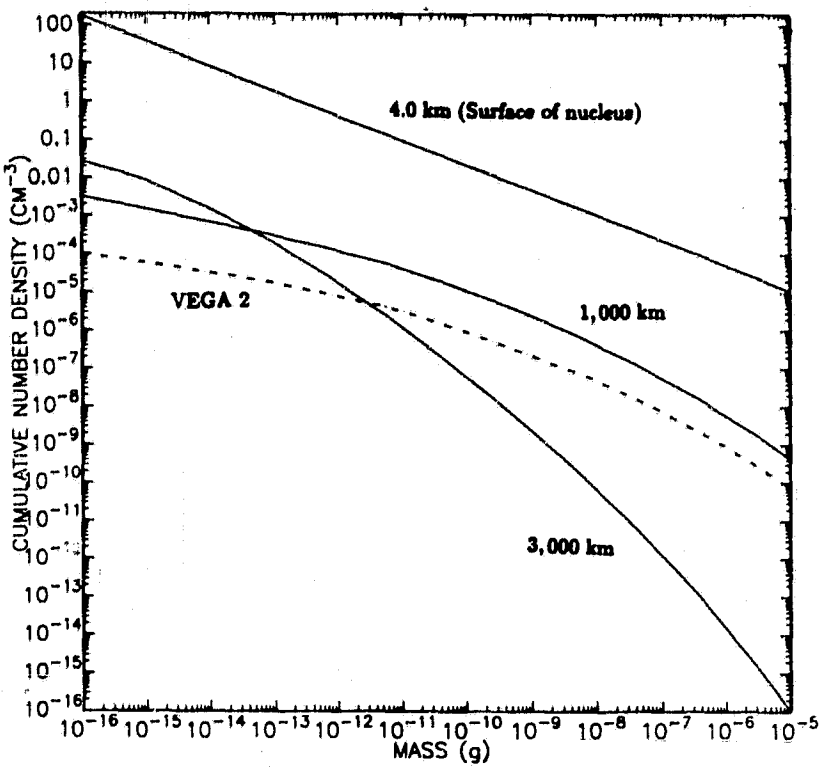

Fig. 3.– Cumulative number density of dust particles as a function of mass. The number density shown indicates the total number of dust particles of the equal or larger mass at the point. The profile deduced from the Vega 2 observations is shown by a dotted-line.

References

Boenhardt, H., Fechtig, H., and Vanysek, V., 1990, *Astron. Astrophys.* **231**, 543.

Gombosi, T.I., Nagy, A.F., and Cravens, T.E., 1986, *Reviews of Geophysics* **24**, 667.

Kitamura, Y., 1986, *Icarus* **66**, 241..

Lamy, P.L., Grün, E., and Perrin, J.M., 1987, *Astron. Astropys.* **187**, 767.

McDonnel, J.A.M., Alexander, W.M., Burton, W.M., Bussoletti, E., Evans, G.C., Evans, S.T., Firth, J.G., Grard, R.J.I., Green, S.F., Grün, E., Hanner, M.S., Hughes, D.W., Igenberg, E., Kissel, J., Kuczera, H., Lindblad, B.A., Langevin, Y., Mandeville, J.-C., , Nappo, S., Pankiewicz, G.S.A., Perry, C.H., Schwehm, G.H., Sekanina, Z., Stevenson, T.J., Turner, R.F., Weishaupt, U., Wallis, M.K., and Zarnecki, J.C., 1987, *Astron. Astropys.* **187**, 719.

Vaisberg, O.L., Smirnov, V., Omelchenko, A., Gorn, L., and Iovlev, M., 1987, *Astron. Astrophys.* **187**, 753.

D. Boice
What is the Gear method?

I. Konno
It is a method to solve stiff differential equations.

P. Weissman
The Vega 2 encounter was at 8,000 km. Why do you compare it with your model curve at 1,000 km?

I. Konno
Lamy et al. [*Astron. Astrophys. 187,* 767 (1987)] deduced the dust size distribution at 1,000 km from the Vega 2 data.

Carey Lisse
Do you plan on extending your dust size distribution model to cometocentric radii layer then 10^3 km?

I. Konno
Yes, we plan to calculate much farther with the one-dimensional model, but we need to use a two-dimensional model when solar radiation pressure on dust becomes significant.

Paul Feldman
Does the Giotto data show a variation in the dust size distribution with distance from the nucleus?

Ichishiro Konno
It may, but the published Giotto data gives only the dust size distribution averaged over a few thousand kilometers.

Ray Russell
Do you calculate the IR emission expected from your model? Thermal images may provide the constraint you need to get a unique determination.

Ichishiro Konno
No, not yet.

N91-21043

A MODEL OF MULTIGENERATION NEUTRALS IN COMETARY COMAE

D.C. Boice
Southwest Research Institute, San Antonio, Texas
and
Max-Planck-Institut für Astrophysik, Garching, FRG

Abstract. The spacial distribution of neutral species in the outer coma of a comet is described using a modified version of the "fountain" model. This model accounts for neutrals that are produced in multiple generations after release from the nucleus (or production in the collision zone of the inner coma) by an iterative application of the "fountain" model. A preliminary description of the model is given; however, results will be presented in a future paper. Suitable applications of the model include the following: (1) distributed coma sources of neutral gas-phase species from anisotropic dust emission, (2) the description of cometary comae at large heliocentric distances, and (3) day/night asymmetry of gas production from the nucleus.

Model Description

Two papers that develop the theory of the "fountain" model by Haser (1957, 1965), form the basis of the present multigeneration model. The neutrals flow freely outside of the collision zone, the extent of which defines the inner boundary of our model, R_c, approximately 10^4 km for Comet Halley at the *Giotto* encounter. The outer boundary of the model, R_g, occurs at approximately 10^7 km in this case, where significant curvature of the particle's trajectory is introduced by the effects of gravity. The inner boundary conditions for the densities and velocities are given by our spherically symmetric, fluid dynamic model with detailed gas-phase chemistry (Schmidt et al. 1988).

Each neutral species is characterized by a lifetime against photo destruction (photodissociation, photodissociative ionization, and photoionization) and charge exchange with the mass-loaded solar wind. The excess energies of the dissociation products are included to

describe the formation of the following generation of neutrals. We assume that the coma is optically thin to visible and UV sunlight, that the neutrals do not undergo collisions in the outer coma (except with the mass-loaded solar wind), and that the conditions can be described in the steady-state approximation. The effect of radiation pressure from sunlight on the different neutral species is incorporated into the model. Each species is characterized by a radiative acceleration parameter, a, that depends on its unique ability to interact with light, folded with the solar spectrum. This effect results in an axisymmetric distribution for the neutrals. Typical reciprocal lifetimes against photodissociation, τ_{PD}^{-1}, and photoionization, τ_{PI}^{-1}, from Schmidt et al. (1988) and values of a from Konno (1990) for important cometary neutrals are presented in Table 1. Also given are stand-off distances, z_{max} (the maximum distance to which the species can travel along the Sun–comet axis), assuming an initial velocity of 1 km s^{-1}.

In addition to the nucleus and inner coma sources of neutrals, each point within the region bounded by the model acts as a source for a subsequent generation when a neutral of the previous generation is destroyed. Just prior to destruction, particles at any point within the outer coma have two peculiar velocities with respect to the nucleus, as given by the original "fountain" model. This results in a skewing of the parabaloid which bounds the set of all possible trajectories of the isotropically emitted, next generation species. When all of the important reaction pathways that lead to the creation of a given neutral are considered, each spacial distribution that results can be superimposed to give the total density distribution. This feature of the model is particularly useful for isolating the most important reactions that contribute to a given species as a function of cometocentric and heliocentric distances.

Computational Grid

The computational grid is axisymmetric, with the Sun–comet line as the axis of symmetry. It has been described by Schmidt and Wegmann (1980) with parameters appropriate to the bounded region discussed above. This grid was chosen for computational efficiency and compatability with our coma chemistry code with solar wind interaction (Schmidt et al. 1988). A complete solution can be obtained along the Sun–comet line with a double integration in a half-plane bounded by this axis of symmetry. The solution for a general point off-axis can be found with a triple integration in a half-volume bounded by this plane.

C-3

Discussion

Whenver possible, we will incorporate data for determining radiative acceleration and photo lifetimes for interesting cometary neutrals. This includes the water group species (such as, OH and O) and other species (such as, C_2, C_3, NH_2, and CH) that have short stand-off distances. Preliminary results along the Sun–comet axis have compared favorably with our previous radially symmetric calculations. Possible applications of the model will be the following: (1) distributed sources of neutral gas-phase species in the coma from anisotropic dust emission, (2) cometary comae at large heliocentric distances, and (3) day/night asymmetry of gas production from the nucleus with possible compositional anisotropies. The results can be applied to observed isophotes for cometary neutrals as well as used for computing two-dimensional, ionic source terms for cometary plasma models.

Acknowledgements. The original concept for this model and many helpful comments are gratefully acknowledged from Dr. H. U. Schmidt. Dr. R. Wegmann kindly supplied the computational grid used in the model and gave valuable comments. This study was supported by a fellowship from the Max-Planck-Gesellschaft.

References

Haser, L. (1957): 'Distribution d'intensité dans la tête d'une comète,' *Bull. de l'Académie royale de Belgique*, 740–750.

Haser, L. (1965): 'Calcul de distribution d'intensité relative dans une tête comètaire,' *Congrès Colloques l'Université de Liège* 37, 233–241.

Konno, I. (1990): Private communication.

Schmidt, H. U., Wegmann, R. (1980): 'MHD-Calculations for cometary plasmas,' *Computer Physics Communications* 19, 309–326.

Schmidt, H. U., Wegmann, R., Huebner, W. F., Boice, D. C. (1988): 'Cometary gas and plasma flow with detailed chemistry,' *Computer Physics Communications* 49, 17–59.

Table 1

Radiation Acceleration and Photolifetimes of Important Cometary Neutrals

	a	z_{max}	τ_{PD}^{-1}	τ_{PI}^{-1}
H_2O	$2.9 \cdot 10^{-4}$ cm s^{-2}	$1.7 \cdot 10^{8}$ km	$1.17 \cdot 10^{-5}$ s^{-1}	$3.34 \cdot 10^{-7}$ s^{-1}
OH	$9.1 \cdot 10^{-3}$	$5.5 \cdot 10^{6}$	$5.00 \cdot 10^{-6}$	
SI	$4.8 \cdot 10^{-4}$	$1.0 \cdot 10^{6}$	–	$1.10 \cdot 10^{-6}$
CO_2	$5.6 \cdot 10^{-4}$	$8.9 \cdot 10^{7}$	$1.22 \cdot 10^{-6}$	$6.55 \cdot 10^{-7}$
CO	$7.6 \cdot 10^{-5}$	$6.6 \cdot 10^{8}$	$3.17 \cdot 10^{-7}$	$3.80 \cdot 10^{-7}$
NH_3	$1.8 \cdot 10^{-4}$	$2.8 \cdot 10^{8}$	$1.76 \cdot 10^{-6}$	$6.10 \cdot 10^{-7}$
C_3	$5.5 \cdot 10^{-1}$	$9.1 \cdot 10^{4}$	$1.00 \cdot 10^{-5}$	
NH_2	$2.7 \cdot 10^{-1}$	$1.9 \cdot 10^{5}$	$2.10 \cdot 10^{-4}$	
C_2	$8.1 \cdot 10^{-1}$	$6.2 \cdot 10^{4}$	$1.40 \cdot 10^{-7}$	$9.10 \cdot 10^{-7}$
CH	$1.4 \cdot 10^{-1}$	$3.6 \cdot 10^{5}$	$4.16 \cdot 10^{-3}$	$7.56 \cdot 10^{-7}$
HCN	$1.7 \cdot 10^{-4}$	$2.9 \cdot 10^{8}$	$2.00 \cdot 10^{-5}$	
CH_4	$3.1 \cdot 10^{-4}$	$1.6 \cdot 10^{8}$	$7.11 \cdot 10^{-6}$	$3.60 \cdot 10^{-7}$
H_2CO	$3.0 \cdot 10^{-4}$	$1.7 \cdot 10^{8}$	$2.78 \cdot 10^{-4}$	$4.04 \cdot 10^{-7}$
CN	$2.8 \cdot 10^{-1}$	$1.8 \cdot 10^{5}$	$4.00 \cdot 10^{-6}$	
HI	$4.6 \cdot 10^{-1}$	$1.1 \cdot 10^{5}$	–	$7.31 \cdot 10^{-6}$
CI[D]	$2.1 \cdot 10^{-3}$	$2.4 \cdot 10^{7}$	–	$3.58 \cdot 10^{-6}$

P. Feldman
CO is hardly a third generation species, particularly for R > 10^4 km.

Dan Boice
I considered CO a third generation species because of the distributed source found by Eberhardt et al. [(*Astron. Astrophys. 187,* 481 (1987)] using Giotto NMS data that existed out to about 20,000 km. I assumed that CO comes from a heavier molecule released by the dust. Additionally, on a larger distance scale (R ~ 10^6 km) CO_2 photodisociates into CO.

532-90
N91-21044

A MULTI-GENERATIONAL MONTE CARLO MODEL OF A COMET COMA

Anthony J. Ferro
Department of Physics and Astronomy
Arizona State University

Introduction

A steady-state multi-generational Monte Carlo model has been developed to describe the distribution of a neutral coma species which has been produced after several photodissociation steps. This distribution can be compared with either line profiles derived from long-slit spectroscopic observations or narrow band imaging, and be used to determine the elemental abundances present in the comet coma. A Monte Carlo model was chosen due to limitations in standard forms of more analytic models, such as those of Haser (1957) and Festou (1981). In contrast to the analytical models, the Monte Carlo method can be modified easily to include new physical parameters.

The Multi-Generational Model

The model can be described using the example of the production of NH in comets by the photodissociation sequence,

$$NH_3 \rightarrow NH_2 \rightarrow NH \rightarrow N. \qquad (1)$$

The grandparent molecules, NH_3, are ejected radially from the nucleus, either symmetrically, or asymmetrically. After a characteristic time, $T_{NH_3} \sim 7700$ s, the solar EUV radiation produces NH_2, with the excess photon energy partitioned into the kinetic and internal energies of the fragments, NH_2 and H. In the current model, the ratios of the energies are set at 9:1. Momentum is conserved in each dissociation, while the directions of the NH_2 fragments are randomized, in the center of mass (NH_3) frame. This process is repeated for NH_2 and NH, using calculated photodissociation rates.

Figure 1 shows a flowchart outlining the model program. Note that the basic structure consists of two nested loops, one for each test particle and one for each dissociation. Typically, each model is run for 10^6 to 10^8 iterations, with three or four dissociation steps for each particle. All calculations are done in three dimensions, centered on the comet nucleus. The final output is a two dimensional map of the observed molecular species. Spatial profiles can be taken from this map to compare with observed spatial profiles, or the map may be directly compared to narrow-band imaging data.

The current model allows simulation of various types of asymmetric ejection of the initial parent from the comet nucleus. The asymmetry can range from simple hemispheric ejection to ejection from very narrow regions, simulating jets. The model currently also can simulate accelerations due to solar radiation pressure. For certain molecules this

radiation pressure, derived from the g-factors, can play a major role in the morphology of the distribution of that molecule and of their daughter products.

In cases where there are several paths for producing a particular molecule, a suite of models may be run, and the results scaled then added. For instance, to model the NH distribution, the sequence in equation (1) is the primary process, with a branching ratio of 97%, 100% and 100%. However, the photodissociation sequence,

$$NH_3 \rightarrow NH \rightarrow N \qquad (2)$$

with a branching ratio of 3% and 100%, can also be considered. A model can be run for each sequence, then the resulting maps multiplied by the appropriate ratio and added.

Results

All results presented were run on the Arizona State University Supercomputing Facility CRAY-XMP/18se. Typical run times for a single model ranged from 20 to 120 cpu minutes.

Figure 2 shows a map of NH_2 generated with the Monte Carlo model in which solar radiation pressure has been taken into consideration. The solar acceleration is 0.17 cm/sec^2. Each side of the map represents 5×10^5 km.

Figure 3 shows a map of NH generated with the model. Again solar radiation pressure has been considered. Each side of the map represents 2×10^6 km. The wide scale of NH is due to its long lifetime. The lifetimes used in this model are given in Table 1.

In figure 4 we show the NH distribution observed in P/Halley, compared with the Monte Carlo model. Data are from S. Wyckoff (*see article in these proceedings*). In this case the model was symmetric and azimuthally averaged to increase signal to noise ratio. The fit, especially at distances greater than 10^6 kms. is quite good.

Future Work

Planned future enhancements to the model include: timed release to model a rotating source, inclusion of collisions by suitable modifications to the expected lifetimes close to the nucleus, addition of distributed sources, and the inclusion of non-gravitational forces. It is also hoped that the code can be modified to run in reasonable times on smaller computers, such as the current generation of high speed workstations.

References

Festou, M.C. 1981, *Astr. Ap.*, **95**, 69.

Haser, L. 1957, *Bull. Acad. Roy. de Belgique, Classe des sci., 5th ser.*, **43**, 740.

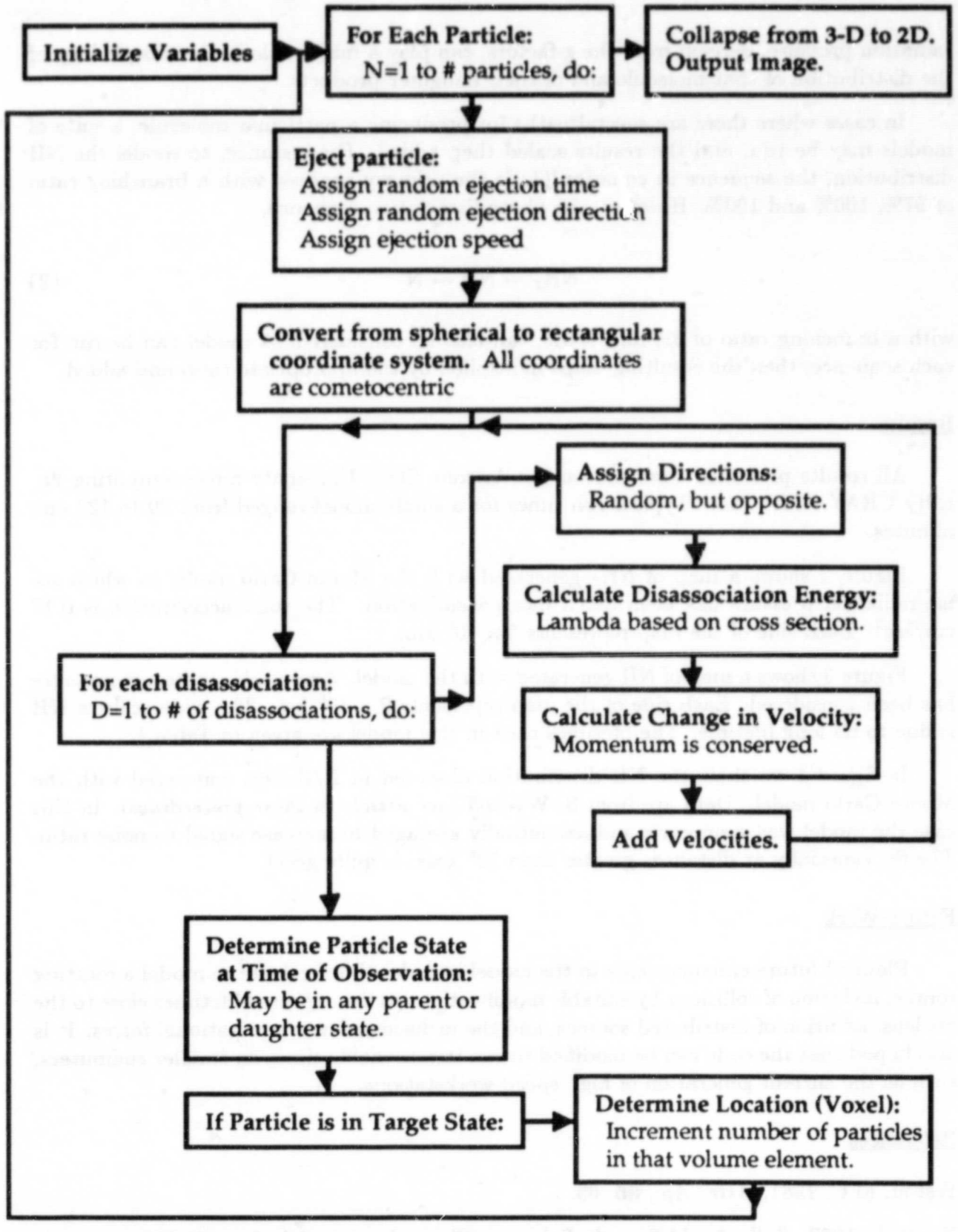

Figure 1: Flowchart of Monte Carlo Model

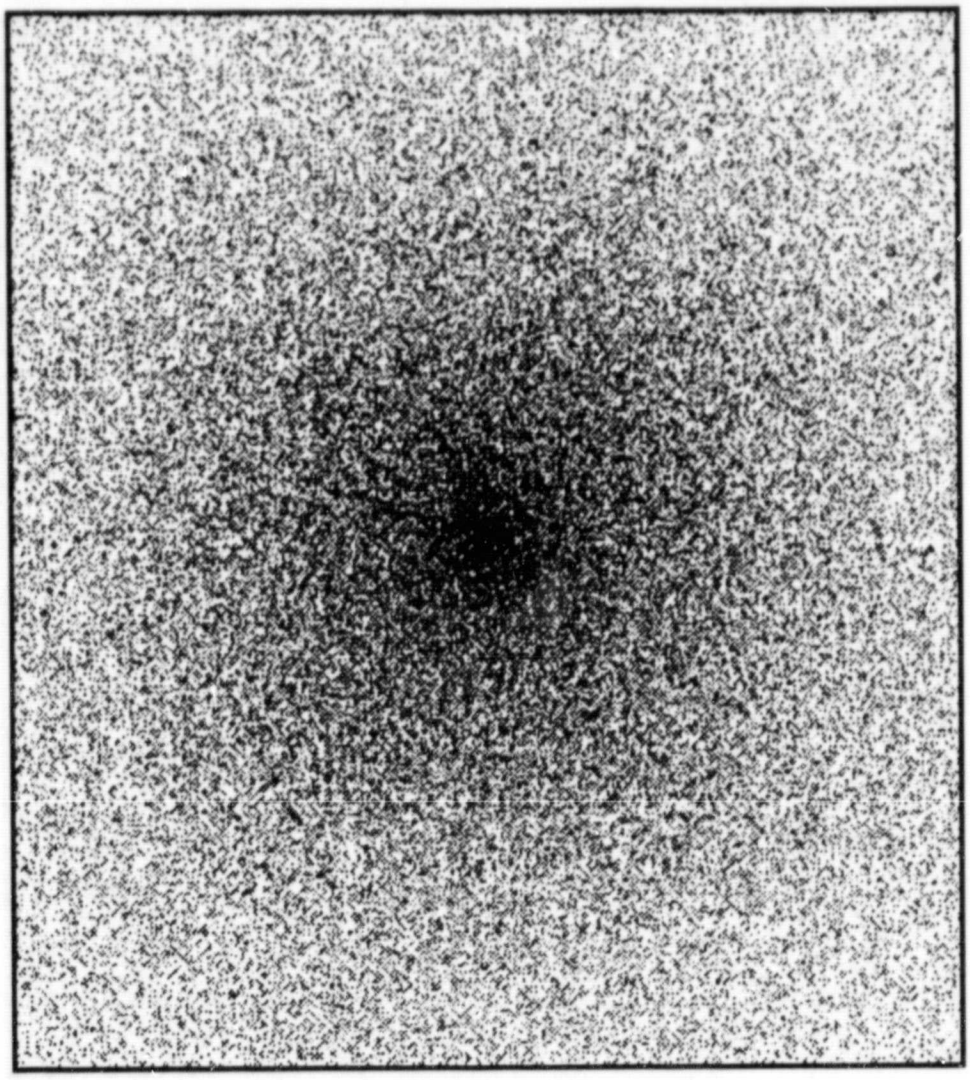

Figure 2: NH2 with solar acceleration.

Table 1: Timescales used in Monte Carlo model.

Molecule	Lifetime (sec)
NH_3	7,700
NH_2	32,600
NH	794,000

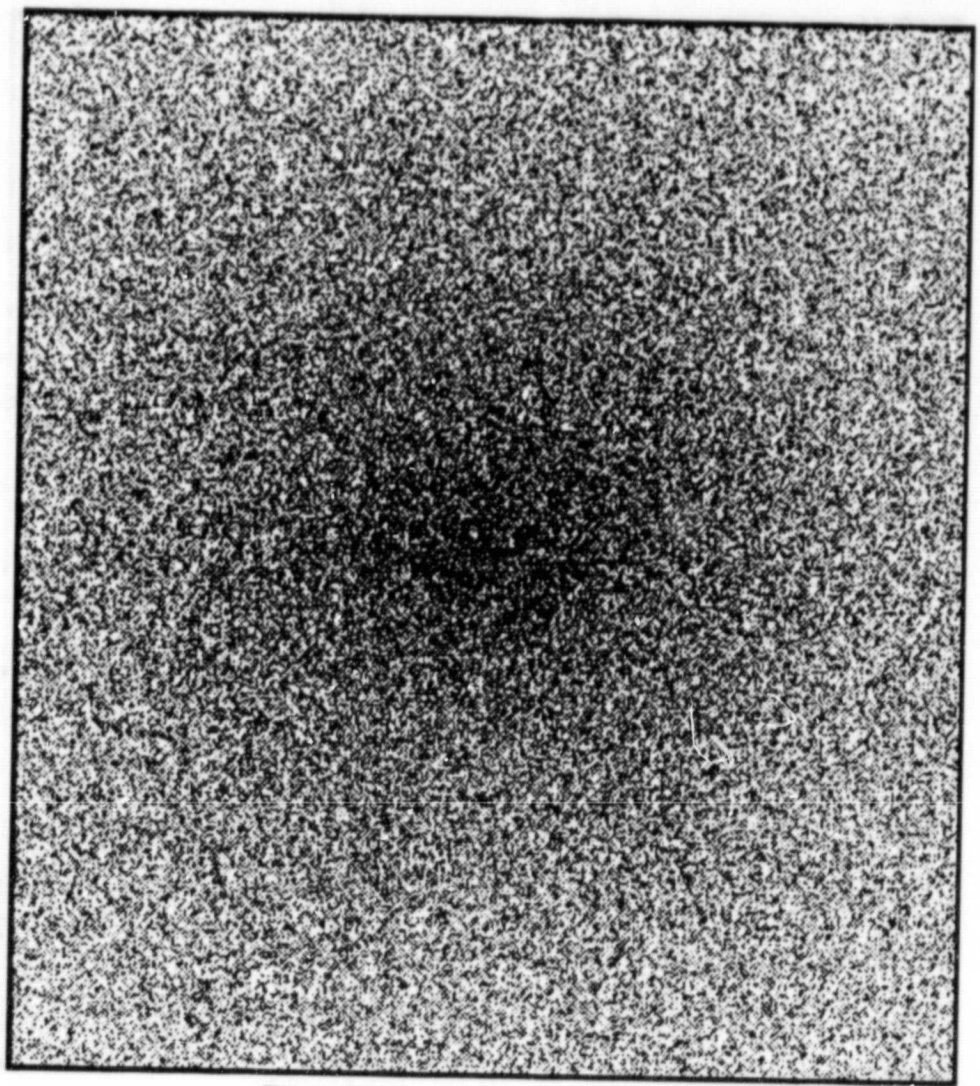

Figure 3: NH with solar acceleration.

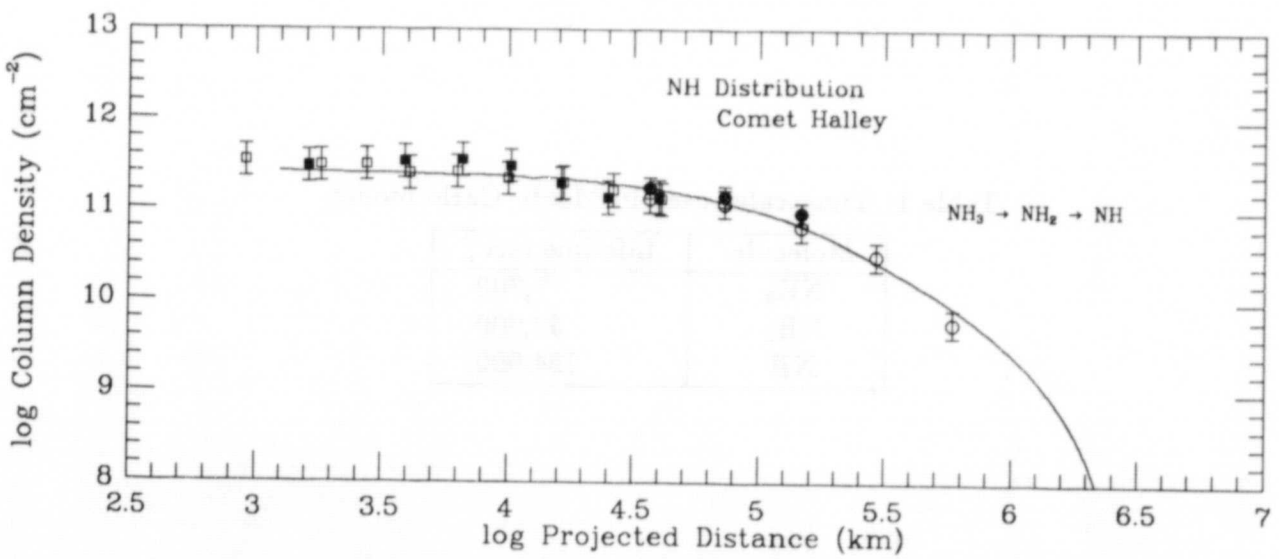

Figure 4: P/Halley and Monte Carlo model.

Dan Boice
This is very interesting and important work. You mentioned that a future extension will be the inclusion of distributed sources. Could you elaborate on how you will do this and what your goals will be?

Tony Ferro
With this model, I believe, that a distributed source could be modeled by simply assuming a very large parent with a mass similar to that of dust grains, and modifying the ejection velocity. This would act as another step in the model.

533-90
NAS. JNG/
P-1

N91-21045

A QUASI-LINEAR THEORY TO EXPLAIN ION ACCELERATION IN THE DISTANT COMETARY ENVIRONMENT.

Raji Sinha (University of New Mexico), S.Peter Gary (Las-Alamos National Lab), Norman Roderick (University of New Mexico).

Spacecraft observations at comet halley as well as computer simulations have demonstrated thar pitch-angle scattering of newborn cometary ions proceeds at a relatively fast rate, leading to relatively isotropic shell-like velocity distribution functions. Energization processes whereby shell distributions become more Maxwellian-like and a few ions are accelerated to high energies appear to proceed more slowly. This paper will describe our research on the latter, slower process, in which the scattering is assumed to be due to the resonant, growing magnetic fluctuations driven by the non-Maxwellian nature of the ion distribution.

We begin with an ion shell distribution which is isotropic in the wave frame and use a Fokker-Plank equation derived from quasilinear plasma theory to describe the broadening and energization of the cometary ion distribution.

N91-21046

MODELS OF THE SPIN STATE OF THE COMET HALLEY NUCLEUS

William H. Julian

Department of Mathematical Sciences, New Mexico State University

Las Cruces, New Mexico 88003 USA

Abstract

Eight rotation-precession models of the comet Halley nucleus have been proposed by various authors: (1) Julian (1987), Sagdeev *et al.*(1989), and Abergel *et al.*(1989); (2) Sekanina (1987); (3-5) Belton (1990); (6) Möhlmann (1989); (7) Festou *et al.*(1987); and (8) Wilhelm (1987) and Watanabe (1989). Julian (1990) has evaluated the eight models in relation to the constraints imposed by: (1) the observed long-axis directions at the Vega 1, Vega 2, and Giotto encounters, (2) the ground-based emission periods harmonically related to 7.4 days (Belton 1990), (3) the need for a two-day spin period in the analysis of the jet morphology, (4) the Smith *et al.*(1987) constraint on the net long-axis roll between Vega 2 and Giotto, (5) the resistance of the spin state of the nucleus to change due to the torque from the jets, and (6) the 7.4-day repetition of the spatial orientation of the nucleus.

Constraint 1. Sagdeev *et al.*(1989) analyzed spacecraft-encounter images to determine the directions of the long axis of the comet Halley nucleus. They found a solution involving a 2.2-day long-axis precession (of the long axis around the spin axis). Belton (1990) re-examined the motion of the nucleus with a 3.7-day long-axis precession and with the ends of the long axis reversed at Vega 1 and reflected in the plane of the sky as seen from Giotto. The eight models (Julian 1990) were constructed to satisfy either Sagdeev's solution (Models 1, 2, 6, 7, and 8) or Belton's solution (Models 3, 4, and 5); all are marked Y (Yes) under constraint 1 in the Table.

The inertial motion of the nucleus consists roughly of the long-axis precession combined with a roll of the nucleus around its long axis. The roll period is close to 7.4 days in Models 1, 2, 3, and 5; to 2.5 days in Model 4; to 5 days in Model 6; and to 15 days in

Models 7 and 8. Models 1, 3, and 8 are SAMs, while the rest are LAMs. In SAMs the roll motion is oscillatory, while for LAMs it is a complete rotation.

Constraint 2. Belton (1990) analyzed observations of the emission from Halley with the windowCLEAN algorithm to determine the dominant observed emission periods. He found that the dominant periods were constrained to be harmonically related to roughly 7.4 days (i.e, 7.4, 3.7, 2.5, and 1.9). He ruled out a 2.2-day periodicity in the observed emission. This calls into question Models 1, 2, 6, 7, and 8 which were constructed with a 2.2-day long-axis precession. Models 3, 4, and 5 satisfy Belton's constraint and are accordingly marked Y under constraint 2 in the Table.

Constraint 3. A two-day spin period derives from the analysis of jet morphology (Hoban *et al.* 1988; Keller and Thomas 1988; Rabinowitz 1988; Schulz and Schlosser 1989). Models 3 and 5 require a re-analysis of the jet morphology with a three-day spin period; the other models are marked Y under constraint 3 in the Table.

Constraint 4. Smith *et al.*(1987) compared the similar profiles of the nucleus that were seen from the Vega 2 and Giotto spacecraft. They deduced that the nucleus rolled an integral number of times between the two images which were taken 4.7 days apart. The models for which the residual net roll computed by Julian (1990) is less than 45° are marked Y under constraint 4 in the Table. Models 3, 4, 6, and 8 are favored; the others are not.

Constraint 5. Constancy of the spin state is required by various analyses. Yeomans and Kiang (1981) have suggested that the spin state of the comet Halley nucleus has been constant for over 27 apparitions. Schleicher and Bus (1990) have determined that the emission periods seen in the 1910 apparition are consistent with a negligible change in spin state between that apparition and 1985/1986. All SAM models (1, 3, and 8) have a spin state that is readily changed by the torques from nine randomly-placed jets (Julian 1990); the other models are marked Y under constraint 5 in the Table.

Constraint 6. Schleicher *et al.*(1990) have concluded that "the data demand that the nucleus returns to essentially the same orientation with respect to the sun each 7.4 ± 0.2 days,

except for longer-time-scale seasonal change." Models 3, 4, and 5 are based on a 3.7-day long-axis precession and on roll periods of 7.4, 2.5, and 7.34 days, respectively. These periods are nearly harmonics of 7.4 days. Thus, the models return to nearly the same inertial orientation each 7.4 ± 0.2 days and are marked Y under constraint 6 in the Table. The other models do not, since 2.2 days is not a harmonic of 7.4 days.

TABLE. CONSTRAINTS.

Constraint Model	1	2	3	4	5	6
1	Y		Y			
2	Y		Y		Y	
3	Y	Y		Y		Y
4	Y	Y	Y	Y	Y	Y
5	Y	Y			Y	Y
6	Y		Y	Y	Y	
7	Y		Y		Y	
8	Y		Y	Y		

Conclusions. All eight models satisfy constraint 1. If we require that the emission periods are harmonics of 7.4 days (constraint 2) then we are left with Models 3, 4, and 5. These are exactly the models that satisfy constraint 6. Model 3 is sensitive to inter-apparition spin state change, as are all the SAM models. Model 4 with a 3.7-day long axis precession and 2.5-day roll satisfies all six constraints. Its emission spectrum is weighted towards the fifth harmonic of 7.4 days, while that of Model 5 is weighted towards the third. Model 5 with 3.7-day long axis precession and 7.4-day roll satisfies constraints 1, 2, 5, and 6. If we accept Model 5, then we must re-examine the Smith *et al.*(1987) long-axis roll constraint, and re-analyze the jet morphology with a three-day spin period.

The roll and long-axis precession periods of Model 4 stand in a 2:3 resonance so the nucleus rolls three times around its long axis in the 7.4 days required for the long axis to precess twice around the spin axis. For Model 5 the resonance is 2:1 so the nucleus rolls once around its long axis in the 7.4 days required for the long axis to precess twice around the spin axis. The next step is to fit the observed ground-based emission waveform (Millis and Schleicher 1986; Schleicher *et al.* 1990) and the jet morphology (Hoban *et al.* 1988; Keller and Thomas 1988; Rabinowitz 1988; Schulz and Schlosser 1989).

Acknowledgements.

The author thanks Michael J.S. Belton and Nancy B. Julian for helpful discussions, and appreciates the kind hospitality of the National Optical Astronomical Observatories.

References.

Abergel, A., J.L. Bertaux, and E. Dimarellis (1989). Surface features and the rotation state of Halley's comet nucleus. *Annales Geophysicae* 7, 129-140.

Belton, M.J.S. (1990). Rationalization of comet Halley's periods. *Icarus* 86, 30-51.

Festou, M.C., P. Drossart, J. Lecacheux, T. Encrenaz, F. Puel, and J.L. Kohl-Moreira (1987). Periodicities in the light curve of P/Halley and the rotation of its nucleus. *Astron. Astrophys.* 187, 575-580.

Hoban, S., N.H. Samarasinha, M.F. A'Hearn, and D.A. Klinglesmith (1988). An investigation into periodicities in the morphology of CN jets in comet P/Halley. *Astron. Astrophys.* 195, 331-337.

Julian, W.H. (1987). Free precession of the comet Halley nucleus. *Nature* 326, 57-58.

Julian, W.H. (1990). The comet Halley nucleus - random jets. *Icarus*, in press.

Keller, H.U., and N. Thomas (1988). On the rotation axis of comet Halley. *Nature* 333, 146-148.

Millis, R.L., and D.G. Schleicher (1986). Rotational period of comet Halley. *Nature* 324, 646-649.

Möhlmann,D., (1989). Rotation and free precession of the comet Halley nucleus. *Astron. Nachr.* 310, 151-154.

Rabinowitz, D.L. (1988). A source map for dust jets observed in the coma of comet P/Halley. *Astron. Astrophys.* 200, 225-247.

Sagdeev, R.Z., K. Szego, B.A. Smith, S. Larson, E. Merenyi, A. Kondor, and I. Toth (1989). The rotation of P/Halley. *Astron. J.* 97, 546-551.

Schleicher, D.G., and S.J. Bus (1990). Comet P/Halley's periodic brightness variations in 1910. *Astron.J.*, submitted.

Schleicher, D.G., R.L. Millis, D.T. Thompson, P.V. Birch, R. Martin, D.J. Tholen, J.R. Piscitelli, N.L. Lark, and H.B. Hammel (1990). Periodic variations in the activity of comet P/Halley during the 1985/1986 apparition. *Astron.J.*, accepted.

Schulz, R. and W. Schlosser (1989). CN-shell structures and dynamics of the nucleus of comet P/Halley. *Astron. Astrophys.* **214**, 375-385.

Sekanina, Z. (1987). Nucleus of comet Halley as a torque-free rigid rotator. *Nature* **325**, 326-328.

Smith, B.A., S.M. Larson, K. Szegö, and R.Z. Sagdeev (1987). Rejection of a proposed 7.4-day rotation period of the comet Halley nucleus, *Nature* **326**, 573-574.

Watanabe, J., (1989). Rotational motion of the nucleus of comet P/Halley. *Pub. Ast. Soc. Japan* **41**, 897-918.

Wilhelm, K. (1987). Rotation and precession of comet Halley. *Nature* **327**, 27-30.

Yeomans, D.K., and T. Kiang (1981). The long-term motion of comet Halley. *Mon.Not.R.Astr.Soc.* **197**, 633-646.

N91-21047

THE CRAF MISSION AND EARTH-BASED COMET OBSERVATIONS

Paul R. Weissman and Marcia Neugebauer
Earth and Space Sciences Division
Jet Propulsion Laboratory
Pasadena, CA 91109

The Comet Rendezvous Asteroid Flyby (CRAF) mission was approved for a New Start in the 1990 NASA appropriation, along with the Cassini (Saturn Orbiter/Titan Probe) mission, to be built simultaneously. Detailed design and planning of the CRAF spacecraft, mission, and scientific payload, are now underway. The CRAF mission will perform detailed studies of a typical short-period comet as it moves around its orbit, building on the information gained from the Giotto, Vega, and Suisei fast flybys of Comet Halley in 1986.

CRAF will be launched in August, 1995 on a Titan IV/Centaur rocket, and will match orbits with short-period Comet Kopff in July, 2000, 850 days before perihelion at a heliocentric distance of 5.05 AU. After a series of close, slow flybys, the spacecraft will be placed in orbit around the cometary nucleus at an altitude of ~ 63 km, yielding better than 1 meter/line-pair imaging resolution on the nucleus surface. One year after arrival, CRAF will fire an instrumented penetrator into the surface of the cometary nucleus to make detailed compositional and thermo-physical measurements over a period of about eight days. Instruments onboard the orbiter will collect and analyze cometary dust and gases, study the interaction of the cometary coma with the solar wind, and image and spectrally analyze both the nucleus surface and the coma, as the comet moves closer to the Sun and activity grows. Current plans call for the spacecraft to fly 50,000 km down the comet's tail, shortly after perihelion passage in late 2002. On the way to Comet Kopff, CRAF will fly by the 88-km diameter, C-type, main belt asteroid 449 Hamburga in January, 1998, at a closest approach distance of about 3,500 km, adding to our knowledge of these primitive bodies which are believed to be the source of many meteorites on Earth. In addition, CRAF will perform a gravity assist flyby of the Earth in July, 1997. CRAF is a joint project between NASA and the Federal Republic of Germany.

Earth-based observations of the target comet, either by ground-based facilities or by Earth-orbiting satellites, can provide essential information for CRAF mission planning, and are needed in support of the rendezvous mission. Estimates of the nucleus size, albedo, shape, rotation period, and rotation pole orientation are needed for preliminary mission planning, resource allocation, and sequence design. Measurement of the target asteroid's rotation period and shape, as well as a detailed spectral reflectance curve, are also needed. Astrometric observations of both the target comet and asteroid can result in improved ephemerides, helping to optimize trajectory design. Ground-based observations of the comet during the rendezvous will allow comparison with *in situ* measurements by the spacecraft, thus improving the interpretation of ground-based observations of other short-period comets.

Opportunities also exist for active participation in CRAF data analysis by scientists not currently associated with the mission. A program of Participating Scientists is planned which will supplement currently selected science teams during flight. Announcements of Opportunity will be issued by NASA approximately one year prior to the Hamburga flyby, and later approximately one year prior to rendezvous with Comet Kopff

The attached table provides orbital data on the future perihelion passages of Comet Kopff, as well as that for two other short-period comets which are prime backup targets for the CRAF mission, Comets Tempel 2 and Wild 2. The CRAF science office is interested in receiving information on any observations of these three comets. Observations of interest include measurements of gas production rates, dust production rates, and visual magnitudes at any point in the comets' orbits, and observations of the bare cometary nuclei at large solar distance. Evidence of cometary activity at large heliocentric distance, beyond 3 AU, would be particularly valuable. Please send any information, preprints, reprints, abstracts, etc. to the authors above.

Comet Kopff is particularly well placed for Earth-based observations during its 1996 perihelion passage, as is Comet Wild 2 in 1997, and Comet Tempel 2 in 1999. Comet Wild 2 is well placed for post-perihelion observations in 1990.

A more complete description of the CRAF mission can be found in: Neugebauer, M., and Weissman, P. R., CRAF mission, *EOS* **70**, 633, 1989.

CRAF Target Comets*

Comet	T	Peri.	Node	Incl.	q	e
Kopff	1990 1 20.3725	162.8291	120.2891	4.7205	1.585125	0.542991
	1996 7 2.1840	162.7631	120.2823	4.7245	1.579523	0.544079
	2002 12 12.0646	162.6860	120.2977	4.7222	1.583575	0.543302
Wild 2	1990 12 16.9253	41.5729	135.5763	3.2494	1.578058	0.540983
	1997 5 6.6533	41.6992	135.5280	3.2481	1.582620	0.540225
	2003 9 25.9857	41.6832	135.5130	3.2457	1.590364	0.538794
Tempel 2	1994 3 16.8162	194.8570	117.5760	11.9783	1.483536	0.522447
	1999 9 8.4247	194.9972	117.5388	11.9798	1.481679	0.522818
	2005 2 15.0423	195.5328	117.1761	12.0208	1.426862	0.535387

*Orbital data from: Yeomans, D. K., and Wimberly, R. N., Cometary apparitions: 1990 - 2010, in *Comets in the Post-Halley Era*, eds. R. L. Newburn, J. Rahe, and M. Neugebauer, Kluwer, Amsterdam, in press, 1990.

OMIT TO END

CONFERENCE SUMMARY

W. F. Huebner
Southwest Research Institute
San Antonio, TX 78228-0510

We had hoped that Jurgen Rahe would prepare and present the summary of this workshop. Unfortunately he is unable to attend. Therefore, I will try to summarize this meeting in his stead.

We have heard reports on the observations of four comets: Brorsen-Metcalf (1989o), Okazaki-Levy-Rudenko (1989r), Aarseth-Brewington (1989a1), and Austin (1989c1). Although only preliminary results are available at this time, the path of research that has been initiated is clear: In many regards it follows closely the directions established by the new Comet P/Halley findings.

The relationship of minor species with each other and with possible parents as well as with dust are being pursued in a number of investigations. Of particular interest are the abundance ratios of CH_4 to CO and NH_3 to N_2, because they give information about the place of origin of comets. These determinations are very difficult because there are no direct observations of CH_4 or N_2 and NH_3 may be detectable only in the radio range and apparently no such observations were made. Thus the determination of these ratios is indirect. Closely related to this line of research and to the place of origin of comets are the isotope ratios of $^{12}C/^{13}C$. Whereas the ^{13}C isotope showed a relatively strong spectrum in Comet Halley, this is apparently not the case with the comets under investigation here.

The relative constancy from comet to comet of some, presumable chemically unrelated minor species may also yield information about the origin of comets. But first it will be necessary to establish whether these species originate in the icy or the dusty component of the nucleus. The fact that some have an almost constant ratio with respect to OH seems to indicate that their abundances are closely correlated to that of water, for example, they may be trapped in water ice to their point of saturation. Establishing a correlation of the minor species to the dust is a much more difficult problem that still needs further investigation.

Other species, such as S_2, appear to vary much more widely. In fact, only upper limits have been established for S_2 in the comets under investigation here. Unidentified lines and the new species CH_3OH and H_2S, reported for the first time at this workshop, give new impetus to comet research.

Observations of dust in the IR and the correlation of the dust with visual brightness of a comet and its chemical composition require close cooperation between various observers. As reported at this workshop, a trend is being established for simultaneous, multi-instrument observations by closely collaborating observing teams. In this regard simultaneous radio and optical observations are also emerging as a new vehicle.

Similar to multi-instrument observations, the time may be ripe for closer collaboration between observing teams and modelers. The Haser model, although very useful for short-lived species and for quick analyses, cannot be used for species involving several, nearly equally effective parents, as may occur in parallel photolytic and chemical reactions. Similarly, the dust size distribution as a function of cometocentric distance needs to be analyzed in closer collaboration between observers and modelers.

This has been a very instructive meeting with many very open discussions. We had

international participation with two poster papers (Kozuka et al. and Watanabe et al.) from our Japanese colleagues and two papers (Bockelée-Morvan et al. and Colom et al.) from our French colleagues, presented by Bockelée-Morvan who made a special trip to present these papers at our workshop. I am very grateful to Dr. Bockelée-Morvan for making this effort and want to thank all of you for attending and participating. I also want to thank Ms. Staglik from the SwRI for taking care of the many details in arranging this workshop and Mr. Sommerfeld from the University of Albuquerque for operating the projection equipment. Finally, I would like to thank my colleagues, Jurgen Rahe, Peter Wehinger, and Ichishiro Konno for their help in organizing this workshop and the NASA Planetary Atmospheres Program for supporting it.